

Design, Engineering and Biological  
Performance of Responsive Lipid Vesicles for  
Enhanced Drug Delivery by Mild Hyperthermia

*Zahraa S. Al-Ahmady*

A thesis submitted in partial fulfilment of the requirements for the  
degree of Doctor of Philosophy

**UCL School of Pharmacy**

**2013**

## Declaration of Academic Integrity

I, Zahraa Al-Ahmady confirm that the work presented in this thesis is my own. Where information has been derived from other sources, I confirm that this has been indicated in the thesis.

---

**Signature**

---

**Date**

## ACKNOWLEDGEMENT

First of all, I would like to thank God for giving me the strength and power through all my life until this stage to finish my PhD studies.

I had an exciting and wonderful experience over the last three years at UCL School of Pharmacy. It was a great opportunity to expand my knowledge and build myself as a scientist. I would like to take this opportunity to express my sincere appreciation for those people who contributed directly to this thesis or were always for me during this journey.

My great appreciation goes to my supervisor professor Kostas Kostarelos for the invaluable guidance, consistent encouragement throughout my doctorate study. Thank you very much professor for offering me this great opportunity, I am really proud to be part of your enthusiastic group. Your deep insight and research expertise enriched my knowledge not only in the liposomes world but in many exciting areas of nanomedical sciences.

I am also very grateful to all our collaborators Dr. Alex Drake, Dr. James Mason, Dr. Tam Bui, Dr. Cheryl Scudamore, Dr. Klazina Kooiman, Dr. Olivier Chaloin, Dr. Louic Vermeer and the European Commission FP7 Program (SONODRUGS) for the funding.

Very special thanks to Jeroen for showing me on the field of liposomes, his continuous help with the design of my liposomes and the fruitful discussions we had during the course of my studies. Tian, although we did not spend much time together, but you were great help at the beginning of my PhD. Many thanks go to Wafa for the training with cell culture, the animal work and all the useful discussions. Hanene, my dearest friend and sister, a big thank for your endless kindness, invaluable advice, listening and taking away my stress. You are a great help whenever I needed a hand. Acelya, our young and lively colleague, you were a great example to follow. Thank you very much for your constant advice and continuous assistance even when you were every busy. Laura and Mariarosa, many thanks for your kind support and the generous help with the animal orders and the setups. Dhifaf, it was great to have you around! We share a lot together. Thank you very much for your understanding and the stress-alleviating chats. Special thanks to Sai for giving me a hand during my last year, you were a great help.

To all my colleagues at the Nanomedicine Lab; Khloud, Takeshi, Chang, Cyrill, Ania, Neus, António, Debora, Katie, Irene, Giulia, James Mei, Dimitris, Sarah and Leon, Thank you very much for your care, kindness, useful feedback and the friendly environment.

Isabel and Katerina you were both a great help solving technical and logistical issues in the lab. John, thank you very much for helping me to design a proper setup for my animal work. I would not have been able to do it without you.

I would also like to thank all my PhD colleagues at UCL School of Pharmacy for the friendly environment. Special thanks to Asma for the help with DSC experiments. Hayder, I know you are always ready to help whenever needed, thank you very much for everything.

Mum and Dad words are not enough to describe what I hold for you. Thank you very much for your never-ending love, support, guidance, prayers and for raising me up with affection to science. My dearest sister you are the irreplaceable part of my life. A big thank for always being so inspiring and thoughtful. You have always been there for me. To my dearest relatives and in-laws, you are my big family. Thank you very much for your continuous love, emotional support, prayers and your faith on me.

Most importantly, I would like to acknowledge my loving husband, Firas. You have been a constant source of strength and motivation. Many thanks for your advice, patience and dedication. There were times during the last three years were everything seemed hopeless, I can honestly say that I would not have been able to get through without you being by my side.

My deep thanks to my five-year old son Ahmed, who grew up during my PhD studies. Thank you very much for giving us so much joy, for always putting a smile on my face and for being so patient for your Mum, you are my escape during periods of despair.

I am so lucky to have you all in my life.

*I would like to lovingly dedicate this thesis to my family;*

*To my wonderful parents & gorgeous sister,*

*To my loving husband &*

*To our precious son*

## ABSTRACT

The design of a delivery system that specifically delivers anticancer drug to the tumour site avoiding normal tissues damage has always been a challenge. In this thesis we describe the engineering and biological performance of novel temperature-sensitive liposomes (TSL) that have both a substantial *in vivo* stability and an efficient content-release by mild hyperthermia (HT).

First, we explain the development of novel lipid-peptide hybrids (Lp-Peptide) by anchoring leucine zipper temperature-sensitive peptide within the liposomal lipid bilayer. The dissociation of the self-assembled coiled-coil structure of the peptide by mild Hyperthermia (HT) is considered to be responsible for triggering drug release. We characterized this system by studying its physicochemical properties and the interaction of the peptide with the lipid bilayer. Then we examined its potential to retain and trigger the release of the anticancer drug, doxorubicin, *in vitro* at physiological temperatures and after exposure to mild HT. The hybrid system was further evaluated at the cellular level by studying its biocompatibility, cellular uptake and cytotoxic activity. In addition, the blood kinetics, tumour and other tissues accumulation were explored when we studied the system *in vivo*. Our data suggested that Lp-Peptide hybrids can increase both immediate and long-term drug accumulation in the tumour. Therefore, we studied their therapeutic activity comparing two different heating protocols to mimic intravascular and interstitial drug release.

The last chapter of this thesis explored the opportunities of increasing the therapeutic specificity of TSL by designing anti-MUC-1 targeted vesicles based on the traditional TSL (TTSL) to trigger drug release after specific uptake into cancer cells. We showed that TTSL liposomes maintain their physicochemical and thermal properties after conjugation to anti-MUC-1 antibody. Moreover, the system was further evaluated by studying the *in vitro* cellular binding, uptake and therapeutic efficacy. Taking this system a step further, its biodistribution and therapeutic potential were also examined. Different protocols were applied to explore the effect of HT on the accumulation of targeted TTSL into the tumour and their therapeutic efficacy.

In summary, this thesis explains the design, engineering and biological performance of novel temperature-responsive vesicles. Our studies demonstrate the critical factors to consider in the design of clinically relevant TSL and the importance of matching the heating protocol to their physicochemical and pharmacokinetic parameters to maximise therapeutic benefits.

# TABLE OF CONTENTS

<b>ACKNOWLEDGEMENT</b>	<b>III</b>
<b>LIST OF TABLES</b>	<b>X</b>
<b>LIST OF FIGURES</b>	<b>XI</b>
<b>LIST OF SCHEMES</b>	<b>XIV</b>
<b>LIST OF ABBREVIATIONS</b>	<b>XV</b>
<b>CHAPTER 1 INTRODUCTION</b>	<b>1</b>
1.1 Development of Liposomes for Cancer Therapy .....	4
1.2 Hyperthermia in Cancer Therapy .....	10
1.2.1 Hyperthermia as a Treatment Modality for Cancer (Ablative Therapy).....	10
1.2.2 The Potential of Hyperthermia in Drug Delivery .....	13
1.3 Evolution of Temperature-Sensitive Liposomes (TSL) .....	16
1.3.1 Rationale Design of TSL for Triggered Drug Delivery .....	16
1.3.2 Critical Parameters Affecting the Choice of Heating Protocol for Triggering Drug Release from TSL .....	50
1.3.3 Image-Guided Drug Delivery of TSL (Paramagnetic TSL) .....	56
1.4 Development of Heating Modalities for Temperature Triggered Drug Delivery .....	61
<b>CHAPTER 2 AIM AND HYPOTHESES</b>	<b>64</b>
<b>CHAPTER 3 MATERIALS AND METHODS</b>	<b>67</b>
3.1 Materials.....	68
3.2 Cell Lines .....	69
3.3 Methods.....	69
3.3.1 Preparation of Liposomes .....	69
3.3.2 Preparation of CF-Loaded Liposomes .....	71
3.3.3 Preparation of DiI-Labelled Liposomes.....	71
3.3.4 Preparation of Targeted TSL Liposomes .....	71
3.3.5 Liposomes Characterization Techniques .....	72
3.3.6 Remote Loading of Liposomes with DOX .....	77
3.3.7 Release Studies from Liposomes .....	77
3.3.8 Biocompatibility Studies.....	78
3.3.9 Cellular Binding and Uptake Studies.....	80
3.3.10 Cellular Cytotoxicity Studies (MTT Assay .....	82
3.3.11 Localisation and Cytotoxicity Studies Using Multicellular Spheroids (MCS) ....	83
3.3.12 Animals and Tumour Models .....	85

3.3.13	Pharmacokinetics and Biodistribution Studies .....	86
3.3.14	<i>In Vivo</i> Optical Fluorescence Imaging.....	88
3.3.15	<i>In vivo</i> Tumour Growth Delay and Survival Studies.....	89
3.3.16	Histopathological Analysis .....	90
3.3.17	Statistical Analysis.....	90
<b>CHAPTER 4</b>	<b>DESIGN AND CHARACTERIZATION OF LP-PEPTIDE HYBRIDS</b>	<b>91</b>
4.1	Introduction.....	93
4.2	Results.....	96
4.2.1	Preparation and Characterization of Liposomes .....	96
4.2.2	Circular Dichroism Studies.....	99
4.2.3	Differential Scanning Calorimetry Measurements.....	102
4.2.4	Fluorescence Anisotropy Measurements .....	104
4.2.5	Solid-State NMR Experiments.....	106
4.2.6	Release Experiments.....	107
4.3	Discussion .....	114
4.4	Conclusion.....	120
<b>CHAPTER 5</b>	<b>BIOLOGICAL PERFORMANCE OF LP-PEPTIDE HYBRIDS</b>	<b>121</b>
5.1	Introduction.....	123
5.2	Results.....	125
5.2.1	Lp-Peptide Hybrids Biocompatibility Studies .....	125
5.2.2	Cytotoxicity of DOX-Loaded TSL .....	128
5.2.3	Pharmacokinetics and Biodistribution Studies .....	130
5.2.4	Pharmacological Activity of Lp-Peptide Hybrids; Choosing the Right Heating Protocol to Maximize Therapeutic Activity.....	136
5.3	Discussion .....	148
5.4	Conclusion.....	154
<b>CHAPTER 6</b>	<b>THE ENGINEERING OF ANTI-MUC-1 TARGETED TSL</b>	<b>155</b>
6.1	Introduction.....	157
6.2	Results.....	160
6.2.1	Preparation and Characterization MUC-1 TTSL-Ab Liposomes .....	160
6.2.2	DOX Release Studies.....	165
6.2.3	Cellular Binding of Anti-MUC-1 Antibody.....	165
6.2.4	Cellular Uptake of TTSL and TTSL-Ab.....	166
6.2.5	Cytotoxic Activity of DOX-Loaded TTSL and TTSL-Ab .....	167



6.2.6	Localisation and Cytotoxic Activity of TTSL and TTSL-Ab in Multicellular Spheroids (MCS) .....	170
6.2.7	Biodistribution and Optical Imaging Studies of TTSL and TTSL-Ab Liposomes .. .....	172
6.2.8	Tumour Growth Retardation and Survival Studies.....	177
6.3	Discussion .....	180
6.4	Conclusion.....	186
<b>CHAPTER 7</b>	<b>FINAL REMARKS AND FUTURE PERSPECTIVE</b>	<b>187</b>
	<b>APPENDENCES</b>	<b>193</b>
	<b>BIBLIOGRAPHY</b>	<b>194</b>

## LIST OF TABLES

Table 1-1: Examples of polymer modified temperature-sensitive liposomes.....	31
Table 1-2: TSL-NHs decorated with gold NPs.....	42
Table 1-3: TSL-NHs decorated with silver NPs.....	43
Table 1-4: TSL-NHs decorated with iron oxide NPs.....	43
Table 1-5: Different examples of actively targeted TSL.....	49
Table 1-6: HT protocols used for trigger release from TSL.....	53
Table 1-7: MR-guided drug delivery from TSL.....	60
Table 3-1: Temperature sensitive and non temperature-sensitive liposome systems studied.	70
Table 4-1: Transition temperature ( $T_m$ ) of different molar ratios of DPPC:DSPC liposomes .....	96
Table 4-2: Transition temperature ( $T_m$ ) of DPPC:DSPC (90:10) liposomes with and without the inclusion of 5 mol% of DSPE-PEG <sub>2000</sub> lipid.....	96
Table 4-3: Physicochemical characterization data; hydrodynamic diameter, polydispersity Index (PDI), zeta-potential, and phase transition temperature ( $T_m$ ) of Lp, Lp- Peptide, Lp-CHOL, LTSL, TTSL and NTSL.....	98
Table 4-4: Physicochemical characterization of DOPE:EPC:DSPE-PEG <sub>2000</sub> liposomes with and without peptide. ....	108
Table 5-1: Therapeutic effect of TSL using the intravascular and interstitial release protocols .....	143
Table 6-1: Survival analysis of MDA-MB-435 tumour-bearing mice treated with DOX- loaded TTSL and TTSL-Ab. ....	179

## LIST OF FIGURES

Figure 1-1: Schematic presentation of the different types of liposome with triggered release properties. ....	9
Figure 1-2: The use of HT in cancer therapy. Adapted from (Kong <i>et al.</i> 1999) .....	10
Figure 1-3: Molecular basis of HT induced cell death. ....	12
Figure 1-4: Schematic presentation of different types of TSL and different chemical components included in their design. ....	16
Figure 1-5: Schematic presentation of phase transition behaviour of TSL.....	18
Figure 1-6: Chemical structures of the lipids used in the design of prototypical TSL. ....	20
Figure 1-7: Schematic presentation for drug leakage and nanopores formation in LTSL. ....	24
Figure 1-8: Chemical structures of the lipids used for the design of lysolipids-containing TSL.....	29
Figure 1-9: Mechanism of drug release from polymer modified TSL.....	30
Figure 1-10: Chemical structures of temperature-sensitive polymers used for the design of TSL. Chemical groups represented in red colour stand for the hydrophobic anchor groups used to fix the polymers into the lipid bilayer. ....	32
Figure 1-11: Different strategies used for the design of TSL-NHs.....	40
Figure 1-12: HT protocols that can be used to enhance drug delivery from TSL.....	50
Figure 1-13: Paramagnetic TSL for image guided drug delivery. ....	57
Figure 2-1: Schematic presentation of main hypothesis studied in this thesis.....	65
Figure 4-1: Schematic presentation of temperature-triggered release from Lp-Peptide hybrids. ....	94
Figure 4-2: Hydrodynamic diameter and zeta potential of the DPPC:DSPC:DSPE-PEG <sub>2000</sub> liposomes (A) before and (B) after incorporation of peptide. ....	97
Figure 4-3: Structural elucidation of Lp-Peptide hybrids. ....	99
Figure 4-4: Temperature-dependent conformational changes and reversibility of Lp-Peptide hybrids. ....	100
Figure 4-5: pH-sensitivity of leucine zipper peptide.....	102
Figure 4-6: Determination of T <sub>m</sub> of liposomes using differential scanning calorimetry. ...	103
Figure 4-7: The effect of peptide anchoring on liposome fluidity and lipid packing. ....	105
Figure 4-8: Solid state NMR studies of the interaction of leucine zipper peptide with liposomes.....	106
Figure 4-9: The effect of peptide on the release rate of DOPE:EPC:DSPE-PEG <sub>2000</sub> -liposomes. ....	108

Figure 4-10: Serum and temperature-sensitivity of Lp-Peptide hybrids.....	110
Figure 4-11: The effect of CHOL on DOX release from DPPC:DSPC:DSPE-PEG <sub>2000</sub> liposomes.....	111
Figure 4-12: Temperature-sensitivity of Lp-Peptide hybrids at 45 °C and 50 °C. ....	111
Figure 4-13: Time dependent DOX release studies in HBS. ....	112
Figure 4-14: CF release from DPPC:DSPC:DSPE-PEG <sub>2000</sub> liposomes with and without peptide. ....	113
Figure 4-15: Schematic presentation of the factors affecting the pH sensitivity of leucine zipper peptide. ....	116
Figure 5-1: Biocompatibility studies of Lp-Peptide hybrids with B16F10 and HUVEC cells. .....	126
Figure 5-2: ELISA studies to check for Lp-Peptide hybrids immunogenicity <i>in vivo</i> .....	127
Figure 5-3: Cellular uptake studies of Lp and Lp-Peptide 200:1 into B16F10 cells. ....	128
Figure 5-4: MTT assay of different types of TSL in comparison to NTSL. ....	129
Figure 5-5: MTT assay of different types of TSL in comparison to NTSL. ....	130
Figure 5-6: The Effect of transition temperature of peptide on the blood profile of Lp- Peptide. ....	131
Figure 5-7: Blood profile of <sup>14</sup> C-Dox loaded LTSL, Lp-Peptide hybrids (200:1) and TTSL. .....	132
Figure 5-8: Body and tumour temperatures monitoring during HT application. ....	133
Figure 5-9: Tumour accumulation of <sup>14</sup> C-Dox after injection of different TSL with HT....	135
Figure 5-10: Organ biodistribution of <sup>14</sup> C-DOX loaded LTSL, Lp-Peptide 200:1 and TTSL. .....	136
Figure 5-11: <i>In vivo</i> optical imaging of DOX fluorescence in athymic mice treated with the intravascular release protocol. ....	139
Figure 5-12: <i>In vivo</i> optical imaging of DOX fluorescence in athymic mice treated with the interstitial release protocol. ....	140
Figure 5-13: <i>In vivo</i> tumour growth delay and survival studies.....	142
Figure 5-14: Histological analysis of tissues following treatment using the avascular release protocol.....	144
Figure 5-15: Histological analysis of tissues following treatment using the interstitial release protocol.....	145
Figure 5-16: Histopathological changes in the kidney 10 days after treatment with TTSL (interstitial protocol).....	146
Figure 6-1: Conjugation of anti-MUC-1 Ab to mal-DSPE-PEG <sub>2000</sub> micelles.....	160

Figure 6-2: SDS-PAGE electrophoresis of anti-MUC-1 antibody. ....	161
Figure 6-3: Quantification of anti-MUC-1 after post insertion into TTSL liposomes.....	162
Figure 6-4: SPR sensograms of anti-MUC-1 antibody binding to MUC-1 epitope.....	163
Figure 6-5: Design and characterization of TTSL and TTSL-Ab.....	164
Figure 6-6: Cellular binding of anti-MUC-1 antibody.....	165
Figure 6-7: Cellular uptake studies of TTSL and TTSL-Ab into MDA-MB-435 cells. ....	166
Figure 6-8: Cellular uptake of DOX-loaded TTSL, TTSL-Ab-I & TTSL-Ab-II.....	168
Figure 6-9: MTT assay of TTSL and TTSL-Ab in: A) MDA-MB-435 and B) C33a cells. 169	
Figure 6-10: Optical microscopy images of MDA-MB-435 MCS. ....	170
Figure 6-11: Evaluation of TTSL and TTSL-Ab liposomes localisation and cytotoxicity on MCS. ....	171
Figure 6-12: Blood profile and tumour accumulation of TTSL and TTSL-Ab. ....	174
Figure 6-13: Biodistribution study of <sup>14</sup> C-DOX loaded TTSL and TTSL-Ab in the organs. .....	176
Figure 6-14: <i>In vivo</i> imaging of athymic nude mice after injection with TTSL and TTSL-Ab. .....	177
Figure 6-15: <i>In vivo</i> tumour growth delay and survival studies.....	178

## LIST OF SCHEMES

Scheme 1-1: schematic presentation of drug delivery from TSL using MR-HIFU. ....	63
Scheme 3-1: Schematic presentation of the time frame of cellular uptake studies of DOX- loaded TTSL, TTSL-Ab-I and TTSL-Ab-II by MDA-MB-435 and C33a cells. .....	82
Scheme 3-2: Schematic presentation of the protocols used to assess the cytotoxicity of TTSL-Ab. ....	83
Scheme 3-3: Time line frame of the protocol used for testing TTSL and TTSL-Ab on MCF-7 MCS. ....	84
Scheme 5-1: Schematic presentation of intravascular and interstitial release protocols.....	137
Scheme 6-1: Schematic presentation of the three different heating protocols applied to study the biodistribution of TTSL-Ab compared to TTSL liposomes. ....	173

## LIST OF ABBREVIATIONS

4T07	mouse mammary carcinoma
5-FU	5-fluorouracil
AA	acrylic acid
AAM	acrylamide
Ab	antibody
ANS	8-Anilino-1-naphthalenesulfonic acid
APr	N-acryloylpyrrolidine
B16F10	murine melanoma
BCA	bicinchoninic acid
BSA	albumin from bovine serum
C12	didodecyl
C33a	human cervix carcinoma
C6-SH	hexanethiol
CD	circular dichroism
CDR	complementarity determining regions
CF	carboxyfluorescein
CHOL	cholesterol
CLSM	confocal laser scanning microscopy
CMC	critical micelle concentration
D.W.	distilled water
DAPI	4',6-Diamidino-2-Phenylindole (double stranded DNA staining)
DiI	1,1'-Diiododecyl-3,3,3',3'-Tetramethylindocarbocyanine Perchlorate
DLS	dynamic light scattering
DMAM	N,N-dimethylacrylamide
DMEM	Dulbecco's Modified Eagle Medium
DMP	2-dodecyl-sulfanylthiocarbonylsulfanyl-2-methylpropionic acid
DMPC	1,2-dimyristoyl- <i>sn</i> -glycero-3-phosphocholine
DMSO	dimethyl sulfoxide
DOPE	1,2-dioleoyl- <i>sn</i> -glycero-3-phosphoethanolamine
DOX	Doxorubicin
DPH	1,6-diphenyl-1,3,5-hexatriene
DPPC	1,2-dipalmitoyl- <i>sn</i> -glycero-3-phosphocholine
DPPE	1,2-dipalmitoyl- <i>sn</i> -glycero-3-phosphoethanolamine
DPPG	1,2-dipalmitoyl- <i>sn</i> -glycero-3-phosphoglycerol
DPPGOG	1,2-dipalmitoyl- <i>sn</i> -glycero-3-phosphoglyceroglycerol
DPTAP	1,2-dipalmitoyl-3-trimethylammonium propane (chloride salt)
DSC	differential scanning calorimetry
DSPE-PEG <sub>2000</sub>	1,2-distearoyl- <i>sn</i> -glycero-3-phosphoethanolamine-N-[methoxy(polyethylene glycol)-2000]
DTPA	diethylenetriamine pentaacetic acid
ECM	extracellular matrix
EDC	N-Ethyl-N'-dimethylaminopropyl carbodiimide
EDTA	ethylenediaminetetraacetic acid
EGM-2	Endothelial Cell Growth Medium-2
ELISA	enzyme linked immunosorbent assay
EMT-6	mammary carcinoma
EOEOVE	2-ethoxyethoxyethylvinylether
EPC	L- $\alpha$ -phosphatidylcholine
EPR	enhanced permeability and retention.
FaDu	human squamous cell carcinoma
FBS	foetal bovine serum
Fe <sub>3</sub> O <sub>4</sub>	magnetite
Gd(HPDO <sub>3</sub> A)	gadolinium-[10-(2-hydroxypropyl)-1,4,7,10-tetraazacyclododecane-1,4,7-triacetic acid]
Glu	Glutamic acid
GMI	gangliosides
H & E	hematoxylin and eosin
h	hour
HaT	DPPC:Brij 96:4
HCC	hepatocellular carcinoma
HCT116	human colon carcinoma
HePC	hexadecylphosphocholine
HEPES	4-(2-Hydroxyethyl) piperazine-1-ethanesulfonic acid
HIFU	High intensity focused

HPMA	N-(2-hydroxypropyl)methacrylamide
HRP	horse radish peroxidase
HSPC	hydrogenated soy phosphatidylcholine
HT	hyperthermia
HUVEC	human umbilical vein endothelial
ICG	indocyanine green
ID	injected dose.
IVIS	in vivo Imaging System
LCST	low critical solution temperature
Lp	DPPC:DSPC: DSPE-PEG <sub>2000</sub> (90:10:5)
Lp-CHOL	DPPC:DSPC:DSPE-PEG <sub>2000</sub> -CHOL (90:10:5:0.5)
Lp-Peptide	DPPC:DSPC: DSPE-PEG <sub>2000</sub> (90:10:5)-Peptide
LTSL	Lysolipid-containing temperature-sensitive liposomes; DPPC:MSPC:DSPE-PEG <sub>2000</sub> (90:10:4)
mAb	monoclonal antibody
Mal- DSPE-PEG <sub>2000</sub>	1,2-distearoyl-sn-glycero-3-phosphoethanolamine-N-[maleimide(polyethylene glycol)-2000]
MCF-7	human breast cancer cells
MCS	multicellular spheroids
MDA-MB-435	human breast cancer cells
MEM	minimum Essential Media
MF	electromagnetic field
min	minute
mol	mole
MPS	mononuclear phagocytic system
MR	magnetic resonance
MSA	mercaptosuccinic acid
MTT	3-(4,5-dimethylthiazol-2-yl)-2,5-diphenyl-tetrazolium bromide
MTX	methotrexate
MUC-1	mucin antigen
N.R	not reported
NBD	N-(7-nitrobenz-2-oxa-1,3-diazol-4-yl)-1,2-dihexadecanoyl-snglycero-3phosphoethanolamine)
NDDAM	N,N- didodecylacrylamide
NHS	N-hydroxysuccinimide
NIPAM	N-isopropylacrylamide
NIPAMAM	N-isopropylmethacrylamide
NIR	near-infrared
NPs	nanoparticles
NTSL	HSPC:CHOL:DSPE-PEG <sub>2000</sub> (56.3:38.2:5.5)
ODA	octadecyl acrylate
ODVE	octadecylvinylether
P-	poly
PAGE	polyacrylamide gel electrophoresis
PBS	phosphate buffered saline
PC3	human prostate adenocarcinoma
PDI	polydispersity index
PEG	polyethylene glycol
Peptide II	(VSSLESK) <sub>6</sub>
RF	radiofrequency
RFA	radiofrequency ablation
ROI	region of interest
rpm	rotation per minute
RPMI	roswell park memorial institute
s	seconds
SCD	average order parameters
SDS	sodium dodecyl sulfate
SEM	standard error of mean
SH	sulfhydryl
SPR	surface plasmon resonance
STD	standard deviation
SW480	human colorectal adenocarcinoma
TBS	tris buffered saline
TEM	transmission electron microscopy
T <sub>m</sub>	phase transition temperature
Traut's Reagent	2-iminothiolane
TSL	temperature-sensitive liposome
TSL-NHs	temperature-sensitive liposomes –nanoparticles hybrids
TTSL	traditional temperature-sensitive liposome ; DPPC:HSPC:CHOL:DSPE-PEG 2000 (54:27:16:3)



TTSL-Ab	anti-MUC-1 targeted TSL
WB	water bath
$\gamma$ -Fe <sub>2</sub> O <sub>3</sub>	maghemite

# **CHAPTER 1**

---

## **INTRODUCTION**

One of the important limitations to the treatment of solid tumours is the inability to achieve effective local drug concentration while avoiding healthy tissue damage, which restricts the dose that can be given systemically. Doxorubicin (DOX) is an effective chemotherapy, however its therapeutic efficiency is limited by delayed cardiotoxicity associated with cumulative damage to myocardial muscle at doses more than 500 mg/m<sup>2</sup> (Rahman *et al.* 1982). The low molecular weight of DOX and other chemotherapeutic drugs results in suboptimal pharmacokinetics characterized by rapid drug clearance (CL) (DOX CL ~45 L/h) and large distribution volumes (VD) (DOX VD ~254 L) (Barenholz 2012). Moreover, physiological barriers at the tumour site including high interstitial pressure (Jain 1987a) and heterogeneous perfusion (Jain 1987b) limit the transport of the free drug to the tumour, resulting in suboptimal therapeutic levels (Jain *et al.* 2010; Lammers 2012).

In an attempt to reduce the drug associated toxicity and improve the biodistribution of chemotherapeutic agents to the tumour site, encapsulation inside site-specific nanoscale delivery systems has been thoroughly investigated (Peer *et al.* 2007; Davis *et al.* 2008). This could lead to a balance between the degree of systemic toxicity and therapeutic efficacy. The key mechanism behind the selective accumulation of nanocarriers into the tumour rather than other healthy organs is the hyperpermeability of the tumour vasculature particularly in implanted animal tumour models (Dvorak *et al.* 1988). This phenomenon is known as enhanced permeability and retention effect (EPR) (Matsumura *et al.* 1986; Maeda 2001) and depends on anatomical difference between healthy tissues and tumour blood vessels. Tumour vasculature characterised by tortuous malformed structure with high permeability that originate during defective tumour angiogenesis. In general, tumour vessels differ from normal tissues vasculature by having poorly aligned endothelial cells, wide inter-endothelial junctions, abnormal and/or lack of perivascular cells, basement membrane and smooth-muscles (Jain 1987a; Iyer *et al.* 2006). These anatomical abnormalities favour the leakage of plasma components including the macromolecules into the tumour. The increase in the extravasation together with the reduced lymphatic drainage means that retention of the nanocarriers in the tumour is prolonged by decreasing their clearance (Maeda 2001; Iyer *et al.* 2006; Lammers 2012). Although the above mentioned factors facilitate the extravasation into the tumour, the size of nanoparticles, the limited flow of interstitial fluid and the

condensed interstitial matrix might hamper their movement into the extracellular matrix especially for big size tumour (Jain 1987a; Chrastina *et al.* 2011). It follows that some areas of the tumour are hyperpermeable whereas other areas have minimal or even absent permeability (Yuan *et al.* 1994a; Gaber *et al.* 1996; Kong *et al.* 2001; Manzoor *et al.* 2012; Li *et al.* 2013a) resulting in heterogeneous extravasation of the chemotherapeutic agents. Importantly, the clinical role of EPR effect in the passive accumulation of nanoparticles in patients is not yet conclusive (Prabhakar *et al.* 2013). In addition, nanoparticles penetration into the tumour is limited by the high tumour cell density and high interstitial fluid pressure which limit their distribution to the perivascular spaces (Lammers 2012).

Despite all these theoretical shortcomings associated with tumour extravasation and penetration, most of the nano-sized drug delivery systems designed for tumour targeting is based on the EPR effect. Among those nanoscale carriers, liposomes have the privilege of being the first and the most extensively used drug delivery system for cancer therapy (Allen 2013) as will be explained in details in the next section.

## 1.1 Development of Liposomes for Cancer Therapy

Liposomes were first described by Alec Bangham in the mid-1960s as spherical phospholipid vesicles consisting of one or more concentric lipid bilayers enclosing an aqueous core (Bangham *et al.* 1964; Bangham *et al.* 1965). Although liposomes form spontaneously by self-assembly of amphiphilic lipids after dispersion in water, they can effectively entrap both hydrophilic (X *et al.* 1998) and hydrophobic compounds (Chen *et al.* 2010; Koudelka *et al.* 2012) in the aqueous core or in the lipid bilayer, respectively. Liposomes are biocompatible, biodegradable, have low toxicity profile and can effectively modify the pharmacokinetic profile of their loaded drugs (Sawant *et al.* 2012). Gregory Gregoriadis was the first to propose the ability of liposomes to entrap drugs (Gregoriadis 1973; Gregoriadis *et al.* 1974b), since then their use in drug delivery has been extensively explored. However, the use of conventional liposomes was limited by their very short half-life due to rapid clearance by mononuclear phagocytic system (MPS) cells, mainly in the liver and spleen (Gregoriadis *et al.* 1974a). The lipid composition, liposome size and opsonisation by serum proteins were considered the most critical factors in the clearance of liposomes (Juliano *et al.* 1975; Gregoriadis *et al.* 1980; Moghimi *et al.* 1989). A promising increase in the circulation half-life of liposomes was achieved by modification with gangliosides ( $G_{M1}$ ) and sphingomyelin that act synergistically to increase the hydrophilic property of liposomes surface and impart bilayer rigidity, respectively (Allen *et al.* 1987; Allen *et al.* 1989). A major breakthrough was accomplished by surface coating with hydrophilic polymer, in particular polyethylene glycol (PEG). PEG imparts steric stabilisation to the liposomes which reduces their interaction with serum proteins, therefore, resulting in a substantial increase in the circulation time (Allen *et al.* 1991a; Allen *et al.* 1991b; Papahadjopoulos *et al.* 1991). Because of the ability of these liposomes to avoid uptake by the MPS cells they were termed “stealth” liposomes. The improved *in vivo* performance of stealth liposomes meant an increase in their passive accumulation at the tumour site as they leaked through malformed blood vessels while avoiding healthy tissues and organs (Gabizon *et al.* 1994; Gabizon *et al.* 1997). Peak drug tumour concentrations in malignant effusions treated with pegylated liposomal DOX 3 to 7 days after injection were 4 to 16 times higher than equivalent dose of free DOX (Gabizon *et al.* 1994).

Another early challenge in the development of liposomes was to achieve stable entrapment of the therapeutic drug concentration inside the liposomes (Senior *et al.* 1982; Barenholz 2003). Drug leakage from liposomes was shown to be affected by several factors; such as the interaction with serum proteins (Allen *et al.* 1980), and the change in lipid composition (Hossann *et al.* 2012) as will be discussed in details later. The stability of drug loading inside the liposomes can be particularly increased by the incorporation of cholesterol (CHOL) into the lipid bilayer and the substitution of fluid phase bilayer with a solid phase lipid membrane (Storm *et al.* 1987). Inclusion of cholesterol can make the lipid membrane stronger by increasing the mechanical stiffness and decreasing the liposomal water permeability (Evans *et al.* 1987; Needham *et al.* 1988). By micromechanical experiments, Needham *et al.* has shown that inclusion of cholesterol into SOPC, stearyl-oleoyl phosphatidylcholine, liposomes at 1:1 molar ratio increased the elastic modulus of the lipid bilayer compared to pure SOPC liposomes (Needham *et al.* 1990). Therefore the inclusion of cholesterol in lipid membrane is expected to increase drug retention and prolong blood circulation (Lasic *et al.* 1995). In addition the higher the elastic modulus is an indication of better resistance to opsonisation (Lasic *et al.* 1995). An example of this strategy is Sphingomyelin:cholesterol (1:1) liposome formulation encapsulating vincristine (Webb *et al.* 1995). Intravenous administration of these liposomes retained 25% of their encapsulated drug in the blood stream up to 72 h. This associated with increased vincristine accumulation to tumours and increased anti-tumour efficacy. This explained by the slow drug release during circulation which represent the basis of vincristine formulation (Webb *et al.* 1995).

Another way to control the loading and retention of drugs inside liposomes is by choosing a drug with the right physicochemical properties. Comparable to biological membranes, liposomal membranes have limited permeability to hydrophilic molecules and high permeability to hydrophobic molecules (Gregoriadis 2006). This hurdle was overcome by the introduction of remote drug loading mechanism by generating a pH gradient across the lipid membrane utilizing either acidic buffers (Mayer *et al.* 1986; Fenske *et al.* 2006) or a proton donating cleavable salts such as ammonium sulphate (Haran *et al.* 1993; Barenholz 2006; Fritze *et al.* 2006). Remote loading process entails drug loading after liposomal formation and is widely used for encapsulation of weakly basic drugs. An excellent example of a drug that can be

encapsulated remotely is doxorubicin which can be efficiently encapsulated inside the liposomes with exceptional retention properties (X et al. 1998). Thus, so far, anthracyclines seem to be the most appropriate chemotherapeutics for liposomal delivery as the rate of drug retention and leakage can be regulated (Barenholz 2012). This has played a great role in the successful development of the clinically approved liposomal drug Doxil<sup>®</sup> encapsulated using transmembrane ammonium sulphate gradient (Barenholz 2006). Remote DOX loading can also be achieved through pH-gradient approach utilizing internal acidic buffer (e.g. citrate)(Mayer *et al.* 1986). When DOX (pKa 8.6) is incubated at neutral pH with liposomes having interior acidic pH, DOX molecules existed in neutral form that readily diffused down their concentration gradient into the liposomes aqueous phase. Once inside the liposomes DOX molecules subsequently protonate and were retained inside liposomes as the lipid membrane is impermeable to charged molecules (Fenske *et al.* 2006). Using internal citrate buffer 300 mM (pH 4), the diffusion process of uncharged DOX will continue until all the drug molecules have been encapsulated (Fenske *et al.* 2006). This technique was employed for ThermoDOX, a temperature-sensitive liposome formulation, that is currently in clinical trials (Needham *et al.* 2013).

Doxorubicin (DOX) exerts its action by acting on the nucleic acids of replicating cells through two ways. First, DOX can intercalate between nucleic acid base pairs leading to inhibition of DNA and RNA synthesis. The second mechanism is by the inhibition of topoisomerase II enzyme that leads to inhibition of super-coiled DNA relaxation, thus prevents DNA transcription and replication (Blum *et al.* 1974; Barenholz 2012). DOX is used as a first line treatment for a variety of cancer such as leukaemia, lymphoma, breast, uterine, ovarian and lung cancers. However, similar to other chemotherapeutics DOX therapeutic potential is limited by collateral damage to healthy tissues (Weiss 1992). The most dangerous and dose-limiting DOX-associated toxicity is a cumulative (dose dependent) cardiotoxicity that leads to irreversible congestive heart failure (Rahman *et al.* 1982). The incidence of this condition is ~ 2% in patients who have received 450-500 mg/m<sup>2</sup> cumulative DOX dose. Therefore, a 21- day regimen of 400-500 mg/m<sup>2</sup> or weekly regimen of 700 mg/m<sup>2</sup> are not recommended (Waterhouse *et al.* 2001).

Encapsulation of DOX inside Pegylated liposomes has been clinically approved for a variety of neoplastic conditions based on its unique safety profile showing lower risk of cardiac toxicity compared to conventional doxorubicin at cumulative doses of 500 mg/m<sup>2</sup> and more (Safra *et al.* 2000; Ewer *et al.* 2004; Solomon *et al.* 2008).

As a result pegylated liposomal DOX (Doxil<sup>®</sup>) was clinically approved in 1995 as the first nano-drug delivery system (Barenholz 2012). To date, several liposomal formulations are now commercially available for a number of clinical applications and many others have progressed into clinical trials (Allen 2013). The significant decrease in cardiac toxicity of DOX after encapsulation into liposomes, did not necessarily translate into improved therapeutic efficacy. Although the tumour accumulation of liposomal DOX can significantly increase compared to free DOX, not all of the drug was bioavailable for tumour cells (Laginha *et al.* 2005). Laginha *et al.* studied the bioavailable DOX levels from Doxil<sup>®</sup> into 4T1 (mammary carcinoma) orthotopically implanted in mice (Laginha *et al.* 2005) using previously described DNase 1 digestion assay (Kirchmeier *et al.* 2001). Administration of Doxil<sup>®</sup> showed higher total tumour DOX accumulation 7 days after injection compared to free DOX (87-fold higher), however this was associated with only 49 % bioavailability (Laginha *et al.* 2005). Similar findings have been observed from the long circulating half-life of liposomal cisplatin that was coupled with poor response in clinical evaluation (Seetharamu *et al.* 2010). After accumulation inside the tumour tissue, drug release from both conventional and stealth liposomes is a slow process that depends on passive leakage of the encapsulated drug overtime or the non-specific degradation of the liposomal lipid membrane (Gabizon *et al.* 2006). As a consequence, the effective drug concentration to the intracellular targets was reduced. In addition, the actual fate of liposomes after extravasation is not clear due to the variation in tumour vascular permeability between different types of tumour and even within the same tumour which affects the therapeutic outcome (Lammers 2012). Moreover, prolonged circulation time of stealth liposomes resulted in the appearance of new toxicity profiles such as swelling and inflammation of hands and feet as a result of the changing biodistribution and pharmacokinetics of the drug (Solomon *et al.* 2008).



Those limitations can be overcome by triggering drug release from the liposomes to make it bioavailable to the tumour cells (Needham *et al.* 2000; Koning *et al.* 2010). Therefore the ideal liposomal formulation of chemotherapy should retain to some extent the drug while circulating in the bloodstream, effectively avoid the MPS cells and finally be able to release the drug locally within the tumour tissues or vasculature via a release profile similar to the pharmacodynamics of the drug. A wide range of research has been conducted over the last two decades to investigate the possibilities of triggering drug release from liposomes. Two main types of triggers have been examined; external, such as heat, light and ultrasound, and internal triggers, those are integrated in the disease site such as pH and enzymes (Figure 1-1). Examples of liposomes with external and internal triggering mechanism include the photosensitive, temperature-sensitive, ultrasound-triggered, enzyme and pH triggered liposomes (Ponce *et al.* 2006b; Kaasgaard *et al.* 2010; Bibi *et al.* 2012).

Although the concept of triggered liposomes seems promising, the practical use of these liposomes has been discouraging with only limited products reaching clinical trials (Landon *et al.* 2011; Allen 2013). This thesis will concentrate on triggered drug release from thermosensitive liposomes by the application of localized mild hyperthermia (HT).

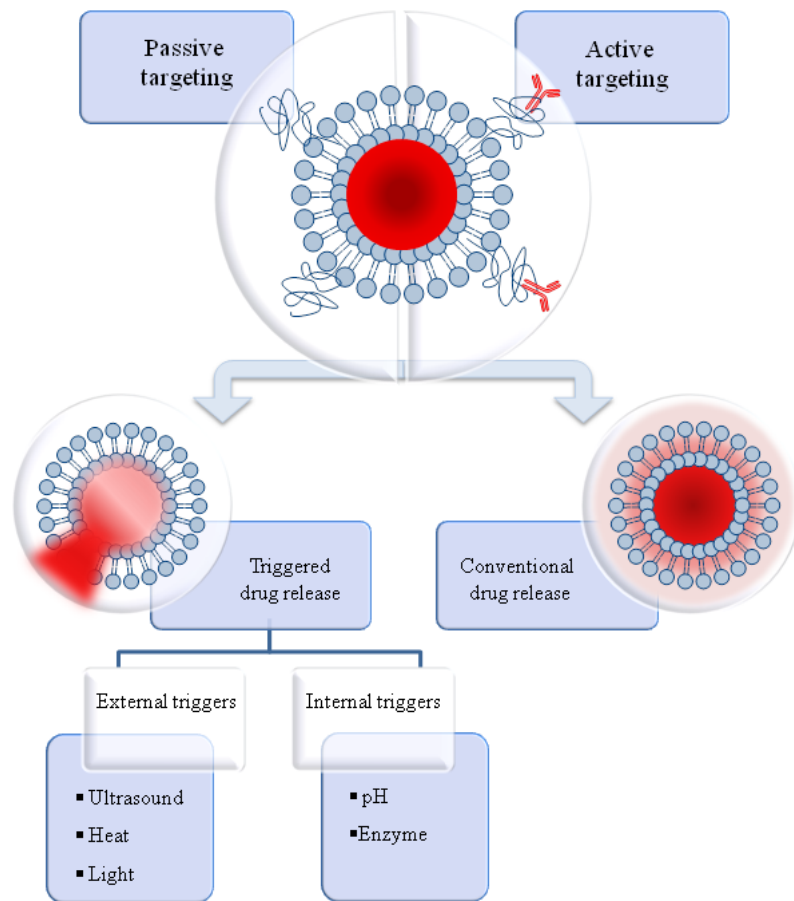


**Figure 1-1: Schematic presentation of the different types of liposome with triggered release properties.**

## 1.2 Hyperthermia in Cancer Therapy

HT has been identified for many years as effective treatment modality for cancer therapy (Schlemmer *et al.* 2004). The potential effectiveness in this area has increased over the last 30 years with the advances in the development of non-invasive image guided thermal techniques. The rationale behind the use of HT to treat cancer is due to either direct cell death that can be induced by HT or the indirect effects obtained when combined with other treatment options. Figure 1-2 describes the various aspect of the use of HT in cancer.

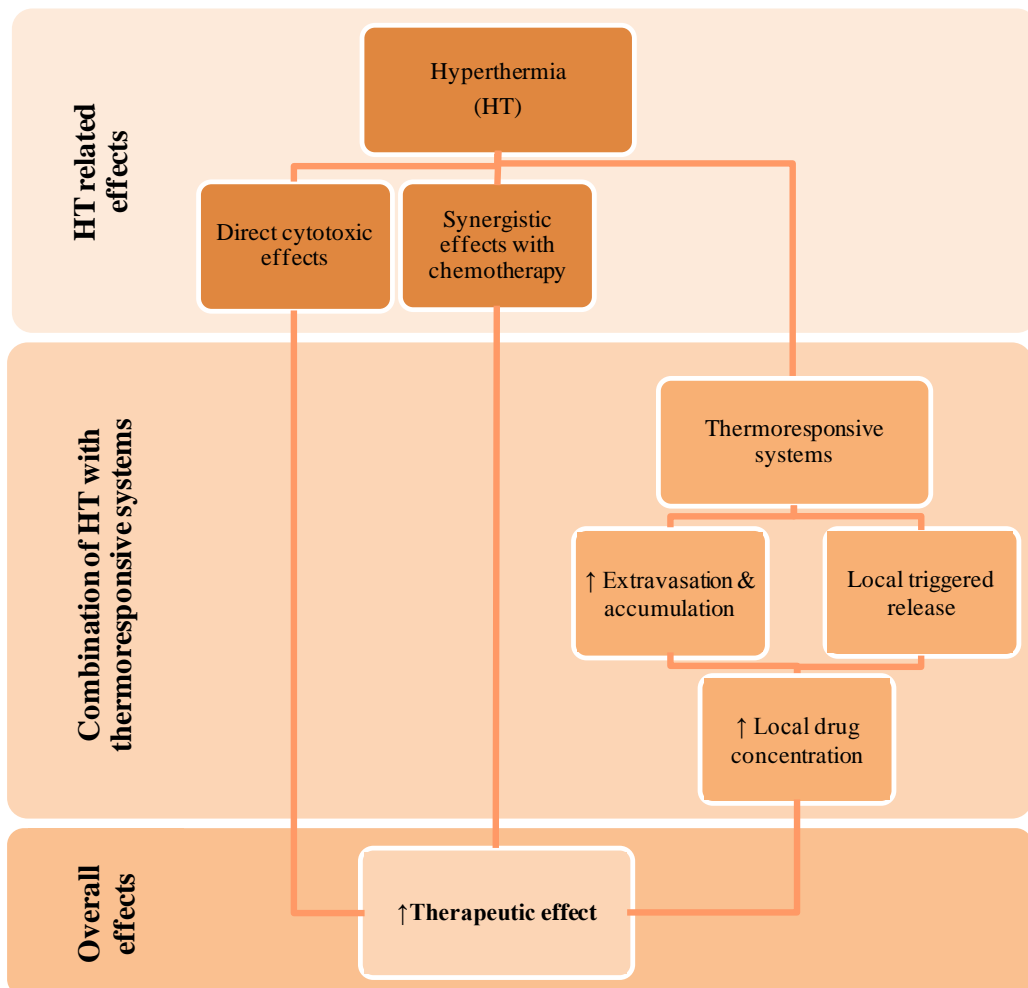


Figure 1-2: The use of HT in cancer therapy. Adapted from (Kong *et al.* 1999)

### 1.2.1 Hyperthermia as a Treatment Modality for Cancer (Ablative Therapy)

HT has been identified for many years as a selective modality for cancer therapy (Bettaieb *et al.* 2013). Thermal ablation is based on direct heating of the tumour to temperatures  $> 50$  °C for short durations (4-6 min) using radiofrequency, laser or

microwave applied by a needle-like applicator (Ahmed *et al.* 2011). The electrical applicator is usually positioned in the centre of the tumour creating a central zone of high temperature surrounded by peripheral areas of sub-lethal heating (Goldberg *et al.* 2000b). Ablative therapy is clinically used for treatment of wide range of unresectable tumours such as focal liver (Livraghi *et al.* 2003), renal (Gervais *et al.* 2003), breast (Zagar *et al.* 2010), bone (Thacker *et al.* 2011), and lung tumours (Dupuy *et al.* 2006). Thermal therapy is mainly important in tumour areas where other treatment modalities such as chemotherapy and radiotherapy have limited effectiveness. This includes tumours that are hypoxic, acidotic and have limited blood supply as the thermosensitivity of tumour cells increases under these conditions (Otte 1988).

The molecular basis behind cellular death induced by ablative therapy is the coagulation of cell membrane and cytosolic proteins and impairment of nucleic acid function and repair (Goldberg *et al.* 2000a; Hildebrandt *et al.* 2002). The result of this coagulative necrosis process is the induction of cell death over several days (Hildebrandt *et al.* 2002). Figure 1-3 summarises the molecular mechanism behind HT induced cellular injury.

Although great emphasis was given to the use of HT in ablative therapy, therapeutic effectiveness of this treatment modality is usually restricted by the failure to get complete tumour ablation especially at the tumour periphery and close to blood vessels (Ahmed *et al.* 2012). Clinical studies in patients with hepatocellular carcinoma (HCC) indicated that RFA is effective in local tumour control in 80-90% of patients having tumour size < 2 cm (Livraghi *et al.* 2008). However, RFA was less satisfactory for treatment of HCC for larger tumour sizes (3.5-5 cm) with 65-75% recurrence (Livraghi *et al.* 2000). Heterogeneous heating results in some cancer cells surviving the thermal ablation treatment; therefore combination with other strategies that can increase tumour damage is needed (Ahmed *et al.* 2012). The synergy of the combination therapy is based on the understanding of the consequences of the biological effects of HT that happens in temperature ranges below those required for cellular damage but yet higher than normal temperature (39-42 °C) (Dewhirst *et al.* 2005). In other words the sub-lethal temperatures observed at the tumour margins in which the centres of those tumours were exposed to ablative thermal treatment. Mild

HT, though well tolerated by cells, can cause reversible cellular injury which improves cellular responsiveness to other therapies such as radiation and chemotherapy (either free or encapsulated inside delivery vehicle) through the increase in blood and oxygen perfusion to the heated areas and the prevention of DNA damage repair (Dewhirst *et al.* 2005; Issels *et al.* 2010). Mild HT can also increase the accumulation and extravasation of nanoscale delivery systems through a number of cellular and physiological mechanisms such as perforation of tumour vasculature and increasing endothelial cells permeability (Ponce *et al.* 2006a).

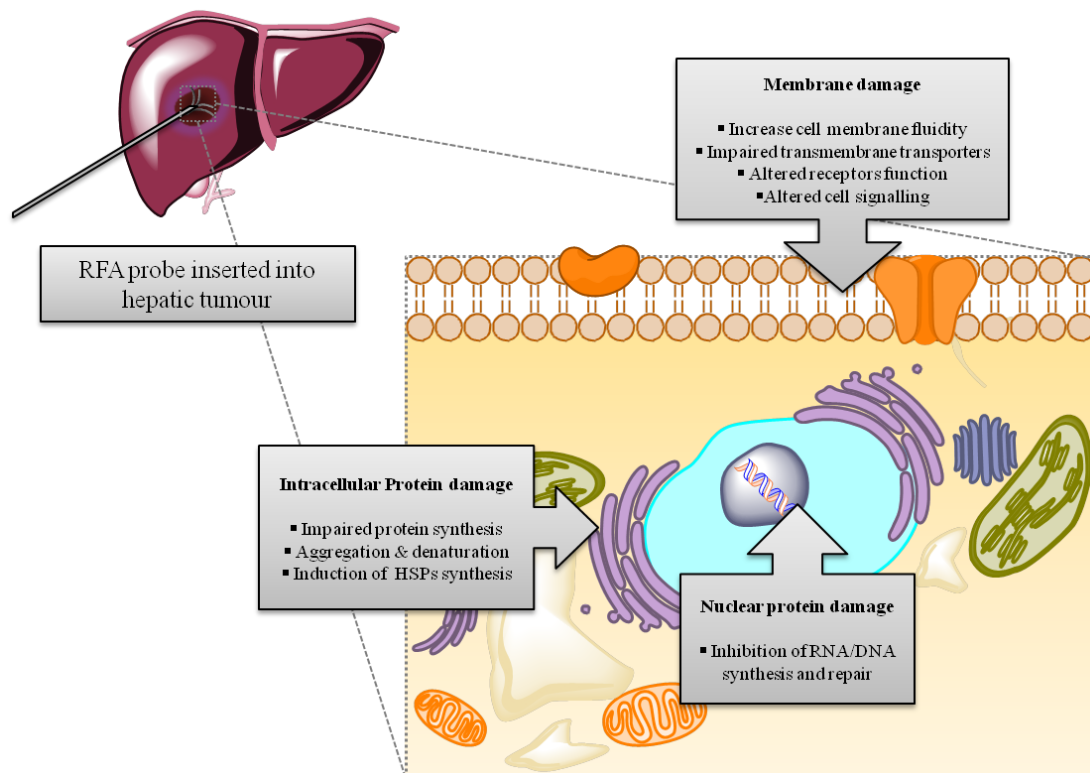


**Figure 1-3: Molecular basis of HT induced cell death.**

Another important parameter in the therapeutic outcome of ablative therapy is the induction of heat shock proteins (HSPs) production which occurs immediately in the peripheral margins of the tumour surrounding the ablative centre (Jaattela 1999). HSPs are known to have a protective effect against cellular damage conditions (Morimoto 1993; Jaattela 1999). They bind to hydrophobic proteins produced from the denaturing effect of HT and prevent their interaction with other functional intracellular proteins, consequently reducing the susceptibility of tumour cells to the cytotoxic effects of HT (Hildebrandt *et al.* 2002). It follows that HSPs can be an

important target in the design of cancer therapy. Recent studies have shown that sensitization of tumour cells to HT can be restored by reducing HSPs level using liposomes encapsulating quercetin, a drug that has an anti-HSPs effect (Yang *et al.* 2012b). Despite the possible role of HSPs in development of thermo-tolerance, the expression of HSPs plays a beneficial role in cancer treatment. An example on that is the stimulation of tumour specific immune responses by induction of cytotoxic T-cell response against tumour cells (Van Der Zee 2002; Kobayashi 2011).

To enhance the therapeutic efficiency of thermal therapy, alternative ways of heat generation have been developed utilizing nanoparticles with specific electrical, optical and thermal properties. These nanoparticles can act as nano-heaters after exposure to external energy. An example of such approach is the use of iron oxide nanoparticles for the generation of magnetic HT (Hilger *et al.* 2012) which has been clinically tested for glioblastoma multiforme (Maier-Hauff *et al.* 2007; Maier-Hauff *et al.* 2011) and prostate cancer (Johannsen *et al.* 2010; Kobayashi *et al.* 2013). As an alternative to iron oxide nanoparticles, other types of nanoparticles haven been used including gold nanoparticles (Huang *et al.* 2007) and nanorods (Tong *et al.* 2007; Huang *et al.* 2010; Park *et al.* 2010; Alkilany *et al.* 2012).

### **1.2.2 The Potential of Hyperthermia in Drug Delivery**

For a long time, great emphasis was given to the use of HT for tumour ablation as treatment modality for cancer therapy. However, over the last 30 years, the rationale of using HT in cancer has been redirected towards lower temperature range (mild HT) due to the compelling advantages that can be attained in that region (Dewhirst *et al.* 2005). It has been well demonstrated that tumour vasculature can be critically hyperpermeable to nanoparticles including liposomes via enlarged endothelial pores through EPR (Dvorak *et al.* 1988). However, this effect has been found to be variable and was dependent on tumour models (Yuan *et al.* 1994a; Yuan *et al.* 1994b).

Besides the well known synergy offered by HT when combined with anticancer drugs (Kowal 1979; Issels 1999), mild HT has a significant influence on tumour pathophysiological parameters that favour an improved nanoparticles extravasation. This increase in permeability is mainly due to structural changes in endothelia cells cytoskeleton that increase the pore cutoff size of the tumour. (Kong *et al.* 2000b;

Kong *et al.* 2001). Mild HT increases local blood flow (2 folds) (Song *et al.* 1984) and decreases tumour interstitial fluid pressure (IFP lowered by 10 folds after 30 min heating at 43 °C) (Leunig 1992), therefore, collectively enhances overall tumour accumulation. Kong *et al.* showed that the extravasation of liposomes of sizes up to 400 nm into a human SKOV-3 ovarian carcinoma xenograft can be achieved by HT (42 °C) compared to normothermic conditions. However, the extravasation magnitudes were less for large nanoparticles. The largest increase in liposomes extravasation with HT was observed in 100 nm liposomes. This was 1.6 and 3.5 times higher than that observed in liposomes sized 200 and 400 nm, respectively (Kong *et al.* 2000b). This indicated the role of HT in increasing the vascular permeability of even impermeable tumour models (Kong *et al.* 2000b). A recent study by Li *et al.* (Li *et al.* 2013a), using high resolution intravital microscopy and the dorsal skin flap window chamber, evaluated the effect of clinically applied HT on the extravasation of TSL in living mice comparing different tumour models. In agreement with kong *et al.* study, liposomes extravasation observed after 30 min heating at 41 °C, while no extravasation occurred without HT. An increase in the gaps between endothelial cells of the tumour vasculature to 10 µm and increase in liposome penetration depth from permeable vessels was observed after 1 h heating to 41 °C. Interestingly this hyperpermeable state of tumour blood vessels was maintained for 8 h after HT; however, the penetration depth was tumour model dependent (extravasation was increase to at least 27.5 µm for the tumour vasculature). No changes were observed in the vasculature of normal tissues with the applied thermal dose (Li *et al.* 2013a).

Alongside the improved tumour extravasation, mild localized HT can be used to boost local drug bioavailability when combined with thermosensitive delivery systems (Kong *et al.* 2000a; Manzoor *et al.* 2012). This can be accomplished by triggering either intravascular release while circulating inside tumour blood vessels or interstitial release after tumour extravasation (Koning *et al.* 2010). The use of HT for this purpose is restricted to solid tumours where surgical intervention is not applicable and cannot be extended to metastatic tumours (Kong *et al.* 1999).

Drug delivery systems for temperature-triggered content release have been studied in a number of different types such as polymers, peptides, hydrogels and metallic

nanoparticles (Bikram *et al.* 2008; Abulateefeh *et al.* 2011; Zhu *et al.* 2013). Whereas most of these systems are under development at their preclinical stages, temperature-sensitive liposomes (TSL) are progressed to an advance stage of development and an example on that is in phase III clinical trials (ClinicalTrials.gov. 2012b). Therefore, the focus of this thesis will be predominantly on TSL and their use with local hyperthermia for heat-triggered drug release.



### 1.3 Evolution of Temperature-Sensitive Liposomes (TSL)

#### 1.3.1 Rationale Design of TSL for Triggered Drug Delivery

Since the concept of TSL was first introduced by Yatvin in late 1970s a lot of effort has been made to explore the potential in that area. Indeed, over the past thirty years the field of TSL has been widely expanded starting from comprehensive design of TSL all the way to testing and understanding the therapeutic aptitude. In this thesis TSL are classified into five subgroups based on the chemical components included in their design. Figure 1-4 illustrates the different types of TSL formulations described in the literature. The design of TSL, mechanism of thermal responsiveness, drug release kinetics, heating protocols and clinical values of TSL are all discussed.

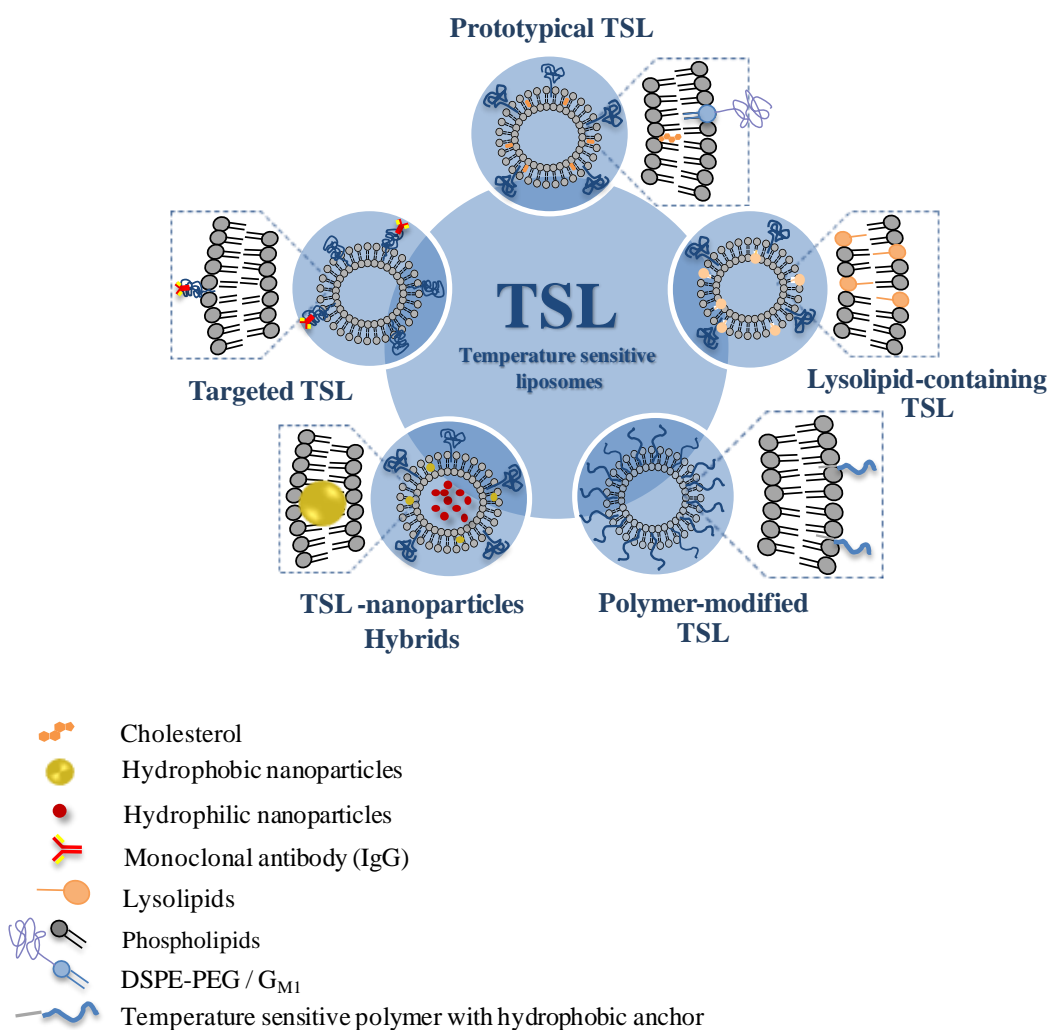


**Figure 1-4: Schematic presentation of different types of TSL and different chemical components included in their design.**

### 1.3.1.1 Prototypical TSL- Exploiting Phase Transition Temperatures of Lipids

The pioneer TSL described by Yatvin *et al.* in 1978 was composed of DPPC:DSPC lipids mixed at certain molar ratios. This formulation showed increase in the release of encapsulated neomycin *in vitro* after heating to their phase transition temperature ( $T_m$ ) which was associated with inhibition of bacterial growth (Yatvin *et al.* 1978). This formulation represents the prototypical type of TSL in this class produced by mixing DPPC lipid which has  $T_m$  of 42 °C with DSPC lipid that has  $T_m$  of 55 °C at 7:3 molar ratios. This ratio allowed a  $T_m$  range between 41-43 °C. The temperature sensitivity of prototypical TSL is based on the tendency of the lipid components to undergo phase transition as a response to heat. When TSL heated through their  $T_m$ , areas of the phospholipid molecules start to change from the solid (ordered) gel phase to the liquid (disordered) crystalline phase creating boundaries between the two phases through which the drug permeability is enhanced (Figure 1-5) (Yatvin *et al.* 1978). In the gel phase, lipid molecules are highly ordered and condensed. The hydrocarbon chains are fully extended and the head groups are immobile at the interface with water. When the temperature is elevated, the head group mobility begins to increase and with further increase in temperature towards the  $T_m$  of lipids, transition of hydrocarbon chains from gel phase to liquid crystalline phase occurs. At  $T_m$  the orientation of the C-C single bonds in the hydrophobic chains is changed from trans to gauche state (Torchilin 2003). The existence of both solid and liquid lipid domains at the  $T_m$  leads to the formation of leaky regions at the interface between these domains. As a result lipid membrane permeability increases at the interfaces, which has been signified previously by dramatic increase in  $\text{Na}^+$  ions diffusion. Although the ions permeability is highest at the  $T_m$ , it reduces as the temperature goes beyond due to the reduction in the existence of those boundary regions. When the lipid membrane fully melts with further temperature increase, the membrane permeability is increased again as the lipid bilayer is predominantly in the fluid phase (Papahadjopoulos *et al.* 1973). Grain boundaries result from defects in the crystalline arrangement of lipid molecules in that region. The crystalline structure is produced during liposome preparation process that involves cooling down of lipid bilayer from its liquid phase into solid phase. When the lipid bilayer is cooled toward  $T_m$  of the lipids, solidification of the lipid membrane appeared as nucleation of solid domain within the melted lipid membrane. These individual solid domains continue

to grow by orienting lipid molecules into crystal-lattice-like structures. The growth of these domains then stops when they approach each other in the final gel phase membrane and this leads to the formation of grain boundaries (Landon *et al.* 2011).

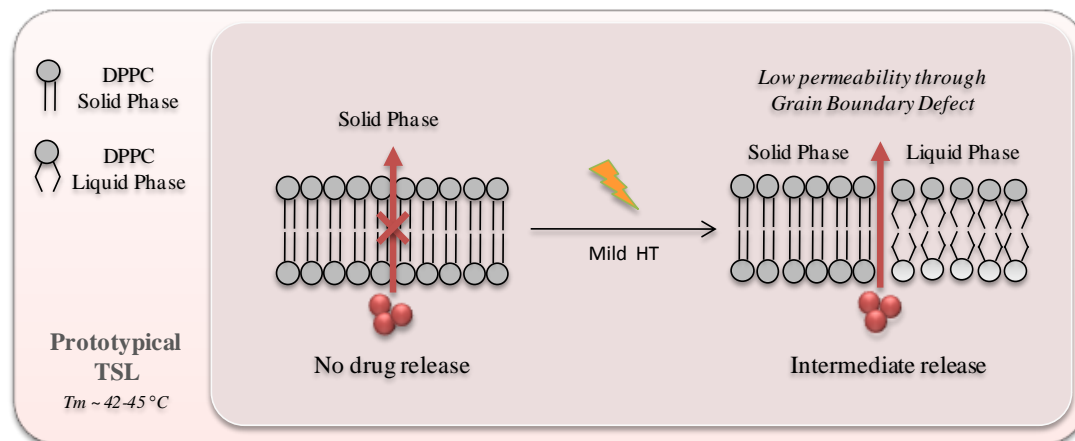


**Figure 1-5: Schematic presentation of phase transition behaviour of TSL.**

When the lipid membrane passes through transition temperature ( $T_m$ ), the bilayer permeability increases. Below that temperature, lipid membranes exist in solid phase only and therefore no drug release is expected. At the  $T_m$ , the existence of both the solid and the liquid phases leads to the formation of grain boundary defects in the bilayer through which drug release occurs. Adapted from (Landon *et al.* 2011).

Similar to Yatvin formulation most of the early examples of prototypical TSL were composed mainly of DPPC or DPPG lipids mixed with other types of lipids like DSPC and HSPC lipids in order to tune the  $T_m$  and the rate of drug release (Yatvin *et al.* 1981; Bassett *et al.* 1986; Iga *et al.* 1991; Maruyama *et al.* 1993; Gaber *et al.* 1995) (Figure 1-6). The use of lipid mixture can also contribute to improved lipid membrane permeability by increasing the defect in lipid packing. Prototypical TSL were further developed by inclusion of cholesterol to optimize their serum stability. However, this can also have a negative effect on the rate and extent of drug release in response to temperature which can be linked to the increase and broadening of  $T_m$  after inclusion of cholesterol (Gaber *et al.* 1995). The blood circulation time of prototypical TSL was also increased by adopting the same approaches used with other stealth liposomes. The inclusion of  $G_{M1}$  or DSPE-PEG<sub>2000</sub> lipids into TSL led to reduced interaction with MPS cells and enhance their blood profile which reflected in better control over tumour growth rate (Maruyama *et al.* 1993; Unezaki *et al.* 1994). Recently Li *et al.* showed that incorporating 5 mol% of PEG is the optimal concentration to provide a balance between the stability of TSL at 37 °C

without jeopardizing the temperature sensitivity at mild HT (Li *et al.* 2010). In addition to the typical benefits provided by DSPE-PEG<sub>2000</sub> as mentioned above, the inclusion of this micelle lipid adds to the thermal sensitivity of prototypical TSL. DSPE-PEG<sub>2000</sub> inclusion at 4-5 mol% drives the switch from mushroom or brush configuration. The heterogeneous structure of DSPE-PEG<sub>2000</sub> causes destabilization of lipid membrane around T<sub>m</sub> and increases contents release without significantly affecting the T<sub>m</sub> (Li *et al.* 2010). An interesting example of that is DPPC:HSPC:CHOL:DSPE-PEG<sub>2000</sub> TSL that contains 3.2 mol% of DSPE-PEG<sub>2000</sub> lipids. The addition of DSPE-PEG<sub>2000</sub> revealed the thermal sensitivity of the liposomes even with the presence of cholesterol as observed from differential scanning calorimetry (DSC) thermograms. This formulation released 60% of DOX *in vitro* in 50% plasma (Gaber *et al.* 1995). Alternatively, Lindner *et al.* showed that the inclusion of DPPGOG lipid (Figure 1-6) into DPPC:DSPC liposomes can prolong their circulation time *in vivo* together with significant enhancement in their content release upon heating (Lindner *et al.* 2004; Hossann *et al.* 2007). In addition, Dicheva *et al.* Described, recently, that targeting TSL to the tumour tissue can be improved by the preparation of a cationic TSL (CTSL) by including 10 mol% of DPTAP cationic lipid (Figure 1-6) into DPPC:DSPC:DSPE-PEG<sub>2000</sub> liposomes. The outcome of that was a slightly positive zeta potential compared to the slightly negative charge of most of other TSL and consequently, better targeting ability to endothelial and tumour cells with contents release upon temperature triggering. (Dicheva *et al.* 2012).

For a long time, prototypical TSL have been mistaken for having slow and incomplete release profiles under mild HT. Likewise, the relatively high T<sub>m</sub> of this class of TSL (42-45°C) suggested that high thermal dose is required to achieve effective drug release (1 h heating at temperature > 42 °C) (Ta *et al.* 2013). However, most of the release profile data were generated in a buffer and this does not reflect the real biological conditions (Unezaki *et al.* 1994; Gaber *et al.* 1995; Hosokawa *et al.* 2003). It is also important to note the difference in the mode of release of DOX compared to other fluorescent dyes such carboxyfluorescein (CF) due to the variation in the encapsulation mechanism adapted. Higher percentage of release usually reported for DOX compared to CF under the same conditions is due to the collapse of the pH gradient mechanism used for DOX loading as a result of the increase in

proton diffusion across the lipid membrane at Tm. Approximately 95% DOX release was reported from DPPC:DSPC:DSPE-PEG<sub>2000</sub> 90:10:5 liposomes after 1 min of heating at 42 °C compared to < 50% of CF under similar conditions (Li *et al.* 2010; Li *et al.* 2013b).

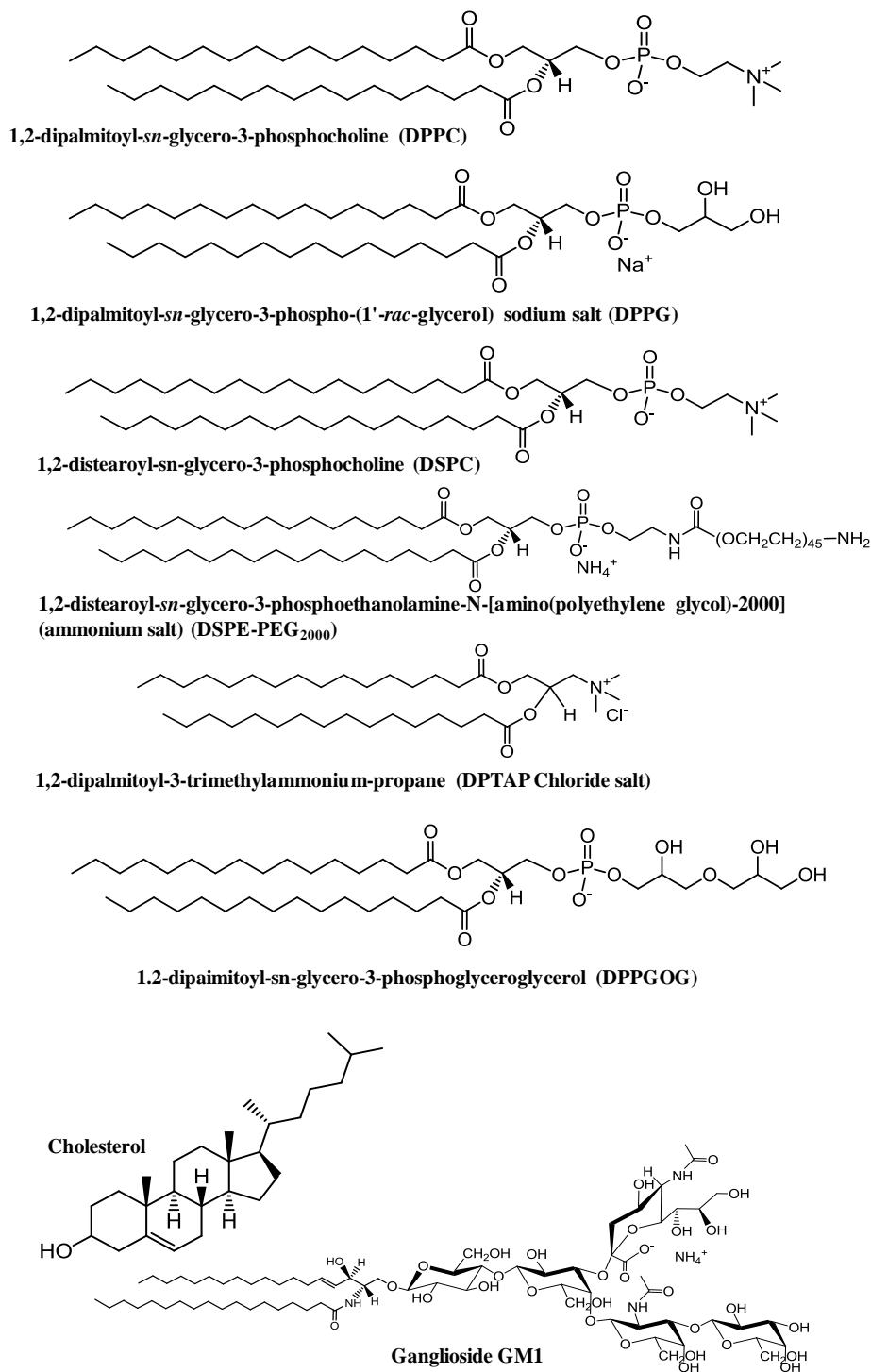


Figure 1-6: Chemical structures of the lipids used in the design of prototypical TSL.

Interestingly, the presence of serum protein can have a favourable effect on temperature sensitivity of this type of TSL and results in an increase in the rate of drug release by gaining access into the grain boundary of lipid membrane at  $T_m$  (Gaber *et al.* 1995; Kong *et al.* 1999; Hosokawa *et al.* 2003; Hossann *et al.* 2007; Hossann *et al.* 2010; Hossann *et al.* 2012). Moreover, the presence of cholesterol in the serum can also contribute to better permeability. The ability of cholesterol to exchange between vesicles leads to disturbance in the lipid packing and causes an improved permeability (Hossann *et al.* 2012). The effect of serum on release profile can vary with the origin of the serum used, its concentration and the duration of exposure. This can explain the discrepancy in the release data reported from prototypical TSL (Gaber *et al.* 1995; de Smet *et al.* 2010). The effect of serum component on the thermal sensitivity of prototypical TSL, can justify the increase in therapeutic activity observed in a number of preclinical studies over wide range of tumour models using mild heating conditions (42 °C) (Kong *et al.* 1999). This was also confirmed recently in real time imaging study by Li *et al.* that showed efficient intravascular DOX release after heating at 42 °C followed by rapid uptake of DOX by endothelial cells and tumour cells. This resulted in high and homogeneous DOX penetration into tumour cells and improves tumour growth control (Li *et al.* 2013b).

### 1.3.1.2 Lysolipids-Containing Temperature-Sensitive Liposomes (LTSL)

The concept of lysolipid-containing thermosensitive liposomes was first described by Anyarambhatla and Needham in 1999 (Anyarambhatla *et al.* 1999) and led to a new concept in the field of drug delivery by triggering drug release in the blood vessels or what is called intravascular drug release (Landon *et al.* 2011; Manzoor *et al.* 2012; Needham *et al.* 2012; Needham *et al.* 2013). They first proposed that the incorporation of ~ 10 mol% of MPPC lysolipids into DPPC:DSPE-PEG (90:4) liposomes lowers the  $T_m$  of DPPC:DSPE-PEG liposomes from 41.9 °C to 41 °C and leads to rapid drug release in a concentration dependent manner (Anyarambhatla *et al.* 1999). Compared to the more traditional thermal sensitive liposomes by Yatvin *et al.* (Yatvin *et al.* 1978) described earlier, lowering the  $T_m$  to 41 °C is a critical parameter for temperature triggered drug release. For clinical applications, mild HT < 43 °C is recommended because higher temperature can result in haemorrhages (Thrall *et al.* 1992) and can also cause necrotic damage to the neighbouring healthy tissues (Ben-Yosef *et al.* 1992; Landon *et al.* 2011).

The design of LTSL requires the presence of three essential components; a solid-phase liposome with grain boundary deformation (DPPC lipids), that acts as a host lipid and forms the bilayer of the liposome, in addition to mono alkyl lysolipids and pegylated lipids at several mol% that act as permeabilising ingredients and steric stabilising components (Needham *et al.* 2013). The combination of these lipid components allows drug release in only few seconds when heated to their phase transition temperature (Mills *et al.* 2005). MSPC lysolipid was then used instead of MPPC to increase the liposome stability during processing and drug retention capability. The longer acyl chain (C18) of MSPC lysolipid increased the  $T_m$  to 41.3 °C and reserved the ultrafast release property (Mills *et al.* 2005).

In order to understand the release mechanism of LTSL liposomes, Mills and Needham studied the permeability of the liposome membrane using a dithionite ( $S_2O_4^{2-}$ ) permeability assay (McIntyre *et al.* 1991). The membrane permeability was studied by preparing NBD (1%) labelled DPPC:DSPE-PEG<sub>2000</sub> (4 %) liposomes with and without MSPC (10%). The addition of dithionite at 30 °C quenched the signal of NBD lipids in the outer membrane only due to the impermeability of the lipid membranes to dithionite ions. Repeating the experiment at the  $T_m$ , quenched the

absorbance of the NBD lipids at the inner membrane since the lipid membranes become permeable to dithionite ions. This decrease in absorbance is faster for DPPC:DSPE-PEG (4%) liposomes having 10 % MSPC and dramatically increased at 42 °C demonstrating the role of lysolipid (MSPC) in increasing the permeability of LTSL liposomes at  $T_m$  (Mills *et al.* 2005). The permeability coefficient of the liposomes membranes with and without MSPC lysolipid was also measured using the following formula;  $C(t) = C_0 (\exp (-m_2 t))$ , where  $m_2$  is the permeability rate constant,  $C(t)$  is the concentration of un-reacted NBD molecules at time  $t$ , and  $C_0$  is the concentration of un-reacted NBD molecules on the inner monolayer at zero time point. The permeability coefficient of DPPC:DSPE-PEG (4%) having 10% MSPC was measured to be  $1.09 \times 10^{-8}$  cm/s, ten folds higher than liposomes without MSPC ( $1.9 \times 10^{-9}$  cm/s). A similar ten folds increase in DOX permeability coefficient at 42 °C was evidence by adding MSPC (10%) compared to liposomes without MSPC measured at  $3.3 \times 10^{-9}$  cm/s and  $3.4 \times 10^{-10}$  cm/s, respectively (Mills *et al.* 2005). Mills and Needham compared the permeabilities of the liposomes to dithionite ion (radius 3 Å) and DOX (radius 500 Å) with and without lysolipid at the  $T_m$ . For pure DPPC membranes dithionite permeability was six times higher compared to DOX indicating easier permeability to smaller ions. Liposomes having 10% MSPC showed three times higher permeability for dithionite ions compared to DOX which was believed to be through a water-filled pore rather than the hydrocarbon chain (Mills *et al.* 2005). Thus, the ultrafast release of LTSL contents appears to be due to the enhancement of the grain boundary and nonporous caused by the inclusion of lysolipid component (Figure 1-7) though which both ions and small molecular weight drugs can permeate (Mills *et al.* 2005). The size of these nanopores appears to be ~ 10 nm as estimated from dextran permeation measurements (Needham *et al.* 2013). Lysolipids have a relatively large head group compared to their single acyl chain, this gives them a positive intrinsic curvature and a tendency for micelles formation in aqueous solution above their CMC (~0.4 µM) (Needham *et al.* 2013). Upon approaching the phase transition, the increase in lateral lipids movements encourages lysolipids accumulation at the melted grain boundaries and the formation of stabilised defects (nanopores) in the lipid membrane. Similar to what was observed before with prototypical TSL, the presence of DSPE-PEG<sub>2000</sub> can add to the thermosensitivity of the system but through a different mechanism.



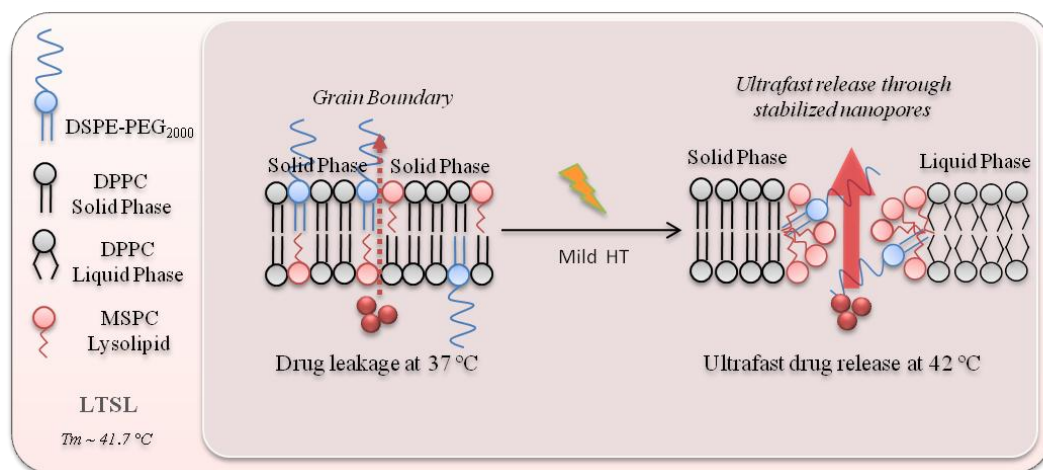


**Figure 1-7: Schematic presentation for drug leakage and nanopores formation in LTSL.**

Below phase transition (37 °C) drug leakage from DPPC:MSPC:DSPE-PEG<sub>2000</sub> (LTSL) bilayer can occur through grain boundary in the bilayer due to the presence of lysolipids. Ultrafast drug release at phase transition region through MSPC nanopores that stabilised by DSPE-PEG<sub>2000</sub>. Adapted from (Needham *et al.* 2013).

Despite having two hydrocarbon chains, DSPE-PEG<sub>2000</sub> still has affinity for micelles formation in aqueous solution. The shape factor of DSPE-PEG<sub>2000</sub> is close to lysolipids as it has much larger head groups in relation to the tail groups because of the PEG<sub>2000</sub> polymer. Therefore, in principle, the presence of DSPE-PEG<sub>2000</sub> lipids can help to some extent in the formation and / or stabilisation of the nanopore structure by bringing a second property, a repulsive forces inside the nanopores (Needham *et al.* 2013). Different concentrations of lysolipids and DSPE-PEG<sub>2000</sub> lipids were matched against the release profiles of DOX and CF. Despite being not optimum regarding DSPE-PEG<sub>2000</sub> coverage (The boundary concentration of DSPE-PEG<sub>2000</sub> between mushroom and brush conformation is 5 mol%), the formulation that progressed into preclinical and clinical studies consisted of DPPC:MSPC:DSPE-PEG<sub>2000</sub> (86.5:9.7:3.8) mol/mol where more than 80% release of encapsulated DOX was achieved after 20 s in mild HT (Landon *et al.* 2011). Mill and Needham demonstrated that the mechanism by which drug release at  $T_m$  is through lysolipids stabilized nanopores rather than enhancement of drug solubility in the lipid membrane (Mills *et al.* 2005). Employing mass spectrometry and dialysis experiments, they also confirmed that the lysolipid was sufficiently retained in the lipid membrane above  $T_m$  after extensive dilution. These studies were ran as control and were performed in buffer to demonstrate the effect of micromolar solubility on the desorption of lysolipids from liposomal membrane. Therefore, these experiments

were performed in the absence of serum proteins and lipids that could act as a sink for lysolipids and, by design, did not simulate the actual physiological conditions (Mills *et al.* 2005). However, in the presence of biological media (serum protein, whole blood) lysolipids could be extracted from liposome membrane to these components. Banno *et al.* showed the dissociation of almost 70% of lysolipids from LTSL liposomes within 1 h after *in vivo* administration and postulated that this might be through exchange with plasma proteins or cellular membranes (Banno *et al.* 2010). Banno and Wood *et al.* showed that the blood circulation half life of DOX retention in LTSL liposomes is ~ 1 h, indicating DOX leakage from LTSL liposomes at 37 °C after *in vivo* administration (Banno *et al.* 2010; Wood *et al.* 2012). However, LTSL limited stability is unlikely due to the loss of the lysolipid because of the reduced permeability of liposomes without lysolipid compared to LTSL liposomes. Needham speculated that DOX loss from LTSL is more likely due to the H<sup>+</sup> ions transport resulted in DOX cation deprotonation and increased its solubility followed by leakage through even solid phase membrane (Needham *et al.* 2013).

The inclusion of DSPE-PEG lipids in LTSL liposomes was expected to stabilise the lipid bilayer from interaction with serum protein, despite that, incubation of LTSL liposomes in serum at 37 °C resulted in ~20-30% leakage of DOX content in 30 min, compared to other TSL formulations (de Smet *et al.* 2010; Hossann *et al.* 2012) having higher serum stability. In addition Chiu *et al.* observed 50% loss of encapsulated DOX within 1 h after *in vivo* administration (Chiu 2005), however in this system DOX encapsulation was performed with transition metal, manganese. On the contrary, Anyarambhatla *et al.* showed that LTSL formulation had good retention to encapsulated CF (in FBS and 50% bovine serum), and DOX (in plasma) at 37 °C (Anyarambhatla *et al.* 1999), which leaves serum and blood DOX leakage data unexplained. In addition, the loss of the lysolipid from LTSL formulation can have a negative effect on the thermal-sensitivity of the formulation. A time dependent decrease in the percentage of DOX release was observed from LTSL liposomes recovered after *in vivo* administration which is consistent with the increase in the percentage of lysolipid loss overtime (Banno *et al.* 2010). DOX leakage from LTSL might be related to the adsorption of serum proteins that could destabilize the lipid bilayer. Although previous data and models of protein adsorption through PEG mushroom coverage (Needham *et al.* 1998), suggested that only monomer

surfactants can penetrate the PEG stabilizing layer. Without enough studies of serum adsorption or association with LTSL, the exact mechanism of serum induced DOX leakage from LTSL cannot be completely resolved. However, this issue become apparent and explained in details by Needham (Needham *et al.* 2013). As a consequence of the relative instability of LTSL towards drug retention upon dilution with biological media, correct timing of LTSL administration with HT represents the most critical parameter for the success of this formulation as will be explained in details in section 1.3.2.

In preclinical studies this formulation showed much effective (20-30 min) local targeted triggered release of DOX compared to free DOX and other TSL and non temperature-sensitive liposomes.

LTSL formulation showed the highest preclinical tumour growth retardation in multiple tumour models (colon HCT116, squamous cell FaDu, prostate PC-3, ovarian SKOV-3 and mammary 4T07). Compared to traditional TSL and NTSL (Yarmolenko *et al.* 2010). In FaDu tumour model LTSL treatment in combination with HT (1 h at 42 °C immediately after injection) showed complete tumour regression up to 60 days compared to only some tumour growth control (31-35 days) from TTSL and Doxil-like NTSL combined with 1 h HT at 42 °C (Kong *et al.* 2000a). Similar results were observed from another study showing 11/11 tumour growth regression 60 days after treatment (Needham *et al.* 2000). The increase in therapeutic efficacy was consistent with the amount of DOX tumour accumulation. Quantification of DOX concentration in the tumour showed that LTSL+ HT resulted in the highest tumour drug level (25.6 ng/mg), 30 fold increase compared to free DOX and 3-5 times higher than other liposomal treatment at the same temperature. In addition the bioavailability of DOX was also improved; LTSL was also the only formulation that showed significant DNA-bound fraction of DOX (quantified by sliver nitrate extraction). Almost half of the DOX delivered to the tumour was bioavailable to tumour cells just 1 h after HT (Kong *et al.* 2000a). In contrast, DOX bioavailable fraction from free DOX, TTSL and NTSL was not detectable. These findings indicated that the increased drug release rate of LTSL is crucial to increase DOX bioavailability, whereas the relatively slow leakage from other liposomal formulations was responsible for their reduce bioavailability (Kong *et al.* 2000a).

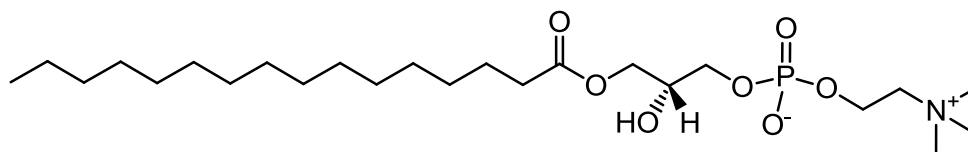
Though DOX quantification data were restricted to only 1 h after injection and longer time points, where increased liposomes extravasation might be anticipated, were not studied. The conclusion from these studies was that both drug release rate and the amount delivered to the tumour were crucial to achieve therapeutic efficacy. LTSL offers a novel concept for the delivery of anticancer drugs by promoting ultrafast drug release inside the tumour blood vessels resulted in LTSL liposomes having both anti-vascular anti-neoplastic effects (Kong *et al.* 2000a; Needham *et al.* 2000). To allow for intravascular drug release, the loaded drug release needs to be faster than the transient time of the liposomes in the vasculature of the heated tumour. This is estimated to be around 50 s for a two-cm tumour (Chen *et al.* 2008). The new paradigm of drug release offered by LTSL overcomes the problems of heterogenous vascularity and limited penetration as it does not depend on liposomal extravasation (Landon *et al.* 2011). Indeed, recent preclinical study by Manzoor *et al.* confirmed that in vivo LTSL injection into preheated tumour not only resulted in DOX release in the blood stream but associated with deeper tumour penetration as observed using intravital fluorescence imaging of DOX delivery into FaDu tumour model (Manzoor *et al.* 2012). Intravascular release of DOX from LTSL significantly increased free drug penetration distance into the interstitial space and the time to which tumour cells exposed to maximum drug concentration compared to free DOX and Doxil-like NTSL (Manzoor *et al.* 2012). LTSL injection into warm tumour delivered 3.5 times higher DOX level than free drug up to 78  $\mu\text{m}$  from both sides from blood vessels (double the penetration distance of Doxil<sup>®</sup>).

LTSL formulation developed by Needham is currently commercially available as ThermoDox<sup>®</sup> (Celsion) and is currently in clinical trials (Celsion.com 2013c). Phase I trial was initiated in canine tumours to determine the maximum tolerated dose (MTD) and pharmacokinetics (PK) parameters (Hauck *et al.* 2006). LTSL MTD was 0.93 mg/kg slightly less than that reported for free drug and Doxil<sup>®</sup>. PK parameters of LTSL were closer to free DOX compared to Doxil<sup>®</sup>. Some variable drug delivery was observed in this study due to variability in tumour heating, especially for bigger sized tumours, and the possibility of increase in core body temperature. Despite that overall DOX tumour level for LTSL was 10 times higher than free DOX that resulted in improved therapeutic outcome. Tumour response observed was encouraging for further evaluation in human (Hauck *et al.* 2006).

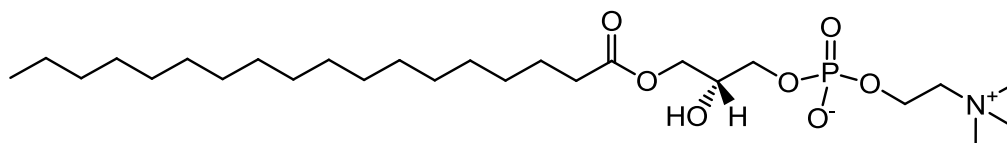
Examples include the combination therapy with radiofrequency ablation (RFA) in patients with hepatocellular carcinoma (HCC) (phase III) (ClinicalTrials.gov. 2012b) and metastatic colorectal cancer (mCRC) (ClinicalTrials.gov. 2013b). ThermoDox® is also being tested in combination with mild HT for chest wall recurrence of breast cancer (RCW) following mastectomy (phase I/II) (ClinicalTrials.gov. 2013a) and palliation of prostate cancer metastases to bone with magnetic resonance (MR) Guided High Intensity Focused Ultrasound (HIFU) (ClinicalTrials.gov. 2012a).

Inspired by LTSL formulation, other TSLs that share similar concept have been recently described in the literature. The HaT formulation, developed by Tagami, is one example. This formulation is based on DPPC lipids with Brij 78 surfactant (Figure 1-8) at 96:4 molar ratios. This formulation shares the same concept with LTSL but in much simplified way. Brij surfactant, comprised of a single acyl chain attached to a PEG moiety, has the properties of both lysolipid and DSPE-PEG, therefore, it can have both the stabilisation and pore-formation properties of LTSL. (Tagami *et al.* 2011b). HaT formulation promoted drug release in a time scale similar to LTSL and had very similar drug retention properties at 37 °C (~20% release in 30 min) *in vitro* which was consistent with blood profile data (only 40% remained in the blood in 1 h). Preclinical studies with this formulation showed slightly higher DOX level in EMT-6 heated tumour at 43 °C compared to LTSL. Single treatment with HaT formulation at 3mg/kg DOX concentration into tumour-bearing mice in combination with HT resulted in enhanced tumour growth retardation compared to LTSL (Tagami *et al.* 2011a). HaT-II is an optimised formulation that was obtained by using Cu<sup>+2</sup> gradient instead of pH gradient for DOX loading. Slight improvement in the pharmacokinetics parameter (2.5 folds reduction in blood clearance compared to HaT and LTSL) and tumour accumulation ( 2 fold relative to LTSL and 1.4 fold vs HaT) were observed from HaT-II compared to HaT and LTSL that resulted in a better therapeutic efficacy (Tagami *et al.* 2012). Liposomes composed of HePC:DPPC:DSPC:DPPGOG designed by Lindner *et al.* are another example of this class of TSL. HePC is structurally similar to MPPC lysolipids but is chemically and metabolically more stable and can act as an anti-cancer drug (Figure 1-8). DPPGOG lipid was used to replace DSPE-PEG<sub>2000</sub> as it was shown previously by the same group to prolong the circulation time of liposomes and enhance temperature sensitivity (Lindner *et al.* 2008). This formulation acts in a very similar way to

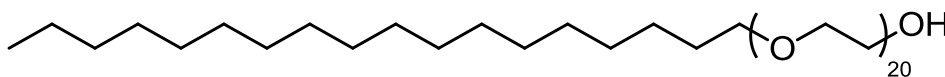
lysolipid-containing formulation resulting in 90 % CF release at 42 °C after 5 min incubation.



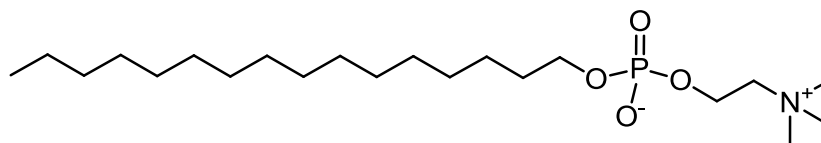
**1-palmitoyl-2-hydroxy-*sn*-glycero-3-phosphocholine (MPPC)**



**1-stearoyl-2-hydroxy-*sn*-glycero-3-phosphocholine (MSPC)**



**Polyoxyethylene stearyl ether (Brij78)**



**Hexadecyl phosphocholine (HePC)**

**Figure 1-8: Chemical structures of the lipids used for the design of lysolipids-containing TSL.**

### 1.3.1.3 TSL Modified with Synthetic Temperature-Responsive Polymers.

Another strategy for designing temperature-responsive liposomal systems is to attach thermosensitive amphiphilic molecules (particularly temperature-responsive polymers) to the liposomal membrane. These polymers have temperature-disruptive effect on the lipid membrane because they change in conformation in response to changes in environmental temperatures. Therefore, temperature-sensitive polymers can either give a thermoresponsive property to non temperature-sensitive liposomes or improve thermal responsiveness of thermosensitive liposomes. At the molecular level, thermosensitive polymer chains undergo a coil to globule transition as the temperature passes through their low critical solution temperature (LCST) (Figure 1-9). Below LCST the polymer is hydrated and sterically stabilises the liposomes surface. As the temperature increases ( $T > LCST$ ), condensation of the polymer results in exposing the liposome surface which leads to destabilisation and content release (Kono 2001). Because the polymers change from hydrophilic to hydrophobic with temperature, stabilisation and destabilisation of polymer-modified TSL can be controlled by temperature, thereby controlling drug release and interaction with cells and serum proteins (Kono 2001). Table 1-1 summarises the different examples of polymer-modified TSL described in the literature. The liposomal formulation, the types of thermosensitive polymers used and their LCST are explained. For chemical structures of temperature-sensitive polymers used, please refer to Figure 1-10.

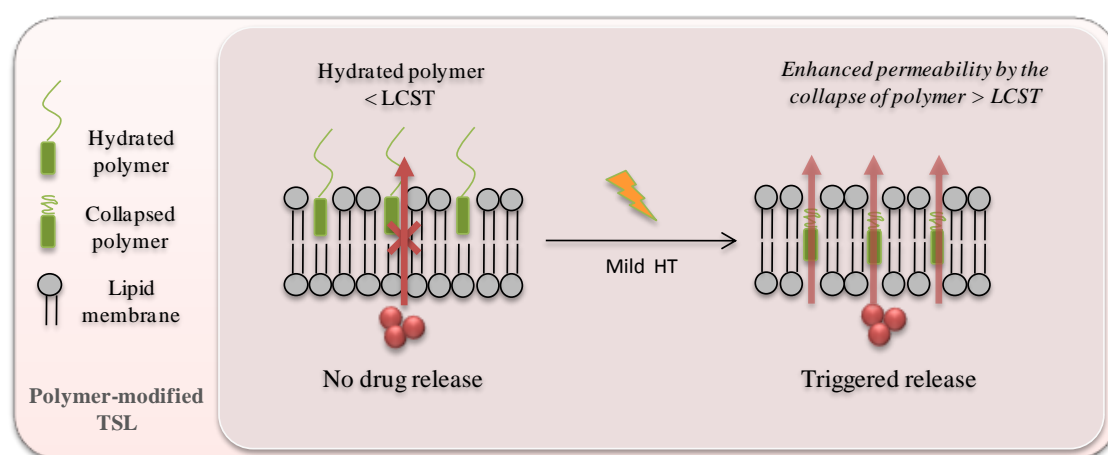


**Figure 1-9: Mechanism of drug release from polymer modified TSL.**

Below LCST polymer chains are hydrated which give a stabilising effect to the liposomes. When the ambient temperature exceeds LCST, the polymer becomes dehydrated and changes into globule status. This destabilises the lipid membrane and releases liposomal content.

**Table 1-1: Examples of polymer modified temperature-sensitive liposomes**

Liposomal Composition	Temperature sensitive polymer	LCST	Dye / Drug	Experimental design	References
EPC & DPPC	p-(NIPAM-ODA)	27 °C	CF Calcein	<i>In vitro</i> release study	(Kono <i>et al.</i> 1994)
DOPE	p-(NIPAM-ODA)	32 °C	Calcein	<i>In vitro</i> release study	(Hayashi <i>et al.</i> 1996)
EPC, DMPC:DPPC DPPC & DSPC	p-(NIPAM-AA-ODA)	30-43 °C	Calcein	<i>In vitro</i> release study	(Kim <i>et al.</i> 1997)
DLPC DPPC DSPC	p-(NIPAM-ODA)	32 °C	Calcein	<i>In vitro</i> release study	(Hayashi <i>et al.</i> 1998)
EPC & EPC:DOPE	p-(NIPAM-NDDAM)	28 °C	Calcein	<i>In vitro</i> release study	(Kono <i>et al.</i> 1999a)
EPC	p-(APr-NIPAM)-2C <sub>12</sub>	40 °C	MTX	<i>In vitro</i> release study and cellular cytotoxicity	(Kono <i>et al.</i> 1999b)
DOPE	p-(APr-NIPAM)-2C <sub>12</sub> p-(APr-NIPAM-NDDAM)	33-34 °C	Calcein	<i>In vitro</i> release study	(Kono <i>et al.</i> 1999c)
DOPE:EPC	p-(NIPAM-NDDAM-AAM) p-(NIPAM-AAM)	39-46 °C	Calcein	<i>In vitro</i> release study (Increasing LCST)	(Hayashi <i>et al.</i> 1999)
DOPE	p-(APr-NIPAM)-2C <sub>12</sub> PEG <sub>550</sub> -2C <sub>12</sub>	38 °C	Calcein	<i>In vitro</i> release study and serum stability (Effect of PEG)	(Kono <i>et al.</i> 2002)
EPC	p-(APr-NIPAM)-2C <sub>12</sub> p-(DMAM-NIPAM)-2C <sub>12</sub> p-(NIPAMAM-NIPAM)-2C <sub>12</sub>	40 °C	Calcein	<i>In vitro</i> release study (Effect of ΔH)	(Yoshino <i>et al.</i> 2004)
DOPE:EPC	p-(EOEOVE-ODVE)	36 °C	Calcein	<i>In vitro</i> release study	(Kono <i>et al.</i> 2005)
DPPC:HSPC:CHOL: DSPE-PEG-2000	p(NIPAM-AAM)	40& 47 °C	DOX	<i>In vitro</i> release and stability study	(Han <i>et al.</i> 2006a)
DPPC:HSPC:CHOL: DSPE-PEG <sub>2000</sub>	p(NIPAM-AAM)	40 °C	DOX	<i>In vitro</i> and <i>in vivo</i> study	(Han <i>et al.</i> 2006b)
DPPC:CHOL & DOPE-EPC	p(HPMA mono/dilactate)- CHOL	42 °C	Calcein	<i>In vitro</i> release study	(Paasonen <i>et al.</i> 2007b)
DPPC:HSPC:CHOL: DSPE-PEG <sub>2000</sub>	p(NIPAM-AA)-DMP	42 °C at pH 6.5	DOX	<i>In vitro</i> pH and temperature sensitivity	(Ta <i>et al.</i> 2010)
EPC:CHOL-DSPE- PEG <sub>2000</sub>	p(EOEOVE-ODVE)	40 °C	DOX	<i>In vitro</i> and <i>in vivo</i> study	(Kono <i>et al.</i> 2010)
EPC:CHOL-DSPE- PEG <sub>2000</sub> -Gd					(Kono <i>et al.</i> 2011)
EPC:DSPE-PEG <sub>5000</sub> - Fe <sub>3</sub> O <sub>4</sub>	p(EOEOVE-ODVE)	40 °C	Pyrene	Magnetic imaging and heat triggered release	(Katagiri <i>et al.</i> 2011)

Studies highlighted in blue represents polymer-modified liposomes progressed to preclinical investigation.



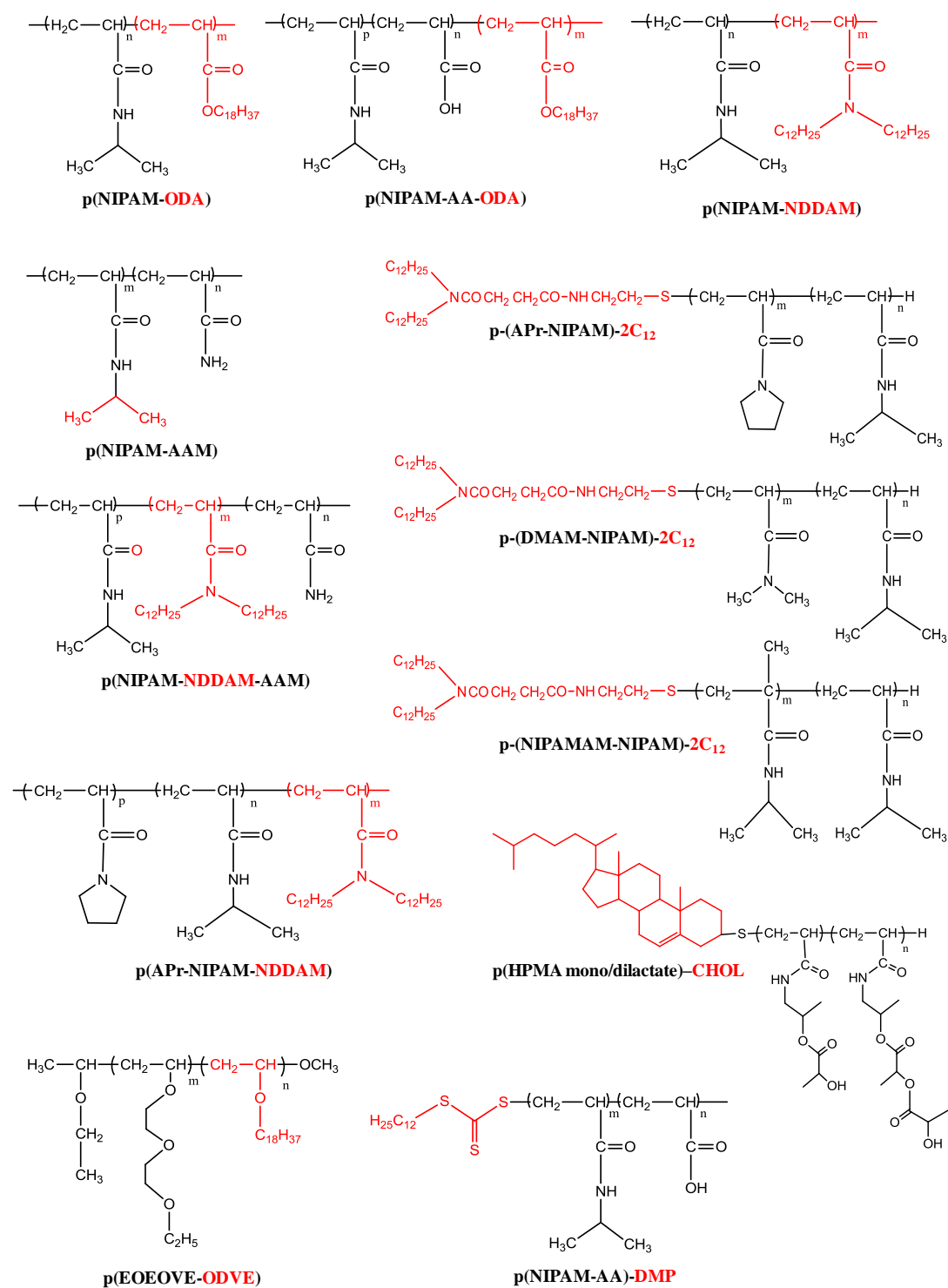


**Figure 1-10: Chemical structures of temperature-sensitive polymers used for the design of TSL.** Chemical groups represented in red colour stand for the hydrophobic anchor groups used to fix the polymers into the lipid bilayer.

Most of the early examples of polymer-modified TSL were designed with N-isopropylacrylamide (p-NIPAM) since it is the most extensively studied thermosensitive polymer. It has LCST around 32 °C, however, its LCST can be adjusted by co-polymerization with other monomers with different hydrophilic or hydrophobic properties (Shibayama *et al.* 1996). LCST decreases by co-polymerization with hydrophobic monomers such as ODA and NDDAM (Kono *et al.* 1994; Kono *et al.* 1999a), and it can be increased by co-polymerization with hydrophilic polymers for example AA or AAM (Kim *et al.* 1997; Han *et al.* 2006a).

Polymer-modified TSL was first proposed by Kono *et al.* where they attached P-(NIPAM-ODA) polymer into the lipid bilayer through the hydrophobic group of ODA. The long alkyl chain of ODA serves as an anchor to fix the hydrated part of the polymer into the liposome surface (Kono *et al.* 1994). In this early study, Kono and co-workers studied the effect of surface modification of both non temperature-sensitive liposomes (EPC) and thermosensitive liposomes (DPPC) with p-(NIPAM-ODA) and found an increased release of encapsulated fluorescent dye at temperature greater than LCST of polymer (~70 % Calcein release from DPPC liposomes and ~45 % CF release from EPC liposomes at 41 °C) with minimum release below LCST (< 10 % at 20 °C). The higher release observed from polymer-modified DPPC liposomes compared to EPC indicated synergistic effect between the thermosensitivity of the DPPC liposomes and membrane destabilisation induced by the polymer.

The hydrophobic anchors used for polymer fixation can be either randomly distributed along the polymer backbone or attached at the end of the polymer. Kono *et al.* has studied the effect of the anchor position on content release properties of calcein-loaded DOPE liposomes. Dramatic release over narrow temperature range was seen from DOPE liposomes modified with polymer having the terminal anchor (p-(APr-NIPAM)-C<sub>12</sub>) (70-90% release over temperature range from 41-42 °C) compared to those modified with the middle anchor p-(APr-NIPAM-NDDAM) (only 60% release at 45 °C) (Kono *et al.* 1999c). Polymers attached to one end can change easily from a hydrophilic to a hydrophobic status compared to polymers fixed through multiple points because of the higher conformational freedom of the former (Kono *et al.* 1999c; Kono 2001). Stronger attachment of the polymer-anchor chain to

liposomes in the gel phase was observed compared to liposomes with fluid nature (Kono *et al.* 1994). The interaction between the polymer and the lipid bilayer is not dependent on the  $T_m$  of the liposomal system, but rather takes place above LCST (Kono *et al.* 1994). This phenomenon was explored systematically by Kono *et al.* and Kim *et al.* by studying the effect of pNIPAM-AA-ODA and pNIPAM-ODA polymers on the release of fluorescent dye from fluid and gel-phase liposomes. The release from liposomes having fluid nature is covered by the LCST of the polymer itself. In contrast, liposomes in the gel phase showed maximum release at the  $T_m$  of the liposomes. In both cases the maximum release achieved from polymer-modified liposomes was higher compared to plain liposomes (Kono *et al.* 1994; Kim *et al.* 1997).

The interaction of the polymer with the lipid bilayer can be improved by changing the lipid composition of liposomes, especially for those with fluid phase as no significant content release was observed from them. Inclusion of DOPE in EPC liposomes-surface coated with p(NIPAM-NDDAM) increased the fraction of content release above LCST. Almost 20 % increase in calcein release was measured from DOPE:EPC liposomes 64:36 mol/mol compared to pure EPC liposomes. This is probably because of H-bond formation between DOPE lipids and the polymer and the affinity of DOPE lipid to exist as a non bilayer structure (Kono *et al.* 1999a).

Early example of polymer-modified TSL were designed with polymers having LCST below body temperature, therefore, they were not clinically suitable. New copolymers of NIPAM were then designed to have LCST around physiological temperature. Hayashi *et al.* showed that LCST of NIPAM can be adjusted around body temperature by free radical copolymerization with AAM monomers. Increase in NIPAM LCST was obtained by increasing the percentage of AAM monomers in a concentration dependent manner (Hayashi *et al.* 1999). Therefore, the release of encapsulated calcein can be adjusted at the desired temperature by controlling LCST of the polymer. Similar findings were observed by Han *et al.* using DOX-loaded DPPC:HSPC:CHOL:DSPE-PEG<sub>2000</sub> modified with p(NIPAM-AAM) (Han *et al.* 2006a).

The effect of comonomers type on content release was also investigated by studying three copolymers of NIPAM having the same LCST (40 °C) but with

different transition endotherms ( $\Delta H$ ); p-(APr-NIPAM)-2C<sub>12</sub>, p-(DMAM-NIPAM)-2C<sub>12</sub> and p-(NIPAMAM-NIPAM)-2C<sub>12</sub>. To test if the structural difference between the polymers affects their interaction with lipid membrane and the percentage of content release, all three polymers were fixed to EPC liposomes by two dodecyl anchors at the termini of the polymer. Although all three polymers tested have the same LCST (40 °C), when interacted with EPC lipid membrane different percentages of calcein was released. Although, LCST of these three polymers measured by cloud point and DSC were almost similar, the enthalpy of their transition ( $\Delta H$ ) was different since it correlates with the destruction of water around the hydrophobic groups. The percentage release of entrapped calcein from polymer-modified EPC liposomes increases with increasing the  $\Delta H$  of the polymers in the following order p-(APr-NIPAM)-2C<sub>12</sub> < p-(DMAM-NIPAM)-2C<sub>12</sub> < and p-(NIPAMAM-NIPAM)-2C<sub>12</sub>. The high  $\Delta H$  of p-(NIPAMAM-NIPAM)-2C<sub>12</sub> indicates that this polymer forms the most hydrophobic domains above LCST and therefore resulted in the highest membrane disruptive effect. Although these liposomes showed rapid drug release at 42 °C, this was associated with poor content retention capacity (~40% released in 15 min) at 37 °C (Yoshino *et al.* 2004).

Modification of liposomes with thermosensitive polymers also has the advantages of increasing the circulation time of liposomes and minimising the uptake by MPS cells in a similar way to surface modification of liposomes with PEG polymer (Han *et al.* 2006b). Han *et al.* has studied the interaction of DPPC:HSPC:CHOL liposomes modified with p(NIPAM-AAM), having LCST of 40 °C, with serum protein, by quantifying the amount of adsorbed protein over time at 37 °C to 48h. Below LCST, the polymer exists in the hydrated state which reduces the amount of adsorbed protein compared to plain liposomes. In the same study protein adsorption was significantly reduced by introducing DSPE-PEG<sub>2000</sub> lipid into p(NIPAM-AAM) modified liposomes (Han *et al.* 2006b).

Along with other types of TSL the inclusion of pegylated lipid into polymer-modified liposomes increases the serum stability at temperatures below LCST and enhances the thermal sensitivity at higher temperatures (Kono *et al.* 2002; Han *et al.* 2006a; Han *et al.* 2006b). Kono *et al.* and Han *et al.* have shown that both PEG<sub>550</sub>-2C<sub>12</sub> and DSPE-PEG<sub>2000</sub> improve serum stability at body temperature and

dramatically increase the percentage of drug release over narrow temperature range (Kono *et al.* 2002; Han *et al.* 2006a; Han *et al.* 2006b). Recently Kono *et al.* reported the optimization of EPC:CHOL liposomes surface coated with p(EOEOVE-ODVE) polymer for in vivo administration by adding 4 mol% of DSPE-PEG<sub>2000</sub> into the formulation. These liposomes showed less than 10% DOX leakage at 37 °C compared to more than 20% from non-pegylated liposomes.

The same concept applies to cellular uptake of polymer-modified liposomes. The uptake of this type of TSL is largely temperature dependent. This effect have been studied by Kono *et al.* looking at the interaction of MTX-loaded EPC liposomes modified with p-(APr-NIPAM)-2C<sub>12</sub> and EPC:CHOL:DSPE-PEG<sub>2000</sub> liposomes modified with p(EOEOVE-ODVE) thermosensitive polymer with CV1 and HeLa cells, respectively. Polymer coated liposomes did not affect cells viability at 37 °C (~ 80 % cell viability), however, cytotoxic activity dramatically enhanced with temperature increase (almost similar to the effect of free drug) (Kono *et al.* 2010). HeLa cells treated with polymer-coated liposomes showed limited drug uptake, however, substantial increase intracellular drug concentration with nuclear localization was observed at 5 minutes heating at 45 °C (Kono *et al.* 2010).

An important drawback to the early work of NIPAM-based polymers was the large polydispersity index and the difficulty to control the molecular weight of the polymer. Overcoming those limitations in recent designs meant a sharp response to temperature over a narrow temperature range (Kono *et al.* 2005). Examples of those polymers include the p(NIPAM-AA) prepared by RAFT chemistry (Ta *et al.* 2010) and the poly(N-vinylethers) synthesized by living cationic polymerization (Kono *et al.* 2005). Liposomes modified with p(NIPAM-AA)-DMP showed interesting temperature and pH sensitivity due to the presence of ionisable carboxyl group that lowers the LCST at acidic conditions (e.g. tumour microenvironment) and enhances drug release (Ta *et al.* 2010).

As an alternative to pNIPAM based polymers, poly(N-vinylethers) has been used recently for the design of TSL. Poly (N-vinylethers) act in the same way as pNIPAM and their LCST can be controlled by copolymerization with hydrophobic monomers that serve as anchor moiety to attach the polymer to the lipid membrane. Recently, Kono *et al.* showed that incorporation of p(EOEOVE-ODVE) polymer has LCST of

40 °C into EPC:CHOL:DSPE-PEG<sub>2000</sub> liposomes leads to less than 10% of DOX leakage at 37 °C and more than 90% of DOX release after 1 min incubation at 45 °C. The interaction of partially dehydrated polymer chains with PEG groups at the surface of liposomes minimized their interaction with lipid membrane at temperatures below LCST (40 °C). As LCST was exceeded, fully dehydrated polymer can result in PEG chains dehydration by H-bond formation. This increases their interaction with lipid membrane causing liposomes destabilisation and drug release (Kono *et al.* 2010). The enhanced stability at body temperature and ultrafast response to hyperthermic conditions suggested the suitability of this formulation for *in vivo* applications (Kono *et al.* 2010).

Despite the interesting results of polymer modified liposomes described *in vitro*, only few preclinical studies were reported to evaluate their *in vivo* therapeutic activity. Han *et al.* studied tumour growth retardation effect of DOX-loaded DPPC:HSPC:CHOL:DSPE-PEG<sub>2000</sub> liposomes modified with p(NIPAM-AAM) polymer after injection into B16F10 tumour-bearing mice at 6 mg/kg DOX in combination with 10 min local HT at 42 °C. Similarly, Kono *et al.* evaluated tumour growth retardation effect EPC:CHOL:DSPE-PEG<sub>2000</sub> liposomes modified with p(EOEOVE-ODVE) after injection into C26 tumour-bearing mice. Therapeutic activity was studied with and without exposure to 10 min local HT at 45 °C 6-12 h after injection (Kono *et al.* 2010). The results of these studies showed promising tumour growth retardation when used in combination with local HT, which agrees with previous *in vitro* data. Multifunctional liposomes based on this formulation have been prepared recently either by surface modification of with Gd chelates (Kono *et al.* 2011) or by incorporation iron oxide nanoparticles into the lipid membrane to provide the capability of monitoring liposomes by MR imaging besides temperature trigger release properties (Katagiri *et al.* 2011).

The Design of polymer-modified TSL offers more flexibility compared to other types of TSL. This helps to overcome some of the limitations of prototypical TSL such as the types of the lipids available, the size of the drug to be released and the temperature range required for content release (Hayashi *et al.* 1998; Kono 2001; Kono *et al.* 2002; Kono *et al.* 2005). Nevertheless, more work is warranted before this type of TSL can have clinical application. The development of temperature-

sensitive polymers that respond under narrow temperature range is necessary to maintain stability under physiological condition and ensure effective drug release under mild HT. Further *in vivo* studies are required to compare the pharmacokinetic parameters and therapeutic efficacy to other types of TSL.

#### **1.3.1.4 TSL Decorated with Metallic Nanoparticles (TSL-Nanoparticle Hybrids)**

While the liposomes and nanoparticles are separately clinically approved, the field of liposome-nanoparticles hybrids is still relatively new and represents a promising approach for designing multifunctional delivery systems (Preiss *et al.* 2011). Liposome nanoparticles hybrids formulation involves either encapsulation of nanoparticles inside the aqueous core of liposomes, embedment in the lipid bilayer, or surface adsorption onto the liposome surface and complex formation (Figure 1-11) (Al-Jamal *et al.* 2011; Preiss *et al.* 2011). Therefore these hybrid systems combine the inherent properties of both liposomes and nanoparticles and present innovative multifunctional platform for therapeutic and imaging applications. In addition, the incorporation of metallic nanoparticles can be used as a heating source when exposed to external stimuli such as alternating electromagnetic field (MF) or lights. (Volodkin *et al.* 2009; Wang *et al.* 2011c; Yoshida *et al.* 2012). Nanoparticles enhanced HT by means of radiofrequency (RF) or photothermal heating have been used to heat local malignant tissues (to temperatures between 40-45 °C or to thermo-ablative therapy (> 50 °C) to induce cellular necrosis and apoptosis by denaturing of intracellular proteins (Hildebrandt *et al.* 2002; Terentyuk *et al.* 2009; Hilger *et al.* 2012). Furthermore nanoparticles induced HT proved to have synergistic effect when used in combination with chemotherapy (Pradhan *et al.* 2010; Yoshida *et al.* 2012) and radiotherapy (Johannsen *et al.* 2010). HT induced with metallic nanoparticles can address some of the problems encountered with conventional HT techniques such as the difficulty to apply heating to deep or not readily accessible tumours (Preiss *et al.* 2011).

When used in conjunction with liposomes, nanoparticles-induced HT can provide a tool for triggered local drug release and theranostic applications. An example is the folate-targeted magnetic liposomes developed by Pradhan *et al.* that co-encapsulate iron oxide nanoparticles and DOX. These targeted magnetic liposomes depicted a significant increase cellular uptake equivalent to free DOX and synergistic cytotoxicity after triggered release with magnetic HT. Besides, the biological targeting against folate receptor, this system can be magnetically guided towards the target of choice (Pradhan *et al.* 2010).



#### 1.3.1.4.1 Formulation of TSL-Nanoparticle Hybrids (TSL-NHs)

The design of TSL-NHs can be divided into three main strategies; encapsulation into the aqueous core of the liposome, lipid membrane embedding and surface adsorption/complexation (Figure 1-11).

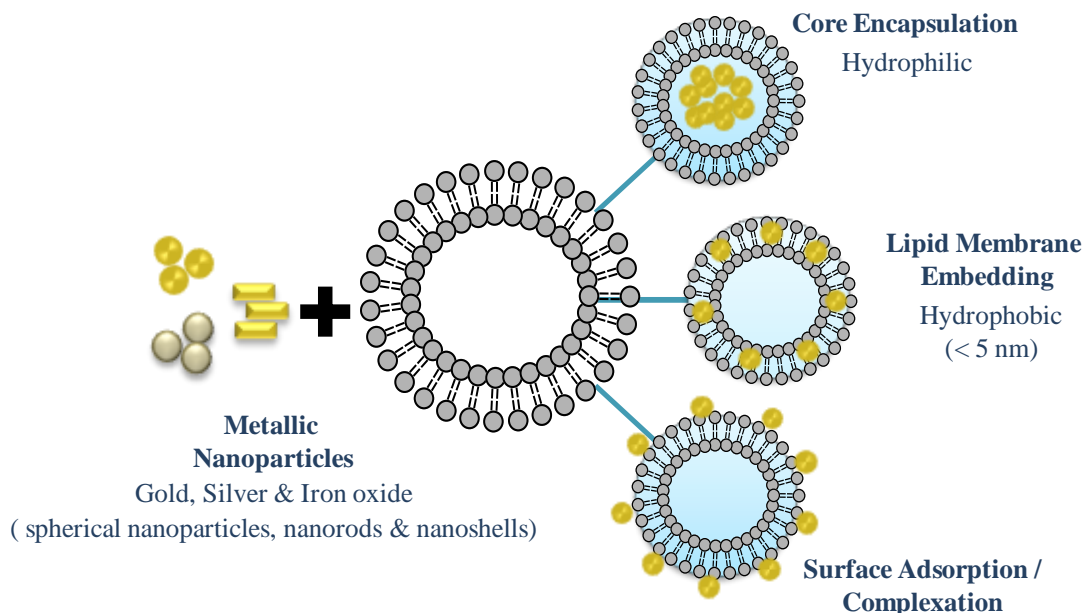


**Figure 1-11: Different strategies used for the design of TSL-NHs.**

Three main strategies have been reported for the preparation of TSL having metallic nanoparticles, namely; encapsulation, lipid bilayer embedment or surface adsorption/complexation.

Encapsulation of preformed metallic nanoparticles into the core of the liposomes is the simplest and can be prepared by thin film hydration (Pradhan *et al.* 2010), reverse phase evaporation (Viroonchatapan *et al.* 1997; Zhu *et al.* 2009) or interdigitated phase transition (Wu 2008). The critical parameters in designing this type of TSL-NHs are the colloidal stability of the nanoparticles solution and the diameter of the nanoparticles which must be smaller than the diameter of aqueous core of liposome. The concentration of nanoparticles also restricts the available volume for co-encapsulation of other water-soluble molecules (Preiss *et al.* 2011). The incorporation of metallic nanoparticles into the lipid membrane is influenced by the differential osmotic pressure across the lipid membrane and the repulsive and attractive forces between the lipid membrane and the nanoparticles (Preiss *et al.* 2011). It also requires the nanoparticles to be hydrophobic with a size that is comparable or smaller than the lipid membrane (5 nm) (Al-Jamal *et al.* 2008). For

larger nanoparticles, lipid molecules can distort to accommodate for the hydrophobic nanoparticles with sizes larger than acyl chain length. This is in agreement with the accommodation of large transmembrane proteins within the cell membrane (Bothun 2008). Nanoparticles adsorption or complexation forms when hydrophilic nanoparticles are coupled to the surface of liposomes by attractive forces or electrostatic interaction. This type of TSL-NHs is relatively easier to prepare by mixing metallic nanoparticles with pre-formed liposomes. Nanoparticles incorporated into the lipid membrane or adsorbed onto liposomes surface have the advantage of providing direct local heating of the bilayer when exposed to external stimuli (Chen *et al.* 2010; Paasonen *et al.* 2010; Katagiri *et al.* 2011; An *et al.* 2013).

#### **1.3.1.4.2 Applications of TSL-NHs**

The applications of TSL-NHs are determined by the type of nanoparticles, liposomal formulation and the interaction between the nanoparticles and the lipid membrane. In general TSL-NHs have the advantage of shielding the nanoparticles which reduces their interaction with external molecules and increases their biocompatibility (Preiss *et al.* 2011). TSL-NHs increase nanoparticles cellular uptake which is important for imaging and hyperthermia applications (Chithrani *et al.* 2010). Besides being a carrier for nanoparticles, TSL-NHs with thermosensitive properties can overcome the limitations of conventional liposomes by offering site specific drug release utilizing nanoparticles heating to control the onset and duration of drug release (Pradhan *et al.* 2010; Tai *et al.* 2010).

The imaging and the thermal characteristics of gold nanoparticles are related to their enhanced surface Plasmon resonance property. The latter allows absorbed light at certain wavelengths to cause oscillation of surface electrons and subsequently, local heat generation. Heat generation can be controlled by the intensity of laser light, duration of exposure and the concentration of gold nanoparticles (Alkilany *et al.* 2012). Photothermal energy can then transfer into the lipid membrane leading to phase transition of the bilayer from gel phase to liquid crystalline phase causing triggered drug release (An *et al.* 2013). Similarly, the magnetic characteristics of iron oxide nanoparticles (magnetite or maghemite) can be used for both imaging and magnetic heating. Iron oxide nanoparticles are approved as a contrast agent for MRI. Moreover, magnetic drug targeting by static magnetic field application and magnetic

heat generation by exposure to alternated magnetic field are now possible. It follows that magnetic hyperthermia is considered as a physiologically accepted non-invasive heating method having good tissue penetration capability (Pankhurst 2003; Laurent *et al.* 2008). For the reasons listed above, interest in design TSL-NHs has increased. Recent examples of this type of TSL decorated with gold, silver and iron oxide nanoparticles are listed in Table 1-2, Table 1-3 and Table 1-4, respectively.

**Table 1-2: TSL-NHs decorated with gold NPs**

Liposomal Formulation	NPs Type / size	Coating	Position	Dye / Drug	Function	References
DPPC	Spherical NPs (3 - 4 nm)	Stearyl amine	Lipid membrane	-	Concentration dependent increase in membrane fluidity	(Park <i>et al.</i> 2006)
DPPC:DSPC	Spherical NPs (2.5 nm)	C6-SH	Lipid membrane	Calcein	UV light triggered release (250 nm)	(Paasonen <i>et al.</i> 2007a)
	Spherical NPs (2.8 nm)	MSA	Core			
	DPPE-nanogold (1.4 nm)	DPPE	Surface adsorbed			
DPPC	Nanoshell (33 nm)	SH-PEG-lipid linker.	Core / lipid membrane / surface adsorbed	CF	NIR triggered release (820 nm)	(Wu 2008)
DPPC:DPTAP: CHOL	Spherical NPs (20 nm)	N.R	Complex	CF	NIR triggered release (830 nm)	(Volodkin <i>et al.</i> 2009)
DSPC:DPPC	Spherical NPs (2.5 nm)	C6-SH	Lipid membrane	Calcein	UV triggered release (365 nm)	(Paasonen <i>et al.</i> 2010)
	Spherical NPs (4 nm)	MSA	Core			
DPPC:CHOL: DSPE-PEG <sub>2000</sub>	DPPE-Nanogold (1.4 nm)	DPPE	surface adsorbed	-	Cellular uptake enhancer	(Chithrani <i>et al.</i> 2010)
EPC:CHOL	Spherical NPs (5 nm)	di-2 ethylhexyl sulfosuccinate	Lipid membrane	berberine	UV light triggered drug release (250 nm)	(An <i>et al.</i> 2010b)
EPC:CHOL	Spherical NPs (5 nm)	Sodium dioctyl sulfosuccinate	Lipid membrane	berberine	UV light triggered drug release (250 nm)	(An <i>et al.</i> 2013)

**Table 1-3: TSL-NHs decorated with silver NPs**

Liposomal Formulation	Nanoparticle Type / size	Coating	Position	Dye / Drug	Function	References
DPPC	Spherical NPs (4 nm)	Stearylamine	Lipid membrane	-	Increase lipid membrane fluidity	(Park <i>et al.</i> 2005)
DPPC	Spherical NPs (5.7 nm)	decane-thiol	Lipid membrane	-	Reduce T <sub>m</sub> and increase lipid membrane fluidity	(Bothun 2008)

**Table 1-4: TSL-NHs decorated with iron oxide NPs**

Liposomal Formulation	Nanoparticle Type / size	Coating	Position	Dye / Drug	Function	References
DPPC	Fe <sub>3</sub> O <sub>4</sub> NPs (5-10 nm)	Dextran	Core	5-FU	MF-induced drug release	(Viroonchapan <i>et al.</i> 1997)
DPPC:CHOL	γ-Fe <sub>2</sub> O <sub>3</sub> NPs (10 nm)	Glutamic acid	Core	MTX	Magnetic targeting	(Zhu <i>et al.</i> 2009)
DPPC:CHOL	γ-Fe <sub>2</sub> O <sub>3</sub> NPs (45- 60 nm)	Dextran	Core	CF	MF-induced release	(Tai <i>et al.</i> 2009)
DPPC	γ-Fe <sub>2</sub> O <sub>3</sub> NPs (5 nm)	Oleic acid	Lipid membrane	CF	MF-induced release	(Chen <i>et al.</i> 2010)
DPPC:CHOL:DSPE-PEG(2000):DSPE-PEG(2000)-Folate	Fe <sub>3</sub> O <sub>4</sub> NPs (10 nm)	SH	Core	Calcein / DOX	MF-induced release by HT	(Pradhan <i>et al.</i> 2010)
DPPC:CHOL	Fe <sub>3</sub> O <sub>4</sub> NPs (12.5 nm)	N.R	Core	-	Lipid bilayer temperature measurement with anisotropy	(Bothun <i>et al.</i> 2011)
DPPC:CHOL	Mn <sub>0.5</sub> Zn <sub>0.5</sub> Fe <sub>2</sub> O <sub>4</sub> NPs (20-30 nm)	N.R	Core	As <sub>2</sub> O <sub>3</sub>	MF-induced drug release by HT	(Wang <i>et al.</i> 2011a; Wang <i>et al.</i> 2011b)
EPC:DSPE-PEG5000-p(EOEOVE-ODVE)	Fe <sub>3</sub> O <sub>4</sub> NPs (12 nm)	Oleic acid	Lipid membrane	pyranine dye	MF-induced release by HT	(Katagiri <i>et al.</i> 2011)
DPPC:DSPC / DPPC:DSPC:DSPE-PEG 2000:Rhod-PE/	γ-Fe <sub>2</sub> O <sub>3</sub> NPs (7 nm)	Citrate ligands	Core	-	Imaging / Targeting and HT	(Bealle <i>et al.</i> 2012)
DPPC:HSPC:CHOL:DSPE-PEG <sub>2000</sub>	γ-Fe <sub>2</sub> O <sub>3</sub> NPs (5 nm)	phosphate salt	Core	-	HIFU- MR imaging	(Lorenzato <i>et al.</i> 2013)

Studies Highlighted in blue represent TSL-NHs progressed to preclinical evaluation

Paasonen *et al.* has shown that incorporating 2-4 nm gold nanoparticles into DPPC:DSPC TSL can trigger calcein release after 5-10 min of continuous exposure to UV light at 250 nm. Three different types of TSL-NHs were compared including; nanoparticles encapsulation, membrane embedment and surface adsorption. The highest content release was observed from membrane embedded Au-C<sub>6</sub>SH NPs and surface adsorbed DPPE-Nanogold<sup>®</sup> NPs. The reason behind that was the potential of direct heat transport from the nanoparticles to the liposomal bilayer compared to encapsulated gold nanoparticles (Au-MSA) (Paasonen *et al.* 2007a). However, the penetration depth limitation and the danger of long term exposure to UV light restrict their clinical applications (Paasonen *et al.* 2007a; Paasonen *et al.* 2010). This limitation was overcome by designing TSL-NHs for triggered drug release with near infrared (NIR) light. NIR can penetrate up to 10 cm allowing non-invasive heating of significant areas of the body (Weissleder 2001). Interesting examples of the above are DPPC liposomes decorated with hollow gold nanoshell by different association types (Wu 2008) and DPPC:DPTAP:CHOL-gold nanoparticles complexes (Volodkin *et al.* 2009). NIR light absorption by gold nanoparticles can be converted into heat by surface resonance resulting in the release of encapsulated CF. Similar to the previous example the percentage of content release is highly dependent on the proximity of the nanoparticles to the lipid bilayer. These results also strongly suggested that mechanism behind trigger release can be due to formation of transient pores or could be due to the mechanical disruption in the lipid membrane (Wu 2008; Volodkin *et al.* 2009).

Few studies have been reported on the development of TSL-NHs having silver nanoparticles. These studies were mainly concerned with investigating the effect nanoparticles on TSL membrane fluidity and T<sub>m</sub> (Park *et al.* 2005; Bothun 2008).

Many examples of TSL decorated with iron oxide NPs have been reported recently. Most of these studies concentrated on investigating the release of a model dye (Tai *et al.* 2009; Pradhan *et al.* 2010) or drugs (Zhu *et al.* 2009; Pradhan *et al.* 2010; Wang *et al.* 2011b) from TSL-NHs incorporating maghemite ( $\gamma$ -Fe<sub>2</sub>O<sub>3</sub>) or magnetite (Fe<sub>3</sub>O<sub>4</sub>) nanoparticles in the liposomal core or into their lipid membrane. Parameters controlling the release process were compared including, lipid: nanoparticles ratios (Chen *et al.* 2010) and the duration and intensity of MF applied

(Chen *et al.* 2010). Increasing the number of incorporated nanoparticles decreases spontaneous content leakage without MF, due to their lipid membrane stabilizing effect, and increases drug release by MF application (Chen *et al.* 2010).

The earliest example of thermosensitive liposomes decorated with iron oxide nanoparticles described by Viroonchatapan *et al.* encapsulated Fe<sub>3</sub>O<sub>4</sub> NPs (10 nm) into the core of DPPC:CHOL liposomes. Successful single and multiple release of 5-fluorouracil (5-FU) was achieved after heating with 500-kHz electromagnetic field (Viroonchatapan *et al.* 1997). The mechanism of release from iron oxide decorated TSL is a combination of enhanced permeability and partial vesicular rupture (Chen *et al.* 2010). Recently Katagiri *et al.* described a new approach for magnetic controlled drug release from polymer modified TSL incorporating hydrophobic iron oxide nanoparticles in the lipid membrane. The temperature-sensitive component of this system is EOEOVE-ODVE block copolymer anchored into EPC liposomes by ODVE moiety. The release of fluorescent dye (pyranine) from this hybrid system was dramatically increased by MF irradiation compared to a negligible release under static conditions. The mechanism behind drug release is believed to be due to changing in the thermosensitive polymer conformation by the heat release from excited Fe<sub>3</sub>O<sub>4</sub> nanoparticles rather than the disruption or rupture of the hybrid systems (Katagiri *et al.* 2011).

The therapeutic effect of iron oxide-TSL at the cellular level in combination with magnetic HT revealed a significant enhancement in cytotoxicity and resulted in effective inhibition of cell proliferation (Pradhan *et al.* 2010; Wang *et al.* 2011b). Zhu *et al.* showed increase accumulation of DPPC:CHOL liposomes encapsulating methotrexate (MTX) and  $\gamma$ -Fe<sub>2</sub>O<sub>3</sub> NPs in the skeletal muscular tissue *in vivo* by application of constant magnetic field compared to the absence of the magnetic field. This observation suggested the potential of iron oxide TSL for magnetic targeting (Zhu *et al.* 2009). In another *in vivo* study by Wang *et al.*, significant VX2 tumour growth retardation in rabbits was achieved from As<sub>2</sub>O<sub>3</sub>-loaded thermosensitive magneto-liposomes. The liposomes were administered arterially via a transcatheter in combination with magnetic HT (Wang *et al.* 2011b).

In addition to triggered drug release, TSL-NHs decorated with iron oxide nanoparticles can have a great role in MR imaging. A change in the MR signal of

encapsulated iron oxide around the phase transition of liposomes is expected since T2 signal of clustered iron oxide nanoparticles is much stronger than dispersed nanoparticles. Encapsulation of iron oxide nanoparticles into liposomes decreases the longitudinal relaxivity compared to free nanoparticles due to restricted water movement across the lipid membrane (Lorenzato *et al.* 2013). Promising *in vivo* imaging studies of magnetic TSL have been reported by Bealle *et al.* and Lorenzato *et al.* suggesting their potential in monitoring tumour accumulation after *in vivo* administration (Bealle *et al.* 2012; Lorenzato *et al.* 2013).

The field of TSL decorated with metallic nanoparticles presents a promising area for the development of multifunctional delivery systems. Further studies are warranted to optimise the choice of TSL formulation, drug leakage at physiological temperature and biocompatibility of the TSL-NHs. Co-encapsulation of therapeutic drugs and nanoparticles needs more optimization as well. Most of the described studies showed the encapsulation of a single component (either a model fluorescent dye or a therapeutic molecule) and only few studies examined the co-encapsulation possibility (Zhu *et al.* 2009; Pradhan *et al.* 2010; Wang *et al.* 2011b). Further *in vivo* evaluation of the performance of those systems is required to optimize their therapeutic potential. In addition to the need for the development of proper clinical techniques for application of MF and NIR light and control their penetration depth into the tissues.

### 1.3.1.5 Targeted TSL

In contrast to passive targeting of liposomes which depends on the EPR effect, active targeting relies on engineering of the liposome surface with targeting ligands. These ligands can be peptides, antibodies or antibody fragments that bind specifically to over-expressed receptors at their target site (Allen 2002; Torchilin 2008). Since pegylated liposomes are rarely taken up by tumour cell *in vitro* and *in vivo* (Gabizon *et al.* 2010), active-targeting can improve target cells recognition and cellular uptake resulting in an increased therapeutic potential (Park *et al.* 2001; Mamot *et al.* 2005). Despite the great amount of preclinical work performed in the field of active targeted nanomedicines (including liposomes), their use in the clinical setting is yet to be proven and only few have progressed into clinical trials. The latter were those designed to improve cellular uptake of certain therapeutics that have, otherwise, no cellular access capability to intracellular targets. An example on that is the cyclodextrin polymeric nanoparticles targeted against transferrin receptor that acts by improving siRNA cytoplasmic delivery (Lammers 2012).

The reason why ligand-targeted nanomedicines have so far failed to show persuasive effectiveness even in preclinical studies lies in the number of anatomical and physiological barriers that limit accumulation into target sites (Kirpotin *et al.* 2006; Lammers 2012). Among the most common barriers in solid tumours are the high cellular density and elevated interstitial fluid pressure. In addition, several cell layers are present between endothelial cells and tumour cells such as pericytes, smooth muscle cells and fibroblasts. As a result of these barriers, the accumulation and penetration of actively targeted delivery systems into solid tumours showed no great difference compared to passive targeting. However, promising therapeutic activity could be achieved when the targets are easier to reach such as tumour blood vessels (Pastorino 2003), metastatic tumours (Moase *et al.* 2001), blood cancers (Cheng *et al.* 2008) and with targeting ligands that have cellular internalisation capacity (Sapra *et al.* 2002).

In addition, the use of extravasation and penetration enhancers; examples are drugs including TNF- $\alpha$ , histamine (Seynhaeve *et al.* 2007), matrix-degrading enzymes (e.g. Hyaluronidase) (Eikenes 2005) or non pharmacological treatment such as radiotherapy (Davies *et al.* 2004) can strongly improve drug delivery from



targeted-liposomes. In addition, mild HT may act as a physical alternative to the accumulation of targeted liposomes at the tumour site since HT is well-known to increase nanoparticles extravasation through several mechanisms such as increasing tumour vascular permeability and blood flow. The other critical issue for active-targeted as well as passive-targeted liposomes is the need for effective content release once they accumulated at their target sites (Allen 2013).

In order to increase the therapeutic potential of liposomal anticancer drugs, interest in developing new generation of liposomes that combine the advantages of both active-targeting and triggered-release has increased including ligand-targeted TSL. Table 1-5 summarises the different examples of actively-targeted TSL. Targeted TSL can be useful in slowing the transient time in the blood by targeting antigens expressed on the tumour vasculature. The cyclic NGR targeted LTSL against tumour vascular CD13 antigen is an example (Negussie *et al.* 2010). In addition, targeted TSL can also be directed towards tumour-specific or tumour-associated antigens. Once bound to the specific antigen on their target tumour cells, targeted TSL can then release its contents by the application of HT either at the surface of the cells (Sullivan *et al.* 1986) or inside the tumour cells after conjugation to an internalising ligands (Puri *et al.* 2008; Smith *et al.* 2011). To further increase the potential of targeted TSL for intracellular delivery, multifunctional targeted TSL have been developed by co-encapsulation of magnetic nanoparticles and doxorubicin. This takes the advantages of both biological targeting and physical targeting by the application of external magnetic field. In this case magnetic nanoparticles can also be utilized for the generation of local heat by applying an alternating magnetic field allowing triggered drug release and further enhance their uptake by the cells (Pradhan *et al.* 2010). Moreover, Kullberg *et al.* has recently reported that cytoplasmic delivery of anti-HER2 TSL can be further improved by attaching them to a pore-forming protein, listeriolysin O (LLO) (Kullberg *et al.* 2009; Kullberg *et al.* 2010).

Targeted TSL studies showed that the liposomes reserve their temperature sensitivity after conjugation to the targeting ligands and this significantly increases the specific uptake and internalisation into tumour cells. Furthermore, the potentiation of intracellular content release by exposure to external HT significantly

improves cytotoxic activity (Pradhan *et al.* 2010; Smith *et al.* 2011). Despite the promising therapeutic activity observed *in vitro*, *in vivo* evaluation of targeted TSL in combination with mild HT has yet to be done. The effects of HT on both targeted TSL accumulation into the tumour and drug release after intracellular uptake have not been previously explored. Further work need to be done to explore this effect in more details.

**Table 1-5: Different examples of actively targeted TSL**

System	Aim	Design	Outcome	Ref.
Mab anti-H2K	Release drug at high concentration at the cell surface	CF / <sup>3</sup> H Uridine release rate	Enhanced release & uptake	(Sullivan <i>et al.</i> 1985; Sullivan <i>et al.</i> 1986)
Anti HER2 Affisomes	Improve targeting potential while retaining thermo-sensitivity	Cellular binding and internalisation	Hyperthermia induce intracellular release of Calcein	(Puri <i>et al.</i> 2008)
Folate-targeted Magnetic TSL	Biological and physical drug targeting	Cellular uptake of DOX and viability study	Synergistically increased cytotoxicity	(Pradhan <i>et al.</i> 2010)
Anti HER2 TSL	Two-component delivery system	2 sets of TSL encapsulated either Rhodamine (RED) or Calcein (GREEN).	two-component delivery system + HT significantly increases specificity to HER2 over-expressing tumour	(Kullberg <i>et al.</i> 2009)
LLO Anti HER2 TSL	Enhance cytoplasmic delivery by pore-forming protein, listeriolysin	Temperature sensitivity, Calcein delivery to cytoplasm	LLO TSL greatly increases cytoplasmic delivery to HER-2-overexpressing cells	(Kullberg <i>et al.</i> 2010)
Anti CD-13 NGR targeted LTSL	To slow the transit time of liposomes in the tumour vasculature	Ab binding/imaging and release studies	Improved affinity for CD13+ cancer cells while retaining temperature sensitivity	(Negussie <i>et al.</i> 2010)

Mab anti-H2K (DPPC)

Anti HER2 Affisomes (DPPC:Mal-DSPE-PEG<sub>2000</sub>:DSPE-PEG<sub>2000</sub>)

Magnetic TSL (DPPC:CHOL:DSPE-PEG<sub>2000</sub>:DSPE-PEG<sub>2000</sub>-Folate)

Anti-HER2 TSL (DPPC:MPPC: DPPG:DSPE-PEG<sub>2000</sub>:DSPE-PEG<sub>3400</sub>)

LLO Anti HER2 TSL (DPPC:MPPC:DPPG:DSPE-PEG<sub>3400</sub>-NHS)

Anti CD-13-NGR targeted LTSL (DPPC:MSPC:DSPE-PEG<sub>2000</sub>)

### 1.3.2 Critical Parameters Affecting the Choice of Heating Protocol for Triggering Drug Release from TSL

HT can be used to enhance drug delivery from TSL in two possible ways; enhancing local drug release and increasing liposomal accumulation into the tumour by increasing local blood flow and endothelial cells permeability (Kong *et al.* 2000b; Kong *et al.* 2001). Based on that, the combination of HT with TSL can be utilized in two approaches; either for intravascular or interstitial drug release (Figure 1-12).

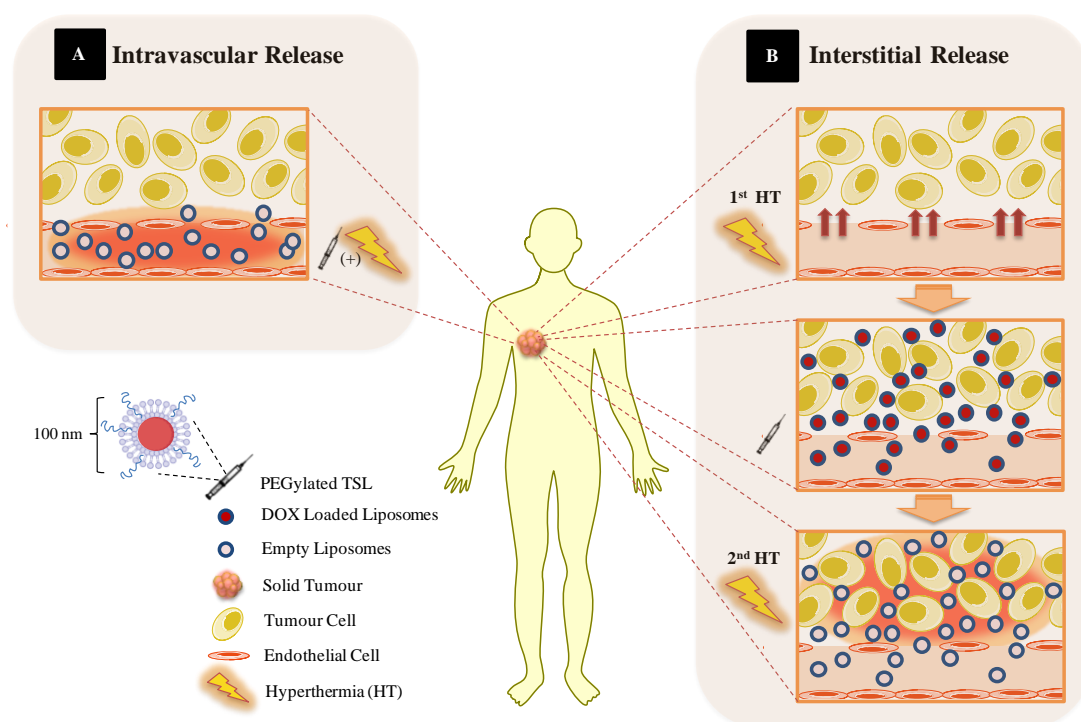


**Figure 1-12: HT protocols that can be used to enhance drug delivery from TSL.**

The combination of hyperthermia and liposomes can be utilized to enhance the drug release from TSL in two different approaches based on the timing between liposomes administration and heat application. In the intravascular release approach, TSL are administered during the heating process, resulting in drug release inside blood vessels, when reaching the heated area (Drug release is represented by the red gradient seen in the blood vessels). This process is then followed by uptake of drug by both tumour and endothelial cells. The increased vascular permeability of the blood vessels in response to 1<sup>st</sup> HT treatment increases the level of liposomes accumulation in the tumour. The interstitial release approach takes the advantage of the fact that stealth small size liposomes have the ability to extravasate the malformed tumour vasculature compared to normal blood vessels. After tumour accumulation a 2<sup>nd</sup> heating session is applied to trigger drug release interstitially (Drug release is represented by the red gradient close to tumour cells).

For the intravascular release approach, TSL are injected just before or during the HT treatment. The formulation needs to have ultra fast drug release to immediately release their contents when arriving at the heated tumour vasculature. This approach

does not rely on the effect of HT to increase the liposomes extravasation (Koning *et al.* 2010).

As mentioned earlier the ultrafast drug release properties of some TSL (e.g. LTSL) offer a new paradigm of liposomal drug release compared to non-temperature-sensitive liposomes that depend mainly on the EPR effect. Previous studies suggested that the ultrafast release property of this formulation allows immediate content release when arriving at the heated tumour vasculature (Chen *et al.* 2004; Chen *et al.* 2008). This type of drug release is called the intravascular release approach which is independent of the tendency of liposomes to accumulate passively into the tumour by EPR effect (Kong *et al.* 2000a). Moreover *et al.* has shown recently that drug release within the vasculature can also increase free drug penetration into the interstitial spaces down its concentration gradient by real time confocal imaging of doxorubicin using skin-fold window chambers (Manzoor *et al.* 2012).

In addition to the beneficial effect of TSL for intravascular drug release, the combination of TSL and HT can also be tailored to achieve interstitial drug release after their extravasation into the tumour area. Since HT is well known to have an enhancement effect on liposomes extravasation, the application of a primary HT prior to TSL injection would be useful to increase tumour vascular permeability. Once the liposomes extravasate to the tumour area, further HT can be used to trigger interstitial drug release (Koning *et al.* 2010). Since the drug release from TSL liposomes vary according to the formulation from ultra fast release within less than 1 min to slow release over 1 h, the duration of the 2nd heat can be adjusted accordingly (Koning *et al.* 2010). The choice and the sequence in which HT and TSL can be administered is critical to achieve the required therapeutic efficacy as the action of TSL depends on the HT protocol selected as well as the activity of the drug itself (Ponce *et al.* 2007). Previously published preclinical studies of TSL in combination with mild HT showed a clear enhancement in tumour uptake and tumour growth delay. Unfortunately, very few studies justified the choice of the HT protocol selected based on the physicochemical properties of the TSL and tumour accumulation (Kong *et al.* 2000a; Ponce *et al.* 2007; Manzoor *et al.* 2012). In most of these studies HT was applied directly after injection (Chen *et al.* 2004; Lindner *et al.*

2004; de Smet *et al.* 2011; Ranjan *et al.* 2012) or shortly after (1-3 h), while the TSL is still circulating in the blood stream (Gaber *et al.* 1996; Ishida *et al.* 2000). Only few studies were specially designed to trigger content release from TSL after accumulation into the tumour (Kono *et al.* 2010; Katagiri *et al.* 2011). Furthermore, these studies were mainly restricted to one type of TSL, which makes it difficult to link the results to the properties of TSL to define the optimum HT timing for each formulation. Recent studies have shown that triggering drug release with HIFU can improve drug distribution into the tumour and increase long-term tumour accumulation from long circulating TSL. This confirms the potential of use HT to trigger interstitial drug release. Table 1-6 summarises the different HT protocols used to trigger drug release from TSL.

The importance of choosing the right heating protocol is demonstrated clearly in the case of LTSL formulation. In preclinical studies, LTSL in combination with mild HT demonstrated significant enhancements in the therapeutic effectiveness compared to free drug, heating alone and liposomes without HT (Kong *et al.* 2000a; Needham *et al.* 2000; Ponce *et al.* 2007). The improvement in therapeutic activity observed is mainly due to the ultrafast release property of LTSL (> 80% release in few seconds) after exposure to mild HT (Anyarambhatla *et al.* 1999; Mills *et al.* 2005). Temperature-induced drug release within tumour vasculature increased the exposure of tumour endothelial cells to DOX causing destruction of tumour vasculature and improve therapeutic efficacy (Chen *et al.* 2004; Chen *et al.* 2008).

Despite that Phase III trial in liver cancer in combination with radiofrequency ablation (RFA) failed to show sufficient evidence of clinical effectiveness (Celsion.com 2013a). Although the results is still being analysed, preclinical studies suggested that the timing between injection and heat application is the most critical factor in the success of this type TSL. A critical limiting fact with ThermoDox<sup>®</sup> is the tendency to leak out DOX once injected into the blood circulation even before HT application (Hauck *et al.* 2006). ThermoDox<sup>®</sup> short blood kinetics of encapsulated drug (only 1.3 h) restrict the time frame of the heating protocol (Poon *et al.* 2009; Banno *et al.* 2010), which then can make its clinical translation prone to errors. Although ThermoDox<sup>®</sup> has longer blood half-life compared to free drug, it is still substantially less than that of Doxil<sup>®</sup>. Bearing in mind that the average clinical

HT duration is 30-60 minutes, it is clear that the optimum treatment would be achieved by starting HT prior to drug administration (Landon *et al.* 2011).

**Table 1-6: HT protocols used for trigger release from TSL**

TSL	Drug	HT Source and Protocol	Experimental design	End Point	Ref.
TTSL	DOX	Water bath (1 h at 42 °C) 1 h after injection 2nd HT 24 h after injection	-Tumour uptake -Drug release	1 h after HT (Data not shown)	(Gaber <i>et al.</i> 1996)
LTSL TTSL NTSL	DOX	Water bath (1 h at 42 °C) immediatly after injection	-Tumour uptake -Growth dealy	-immdeiatly after HT -5x tumour volume or up to 60 days	(Kong <i>et al.</i> 2000a)
LTSL TTSL NTSL	DOX	Water bath (1 h at 42 °C) immediatly after injection	-Growth delay	5x tumour volume or up to 60 days	(Needham <i>et al.</i> 2000)
PEG-TSL	DOX	RF (20 min at 42 °C) 3 h after injection	-Tumour uptake -Survival	-5 min after HT -Up to 90 days	(Ishida <i>et al.</i> 2000)
DPPGOG-CF	CF	Water bath (1 h at 42 °C) immediatly after injection	-Tumour uptake	up to 6 h after HT	(Lindner <i>et al.</i> 2004)
LTSL NTSL	DOX	HIFU (15-20 min 42 °C) immediatly or 24 h after injection	-Tumour uptake -Growth delay	- immediatly after HT -Time to reach 500 mm <sup>3</sup>	(Dromi <i>et al.</i> 2007)
LTSL	DOX & Mn	Catheter (30 min at 42 °C) -injection 15 min after HT -injection 15 min before HT -split dose before & during HT	-Tumour uptake -Growth delay -Survival:	-30-45 min after injection -5x tumour volume -up to 60 days	(Ponce <i>et al.</i> 2007)
LTSL	DOX	Water bath (1 h at 42 °C) immediatly after injection	-Tumour uptake -Growth dealy	-immdeiatly after HT -5x tumour volume or up to 60 days	(Yarmolenko <i>et al.</i> 2010)
Polymer-modified EPC:CHOL:DSPE- PEG	DOX	RF (10 min at 45 °C) 6 h & 12 h after injection	-Growth dealy	-up to 8 days	(Kono <i>et al.</i> 2010)
Polymer-modified EPC:CHOL:DSPE- PEG-Gd	DOX	RF (10 min at 44 °C) 8 h after injection	-Tumour uptake -Growth dealy	-1 h, 3 h & 8 h -up to 8 days	(Kono <i>et al.</i> 2011)
TTSL	DOX & Gd	MR-HIFU (2x 15 min) -injection after HT initiation (42 °C)	- Tumour uptake (DOX quantification & MR imaging)	20-30 min after injection	(de Smet <i>et al.</i> 2011)
LTSL	DOX & Gd	MR-HIFU (4x 10 min at 41 °C) immediatly after injection	- Tumour uptake (MR maging)	-immdeiatly after HT	(Negussie <i>et al.</i> 2011)

HaT LTSL	DOX	Water bath (1 h at 43 °C) 10 min before injection	- Tumour uptake -Growth delay	-immediatly after injection - up to 21 days	(Tagami <i>et al.</i> 2011a)
HaT	DOX & Gd	Water bath (1 h at 43 °C) 10 min before injection	- Tumour uptake (DOX quantification & MR imaging)	-immediatly after injection	(Tagami <i>et al.</i> 2011c)
HaT-II LTSL	DOX- Cu <sup>+2</sup>	Water bath (1 h at 43 °C) 10 min before injection	- Tumour uptake -Growth delay	-immediatly after injection -up to 21 dyas	(Tagami <i>et al.</i> 2012)
LTSL	DOX	Heating coil (30 min at ~41°C) HT plus injection	- Tumour uptake	CLSM imaging every 5 s for 20 min	(Manzoor <i>et al.</i> 2012)
LTSL	DOX	MR-HIFU (3x 10 min at 40-41 °C) within 1 h of LTSL infusion	-Tumour uptake (DOX quantification)	4 h after injection	(Ranjan <i>et al.</i> 2012)
TTSL	DOX & Gd	MR-HIFU (2x 15 min) immediatly after injection	-Tumour uptake	-1.5 & 48 h after injection	(de Smet <i>et al.</i> 2013)
Optimized PEG-TSL-Rho-PE	-	Heating coil (0.5-1 h at 41 °C) 20 min after injection	-Tumour uptake -Blood vessles permeability	-CLSM up to 2h -4 h, 8 h & 24 h post HT	(Li <i>et al.</i> 2013a)
Optimized PEG-TSL-Rho-PE	DOX	Heating coil (1 h at 42 °C) 20 min after injection	-Tumour uptake -Growth delay & survival	-CLSM up to 80 min after injection -up tp 26 days	(Li <i>et al.</i> 2013b)

HaT: DPPC:Brij 78  
 NTSL (HSPC:CHOL:DPPE-PEG<sub>2000</sub>)  
 PEG-TSL (DPPC:DSPC:CHOL:DSPE-PEG)  
 Polymer-modified EPC:CHOL:DSPE-PEG (EPC:CHOL:copoly(EOEOVE-block-ODVE):DSPE-PEG<sub>2000</sub>)  
 Polymer-modified EPC:CHOL:DSPE-PEG-Gd (EPC:CHOL:copoly(EOEOVE-block-ODVE):DSPE-PEG<sub>5000</sub>-G3-DL-DOTA-Gd)

Studies highlighted in blue represent HT protocols designed for interstitial drug release or studies that quantify prolonged drug accumulation.

The importance of this parameter on the therapeutic efficacy of LTSL formulation has been revealed before in preclinical studies by Ponce *et al.*, when, they studied the effect of timing between HT and injection on the tumour distribution and therapeutic activity of LTSL encapsulating Mn<sup>+2</sup>. For this type of TSL, higher and faster DOX accumulation into the tumour occurs when injected during HT compared to injection before that since this sequence takes the advantage of having the maximum intravascular LTSL concentrations. Thus preheating the tumour before LTSL injection is essential to get the maximum therapeutic activity from this formulation to get rapid drug release in the tumour vasculature. Despite the whole tumour is heated, LTSL release most of the drug at the periphery of the tumour before reaching the

tumour centre causes peripheral drug accumulation. In contrast LTSL injection before HT allows liposomes to perfuse into the tumour interstitium before drug release and therefore central distribution is achieved. Phase I clinical study data of ThermoDox<sup>®</sup> showed that the maximum plasma level of drug is at the end of 30 min infusion, suggesting that this is the optimum time for RFA application (Poon *et al.* 2009). Yet, in clinical trial, RFA, started at least 15 min after the initiation of infusion and completed no longer than 3 h (ClinicalTrials.gov. 2012b). This modification in the timing of ThermoDox<sup>®</sup> administration and HT treatment between pre-clinical and clinical studies, together with the short blood circulation may explain in part the unsuccessful clinical outcome. Recently, Celsion announced meta-analysis of the data extracted from the Phase III heat study showed that ThermoDox<sup>®</sup> noticeably improves progression free survival and overall survival in patient received RFA for at least 45 min. This applied to patients having small-sized HCC lesions (3-5 cm and 5-7 cm). This analysis suggests that the duration of heat from the RFA procedure is a key parameter to get a successful clinical outcome when combined with TSL (Celsion.com 2013b).

Taking all the above into consideration, it is evident that systematic preclinical studies are required to get insight into the choice of the correct HT protocol that best matches the physicochemical properties, drug release rate, pharmacokinetic parameters and tumour accumulation.



### 1.3.3 Image-Guided Drug Delivery of TSL (Paramagnetic TSL)

An important issue to consider in the design of triggered local delivery systems is to guarantee the release process at the correct timing, location and therapeutic dose needed. Ensuring this level of control requires monitoring of both the liposomal tumour accumulation and the drug release process. Progressive development in the field of molecular imaging and nanotechnology inspired the development of delivery systems that combine imaging and therapeutic moieties (theranostics). Several studies have shown combined delivery of DOX and contrast agent from TSL. In these cases, MR imaging was used to monitor drug release from TSL and to track the liposomal tissue distribution providing non invasive and dynamic monitoring of drug release under hyperthermia condition. No nanoparticles were included for this purpose in comparison with TSL with metallic nanoparticles (Figure 1-13A).

It is important to note here that what is monitored by these techniques is the effect of contrast agent on the surrounding water protons rather than the actual drug release process. However, because both the drug and the contrast agent are available in the compartment and have similar release and distribution profile, then this can be used as an indirect way to estimate the drug release profile (May *et al.* 2013). Encapsulation of low molecular weight MR contrast agents into the aqueous compartment of the liposome affects the  $T_1$  relaxation time of accompanied intraliposomal water protons. Water exchange between inside and outside of the liposomal compartments is limited by its exchange rate across the lipid bilayer. Therefore, the interaction of MR contrast agent with the bulk water protons is restricted when encapsulated inside liposomes as compared to free contrast agent and this can be used as an indirect measure of the water membrane permeability (Bacic *et al.* 1988). The release of MR contrast agent from TSL at the  $T_m$  of liposomes is associated with dramatic increase in this interaction which consequently decreases  $T_1$  relaxation time of bulk water protons. This property has been exploited for MR image-guided drug delivery (Viglianti *et al.* 2006). The increase in MR signal after release of encapsulated MR contrast agent and drug from liposomes provides information about spatial and temporal drug release. This concept of MR-based drug quantification is referred to as “dose-painting” or “chemodosimetry” described by

Viglianti and Ponce *et al.* using TSL encapsulating  $Mn^{+2}$  and DOX (Viglianti *et al.* 2006; Ponce *et al.* 2007).

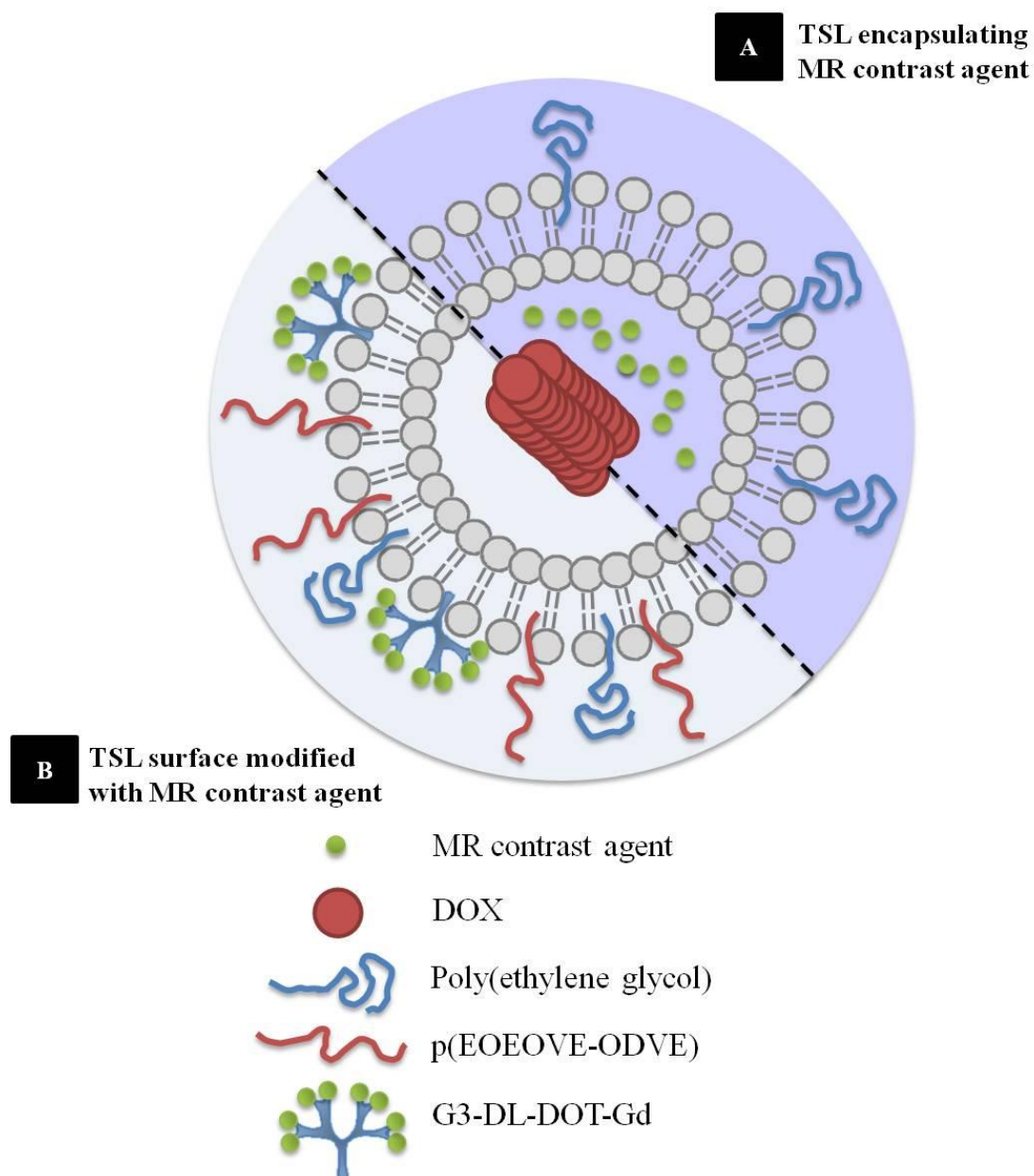


**Figure 1-13: Paramagnetic TSL for image guided drug delivery.**

Schematic illustration of different types of paramagnetic TSL used for image guided drug delivery in conjugation with mild HT. A) TSL encapsulating MR contrast agent. B) Multifunctional polymer-modified TSL surface modified with MR contrast agent.

The release of contrast agent from TSL has been used to image drug release *in vivo*. Good correlation was reported between MR imaging and thermal ablation (Frich *et al.* 2004), drug delivery (Viglianti *et al.* 2004; de Smet *et al.* 2010; de Smet *et al.* 2011) and therapeutic efficacy (Ponce *et al.* 2007; Tagami *et al.* 2011c).

The estimated DOX tissue concentration determined from the shortening in  $T_1$  relaxation time demonstrated a linear relationship with actual DOX concentration quantified by HPLC and histological fluorescence analysis. Imaging drug release from liposomes is an important tool to control drug delivery. By using this technology, release from DOX/ $Mn^{+2}$ -LTSL liposomes administered during HT was detected immediately upon entry into the heated tumour from peripheral circulation. This observation indicated that the release profile from LTSL liposomes is much dependent on the tumour vascularisation pattern as well as on tumour temperature at the time of injection (Ponce *et al.* 2007). Similar findings have been reported by de Smet *et al.* where MR images revealed a variation in drug distribution in the tumour that was related to the variation in the vascularisation, permeability and the presence of necrotic core (de Smet *et al.* 2011). The results of those studies demonstrated the suitability of the concept of using real time imaging of drug distribution to optimise the choice of HT protocol.

Although  $Mn^{+2}$  has been used to image drug delivery from TSL (Viglianti *et al.* 2004; Ponce *et al.* 2007), its toxicity can limit its clinical applications (Silva *et al.* 2004). Gadolinium based contrast agents are better alternatives because of their safety profile that makes them more acceptable for clinical applications. Therefore, much of the recent work of image guided TSL involved the use of Gd(HPDO<sub>3</sub>A), ProHance<sup>®</sup>, a clinically approved MR contrast agent co-encapsulated into TSL with DOX (de Smet *et al.* 2010; de Smet *et al.* 2011; Negussie *et al.* 2011). It might be worthwhile to point out that encapsulation of Gd(HPDO<sub>3</sub>A) inside liposomes did not interfere with DOX loading and formation of DOX crystals inside liposomes (de Smet *et al.* 2010).

Paramagnetic TSL, described above, involved the encapsulation of MR contrast agent in the lumen of the liposome. An alternative way to formulate paramagnetic TSL includes the attachment of an MR contrast agent to the liposomal surface. An example of this type has been reported by Kono *et al.* (Kono *et al.* 2011) (Figure 1-13 B). This type of polymer-modified TSL has Gd-chelate-dendron attached to their surface which can be used to probe liposome accumulation into the tumour but cannot monitor drug release as the MR contrast agent is not encapsulated inside the

liposome (Kono *et al.* 2011). In this case  $T_1$  shortening of surface attached metal ions was equivalent to the free metal ions (Viglianti *et al.* 2004).

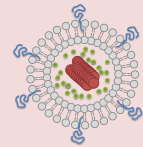
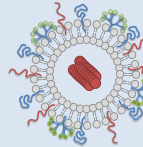
Table 1-7 summarises the recent studies using MR-guided drug delivery from TSL. Different experimental details encountered by these studies are explained including, liposomal formulation, injected dose, contrast agent, heating protocol, HT duration, and animal model.

Besides being useful for imaging, paramagnetic TSL proved to be a good tool for MR-thermometry (Lindner *et al.* 2005). In addition to providing guidance during treatment planning and following drug release from paramagnetic TSL, it can also provide accurate temperature feedback from heated tissue in real time. MR guided temperature mapping can be used to control the power of heat input using either MR-HIFU system or an ultrasound transducer to maintain the target temperature at the heated tissue (de Smet *et al.* 2011; Negussie *et al.* 2011; Staruch *et al.* 2011).

MR image-guided drug delivery may also help to individualise treatment regimen as it is widely used for tumour diagnosis for being non-invasive and safe for repeated applications (Tagami *et al.* 2011c) as will be explained in the next section.

An alternative to magnetic and paramagnetic imaging described earlier, fluorescence-based *in vivo* imaging in the NIR region is also proved to be of great benefit for image-guided drug delivery. Besides being non-invasive, NIR imaging has the advantage of high signal to noise ratio and deep tissue penetration because of the limited photon absorption at the NIR region. For this purpose, the TSL system (DPPC:HSPC:CHOL 100:50:30 mol/mol), surface coated with either DSPE-PEG<sub>2000</sub> or DSPE-Dextran, and encapsulating indocyanine green (ICG), NIR fluorophores, has been developed for theranostic applications. ICG-TSL was shown to provide reliable biodistribution profile and tumour accumulation of liposomes *in vivo*. ICG signal in the tumour can be detected up to 72 h after injection but fades rapidly after release from liposomes because of its short circulation half-life. This allows its use as an indicator of triggered release from TSL (Turner *et al.* 2012).

**Table 1-7: MR-guided drug delivery from TSL**

Liposomal Formulation (mol/mol)	Dox Dose	MR Contrast Agent	Animal / Model	HT Source and Protocol	References
MR-guided tsl co-encapsulate contrast agent inside the liposomal compartment					
LTSL	10 mg / kg	Mn <sup>+2</sup>	Rat / Fibrosarcoma	Catheter (60 min at 44 °C started before injection)	(Viglianti <i>et al.</i> 2004)
LTSL	5mg / kg	Mn <sup>+2</sup>	Rat / Fibrosarcomas	Catheter (60 minutes at 42 °C before and / or with HT injection)	(Ponce <i>et al.</i> 2007)
LTSL TTSL NTSL	N/A	Gd(HPDO <sub>3</sub> A)	In vitro	-	(de Smet <i>et al.</i> 2010)
HaT	5mg / kg	Gd-DTPA	Mice / EMT-6	Water bath (60 at 43 °C min started before injection)	(Tagami <i>et al.</i> 2011c)
LTSL	5mg / kg	Gd(HPDO <sub>3</sub> A)	Rabbit / VX2	MR-HIFU (4 × 10 min at 41.5 °C)	(Negussie <i>et al.</i> 2011)
TTSL	5 mg /kg	Gd(HPDO <sub>3</sub> A)	Rat / 9L gliosarcoma	MR-HIFU (2 × 15 min at 41.5 °C after injection)	(de Smet <i>et al.</i> 2011)
TTSL	5mg / kg	Gd(HPDO <sub>3</sub> A)	Rat / Rhabdomyosarcoma	MR-HIFU (2 × 15 min at 41 °C started immediately after injection)	(de Smet <i>et al.</i> 2013)
MR-guided tsl surface modified with MR contrast agent					
EYPC:CHOL:p(EOEOVE-ODVE):PEG-PE:G3-DL-DOTA-Gd (42:42:4:2:5-10)	6mg/kg	G3-DL-DOTA-Gd	Mice/ colon carcinoma 26	Radio Frequency / (10 min HT at 44 °C 8 h after injection)	(Kono <i>et al.</i> 2011)
TTSL: DPPC:HSPC:CHOL:DPPE-PEG2000 (50:25:15:3) LTSL: DPPC:MSPC:DSPE-PEG2000 (90:10:4) HaT: DPPC:Brij78 (96:4) NTSL: HSPC:CHOL:DPPE-PEG2000 (75:50:3)					

#### **1.4 Development of Heating Modalities for Temperature Triggered Drug Delivery**

Although the theory of triggered drug delivery by HT has been described since the late 1970, several chemical and technical obstacles had to be overcome before this technology could be tamed for clinical application. The most important challenge was to achieve controlled non-invasive focal heating of the tumour site (Grull *et al.* 2012). Moreover, monitoring of the tumour temperature restricts the clinical translation of TSL (Grull *et al.* 2012).

The majority of heating techniques available are limited by several factors including, the invasiveness of the techniques, the poor control of the temperature, the inability to adapt to the change in tumour size and perfusion and the restrictions imposed by the location of the tumour. Several techniques have been applied for heat triggered release from TSL, including, regional superficial heating employing heated water baths (Gaber *et al.* 1996; Kong *et al.* 2000a; Needham *et al.* 2000; Needham *et al.* 2001), localized superficial heating with external electromagnetic sources (Hauck *et al.* 2006) and implanted electrodes heated by continue flow of hot water (Viglianti *et al.* 2006; Ponce *et al.* 2007).

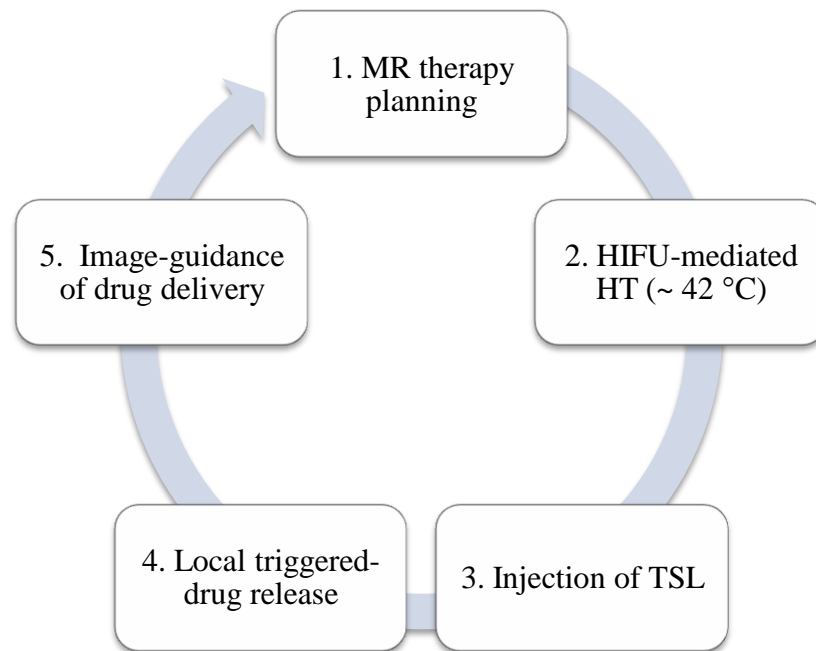
In clinical trials, two heating techniques have been applied for local tumour heating; percutaneous radiofrequency ablation (RFA) used for hepatocellular carcinoma (HCC) and superficial microwave heating for chest wall recurrence of breast cancer.(ClinicalTrials.gov. 2013a). In both heating techniques tissue temperature was monitored with interstitial probes and, therefore, the control on spatial temperature changes was limited, which is reflected on drug release (Van Der Zee *et al.* 2010; Ahmed *et al.* 2011). To enhance clinical favourability, the development of heating and monitoring techniques to achieve non-invasive spatial and temporal control of temperature is crucial. One promising techniques is the HIFU system guided with MR. Ultrasound has been used clinically to apply HT non-invasively (40-45 °C) to tumour areas that are difficult to reach by other heating methods (Hynynen 2011). MR linking to this procedure include its crucial role to provide soft tissue imaging and real-time thermometry, hence, providing precise 3D temperature feedback (Salomir *et al.* 2000; de Senneville *et al.* 2007). MR can also be useful to monitor temperature-triggered drug release from TSL by co-

encapsulation of a paramagnetic contrast agent inside the lumen of TSL with the drug compartment as described earlier (de Smet *et al.* 2011; Negussie *et al.* 2011; Tagami *et al.* 2011c).

MR-HIFU has recently been used for thermoablation applications (Zhou 2011; Li *et al.* 2012) and it also holds a great promise to trigger drug delivery in pre-clinical phase as a new paradigm in localized treatment (Grull *et al.* 2012). Promising temperature-triggered drug release from TSL with MR-HIFU has been demonstrated in several preclinical studies in normal tissues (Staruch *et al.* 2011), and in animal tumour models (Dromi *et al.* 2007; de Smet *et al.* 2011; Ranjan *et al.* 2012; Staruch *et al.* 2012). HT induced by HIFU triggered drug release from TSL and increased the long term liposomal drug uptake into the tumour in the period after HT. As a result, MR-HIFU proved to provide homogeneous intra-tumoural drug distribution over bigger area and to a larger distance away from blood vessels (de Smet *et al.* 2013). Improved distribution of DOX into the tumour was observed by the combination of TSL with MR-HIFU. This enabled DOX delivery to the core and the periphery of the tumour as compared to the distribution seen with LTSL or DOX alone which was mainly restricted to the periphery of the tumour. This improvement in DOX delivery to the tumour did not increase DOX bio-distribution into other organs which was very similar to that observed in non treated animals.(Ranjan *et al.* 2012). Gasselhuber *et al.* has shown recently that by using computer simulation studies, the amount of drug delivered to the tumour after heating with HIFU can be predicted and used to estimate cell killing induced by both, DOX and hyperthermia. Simulation studies agreed with *in vivo* data that used rabbit animal model for both temperature and drug. These promising results suggested the potential of using these computational studies for quantifying drug release in response to HT (Gasselhuber *et al.* 2012).

As a consequence to the emergence of MR system with HIFU in a bed-side system (MR-HIFU) a non-invasive option for proper treatment planning and monitoring for many patient with advance solid tumours can be offered (Grull *et al.* 2012). Individual monitoring of local drug concentration and bio-distribution during and after heating procedure can be achieved. Scheme 1-1 summarizes the potential of MR-HIFU use for heat-triggered drug release from TSL. The advantages offered by MR-HIFU- would be useful to decide on: 1) treatment modification to have a

uniform drug delivery and 2) select patients that are more likely to benefit from triggered liposomal treatment (Viglianti *et al.* 2004).



**Scheme 1-1: schematic presentation of drug delivery from TSL using MR-HIFU.**

Triggered drug release from TSL co-encapsulating drug and MR contrast agent by MR-HIFU can play a pivotal role in individualised and controlled treatment. MR plays a crucial role in therapy planning, temperature control during treatment and imaging of drug delivery. Temperature and drug release mapping provide continuous feedback to the HIFU system transducer to adjust the sonication time and/or dose until the desired signal is obtained. Adapted from (Tagami *et al.* 2011c; Grull *et al.* 2012).



## **CHAPTER 2**

---

### **AIM AND HYPOTHESES**

In this thesis we studied the possibilities of designing new types of temperature-sensitive liposome systems that have effective temperature triggered drug release in the region of interest, yet with reasonable *in vivo* drug retention. In order to achieve this goal we studied;

- Design and characterisation of novel lipid-peptide hybrid vesicles (Lp-Peptide).

To test if the incorporation of a temperature-sensitive amphiphilic peptide within the liposomal bilayer can trigger drug release by mild HT (42 °C) (Figure 2-1 A).

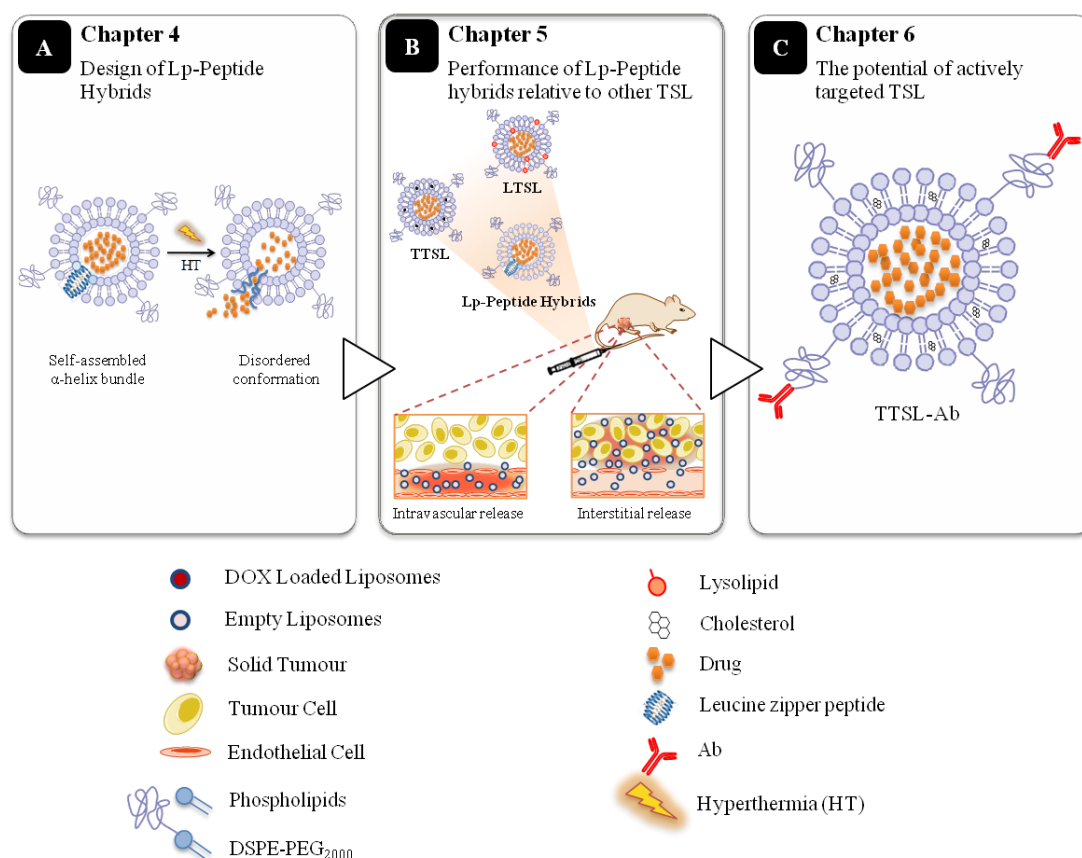


**Figure 2-1: Schematic presentation of main hypothesis studied in this thesis.**

- A) The rationale behind the design of Lp-Peptide hybrid system is to achieve triggered drug release by HT while maintaining substantial drug retention at body temperature. B) Performance of the system was studied *in vivo* in comparison to other TSL such as LTSL and TTSL with the aim to identify the critical parameters that affect the choice of the optimum HT protocol. C) The potential of enhancing the therapeutic specificity of TSL by designing anti-MUC-1 targeted TTSL was explored *in vitro* and *in vivo*.

- Biological performance of Lp-Peptide hybrids.  
To test if rapid drug release and substantial serum stability of the Lp-Peptide hybrids can increase both immediate and long-term drug accumulation in the tumour (to mimic intravascular and interstitial drug release) compared to other TSL (Figure 2-1 B).
- The engineering of anti-MUC-1 targeted TSL.  
To test if anti-MUC-1 targeted vesicles based on the traditional TSL (TTSL) can increase therapeutic specificity of TSL and trigger drug release after specific uptake into cancer cells (Figure 2-1 C).

In summary, this thesis aims to maximise the potential of TSL in cancer therapy through rationale design and engineering of TSL, understanding the critical parameters that affect their clinical translation and exploring new opportunities to increase their therapeutic benefits.

## **CHAPTER 3**

---

### **MATERIALS AND METHODS**

### 3.1 Materials

Leucine zipper peptide was purchased from Peptide Synthetics (Peptide Protein Research Ltd, Hampshire, UK). hCTMO1; anti MUC-1 IgG antibody (Ab) (150 kDa) was a kind gift from UCB (UK). 1,2-dipalmitoyl-*sn*-glycero-3-phosphocholine (DPPC), 1,2- distearoyl 1-*sn*-glycero-3-phosphocholine (DSPC), 1-stearoyl-2-hydroxy-*sn*-glycero-3-phosphocholine (MSPC), hydrogenated soy phosphatidylcholine (HSPC) , 1,2-distearoyl-*sn*-glycero-3-phosphoethanolamine-N-[methoxy(polyethylene glycol)-2000 (DSPE-PEG<sub>2000</sub>) and L- $\alpha$ -phosphatidylcholine (EPC) were kind gifts from Lipoid GmbH (Germany). 1,2-distearoyl-*sn*-glycero-3-phosphoethanolamine-N-[maleimide(polyethylene glycol)-2000] (ammonium salt) (Mal-DSPE-PEG<sub>2000</sub>) and 1,2-dioleoyl-*sn*-glycero-3-phosphoethanolamine (DOPE) were purchased from Avanti Polar Lipids (USA).

8-Anilino-1-naphthalenesulfonic acid (ANS), Triton-X 100, chloroform, methanol, 4-(2-Hydroxyethyl) piperazine-1-ethanesulfonic acid (HEPES), Tris base, hydrogen peroxide solution 30%, doxorubicin hydrochloride (DOX), Cholesterol, sepharose CL-4B, carboxyfluorescein (CF), sterile filtered dimethyl sulfoxide (DMSO), 2-iminothiolane (Traut's Reagent), albumin from bovine serum (BSA), goat serum, 3-(4,5-dimethylthiazol-2-yl)-2,5-diphenyl-tetrazolium bromide (MTT) and Streptavidin were obtained from Sigma (UK).

1,1'-Dioctadecyl-3,3,3',3'-Tetramethylindocarbocyanine Perchlorate (DiI) and 1,6-diphenyl-1,3,5-hexatriene (DPH) are from Invitrogen, UK. Soluene<sup>®</sup>-350 and doxorubicin HCL [14-14C] were bought from PerkinElmer (USA). Scintillation cocktail high performance scintisafe gel (Fisher). 1,2-dipalmitoyl(d62)-*sn*-glycero-3-phosphocholine (Avanti Polar Lipids, Alabaster, AL) was a kind gift from Dr Richard Harvey. Ethylenediaminetetraacetate dehydrate (EDTA) was from VWR. Cy3-conjugated affiniPure goat anti-human IgG (Jackson ImmunoResearch Laboratories). BCA Protein Assay Reagent and paraformaldehyde (PFA) were from thermo scientific, UK. The amine coupling kit containing N-hydroxysuccinimide (NHS) and N-Ethyl-N'-dimethylaminopropyl carbodiimide (EDC), were from BIACORE (Upsala, Sweden). Vectashield mounting medium with DAPI H-1200 is from Vector Laboratories.

DMEM (Dulbecco's Modified Eagle Medium), MEM (Minimum Essential Media), Advanced RPMI 1640 (Roswell Park Memorial Institute) and L-glutamine (200mM) were from Gibco Life Technologies (UK). All chemical substances and solvents were used without further purification.

## 3.2 Cell Lines

B16F10, a murine melanoma cancer cell line (ATCC, USA), C33a, a human, cervix carcinoma cell line (ATCC, USA) and SW480, a human colorectal adenocarcinoma cell line (ATCC, USA) were cultured in advanced RPMI-1640 supplemented with 10% FBS, 1% L-Glutamine and 1% penicillin/streptomycin. HUVEC, primary human umbilical vein endothelial cells (C2519A; Lonza, Verviers, Belgium) were cultured in EGM-2 medium (CC-3162; Lonza). MDA-MB-435, human breast cancer cells, transfected to produce MUC-1 antigen were kind gift from Dr. John Maher, King's College London (Wilkie *et al.* 2008). MDA-MB-435 and MCF-7, human breast cancer cells (ATCC, USA), were grown in DMEM & MEM, respectively, supplemented with 10% FBS and 1% penicillin/streptomycin.

The cells were incubated in a humidified atmosphere at 37 °C in 5% CO<sub>2</sub>. Cells were routinely grown in 75 cm<sup>2</sup> tissue flask (TPP, Switzerland), splitted twice a week using sterile phosphate buffer saline (PBS) pH 7.4 (Gibco) for washing and trypsin-EDTA (Ca<sup>+2</sup> and Mg<sup>+2</sup> free) (Gibco) for trypsinisation after reaching 80% confluency.

## 3.3 Methods

### 3.3.1 Preparation of Liposomes

Both temperature-sensitive and non temperature-sensitive liposomes studied in this thesis were prepared by thin lipid film hydration method followed by extrusion (Hossann *et al.* 2007; Al-Jamal *et al.* 2009a). Table 3-1 shows the liposomal formulations studied, their lipid composition and the molar ratios used. Briefly, lipids of different types were dissolved in chloroform:methanol mixture (4:1) in a total volume of 2 ml in a 25 ml round bottom flask. To engineer Lp-Peptide hybrids, the respective amount of peptide dissolved in methanol was added to the lipid mixture before the formation of the lipid film. Organic solvents were then evaporated using a

rotary evaporator (Buchi, Switzerland) at 40 °C at 120 rotations/min. After 1 h under vacuum, lipid films were further dried for 2-3 min under a nitrogen gas stream followed by hydration with ammonium sulphate 250 mM (pH 8.5) at 60 °C. Small unilamellar liposomes were produced by extrusion through 800 nm and 200 nm polycarbonate filters (Whatman, VWR, UK) 5 times each then 10 times through 100 nm extrusion filters (Whatman, VWR, UK) using a mini-Extruder (Avanti Polar Lipids, Alabaster, AL). For animal experiments liposomes (25 mM) were also extruded for additional 10 times through 80 nm extrusion membrane (Whatman, VWR, UK).

**Table 3-1: Temperature sensitive and non temperature-sensitive liposome systems studied.**

Liposomal formulation	Lipid molar ratios	Lipid:Peptide (mol/mol)	Lipid concentration (mM)
<b>Temperature-sensitive liposomes</b>			
DPPC:DSPC: DSPE-PEG <sub>2000</sub>	90:10:5		
-Lp		-	5 & 25
-Lp-Peptide 600:1		600:1	5
-Lp-Peptide 200:1		200:1	5 & 25
-Lp-Peptide 100:1		100:1	5
DPPC:DSPC:DSPE-PEG <sub>2000</sub> :CHOL (Lp-CHOL)	90:10:5:0.5	-	5
DPPC:MSPC:DSPE-PEG <sub>2000</sub> (LTSL)	90:10:4	-	5 & 25
DPPC:HSPC:CHOL:DSPE-PEG <sub>2000</sub> (TTSL)	54:27:16:3	-	5 & 25
<b>Non temperature-sensitive liposomes</b>			
HSPC:CHOL:DSPE-PEG <sub>2000</sub> (NTSL)	56.3:38.2:5.5	-	5 & 25
DOPE:EPC:DSPE-PEG <sub>2000</sub>	64:36:5		5
DOPE:EPC:DSPE-PEG <sub>2000</sub> -Peptide	64:36:5	200:1	5

### **3.3.2 Preparation of CF-Loaded Liposomes**

CF-loaded liposomes were prepared by hydrating the lipid film with 100 mM CF solution in HBS (pH 7.4) to a final lipid concentration of 5 mM. CF-loaded liposomes were then purified using Sepharose CL-4B column equilibrated with HBS (pH 7.4) to remove the non-encapsulated CF before use for release experiments.

### **3.3.3 Preparation of DiI-Labelled Liposomes**

To prepare DiI-labelled liposomes for cellular uptake studies, 5 mol% of DiI in ethanol (1mg/ml) was added to the lipid mixture and liposomes were prepared by thin lipid film hydration method as described earlier. Lipid films were kept protected from light and hydration was performed with ammonium sulphate (pH 8.5) to a final lipid concentration of 5 mM. DiI-labelled liposomes were purified by passing them through Sepharose CL-4B column equilibrated with HBS (pH 7.4) before use.

### **3.3.4 Preparation of Targeted TSL Liposomes**

#### **3.3.4.1 Conjugation of Anti-MUC-1 Antibody to Maleimide-DSPE-PEG<sub>2000</sub> (Mal-DSPE-PEG<sub>2000</sub>) Micelles**

For the preparation of targeted TTSL-Ab liposomes, TTSL liposomes (25 mM) composed of DPPC:HSPC:CHOL:DSPE-PEG<sub>2000</sub>; 54:27:16:3 mol/mol% were first prepared as mentioned earlier followed by post-insertion of anti-MUC-1 mal-DSPE-PEG<sub>2000</sub> micelles using the previously described procedure with slight modifications (Iden *et al.* 2001). Anti-MUC-1 antibody was first thiolated as describe in (Figure 6-1 step 1) by mixing with Traut's reagent at Ab:Traut's reagent molar ratio of 1:20 for 1 h at room temperature with continuous stirring at concentration of 10 mg Ab/ml buffer, pH 8.0 (25 mM HEPES, 140 mM NaCl, 3mM EDTA). Unreacted Traut's reagent was removed using Sephadex G50 column equilibrated with deoxygenated HBS (pH 7.4). The coupling reaction was run by mixing thiolated Ab with mal-DSPE-PEG<sub>2000</sub> micelles at 1:10 molar ratio in HBS (pH 7.4) overnight at room temperature (Figure 6-1 step 2). All above reactions were performed at oxygen free conditions. At the end of reaction any uncoupled mal-DSPE-PEG<sub>2000</sub> groups were blocked by mixing with cysteine HCl to a final concentration of 1 mM for 30 min



(Loomis *et al.* 2010). Ab micelles were then concentrated by centrifugation using Viva spin 6 columns (Sartorius, fisher) at 9000 rpm for 10-12 min.

To confirm the conjugation of the anti-MUC-1 antibody to mal-DSPE-PEG<sub>2000</sub> micelles, SDS-PAGE electrophoresis was performed by mixing 10 µl of Ab samples after each chemical step with 3 ul of LDS sample buffer (lithium dodecyl sulphate, Life Technologies, UK). 10 ul samples were then loaded onto each lane of 4-12% Nupage<sup>®</sup> Novex<sup>®</sup> Bis-tris polyacrylamide gel (Life Technologies, UK). The gel was run for 40 min at 220 V in 20 times diluted Nupage<sup>®</sup> MOPS running buffer (Life Technologies, UK). Staining was performed with Instant Blue stain<sup>™</sup> (Expedeon, UK) for 15-20 min followed by washing in distilled water (D.W.) for 2 h. The gel was then scanned using a Canon LiDE80 scanner (Canon, Uxbridge, UK).

#### **3.3.4.2 Post Insertion of Maleimide-DSPE-PEG<sub>2000</sub> (Mal-DSPE-PEG<sub>2000</sub>) Micelles into TTSL Liposomes**

Mal-DSPE-PEG<sub>2000</sub> Ab micelles were then post inserted into preformed TTSL liposomes at two different Ab: lipids molar ratios (1:500 and 1:1000) by 1 h incubation at 60 °C. TTSL-Ab liposomes were then separated from non-incorporated mal-DSPE-PEG<sub>2000</sub> Ab micelles by using Sepharose CL-4B column in HBS (pH 7.4). Post-insertion efficiency was determined by collecting elution fractions (1 ml each) and analysed spectrophotometrically for the presence of Ab (BCA protein assay, at 562 nm) (Yang *et al.* 2007) and liposomes (Stewart's assay, at 485 nm), using Cary 50 Bio Spectrophotometer (Agilent Technologies). In order to allow for direct comparison, TTSL and TTSL-Ab liposomes were prepared following the same steps, except for the post-insertion process where HBS (pH 7.4) was used instead of mal-PEG<sub>2000</sub> Ab micelles in the case of TTSL liposomes.

### **3.3.5 Liposomes Characterization Techniques**

#### **3.3.5.1 Size and Zeta Potential Measurements Using Dynamic Light Scattering (DLS)**

Liposome size and surface charge were measured by using Zetasizer Nano ZS (Malvern, Instruments, UK). For size measurement samples were diluted with HBS (20 mM HEPES, 150 mM NaCl ) pH 7.4 and measured in 1 ml cuvettes. Zeta potential

was measured in disposable Zetasizer cuvettes and sample dilution was performed with distilled water. Size and zeta potential data were taken in three and five measurements, respectively.

### **3.3.5.2 Transmission Electron Microscopy (TEM)**

Liposomes of different compositions were visualized with transmission electron microscopy with and without incorporation of different peptide concentrations (CM 120 BioTwin/Philips, USA). Samples were diluted to 2.5 mM lipid concentration then a drop from each liposome suspension was placed onto the copper grid and the excess suspension was removed with a filter paper. Staining was performed using aqueous uranyl acetate solution 1%. Each liposome suspension was imaged at room temperature and after 15 min heating at 60 °C. TEM images were performed by Mr David McCarthy, UCL School of Pharmacy.

### **3.3.5.3 Circular Dichroism Studies (CD)**

CD thermal scan measurements were performed on a Chirascan Spectrometer (Applied Photophysics, Leatherhead, UK) supplied with a thermoelectric temperature control system. Temperature-dependent conformational changes were measured for leucine zipper peptide solutions (20 µM) in Tris amine buffer (5 mM) and for Lp-Peptide hybrids (200:1 lipid: peptide molar ratio, total lipid concentration 4 mM). Measurements were performed in Tris buffer at pH ≈ 8.8 as this pH was close to the pH used for DOX loading experiments. CD spectra of the samples were recorded from 260 to 180 nm using 0.5 mm cuvette, at 6 °C before starting the thermal scan. The temperature-sensitivity was then tested by increasing the temperature from 6 °C to 94 °C at 1 °C/min heating rate and 2 °C/step. At the end of the thermal scan the sample was equilibrated at 94 °C and the CD spectrum was recorded. Once the thermal scan is completed, the samples were cooled to 6 °C and equilibrated for 15 min before recording the CD spectra. Data Analysis was performed using Applied Photophysics Chirascan Software and the transition temperatures were determined with Global 3 analysis software for dynamic multi-mode spectroscopy.

To study the effect of pH on the conformation of the peptide, pH titration measurements were performed as described previously (Lan *et al.* 2010a). Peptide

samples were prepared in 5 mM tris buffer pH  $\approx$  8.0 - 8.5 at 0.17 mg / ml (37.5  $\mu$ M). Acid titration was done by adding few  $\mu$ l of perchloric acid (HClO<sub>4</sub>) 0.5% – 5% (v/v) followed by back titration using NaOH (0.5-1 M). CD spectra of the samples were then recorded at each pH value with a Chirascan Spectrometer (Applied Photophysics, Leatherhead, UK) over the wavelength range from 260 to 180 nm using 0.5 mm cuvette. Data were analysed using Chirascan software after correcting the spectra by subtracting the spectrum of peptide-free Tris buffer solution. CD analysis was done in collaboration with Dr. Alex Drake, Dr. James Mason and Dr. Tam Bui from King's College London, UK.

#### **3.3.5.4 Solid-State NMR Experiments**

For solid-state NMR, samples with the lipid composition DPPC-d62:DSPC:DSPE-PEG<sub>2000</sub> (90:10:5) with or without peptide 200:1 & 100:1 mol/mol were prepared. A total of around 4.2 mg lipids per sample was dissolved and mixed together with the peptide in chloroform:methanol mixture and dried using a rotary evaporator at room temperature. In order to remove all organic solvent, the lipid films were exposed to vacuum overnight. The films were then rehydrated with 4 ml of ammonium sulphate 250 mM (pH 8.5) at 60 °C. Samples were subjected to five rapid freeze–thaw cycles for further sample homogenization, generating multi-lamellar vesicles, and then centrifuged at 21,000 g for 30 min at room temperature. The pellets, containing lipid vesicles and associated peptides were transferred to Bruker 4 mm MAS rotors for NMR measurements. Lipid vesicles were also prepared in this way in the absence of peptide. <sup>2</sup>H quadrupole echo experiments (Davis 1983) for samples containing DPPC-d62 were performed at 61.46 MHz on a Bruker Avance 400 NMR spectrometer using a 4 mm MAS probe, a spectral width of 100 KHz and with recycle delay, echo delay, acquisition time and 90° pulse lengths of 0.25 s, 100  $\mu$ s, 2.6 ms and 3  $\mu$ s respectively. The samples were maintained at different temperatures (41°C, 42°C, 43°C, 45°C & 50°C). During processing, the first 10 points were removed in order to start Fourier-transformation at the beginning of the echo. Spectra were zero filled to 1k points and 50 Hz exponential line-broadening was applied. Smoothed deuterium order parameter profiles were obtained from symmetrised and dePaked <sup>2</sup>H-NMR powder spectra of DPPC-d62 using published procedures (Davis 1983; Sternin *et al.* 1983; Schafer *et al.* 1995). Order parameters

were averaged along the length of the acyl chain and plotted as a function of temperature (Iacobucci *et al.* 2012). Solid-state NMR studies were performed in collaboration with Dr. James Mason, King's College London, UK.

### 3.3.5.5 Differential Scanning Calorimetry Measurements (DSC)

In order to determine the phase transition ( $T_m$ ) temperatures of the liposomes, 20  $\mu$ l samples of liposome suspension (10 mM) were placed in T zero hermetic aluminium pans sealed with lids. Samples were then thermally scanned from 30 °C to 60 °C at 1 °C/min heating rate using differential scanning calorimetry (Q2000 differential scanning calorimeter, TA Instruments, USA).

### 3.3.5.6 Fluorescence Anisotropy Measurements

Lp and Lp-Peptides hybrids were prepared then further diluted to 0.025 mM and divided into two 4 ml aliquots. DPH solution in tetrahydrofuran (0.8 mM, 2.5  $\mu$ l) or an aqueous ANS solution (10 mM, 4  $\mu$ l) was mixed with the liposomes at 500:1 lipid:DPH or 25:1 lipid:ANS. To allow the probes to be incorporated, the samples were shaken at room temperature for two hours then left overnight before starting measurements. Fluorescence polarization was then measured by LS-50B Fluorimeter (PerkinElmer) equipped with automated polarizer and thermostatic cell holder connected to a water bath to control the sample temperature. For the DPH experiment the anisotropy measurements were carried out at excitation slit 10 nm and emission slit of 5 nm and ,excitation and emission wavelengths of 361 nm and 425 nm respectively. ANS anisotropy was measured at slits of 10 nm and excitation and emission wavelengths of 395 nm and 476 nm, respectively. Measurements were started at 25 °C and then temperature increased gradually up to 60 °C. Sigmoidal curve fitting of the experimental points were performed using Origin software. The samples were equilibrated for at least 6 min after each temperature change. Fluorescence anisotropy was then measured automatically by the fluorimeter based on the following equation (Liaubet *et al.* 1994):

$$r = \frac{I_{V_V} - GI_{V_H}}{I_{V_V} + 2GI_{V_H}}$$

Where  $r$  is the fluorescence anisotropy,  $I_{V_V}$  and  $I_{V_H}$  are the emission intensity excited with vertically polarized light and measured with emission polarizer oriented in a parallel or perpendicular direction to the plane of excitation, respectively.  $G$  is an instrument specific factor calculated to correct the instrument polarization, which is equal to  $I_{HV}/I_{HH}$ , and obtained by measuring the vertically and horizontally polarized emission intensities after excitation with horizontally polarized light (Nagy *et al.* 2000).

### **3.3.5.7 Surface Plasmon Resonance (Francis *et al.*) Study of anti-MUC-1 TTSL-Ab Liposomes**

In order to confirm the anti-MUC-1 antibody binding capacity after conjugation to mal-DSPE-PEG<sub>2000</sub> and post-insertion into TTSL liposomes, SPR measurements were performed using a BIAcore 3000 (BIAcore, Upsala, Sweden) by assessing the binding of anti-MUC-1 antibody to MUC-1 epitope. Biot-MUC-1 or Biot-scrambled MUC-1 (control channel) was immobilized on the surface of a CM5 sensor chip using amine coupling kit. Immobilisation of streptavidin was performed by injecting, onto the activated surface by EDC/NHS of a sensor chip CM5, 35  $\mu$ l of streptavidin (100  $\mu$ g/ml in formate buffer, pH 4.3), which gave a signal of approximately 5000 RU, followed by 20  $\mu$ L of ethanolamine hydrochloride, pH 8.5, to saturate the free activated sites of the matrix. Biotinylated MUC-1 and scramble MUC-1 (1  $\mu$ M in HEPES buffer) were allowed to interact with streptavidin until a response of 700 RU was obtained.

All the binding experiments were carried out at 25 °C with a constant flow rate of 20  $\mu$ l/min. All biosensor assays were performed with HEPES-buffered saline (HBS-N) as running buffer (10 mM HEPES, 150 mM sodium chloride, pH 7.4). The different compounds were dissolved in the running buffer. Different concentrations of samples were injected for 3min., followed by a dissociation phase of 3min. The sensor chip surface was regenerated after each experiment by injection of 10  $\mu$ l of 100 mM HCl. The kinetic parameters were calculated using the BIAeval 4.1 software on a personal computer. Global analysis was performed using the simple Langmuir binding model 1.1. The specific binding profiles were obtained after subtracting the response signal from the peptide control. The fitting to each model was judged by the reduced chi

square and randomness of residue distribution. This work was done in collaboration with Dr. Olivier Chaloin (CNRS, France).

### 3.3.6 Remote Loading of Liposomes with DOX

For DOX loading, the ammonium sulphate gradient method was used (Haran *et al.* 1993). Liposomes were hydrated with ammonium sulphate 250 mM (pH 8.5) at 60 °C followed by extrusion and then flushed with N<sub>2</sub> gas and kept in the fridge for annealing overnight. Exchanging the external unencapsulated ammonium sulphate was performed by gel filtration through Sepharose CL-4B column (15 cm ×1.5 cm) (Sigma, UK) equilibrated with HBS (pH 7.4). Doxorubicin hydrochloride (5 mg/mL) was added to the liposome suspensions at 1:20 DOX:Lipids mass ratio in respect to the original total lipid concentration. Subsequently, samples were incubated at 37 °C (1.5 h) for LTSL or at 39 °C for Lp-Peptide hybrids (2 h) and TTSL (5 h). DOX loading into non temperature-sensitive liposomes was performed by incubation at 60 °C for either 1 h in case of NTSL or 10 min for DOPE:EPC:DSPE-PEG<sub>2000</sub> with and without peptide. After incubation liposomes were passed again through Sepharose CL-4B column to remove any free DOX. Encapsulation efficiency (% EE) was calculated by comparing the total fluorescence intensity of DOX post and pre gel filtration, diluted to the same final lipid concentration (Mills *et al.* 2005).

$$\% EE = I_{(t)} \text{ post column} / I_{(t)} \text{ pre column} * 100$$

Where,  $I_{(t)}$  is the total fluorescence intensity of the liposome suspension after adding 2 µl Triton X-100 (10% in HBS, pH 7.4). Liposomes used for animal experiments were concentrated to their original concentration using Viva spin 20 centrifuge tubes (Sartorius, Fisher) at 9000 rpm for 20-40 min. Liposomes for *in vivo* biodistribution studies were loaded with radio-labelled <sup>14</sup>C-DOX. All liposomes used for cell culture and *in vivo* studies were sterile filtered through 0.22µm filter before use.

### 3.3.7 Release Studies from Liposomes

CF and DOX release data were measured by taking advantage of the fluorescence quenching process. When CF or DOX are encapsulated inside the liposomes, their concentrations are very high resulting in self-quenching of their fluorescence signal.

When the ambient temperature exceeded the liposome transition temperature, CF and DOX were released from the liposomes and their concentrations are diluted resulting in increase in fluorescence intensity, which was used to monitor the release process. Release experiments were performed over 1 h at different temperatures in HBS or 50% CD-1 mouse serum (Sera Laboratories International, UK) at 0.8 mM final lipid concentration. For liposome stability studies, release in 50% CD-1 mouse serum was continued at 37 °C over night. At different time points samples were withdrawn and further diluted to 200 µL with HBS (pH 7.4) and measured in a quartz cuvette at either 480/595 nm excitation and emission wavelengths (slit 15/20 nm) in case of DOX or at 492/516 nm (slit 2.5/5) for CF using PerkinElmer Luminescence Fluorimeter (LS50B). The intensity of the fluorescence signals was then normalized and the percentage of DOX release was calculated as;

$$\% \text{ release} = [I_{(s)} - I_{(0)}] / [I_{(t)} - I_{(0)}], \text{ (Tai } et \text{ al. 2009)}$$

Where,  $I_{(s)}$  is the fluorescence intensity of individual samples at different time points,  $I_{(0)}$  is the background fluorescence intensity of liposome samples after purification and  $I_{(t)}$  is the fluorescence intensity of liposomes suspension after the addition of 2 µL of 10% Triton X-100 in HBS (pH 7.4).

### **3.3.8 Biocompatibility Studies**

#### **3.3.8.1 Lp-Peptide Hybrids Biocompatibility with B16F10 Cells**

To check for the cellular biocompatibility of Lp-Peptide hybrids, their effect on cellular viability was tested on B16F10 murine melanoma cancer cells. Cells were seeded overnight into 96-well plates (Corning Costar Corporation, USA) at a density of 6,000 cells per well. Next day, media was aspirated and cells were treated with 100 µl of Lp or Lp-Peptide hybrids (without DOX) diluted with medium to 0.5, 0.145 and 0.0145 mM total lipid concentration. Cells were incubated with liposomes for either 3 h or 24 h at 37°C. At the end of incubation culture media containing the liposomes was removed and cell viability was assessed with MTT assay. In brief, media were aspirated and replaced with 120 µl of MTT solution (5mg/ml), at 1:5 dilutions in fresh media and incubated for 1.5-2 h at 37 °C to allow for the formation of Formazan crystals. At the end of incubation, culture medium was removed by gentle tapping and the Formazan crystals were dissolved by adding 150 µl of DMSO

solution (Fisher Scientific, UK) using multichannel pipette. Plates were incubated for another 15 min at 37 °C to remove any air bubbles. The Formazan absorbance (A) was measured at 570 nm in Fluostar Omega plate reader (BMGLabtech,UK). The results were expressed as the percentage of cell viability ( $n = 6 \pm S.D$ ) compared to control untreated cells using the following formula:

$$\% \text{ cell viability} = A \text{ treated cells} / A \text{ control} \times 100$$

Where, A treated cell is the absorbance of treated cells and A control is the absorbance of control cells treated with media only.

### **3.3.8.2 Lp-Peptide Hybrids Biocompatibility with HUVEC Cells**

In addition to testing the biocompatibility of Lp-Peptide hybrids on B16F10 cells, we also checked their effect on primary human umbilical vein endothelial (HUVEC) cells. HUVEC cells were plated into 96-well plates (Costar, Corning Life Sciences, Amsterstam, the Netherlands) at a density of  $4 \times 10^4$  cells/well (100  $\mu$ l medium per well). Before plating, the 96-well inserts were treated for 30 min with 50  $\mu$ l of 1% gelatine in MilliQ (Merck, Schiphol-Rijk, The Netherlands) at 37 °C in a humidified cell incubator followed by incubation for 30 min with 95  $\mu$ l of 5  $\mu$ g/ml fibronectin (Roche Diagnostics, the Netherlands) at 37 °C in a humidified cell incubator.

The experiment was performed the day after plating. Throughout the experiment, cells were kept in the humidified cell incubator. EGM-2 medium was replaced by EGM-2 medium containing Lp or Lp-Peptide hybrids (0.145 mM) without DOX. After 4 h or 24 h, the EGM-2 medium containing liposomes was removed and the cells were washed once with fresh EGM-2 medium. HUVEC cells were allowed to recover for 24 h and cell viability was assessed by MTT assay (Cell Proliferation Kit I, Roche Diagnostics, the Netherlands). Briefly, 10  $\mu$ l MTT labelling reagent was added per well. After 4 h, 100  $\mu$ l of solubilisation solution was added and the 96-well plate incubated overnight in the humidified cell incubator. Absorbance was measured at 595 nm and 655 nm in a Model680 microplate reader from Bio-Rad (Veenendaal, the Netherlands). Absorbance (595 nm minus 655 nm) was expressed as percentage of control treated HUVEC cells (i.e. HEPES buffer only). HUVEC cells treated with 1% Triton X-100 were used as positive controls. The experiment was performed in



triplicates. This experiment was done in collaboration with Dr. Klazina Kooiman (Erasmus MC, Netherlands).

### **3.3.8.3 ELISA Studies**

To check the biocompatibility of the Lp-Peptide hybrids after *in vivo* administration, B16F10 tumour-bearing C57 mice were injected with either empty Lp-Peptide 200:1 or DOX-loaded Lp-Peptide 200:1 followed by local heating of the tumour in a water bath at 42 °C for 1 h. To check for the development of immune response against Lp-Peptide hybrids, serum was collected 1 week after injection and the total antibody level was quantified by ELISA and compared to control (non-injected mice). High-binding ELISA plates (Costar, UK) were coated overnight with serum samples (100 µl) at a dilution of 1:1000 at 4 °C. After washing with PBS containing 0.01% Tween 20, the plates were blocked with 3% BSA in PBS for 2 h. Plates were then washed with TBS for 3 times and incubated with HRP-label anti-mouse IgG at 1:1000 dilution (100 µl) for 1 h at room temperature. 1-Step Ultra TMB-ELISA was used as a detection system. Then the reaction was stopped by adding sulphuric acid (2 M) and absorbance was measured at 450 nm in Fluostar Omega plate reader (BMGLabtech, UK). This experiment was performed in collaboration with Dr. Açelya Yilmazer (Nanomedicine Lab, UCL School of Pharmacy).

### **3.3.9 Cellular Binding and Uptake Studies**

Cells were grown overnight on glass cover slip in 24 tissues culture well plate (corning USA) at either 20,000 cells per well (B16F10) or 40,000 cells per well (MDA-MB-435, MCF-7 & C33a) to reach confluency. Different incubation procedures were applied which are explained below under each section. At the end of incubation, cells were washed with PBS and fixed with paraformaldehyde (PFA) 4% (Thermoscientific, UK) for 10-15 min at room temperature then mounted using 3 µl Vectashiled mounting medium with DAPI H-1200 (Vector Laboratories). Cells were then imaged with confocal laser scanning microscopy (CLSM) Zeiss LSM 710 (Oberkochen, Germany) using EC Plan-Apochromat 40x/1.3 oil lense. DAPI staining of nucleus was detected at 405 nm laser excitation source and 410 nm output filter, whereas DiI and Cy3 were imaged at 514 nm laser excitation source and 585 nm

output filter. DOX fluorescence signal was detected at 488nm laser excitation source and 535–674 nm output filters.

### **3.3.9.1 Cellular Uptake of Lp-Peptide Hybrids**

The cellular uptake of Lp-peptide hybrids was studied in B16F10 cells and compared to liposomes without the peptide. Cells were treated with DiI-labelled Lp and Lp-peptide hybrids (without DOX) at 0.145 mM and 0.5 mM total lipid concentration for 3 h and 24 h at 37 °C. At the end of incubation cells were washed with PBS, fixed, mounted and imaged with CLSM as described above.

### **3.3.9.2 Cellular Binding of MUC-1 Ab**

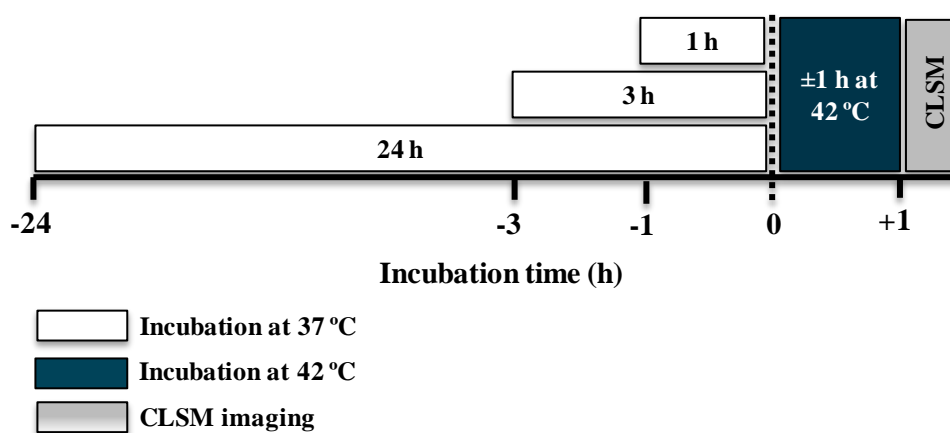
To investigate the expression of MUC-1 antigen MDA-MB-435, MCF-7 and C33a cancer cell lines were incubated with anti-MUC-1 antibody (1 µg/ml) for 3 h at 37 °C. At the end the incubation, cells were washed with PBS and fixed with PFA 4% (Thermoscientific, UK) for 10-15 min at room temperature. Cells then washed with PBS and permeabilize with 0.5% Triton X-100 for 10 min and incubated with a blocking solution composed of 4% goat serum and 3% BSA in PBS for 30 min. At the end of incubation, cells were washed and incubated with anti-human Cy3-labelled secondary antibody at 1:220 dilution in blocking solution (2 h at room temperature protected from light). Cy3-labelled antibody was then removed and cells were mounted using 3 µl Vectashiled mounting medium with DAPI H-1200 (Vector Laboratories). Anti-MUC-1 antibody binding capability was also checked after each step of conjugation to TTSL liposomes and DOX loading by incubation with MDA-M-435 (MUC-1+ve) at 1 µg/ml for 1 h at 37 °C. Cells were then stained after incubation with Cy3-labelled antibody using the same procedure described above and imaged with CLSM.

### **3.3.9.3 Cellular Uptake of MUC-1 TTSL-Ab**

Cellular uptake studies of DOX-loaded and DiI-labelled TTSL and TTSL-Ab liposomes (150 µM lipid, 10 µM DOX) were performed independently due to the overlap in the fluorescent spectrum of DOX and DiI. First, to study the cellular uptake kinetics, DOX-loaded TTSL, TTSL-Ab-I and TTSL-Ab-II uptake by MDA-MB-435 and C33a was studied after 1 h, 3 h and 24 h incubation at 37 °C. At the end

of incubation cells were washed with PBS to remove any unbound liposomes, and imaged with CLSM with or without 1 h heating at 42 °C at the end of incubation time (Scheme 3-1).

The effect of antibody conjugation on the uptake of the liposomes itself by MDA-MB-435 cells was also studied after 1 h and 3 h incubation with DiI-labelled liposomes at 37 °C. At the end of incubation time, cells were washed with PBS to remove unbound DiI-labelled liposomes and visualized with CLSM as described above.



**Scheme 3-1:** Schematic presentation of the time frame of cellular uptake studies of DOX-loaded TTSL, TTSL-Ab-I and TTSL-Ab-II by MDA-MB-435 and C33a cells.

### 3.3.10 Cellular Cytotoxicity Studies (MTT Assay)

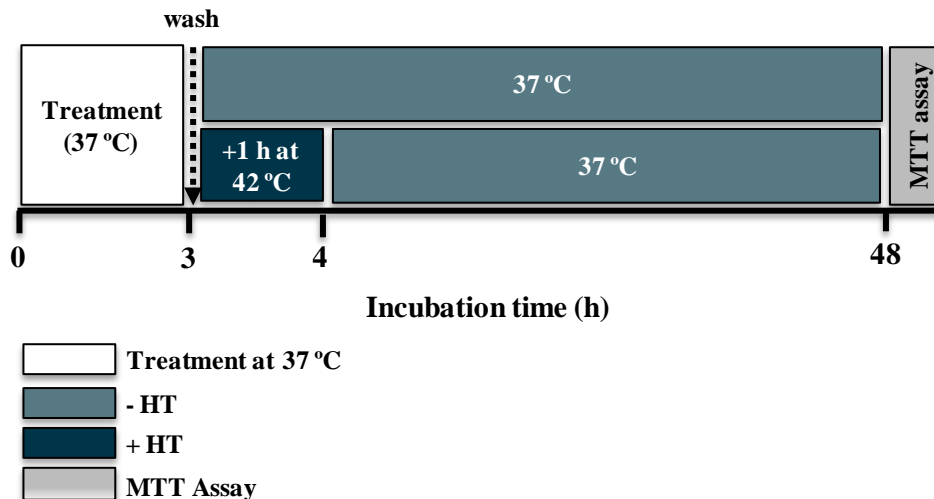
#### 3.3.10.1 Cytotoxic activity of DOX-Loaded Lp-Peptide Hybrids

*In vitro* cytotoxicity of DOX-loaded LTSL, Lp-Peptide 200:1 hybrids and TTSL were compared using MTT reduction assay. Briefly, B16F10 and SW480 cells were plated into 96 well plates (Coster, USA) at 6,000 and 10,000 cells per well, respectively. Cells were incubated overnight at 37 °C before treatment. To assess the stability and the thermal sensitivity of Lp-Peptide hybrids compared to LTSL and TTSL, liposomes were heated for 1 h at 42 °C in complete media before incubation with the cells and compared to non-heated liposomes. Cells were then treated with both heated and non-heated liposomes at 10 µM DOX concentration for 3h at 37 °C in CO<sub>2</sub> Incubator. At the end of treatment, cells were washed and replaced with liposomes-free media and incubated at 37 °C for either 24 h or 48 h. Cell viability

was then assessed with MTT assay as explained in section 3.3.8.1 and the results were expressed as percentage of untreated control cells.

### 3.3.10.2 Cytotoxic activity of MUC-1 TTSL-Ab

Cytotoxicity of DOX-loaded TTSL and TTSL-Ab was also studied by MTT reduction assay; however, different incubation protocol was applied. Briefly, MDA-MB-435 (MUC-1+ve) and C33a (MUC-1-ve) cells were plated in 96 well plates (Coster, USA) at 8,000 and 10,000 cells/well, respectively and incubated at 37 °C overnight before treatment. Cells were then treated with free DOX, TTSL, TTSL-Ab-I and TTSL-Ab-II at 10 µM for 3 h at 37 °C in CO<sub>2</sub> incubator. At the end of 3 h treatment, cells were washed and replaced with liposomes-free media. At this stage plates were either incubated at 37 °C for 48 h or treated for 1 h at 42 °C in CO<sub>2</sub> incubator followed by incubated at 37 °C for 48 h (Scheme 3-2), to evaluate the effect of triggering the drug release after cellular binding and internalisation. Cell viability was then assessed with MTT assay and expressed as % of untreated cells as described in section 3.3.8.1.



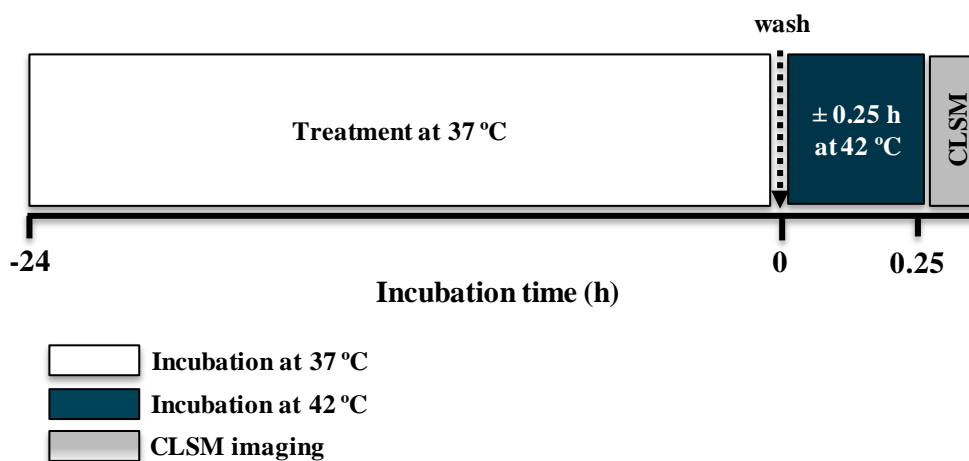
Scheme 3-2: Schematic presentation of the protocols used to assess the cytotoxicity of TTSL-Ab.

### 3.3.11 Localisation and Cytotoxicity Studies Using Multicellular Spheroids (MCS)

MCF-7 (MUC-1+ve) MCS were used in these experiments instead of MDA-MB-435 due to the inability of the later to form MCS. MCF-7 spheroids were prepared

using a previously published liquid overlay technique (Yuhas *et al.* 1977). Briefly, MCF-7 cells obtained by trypsinization of monolayer growth cultures were seeded at 10,000 cells/well into 96 well plates coated with 100  $\mu$ l of sterile 1% purified agar (Oxoid, UK) in D.W.

After 4 days culture on agar spheroids with diameters of approximately 500  $\mu$ m were selected under an inverted phase-contrast microscope with an ocular graticule. MCS were pooled into 15 ml plastic tubes and allowed to sediment for few min. After sedimentation, the bulk of the medium was removed, leaving the spheroids in the bottom of the tubes. MCS were then mixed with 5 ml medium containing either free DOX, TTSL or TTSL-Ab (26  $\mu$ g Ab/ $\mu$ mol lipid) at 10  $\mu$ M DOX concentration and transferred to 50 mm diameter Petri dishes coated with 10 ml of 1% agar and incubated for 24 h at 37 °C. At the end of incubation, MCS were washed 3 times with PBS and placed in fresh incubation medium. To evaluate the effect of HT on DOX penetration and MCS growth retardation, MCS incubated with TTSL-Ab were heated for 15 min at 42 °C in a water bath with continuous shaking and compared to untreated MCS (Scheme 3-3).



**Scheme 3-3:** Time line frame of the protocol used for testing TTSL and TTSL-Ab on MCF-7 MCS.

DOX penetration into the MCS was imaged with CLSM (Zeiss LSM 710, Oberkochen, Germany) using sterile 35 mm glass-bottom culture dishes (MatTek, USA) at 488 nm laser excitation source and 535–674 nm output filter using EC Plan-Neofluar 10x objective to detect DOX fluorescence signals. Distribution of DOX

signal throughout the MCS was studied with Zeiss LSM 710 confocal microscope using Z-stack imaging at 58.8  $\mu\text{m}$  penetration depth. Images were then analyzed using LSM 710 image software.

To evaluate the growth retardation effect of anti-MUC-1 TTSL-Ab, MCS were transferred into 50 mm Petri dishes coated with 1% agar and incubated with fresh medium at 37 °C over 3 weeks with replacement of the media twice a week. MCS were then regularly imaged at 10x inverted microscope. MCS volume ( $v$ ) was then calculated by measuring MCS dimensions using Image J software applying the following equation:

$$v = \frac{L \times W^2}{2}$$

Where, L and W are the length and width of the MCS respectively. Normalized volume ratio was then calculated as  $v/v_0$ , where  $v_0$  is the volume of the spheroids on the first day of treatment.

### **3.3.12 Animals and Tumour Models**

5-6 week-old females C57BL6 mice (15-20 g) were purchased from Harlan (UK Limited, U.K). 5-6 week-old female athymic nude mice (20-25 g) were purchased from Charles River Laboratories, UK. Mice were housed in groups of 5 with free access to water at 19-22 °C, relative humidity of 45-65% and a 12 h light/dark cycle. Individually vented cages (IVC; Allentown, USA) were used in case of athymic nude mice. Animal procedures were performed in compliance with the UK Home Office Code of Practice for the Housing and Care of Animals used in Scientific Procedures. Mice were acclimatized to the environment for at least 7 days before performing the procedures and tumour implantation.

Tumour implantation was performed by injection tumour cells into the right lower leg using 26G needles. B16F10 melanoma was established by subcutaneous injection of  $2.5 \times 10^5$  B16F10 melanoma cells in a volume of 20  $\mu\text{l}$  of PBS. SW480 human colon adenocarcinoma tumour model was inoculated by subcutaneous injection of  $5 \times 10^6$  SW480 cells in a volume of 100  $\mu\text{l}$  of serum free advanced RPMI media supplemented with 1% L-glutamine. MUC-1 overexpressing MDA-MB-435 tumour

model was established by subcutaneous injection of  $1 \times 10^7$  MDA-MB-435 cells in a volume of 150  $\mu\text{l}$  of DMEM media.

The tumour volume was estimated by measuring three orthogonal diameters (a, b, and c) with calipers; the volume was calculated as  $(a \times b \times c) \times 0.5 \text{ mm}^3$ . The experiments were performed when the tumour volume reached 200-400  $\text{mm}^3$  for biodistribution and 100  $\text{mm}^3$  for therapy.

### **3.3.13 Pharmacokinetics and Biodistribution Studies**

To study the pharmacokinetics and biodistribution profile of liposomes, they were prepared in 25 mM (total lipid concentration) as describe earlier and loaded with radiolabelled  $^{14}\text{C}$ -DOX (equivalent to 0.2  $\mu\text{Ci}/\text{dose}$ ). Mice (n = 3-4) were anesthetized by inhalation of isoflurane and injected *via* the tail vein with 200  $\mu\text{l}$  of the liposomes suspension (equivalent to 2.5  $\mu\text{mol}$  of lipids/200  $\mu\text{l}$ , DOX 5 mg/kg) in HBS.  $^{14}\text{C}$ -DOX levels in blood profile, organs and tumour were then quantified.

Local hyperthermia was applied by immersing the tumour-bearing leg in a water bath stabilized at 43  $^{\circ}\text{C}$ . Animals were anesthetized by inhalation of isoflurane and the body temperature of the mice was monitored with a rectal thermocouple. A fan and a heating pad were used to maintain the body temperature at 36-37  $^{\circ}\text{C}$ . Experimental conditions and HT protocols applied for each study are explained in details below.

#### **3.3.13.1 Pharmacokinetics and Biodistribution Studies of $^{14}\text{C}$ -DOX Loaded Lp-Peptide Hybrids**

The blood circulation profile of Lp-Peptide 200:1, LTSL and TTSL were studied after *in vivo* administration into C57BL6 mice. At different time points, mice were bled by tail vein puncture and 70  $\mu\text{l}$  of blood was collected using a heparinized capillary tube. Blood withdrawn did not exceed 10% of the mouse blood volume per day. The mice were killed after 1 h and 24 h by cervical dislocation (Al-Jamal *et al.* 2009a). The total radioactivity in the blood was calculated based on the assumption that the total blood volume is accounting 7.3% of the total body weight (Buiting *et al.* 1996). Blood profile of Lp-Peptide 200:1 was also studied in comparison to Lp

without peptide and Lp-Peptide II 200:1, which has leucine zipper peptide of higher transition temperature (VSSLESK)<sub>6</sub> using the same procedure described above.

The amount of <sup>14</sup>C-DOX accumulated in the tumours and organs in response to heat treatment was also quantified by applying local HT immediately after injection and maintained for 60 min. At 1 h and 24 h post injection and heat application, the mice were killed and organs, including tumours, were excised. The results were represented as the percentage of the injected dose (% ID) per gram tissue.

### **3.3.13.2 Biodistribution Studies of <sup>14</sup>C-DOX Loaded TTSL and TTSL-Ab**

The effect of anti-MUC-1 antibody conjugation to TTSL liposomes on their pharmacokinetics and biodistribution parameters was also studied after *in vivo* administration into MDA-MB-435 tumour-bearing athymic nude mice. <sup>14</sup>C-DOX level in the blood and accumulation in the organs and tumour from TTSL-Ab (26 µg Ab/µmol lipid) was quantified and compared to non-targeted TTSL applying three different heating protocols as described in Chapter 6 (Scheme 6-1). HT protocols were classified depending on whether or not 60 min local HT was applied and the timing of HT application relative to the injection. The purpose of such variation is to study the effect of HT on the extravasation of targeted TTSL-Ab into solid tumours. In all three heating protocols studied a 2nd HT was applied over 30 min 24 h after injection to trigger intracellular drug release. Organs and tumours were collected 1 h and 24 h after injection, before and after, the application of 2nd HT. The results were represented as the percentage of the injected dose (% ID) per gram tissue.

### **3.3.13.3 Radioactivity Measurements in the Blood and Tissues**

The quantification <sup>14</sup>C-DOX was carried out as previously described (Al-Jamal *et al.* 2009b). Blood and whole organs samples (except liver 100 mg) were transferred to 20 mL scintillation vials and solubilised with 1 mL of Soluene-350 tissue solubilizer (PerkinElmer, UK), with continuous shaking overnight at 55°C. Samples were decolourized before adding the scintillation cocktail by adding 0.3 ml of 30% H<sub>2</sub>O<sub>2</sub> and 0.3 ml of isopropanol as an antifoaming agent. Samples were shaken at 55 °C for at least 1-3 h to expel H<sub>2</sub>O<sub>2</sub> before adding the scintillation cocktail. Samples were then mixed with 20 ml of Optiphase “Safe” scintillation cocktail (Fisher Scientific, UK) acidified with 0.7% (v/v) glacial acetic acid to eliminate any chemi-



luminescence, and counted in an LS6500 multipurpose scintillation counter (Beckman, USA).

### **3.3.14 *In Vivo* Optical Fluorescence Imaging**

*In vivo* optical imaging was used to study the accumulation of DOX into tumour-bearing mice by looking at the optical fluorescence signal in live animals. Mice were imaged by IVIS Lumia II imaging system (Caliper Life Sciences Corp., Alameda, CA) using the following setting; exposure 10 seconds, binning medium, F stop 2, FOV D and height 1.5. Images were taken at 500 nm/DsRed excitation and emission filters and corrected by subtraction from background images performed at 430 nm excitation wavelength and GFP emission filter. Images analysis was done with Living Image software 3.2 (Caliper Life Sciences Corp) and displayed as fluorescent efficiency images, where the value of each pixel represents the fractional ratio of fluorescent emitted photons per incident excitation photon. Optical imaging was used to study the effect of HT protocols on DOX accumulation into SW480 and MDA-MB-435 tumours as will be explained in the following sections. DOX fluorescent intensity at the tumour site was quantified by drawing region of interest (ROI) that covers the tumour-bearing leg and values expressed as total efficiency, which is a unitless value represents the ratio of emitted light to incident light.

#### **3.3.14.1 Optical Imaging of DOX Accumulation into SW480 Tumour Using Intravascular and Interstitial Release Protocols**

Optical imaging was used to study DOX accumulation into SW480 tumour-bearing athymic nude mice from LTSL, Lp-Peptide 200:1 hybrids and TTSL comparing both intravascular and interstitial release protocols. For intravascular release protocol IVIS acquisition was performed 1 h and 24 h after injection, while for the interstitial release protocol images were taken 24 h after injection, before and after 2nd HT, using the imaging settings described earlier.

#### **3.3.14.2 Optical Imaging of DOX Accumulation into MDA-MB-435 Tumour by MUC-1 TTSL-Ab**

In addition to quantification of <sup>14</sup>C-DOX accumulation in the tumour, DOX retention in the tumour *in vivo* was studied by optical imaging in live animals. TTSL

and TTSL-Ab (26  $\mu\text{g}$  Ab/ $\mu\text{mol}$  lipid) injected tumour-bearing athymic nude mice were imaged using IVIS Lumia II imaging system. Images were taken at the same time points used for biodistribution experiment studying the same HT protocols described in Chapter 6 (Scheme 6-1).

### **3.3.15 *In vivo* Tumour Growth Delay and Survival Studies**

Therapeutic activity of TSL studied in this thesis was evaluated by their effect on tumour growth retardation after *in vivo* administration. Tumours were measured with calipers as described under tumour establishment. Mice were also examined for any change in the body weight or signs of toxicity twice a week. Tumour measurements were blinded to the experimental conditions. Therapy experiments were terminated when tumours reached 1000  $\text{mm}^3$  and mice were scarified by cervical dislocation.

#### **3.3.15.1 *In Vivo* Tumour Growth Delay and Survival of TSL Comparing Intravascular and Interstitial Release Protocols**

The therapeutic activity of Lp-Peptide hybrids was studied after *in vivo* administration into SW480 tumour-bearing athymic nude mice. We studied the therapeutic activity of Lp-Peptide hybrids using two HT protocols to mimic intravascular and interstitial drug release (in comparison with LTSL and TTSL).

When the tumour volume reached 100  $\text{mm}^3$  (day 11 after implantation), mice were divided into groups (5-7 mice/group) and treated with single administration of LTSL, Lp-Peptide 200:1 hybrids or TTSL (5mg/kg DOX) by intravenous injection applying either intravascular or interstitial release protocols described in Chapter 5 (Scheme 5-1). Control mice in both protocols are mice treated with HT only without receiving any injection.

For the intravascular drug release single, HT was applied directly after TSL intravenous injection to trigger drug release from TSL within the heated tumour vasculature. Alternatively, for the interstitial release protocol, two HT sessions were used. The 1st HT was over 1 h prior to TSL injection to increase the local tumour endothelial cells permeability. 24 h after TSL injection a 2nd HT treatment was given (over 30 min) to trigger drug release interstitially from TSL accumulated within the tumour.

### **3.3.15.2 *In Vivo* Tumour Growth Delay and Survival of MUC-1 TTSL-Ab**

The therapeutic activity of MUC-1 targeted TTSL-Ab (26 µg Ab/µmol lipid) compared to non-targeted TTSL was evaluated after *in vivo* administration into MDA-MB-435 (MUC-1+ve) tumour-bearing athymic nude mice. TTSL and TTSL-Ab (5mg/kg DOX) were administered by single intravenous injection on day 13 after tumour inoculation using HT protocol 3 (Scheme 6-1) with and without application of 2nd heating 24 h after injection. Tumour volume and body weight was monitored twice a week as described earlier.

### **3.3.16 Histopathological Analysis**

To assess for any histological changes as a result of treatment with DOX loaded TSL, major organs were collected from treated mice and compared to control mice. Mice were sacrificed by cervical dislocation 3-5 weeks after injection with the exception of mice treated with TTSL liposomes (interstitial release protocol) who had to be euthanized earlier (10 days after injection) because of the severe weight loss (15-20% of initial weight). Tissue samples were fixed in neutral buffered formalin and processed routinely into paraffin before sectioning and staining with Haematoxylin and Eosin (H & E).

### **3.3.17 Statistical Analysis**

Statistical analysis of the data was performed using Graph Pad Prism software. Two-tailed unpaired student t-test and one-way analysis of variance (ANOVA) followed by the Tukey multiple comparison test were used and p values < 0.05 was considered significant.

## **CHAPTER 4**

---

### **DESIGN AND CHARACTERIZATION OF LP- PEPTIDE HYBRIDS**

This chapter describes the design and characterization of leucine zipper lipid-peptide hybrid vesicles (Lp-Peptide) engineered by self-assembled anchoring of the amphiphilic peptide within the lipid bilayer. These hybrid vesicles aim to combine the advantages of traditional temperature-sensitive liposomes with the dissociative, unfolding properties of a temperature-sensitive peptide to optimize drug release under mild hyperthermia and maintain *in vivo* drug retention. The secondary structure of the peptide and its thermal responsiveness after anchoring onto liposomes were studied with CD. In addition, the interaction of the peptide with the lipid bilayer was studied with fluorescent anisotropy and solid state NMR studies. A model drug molecule, doxorubicin, was successfully encapsulated in the Lp-Peptide vesicles at higher than 90% encapsulation efficiency following the remote loading, using ammonium gradient methodology. The release of doxorubicin from Lp-Peptide hybrids *in vitro* was studied at physiological temperatures and after exposure to mild HT (42 °C).

## 4.1 Introduction

Poly- and oligopeptides can be readily produced with a defined sequence and chain length offering better control of transition temperatures compared to general synthetic polymers (Aluri *et al.* 2009). MacKay and Chilkoti have proposed that oligopeptides with repeated short sequences (< 7 amino acids in length) can generate a highly ordered biopolymer with complex temperature-responsive properties that could provide new tools for engineering hyperthermia mediated drug delivery systems (Mackay *et al.* 2008). From the drug delivery point of view, two important properties of temperature-sensitive peptides should be considered; directionality and reversibility. Directionality usually refers to the self-association and dissociation changes of the peptide in response to heating. Reversibility describes whether or not the peptide secondary structure is retained upon cooling (Mackay *et al.* 2008). Elastin-like polypeptides (ELPs) are examples of temperature-responsive peptides that have shown promising results in cancer therapy due to their ability to deposit and switch conformation in heated tissues and tumours. ELPs have been incorporated into self-assembled nanoparticles encapsulating drug or directly conjugated to drug molecules (Mackay *et al.* 2008). Aluri *et al.* and McFarlane *et al.* have described conformationally ordered peptides that can potentially be used in drug delivery systems by trapping therapeutics in assembled particulate drug carriers or in the form of switchable hydrogels to control the drug release at elevated temperature (Aluri *et al.* 2009; McFarlane *et al.* 2009).

In the present work we have investigated the engineering of previously characterized thermo-responsive liposome systems based on anchoring a temperature-sensitive amphiphilic peptide within a temperature-responsive lipid bilayer (Lp-Peptide). Our approach aims to combine the traditional temperature-responsive liposome system technology with the dissociative/unfolding properties of a leucine zipper sequence peptide to allow better control, modulation and timing of drug release under mild hyperthermia, while improving *in vivo* drug retention.

We have chosen a leucine zipper with the amino acid sequence [VSSLESKVSSLESKVSKLESKKSLESKVSKLESKVSSLESK]-NH<sub>2</sub> for its interesting ability to dissociate above its melting temperature (~40 °C) into a disordered conformation in the temperature range that is clinically attainable



Our results in this chapter show that leucine zipper peptides successfully incorporate into lipid bilayers during liposome preparation without affecting the liposome morphology or size characteristics. In addition, Lp-Peptide hybrids have fast release of DOX following localized mild HT application which was comparable to LTSL. The leucine zipper peptide appears to be in an unfolded state at the higher temperatures required for drug release. Lp-Peptide Hybrids exhibit a promising enhancement in serum stability at physiological temperature compared to LTSL without compromising the thermo-responsiveness of the system at 42 °C. The engineered Lp-Peptide hybrids incorporating a temperature-sensitive peptide provide a new class of clinically-relevant thermosensitive liposomes suitable for *in vivo* applications.



## 4.2 Results

### 4.2.1 Preparation and Characterization of Liposomes

Liposome-Peptide (Lp-Peptide) hybrids were prepared by incorporating the peptide into temperature-responsive DPPC:DSPC:DSPE-PEG<sub>2000</sub> (90:10:5) liposomes. To study the effect of peptide incorporation into liposomes on their *in vitro* properties, different lipid:peptide molar ratios (600:1, 200:1 and 100:1) were studied. The lipid composition of the formulation was optimized based on DSC data by testing different molar ratios of DPPC:DSPC liposomes (Table 4-1). DPPC:DSPC 90:10 mol/mol was chosen since its  $T_m$  is around 42 °C which can be clinically attainable.

**Table 4-1: Transition temperature ( $T_m$ ) of different molar ratios of DPPC:DSPC liposomes**

Liposomes composition (mol/mol)	Transition temperature ( $T_m$ ) mean $\pm$ STD (n=3)
DPPC:DSPC 90:10	41.64 $\pm$ 0.38
DPPC:DSPC 80:20	42.99 $\pm$ 0.20
DPPC:DSPC 70:30	43.65 $\pm$ 0.28
DPPC:DSPC 60:40	46.41 $\pm$ 0.06
DPPC:DSPC 50:50	47.83 $\pm$ 0.35

To impart stealth properties to the liposomes and to increase their circulation time in the blood stream, 5 mol% of DSPE-PEG<sub>2000</sub> lipids were included into DPPC:DSPC (90:10) liposomes (Li *et al.* 2010). A slight increase in  $T_m$  (Table 4-2) was observed after addition of DSPE-PEG<sub>2000</sub> lipid which agrees very well with previous studies (Gaber *et al.* 1995).

**Table 4-2: Transition temperature ( $T_m$ ) of DPPC:DSPC (90:10) liposomes with and without the inclusion of 5 mol% of DSPE-PEG<sub>2000</sub> lipid**

Liposomes composition (mol/mol)	Transition temperature ( $T_m$ ) mean $\pm$ STD (n=3)
DPPC:DSPC 90:10	41.9 $\pm$ 0.10
DPPC:DSPC:DSPE-PEG <sub>2000</sub> 90:10:5	42.64 $\pm$ 0.15

Also included in the study are two different types of TSL as positive controls; LTSL that have shown ultrafast release properties (Needham *et al.* 2000; Mills *et al.*

2005) and TTSL that have intermediate drug release rate (Gaber *et al.* 1996). As a negative control, non temperature-sensitive liposomes (NTSL) based on the formulation of clinically approved liposomal doxorubicin (Doxil<sup>®</sup>) were also included in our experiments.

Table 4-3 shows that Lp and Lp-Peptide hybrids had a hydrodynamic diameter of around 100 nm with low polydispersity index ( $PDI \leq 0.1$ ) and are slightly negatively charged. The incorporation of the peptide, at all ratios, did not affect the size or surface properties of the liposomes (Figure 4-2 A & B).

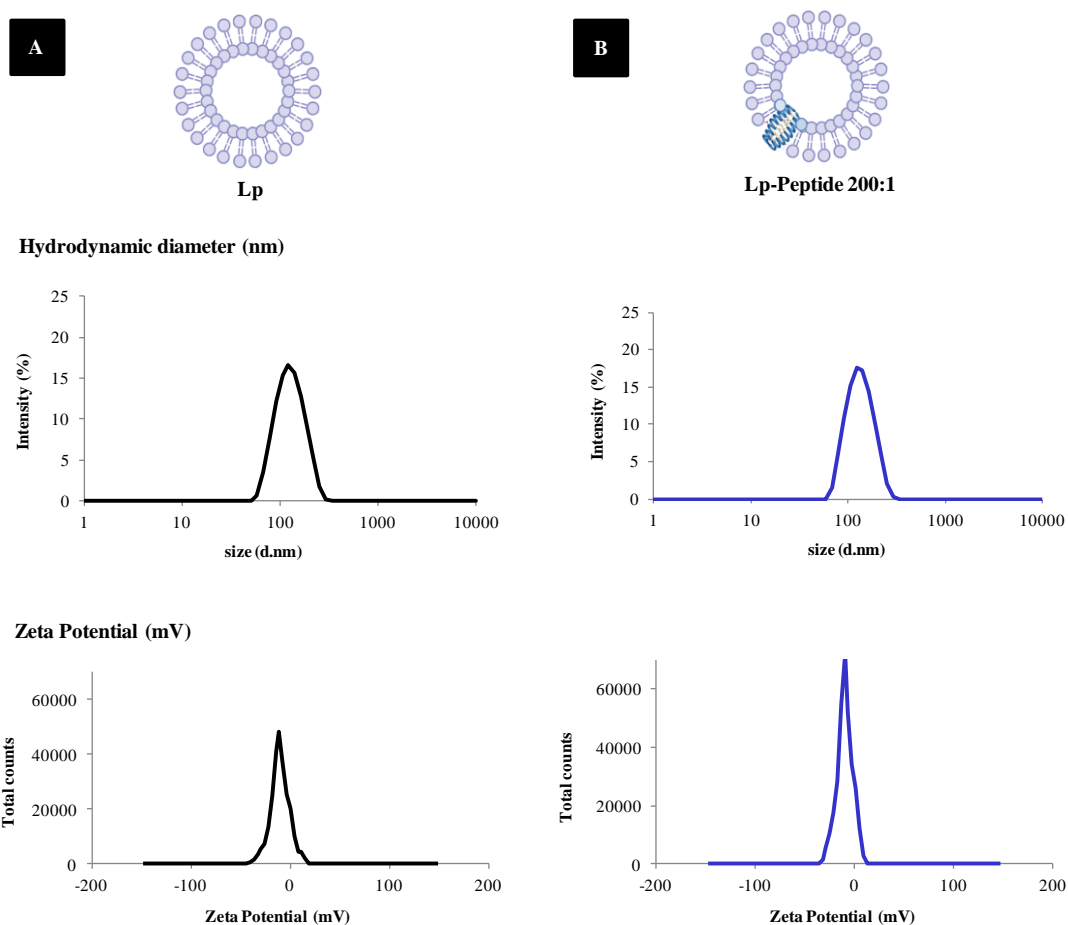


**Figure 4-2: Hydrodynamic diameter and zeta potential of the DPPC:DSPC:DSPE-PEG<sub>2000</sub> liposomes (A) before and (B) after incorporation of peptide.**

**Table 4-3: Physicochemical characterization data; hydrodynamic diameter, polydispersity Index (PDI), zeta-potential, and phase transition temperature (T<sub>m</sub>) of Lp, Lp-Peptide, Lp-CHOL, LTSL, TTSL and NTSL.**

Liposomes composition (mol/mol)	Peptide mol%	Lipid:Peptide (mol/mol)	Size (nm)	PDI	Zeta Potential (mV)	DOX loaded liposomes		
						Size (nm)	PDI	T <sub>m</sub> (°C)
DPPC:DSPC: DSPE-PEG <sub>2000</sub> (90:10:5)								
Lp	0.0%	-	123 ± 11.0	0.10 ± 0.050	-12.0 ± 3.00	118 ± 0.80	0.06 ± 0.020	42.6
Lp-Peptide 600:1	0.0017%	600:1	128 ± 0.40	0.07 ± 0.003	-8.00 ± 0.82	128 ± 1.14	0.08 ± 0.016	42.6
Lp-Peptide 200:1	0.5%	200:1	114 ± 1.70	0.06 ± 0.020	-9.89 ± 1.32	128 ± 2.30	0.09 ± 0.015	42.9
Lp-Peptide 100:1	1.0%	100:1	128 ± 1.62	0.05 ± 0.003	-9.10 ± 0.45	127 ± 0.68	0.01 ± 0.015	42.6
DPPC:DSPC:DSPE-PEG <sub>2000</sub> :CHOL (90:10:5:0.5) (Lp-CHOL)								
	-	-	126.0 ± 18.0	0.09 ± 0.055	-13.3 ± 0.51	123 ± 0.10	0.07 ± 0.009	42.8
DPPC:MSPC:DSPE-PEG <sub>2000</sub> (90:10:4) (LTSL)								
	-	-	97.00 ± 5.01	0.07 ± 0.03	-9.69 ± 0.11	99 ± 1.53	0.06 ± 0.010	41.4
DPPC:HSPC:CHOL:DSPE-PEG <sub>2000</sub> (54:27:16:3) (TTSL)								
	-	-	105.2 ± 3.61	0.05 ± 0.02	-8.40 ± 1.10	101 ± 1.03	0.05 ± 0.02	44.2
HSPC:CHOL:DSPE-PEG <sub>2000</sub> (56.3:38.2:5.5) (NTSL)								
	-	-	105.0 ± 1.53	0.05 ± 0.01	-7.97 ± 0.77	107 ± 2.89	0.07 ± 0.01	-

Data expressed as mean ± STD (n=3)

The morphology of the Lp-Peptide hybrids was examined by transmission electron microscopy (TEM) (Figure 4-3, top panel). TEM images showed well-dispersed, round shaped vesicles that correlated with dynamic light scattering (DLS) measurements. In addition, TEM images showed that the morphology of the liposomes did not change after 15 min incubation at 60 °C (Figure 4-3, bottom panel) confirming that the vesicular structure of the Lp-Peptide hybrids was maintained at high temperature.

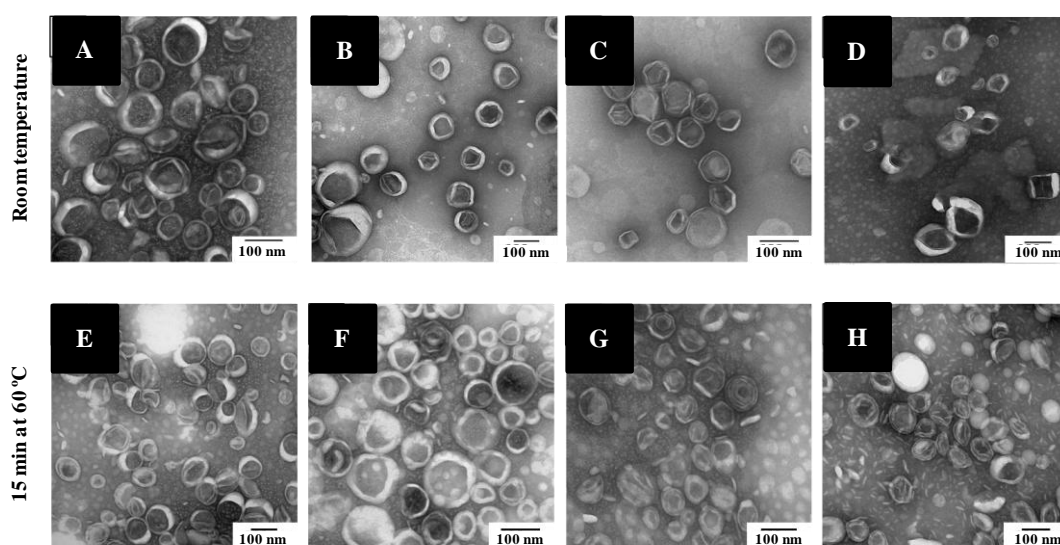


**Figure 4-3: Structural elucidation of Lp-Peptide hybrids.**

Transmission electron microscopy images at room temperature (top) and after 15 min incubation at 60 °C (bottom) of DPPC:DSPC:DSPE-PEG<sub>2000</sub> (90:10:5) liposomes (A & E) and Lp-Peptide hybrids at 600:1 (B & F); 200:1 (C & G); and 100:1 (D & H) lipid: peptide molar ratios.

#### 4.2.2 Circular Dichroism Studies

To assess the conformation of the peptide and whether anchoring into the liposome bilayer affected response to temperature, far-UV Circular Dichroism (CD) analysis was applied for both free peptide and Lp-Peptide hybrids at 200:1 molar ratio. Both unbound peptide (Figure 4-4 A) and peptide anchored in liposomes (Figure 4-4 B) adopted a predominantly  $\alpha$ -helix conformation at 6 °C with well-defined characteristic negative bands at 208 nm and 222 nm and a positive band at 192 nm (arrows). To characterize the temperature-switchable unfolding process of the peptide, CD changes were assessed with thermal scans from 6 °C to 94 °C (1 °C/min heating rate). For both the unbound peptide and the Lp-Peptide hybrids, the

positive band at 192 nm and the negative bands at 208 and 222 nm collapsed together with the appearance of the typical disordered conformation CD spectrum (negative band at 200 nm).

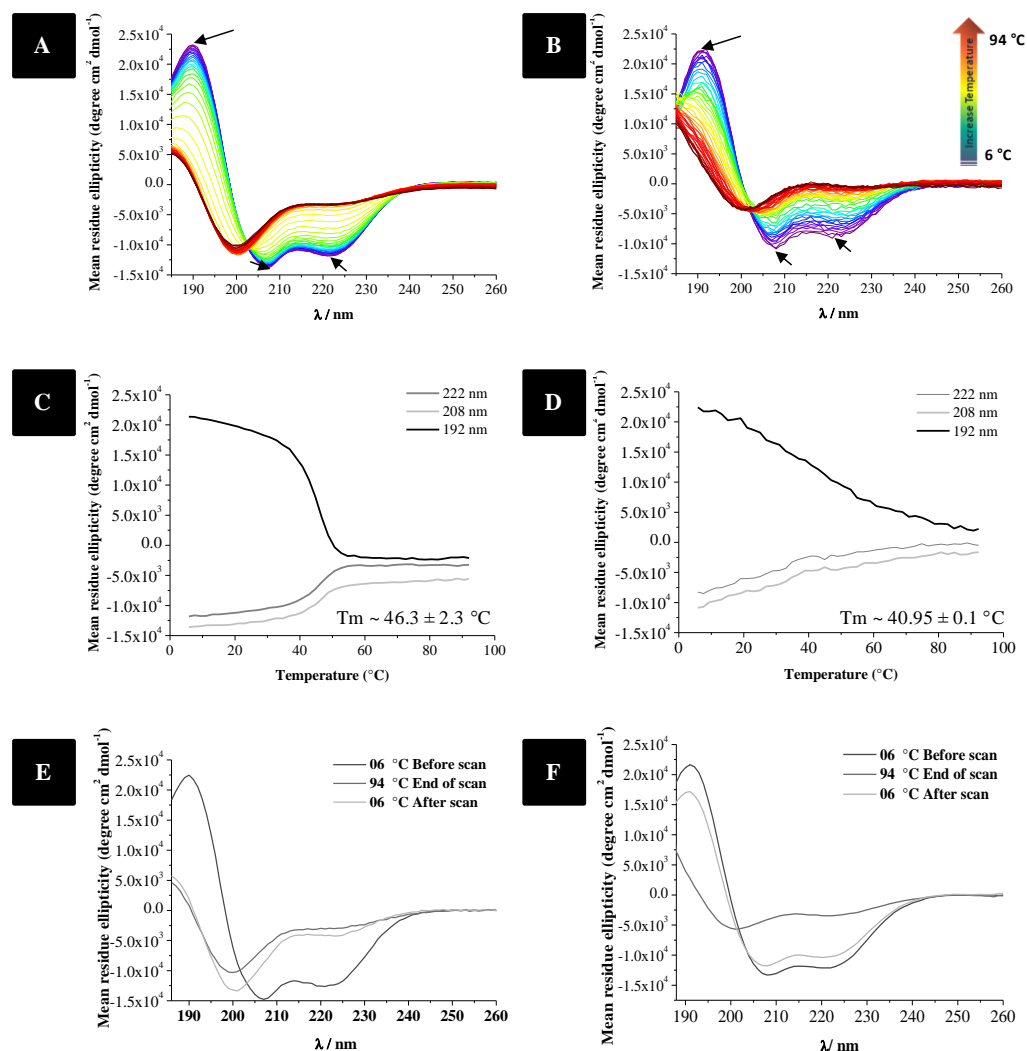


**Figure 4-4: Temperature-dependent conformational changes and reversibility of Lp-Peptide hybrids.**

Far UV CD spectra of: A) free Leucine zipper peptide, and B) Lp-Peptide hybrids (200:1 lipid: peptide). The peptide adopts an  $\alpha$ -helix conformation at low temperature and becomes increasingly disordered as the temperature is raised, both in solution and in liposomes. The same colour scheme was used for both graphs. Peptide melting temperatures of: C) free leucine zipper peptide, and D) Lp-Peptide hybrids (200:1). The mean residue ellipticity ( $\text{degree cm}^2 \text{dmol}^{-1}$ ) at the wavelength values characteristic to  $\alpha$  helix peptide (222 nm, 208 nm and 192 nm) were plotted as a function of temperature and the transition temperature of the peptide was determined with the Applied Photophysics Global 3 analysis software for dynamic multi-mode spectroscopy. Far-UV CD spectra were also recorded after 15 min equilibration at different specified temperatures for the reversibility of peptide at the end of thermal scan of: E) unbound leucine zipper peptide, and F) Lp-Peptide hybrids (200:1).

The CD spectroscopy confirmed a change from an  $\alpha$ -helix content at room temperature to a more disordered state at higher temperatures (Figure 4-4). The peptide conformation melting temperature ( $T_m$ ) was determined from the global analysis software associated with the Chirascan spectrometer.  $T_m$  of  $46.3 \pm 2.3$  °C was found for the unbound peptide and  $T_m$  of  $40.95 \pm 0.1$  °C for Lp-Peptide (Figure 4-4 C & D). Reversibility of the peptide conformation was assessed by measuring CD spectra at 6 °C, after cooling (Figure 4-4 E & F). No change in the far-UV CD spectra of the unbound peptide was obtained on rapid cooling of the sample. No recovery of the  $\alpha$ -helical structure was observed. Even after four hours incubation at 4 °C, a  $[\Theta]_M(222 \text{ nm}) \sim -7000 \text{ deg cm}^2 \text{ dmol}^{-1}$  was observed with no further changes over one week (data not shown). Clearly, the  $\alpha$ -helix conformation of the leucine zipper peptide is not reversible and is stabilised by self-association. In contrast, CD spectra of the Lp-Peptide hybrids indicated that the  $\alpha$ -helix unfolding is reversible giving  $[\Theta]_M(222 \text{ nm}) \sim -10000 \text{ deg cm}^2 \text{ dmol}^{-1}$  at 6 °C after rapid cooling to 6 °C. Taken together, the CD results confirmed that the leucine zipper peptide was anchored in the vesicle bilayer with an  $\alpha$ -helical self-association status that is temperature reversible.

In addition to studying the temperature sensitivity of the peptide, the pH sensitivity was also investigated by titration with perchloric acid starting from a pH  $\approx 9$  to a pH of 2 at 25 °C. The reversibility of the pH effect was also monitored through backward titration by small additions of NaOH starting from a pH 2 up to a pH  $\approx 9$ . At basic pH, the peptide showed a predominant helical structure, characterized by two negative bands at 208 nm and 222 nm and a positive band 192 nm. In the perchloric acid titration experiment, a gradual reduction in the  $\alpha$ -helix content was observed as the pH decreases down to a pH 6. No further changes were observed at lower pH values (Figure 4-5 A & C). When NaOH was used for the backward pH titration experiment, opposite behaviour was observed. The mean residue ellipticity at 222 nm decreased gradually with increasing the pH, indicating an increase in the helical content of the peptide (Figure 4-5 B & D).

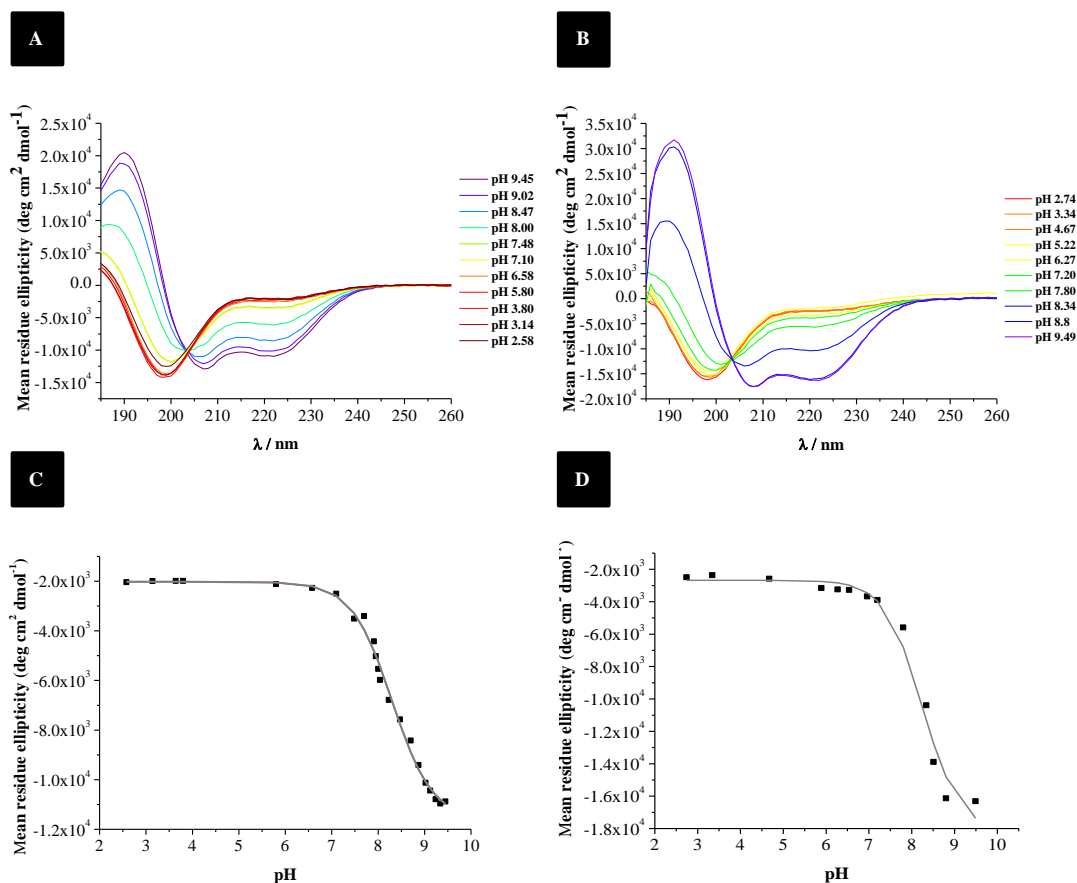


**Figure 4-5: pH-sensitivity of leucine zipper peptide.**

pH-dependent conformational changes of leucine zipper peptide obtained by titration with A) perchloric acid, B) NaOH at 25 °C. Leucine zipper peptide shows conformational change from  $\alpha$ -helix to unfolded state as the pH decreases. C & D) Corresponding mean residue ellipticity ( $\text{deg cm}^2 \text{dmol}^{-1}$ ) at 220 nm versus pH obtained from the titration with perchloric acid and NaOH, respectively.

### 4.2.3 Differential Scanning Calorimetry Measurements

To investigate the effect of peptide anchoring on the phase transition of the lipid bilayer, DSC was used. Table 4-3 and Figure 4-6 show the DSC thermograms of the different liposomal systems studied, indicating that the incorporation of different molar ratios of peptide in the lipid bilayer did not substantially affect the phase transition temperature of the liposome ( $\sim 42.5$  °C) (Figure 4-6 A). In order to compare the effect of peptide incorporation into the bilayer with that of cholesterol, we investigated vesicles containing cholesterol (CHOL) at a molar ratio of 200:1. Cholesterol is commonly used to modulate the release rate from liposomes and increase their in vitro and in vivo stability by protecting against serum destabilization effects (Kirby *et al.* 1980; Gaber *et al.* 1995). Incorporating small amounts of CHOL

in the lipid bilayer (200:1 lipid:CHOL molar ratio, equivalent to 0.5 mol%) did not affect the phase transition of the liposomes which was similar to unmodified liposomes and Lp-Peptide hybrids (Figure 4-6 A).

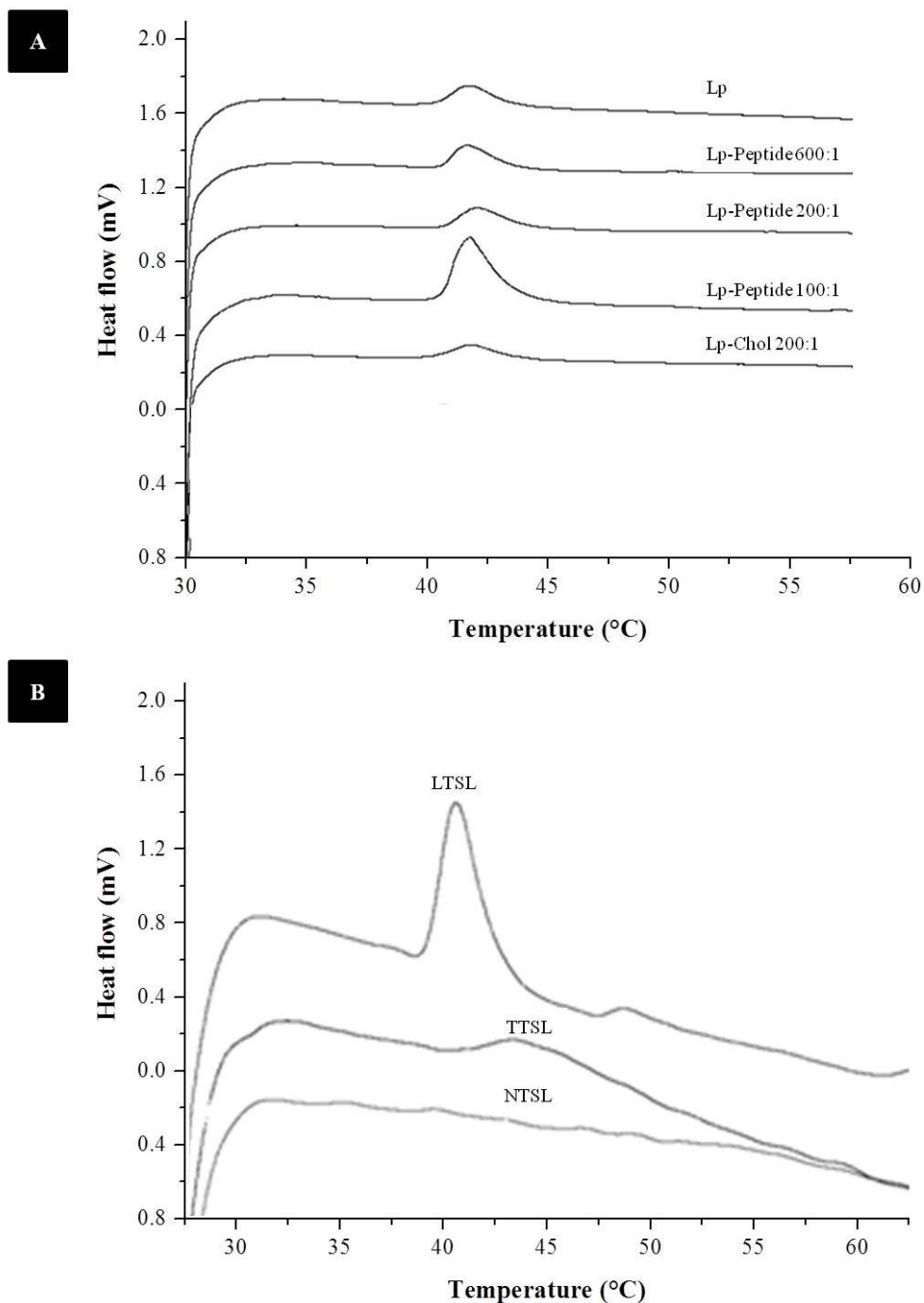


**Figure 4-6: Determination of T<sub>m</sub> of liposomes using differential scanning calorimetry.**

DSC thermograms of A) unmodified DPPC:DSPC:DSPE-PEG<sub>2000</sub> liposomes, Lp-Peptide hybrids, Lp-CHOL and B) LTSL, TTSL and NTSL. DSC thermograms were recorded at 1 °C/min from 25 °C to 60 °C.



As expected, the DSC thermogram of LTSL showed a lower transition temperature of about 41.4 °C due to the incorporation of MSPC lysolipid in the bilayer that led to slightly less ordered packing of phospholipid molecules in the gel phase (Needham *et al.* 2000). Higher transition temperature was detected for TTSL liposomes (44.2 °C), while it was impossible to detect the transition peak for NTSL due to their high cholesterol content (Figure 4-6 B)(Gaber *et al.* 1995; de Smet *et al.* 2010).

#### 4.2.4 Fluorescence Anisotropy Measurements

In order to obtain a better understanding of the interactions between the lipid bilayer and the anchoring peptide molecules, fluorescence anisotropy measurements were performed. Two different types of membrane bound probes were used: DPH which reflects perturbations in the hydrophobic region of the membrane and ANS which resides at the head group region and can better reflect changes in the bilayer fluidity at the lipid-water interfaces (Sospedra *et al.* 1999). The temperature-dependent anisotropy curves of both DPH and ANS (Figure 4-7) show that both liposomes and Lp-Peptide hybrid vesicles exhibited a gradual decrease in anisotropy values with increasing temperature. Around 42 °C this reduction was dramatic, since this was close to the phase transition temperature of the DPPC:DSPC:DSPEPEG<sub>2000</sub> (9:1:0.5) liposomes (~42.5 °C) (Kono *et al.* 2005).

On the other hand, when the bilayer fluidity was monitored with DPH spectroscopy (Figure 4-7 A), Lp-Peptide hybrids showed higher anisotropic values below T<sub>m</sub>, which was not observed with unmodified liposomes and liposomes containing CHOL (Figure 4-7 C). This indicated that, in the gel phase, DPH probe mobility was constrained by anchoring the peptide in the lipid bilayer. When the ANS probe was studied (Figure 4-7), the opposite trend was observed. Lp-Peptide hybrid vesicles showed a concentration-dependent reduction in the ANS anisotropy values, indicating an increase in the ANS probe mobility in the presence of peptide at the bilayer interface. In contrast, Lp-CHOL system showed higher anisotropic values below T<sub>m</sub> compared with Lp and Lp-Peptide hybrids (Figure 4-7 D) indicating a bilayer rigidifying effect below the phase transition temperature.

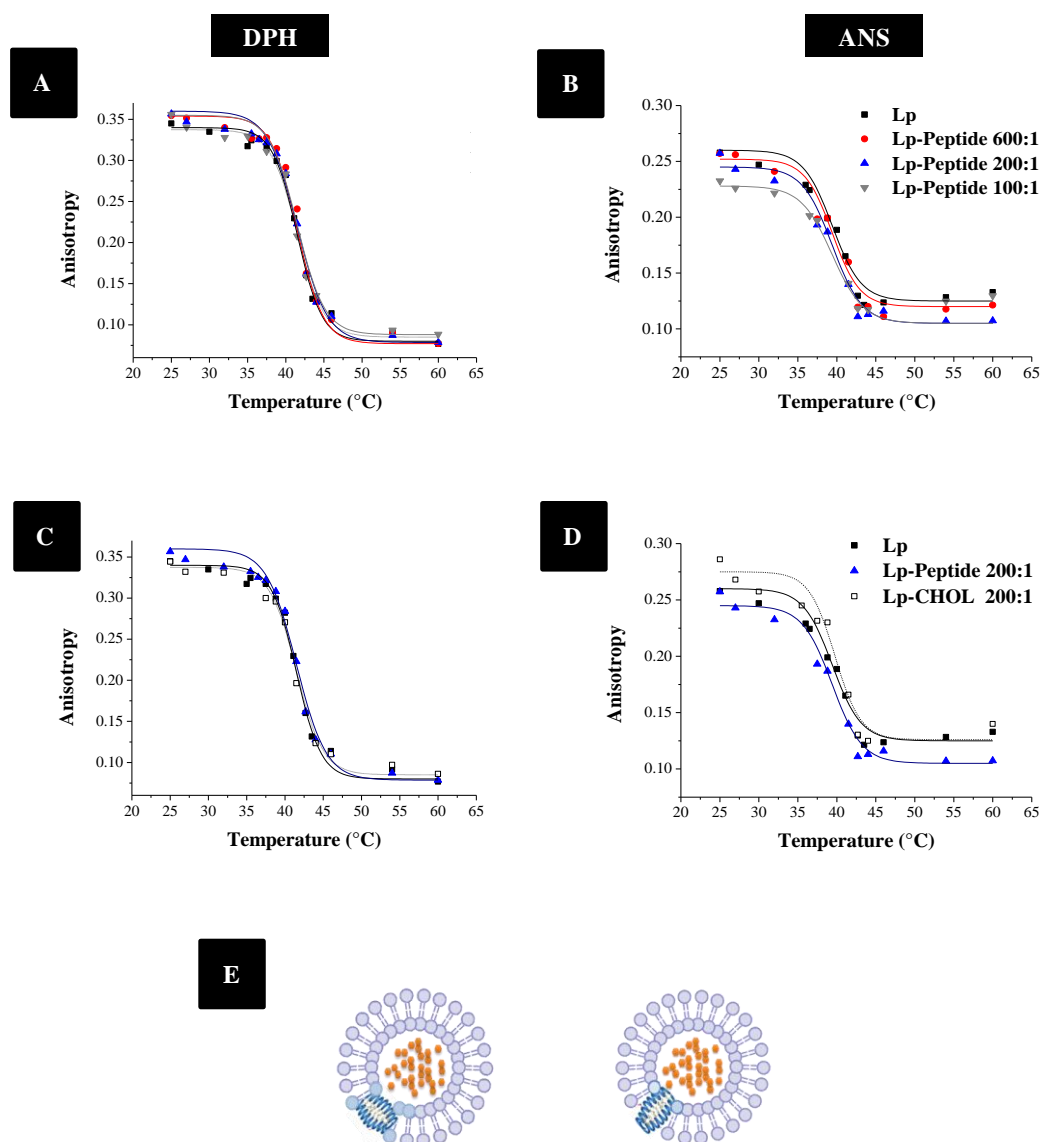


**Figure 4-7: The effect of peptide anchoring on liposome fluidity and lipid packing.**

The fluorescence anisotropy of: A & C) DPH; and B & D) ANS incorporated into DPPC:DSPC:SDPE-PEG<sub>2000</sub> (90:10:5) with and without peptide was measured as a function of temperature. A & B showed the effect of increasing the peptide molar ratio. C & D compared the effect of peptide incorporation at 200:1 molar ratio to equivalent ratio of CHOL. E) The two possible orientations of the self-associated leucine zipper peptides in the liposome bilayer.

Overall, the fluorescence anisotropy studies showed that Lp-Peptide vesicles had a reduction in bilayer fluidity at the inner-core below  $T_m$  (as observed with DPH anisotropy) while increasing the bilayer fluidity at the interface both below and above  $T_m$  (ANS anisotropy results). This was thought to indicate that the peptide interacts with both regions of the liposomal membrane rather than attaining only a superficial conformation (Figure 4-7 E).

#### 4.2.5 Solid-State NMR Experiments

The interaction of the peptide with the liposomal membrane was also studied by solid-state NMR studies using DPPC-d62 as the deuterated reporter lipid (Figure 4-8). Quadrupole echo spectra obtained for liposomes above the main phase transition revealed that the presence of peptide at 0.5 mol% and, more notably, at 1 mol% increased the DPPC-d62 acyl chain order parameters. The peptide was consequently responsible for a concentration dependent ordering effect on DPPC lipids in the Lp-Peptide hybrid system.

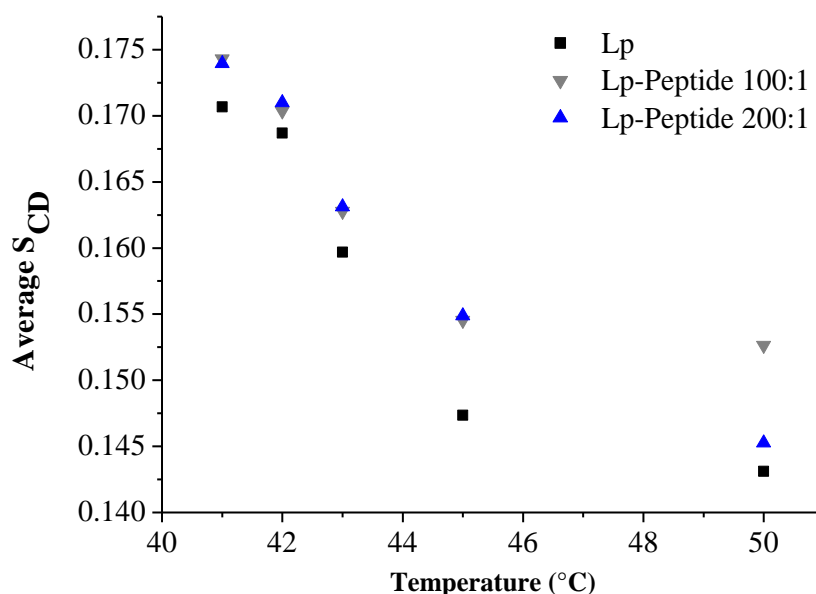


**Figure 4-8: Solid state NMR studies of the interaction of leucine zipper peptide with liposomes.** Solid-state NMR of chain deuterated lipids revealed the concentration dependent effect of leucine zipper temperature-sensitive peptides on the average order parameters of the DPPC lipid acyl chains as a function of temperature. Average order parameters (SCD) are shown for the deuterated acyl chains in membranes comprising DPPC-d62:DSPC:DSPE-PEG<sub>2000</sub> in the absence or presence of 0.5 mol% or 1 mol% peptide. In the presence of peptide, increasingly ordered membranes are observed over the temperature range tested. The samples were maintained at pH 8.5.

#### 4.2.6 Release Experiments

In order to study the drug retention properties (stability) of Lp-Peptide hybrid vesicles at body temperature and their triggered-release properties by HT, CF and DOX were encapsulated inside Lp and Lp-Peptide hybrids and their leakage/release profiles were studied over time. Leucine zipper peptide showed to be folded at high pH values (~8-9.5) compared to acidic pH, therefore, DOX encapsulation was performed using the ammonium sulphate gradient method (pH 8.5) (X et al. 1998; Gregoriadis 2006; Tian et al. 2011) instead of pH gradient using citrate (pH 4) (Fenske *et al.* 2006). Our results show that the incorporation of the peptide did not interfere with DOX loading and the encapsulation efficiencies. Furthermore, the size and polydispersity did not change after DOX encapsulation (Table 4-3 & Table 4-4).

##### 4.2.6.1 Incorporation into DOPE:EPC:DSPE-PEG<sub>2000</sub> Liposomes

First, to prove our hypothesis that the incorporation of temperature-sensitive leucine zipper peptide can trigger liposomal drug release, we studied its effect on the release profile of DOPE:EPC:DSPE-PEG<sub>2000</sub> (64:36:5) liposomes since these liposomes have no thermosensitive release property (Kono *et al.* 1999a; Kono 2001). DOPE was included because it can form hydrogen bonds through primary amino group and phosphate group of the head group (Kono *et al.* 1999a). Peptide was incorporated into DOPE:EPC:DSPE-PEG<sub>2000</sub> liposomes at 200:1 molar ratio and the release of both CF and DOX was studied at 37 °C and 42 °C. CF and DOX release data at 37 °C did not show significant release from DOPE:EPC:DSPE-PEG<sub>2000</sub> liposomes with and without the peptide which indicated their stability at body temperature (Figure 4-9 A & B). Interestingly, DOPE:EPC:DSPE-PEG<sub>2000</sub>-Peptide 200:1 liposomes released approximately 20% of encapsulated CF and DOX immediately after incubation at 42 °C (Figure 4-9 C & D). This enhancement in drug release is thought to be due to the structural changes caused by unfolding of coiled-coil state of peptide after heating, since liposomes without the peptide did not show any release at 42 °C. Despite these interesting findings the triggered property of the peptide was not strong enough to cause the release of the entire liposomal content.

#### 4.2.6.2 Incorporation into DPPC:DSPC:DSPE-PEG<sub>2000</sub> Liposomes

To improve the thermal sensitivity of the Lp-Peptide hybrid system and achieve significant fast drug release suitable for *in vivo* applications, we investigated the incorporation of the peptide into DPPC:DSPC:DSPE-PEG<sub>2000</sub> liposomes. By this we can combine the advantages of traditional TSL with the dissociation unfolding nature of leucine zipper peptide to achieve enhanced drug release by mild HT.

**Table 4-4: Physicochemical characterization of DOPE:EPC:DSPE-PEG<sub>2000</sub> liposomes with and without peptide.**

Liposomes Composition	Size (nm)	PDI	Zeta Potential (mV)	% EE
CF-Loaded liposomes				
DOPE:EPC:DSPE-PEG <sub>2000</sub>	121 ± 0.53	0.03 ± 0.04		
DOPE:EPC:DSPE-PEG <sub>2000</sub> -Peptide 200:1	108 ± 0.03	0.04 ± 0.01		
DOX-loaded liposomes				
DOPE:EPC:DSPE-PEG <sub>2000</sub>	125 ± 0.73	0.07 ± 0.02	- 40.4 ± 0.63	86.4
DOPE:EPC:DSPE-PEG <sub>2000</sub> -Peptide 200:1	123 ± 0.43	0.06 ± 0.12	- 6.01 ± 1.62	70.0

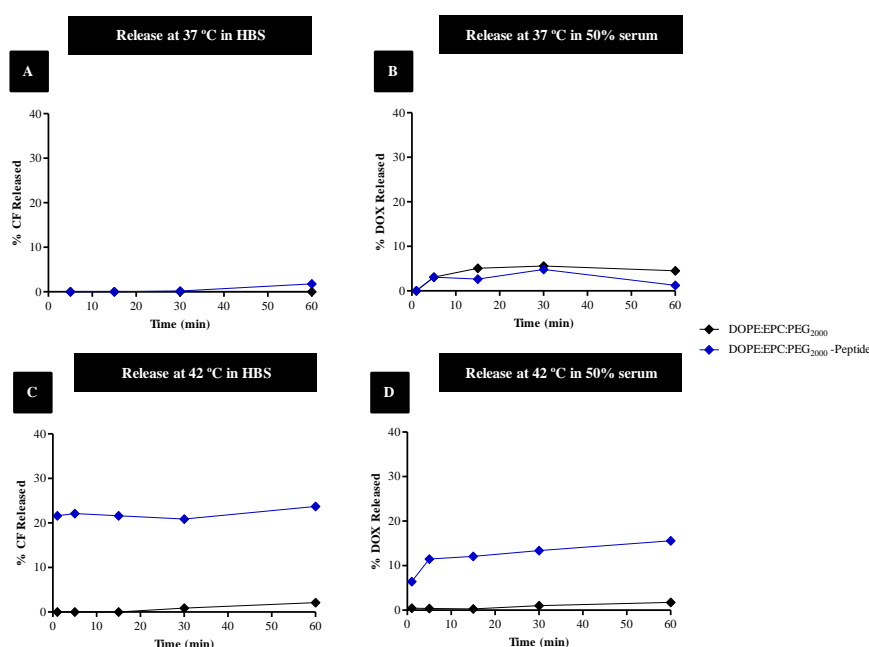


**Figure 4-9: The effect of peptide on the release rate of DOPE:EPC:DSPE-PEG<sub>2000</sub>-liposomes.**

Leucine zipper peptide was incorporated into DOPE:EPC:DSPE-PEG<sub>2000</sub> at 200:1 molar ratio and the effect of the peptide incorporation on the release profile was studied by monitoring both, the percentage of CF release in HBS (A & C) and the percentage of DOX release over time in 50% serum (B & D). Data represented as average ± STD.

The stability of the Lp-Peptide hybrid vesicles after peptide anchoring and their temperature-response were investigated by studying the release profile of encapsulated CF and DOX.

To study the serum stability of Lp-Peptide hybrids in simulated *in vivo* conditions, DOX leakage was quantified over time at 37 °C in 50% CD-1 mouse serum (Figure 4-10 A & B). During the first hour a significant improvement in drug retention was observed ( $p < 0.05$ ) with only 10% drug leakage observed from liposomes without peptide, Lp-Peptide hybrids and TTSL compared to over 60% leakage with LTSL and Lp-CHOL (Figure 4-10 A & Figure 4-11 A). The drug leakage profile of DPPC:DSPC:DSPE-PEG<sub>2000</sub> liposomes (Lp) was significantly improved ( $p < 0.05$ ) by anchoring of the peptide in a concentration-dependent manner, with almost 50% and 60% of the encapsulated DOX retained in Lp-Peptide hybrids at 200:1 and 100:1 lipid:peptide molar ratios (respectively) over 24 h (Figure 4-10 B). Similar stabilising effect observed from TTSL liposomes because of their high cholesterol content (16 mol%). TTSL drug retention at body temperature was comparable to the stabilisation effect of peptide incorporated at 200:1 and 100:1 molar ratios.

To study the effect of peptide anchoring on temperature-responsiveness of the vesicles, DOX release was studied at 42 °C in 50% serum (Figure 4-10 C). Almost 100% of DOX was released from LTSL in the first min of incubation. In comparison, the drug release from Lp increased overtime between 80% and 100% after 5 and 30 min, respectively. No significant difference in DOX release was observed between Lp and Lp-Peptide hybrids up to 200:1 lipid: peptide ratio. However, at 100:1 ratio only 60% of DOX was released from Lp-Peptide hybrids over 1 h. Similar to peptide anchoring, the presence of cholesterol did not affect the DOX release at 42 °C (Figure 4-11 B). While DOX release from TTSL liposomes increased gradually over time from 70% in the first 5 min to almost 100% release after 15 min of incubation at 42 °C (Figure 4-10 C), no DOX release was quantified from NTSL liposomes under all the conditions tested (Figure 4-10 A, B & C).

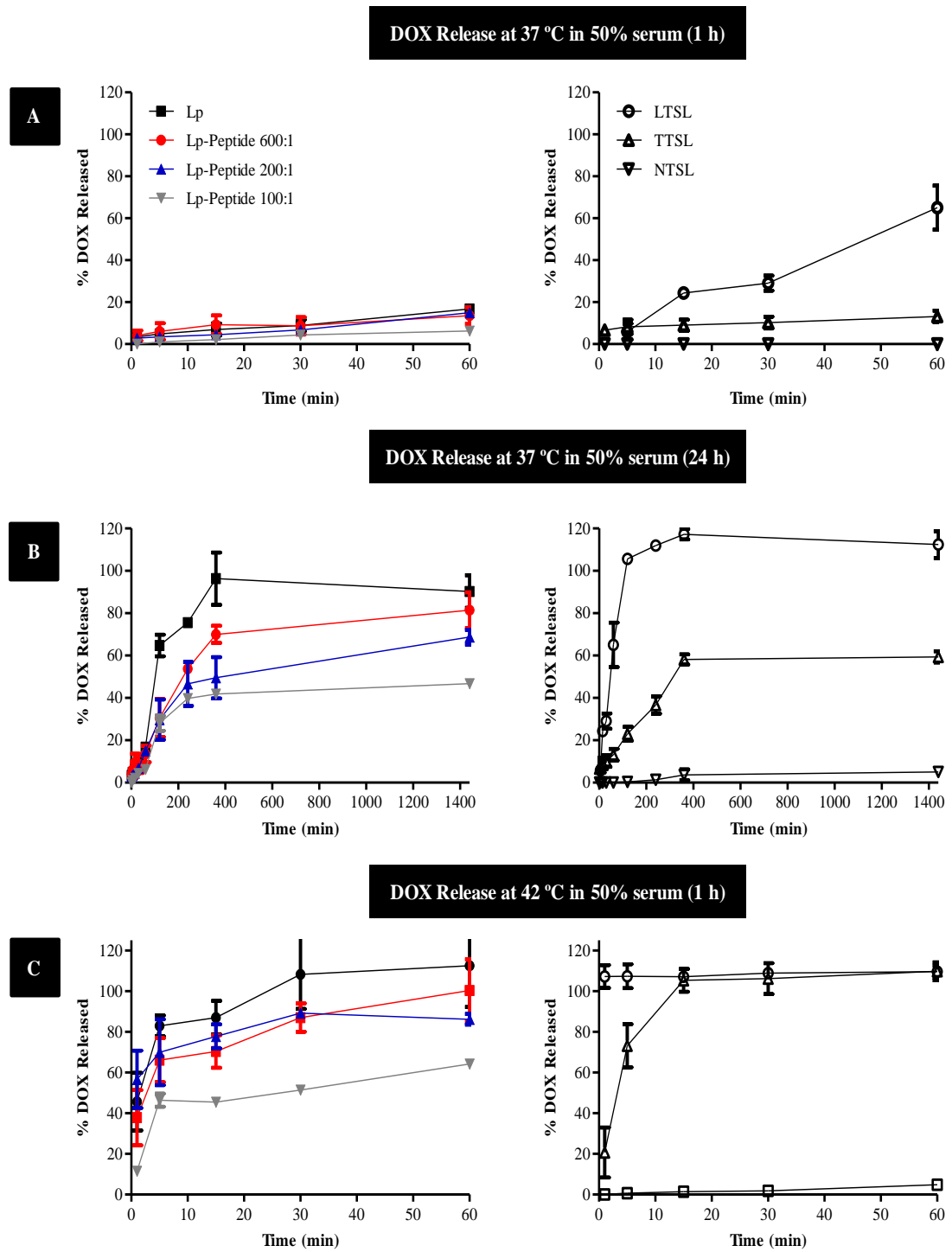


**Figure 4-10: Serum and temperature-sensitivity of Lp-Peptide hybrids.**

The percentage of DOX release from unmodified liposomes; Lp-Peptide hybrids incorporating different molar ratios of peptide were studied in 50% CD-1 mouse serum at A) 37 °C over 1 h; B) 37 °C over 24 h and C) 42 °C over 1 h. Release profiles were compared to LTSL, TTSL and NTSL (A, B & C right graphs) studied under the same conditions. Data are expressed as average  $\pm$  STD (n=3).

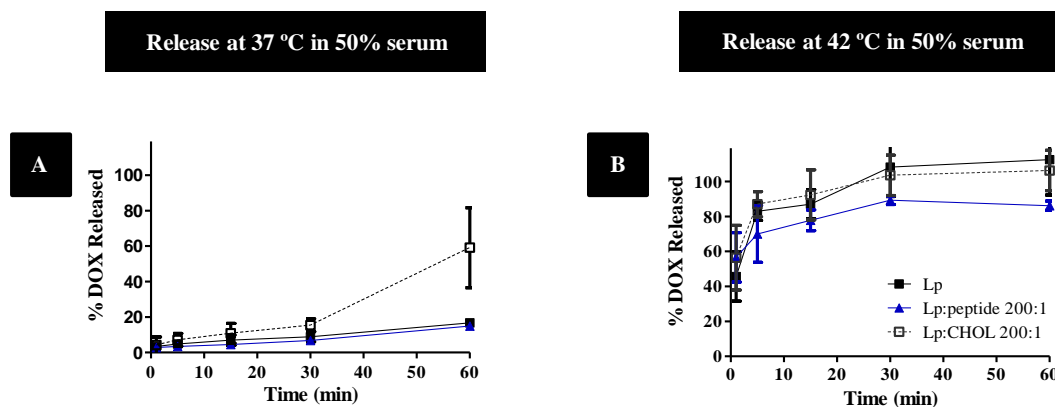


**Figure 4-11: The effect of CHOL on DOX release from DPPC:DSPC:DSPE-PEG<sub>2000</sub> liposomes.** The percentage of DOX release from unmodified liposomes; Lp:Peptide hybrids (200:1) and Lp-CHOL (200:1) were studied in 50% CD-1 mouse serum at: A) 37 °C and B) 42 °C.

To evaluate the effect of even higher temperatures, DOX release from plain liposomes and Lp-Peptide hybrids was studied by incubation at 45 °C and 50 °C. No significant differences in the drug release profile were observed compared to those at 42 °C (Figure 4-12).

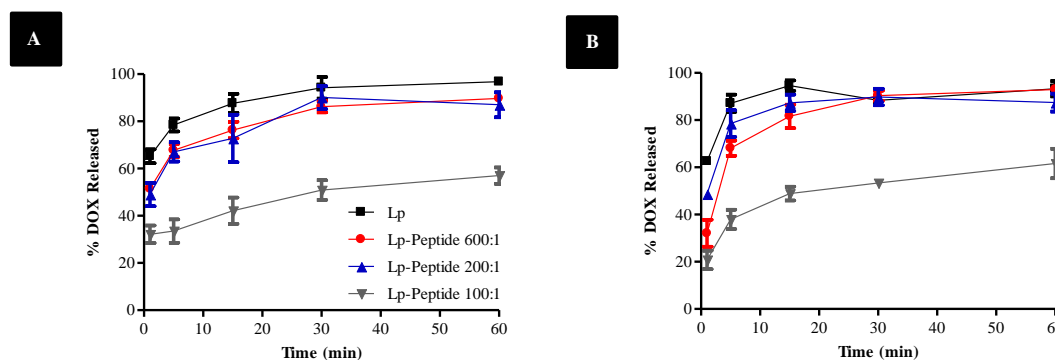
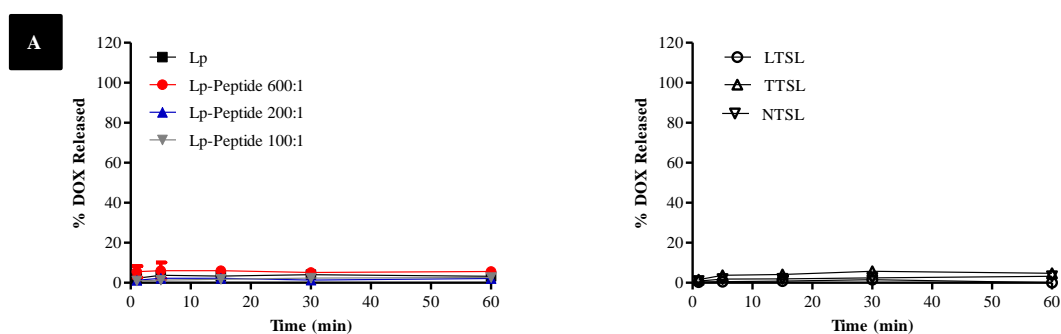


**Figure 4-12: Temperature-sensitivity of Lp-Peptide hybrids at 45 °C and 50 °C.** The percentage of DOX released from unmodified liposomes and Lp-Peptide hybrids in 50% CD-1 mouse at: A) 45 °C and B) 50 °C.

DOX release was also studied in HBS both at 37 °C and 42 °C. In contrast to the release data in 50% serum, the amount of DOX release at both temperatures was very low from all the formulations except LTSL at 42 °C which showed a similar release profile to that observed in serum (Figure 4-13 A & B), since this formulation has 10% MSPC lysolipid that stabilise nanopores in the grain boundary region of the lipid membrane at the  $T_m$ .



### DOX Release at 37 °C in HBS (1 h)



### DOX Release at 42 °C in HBS (1 h)

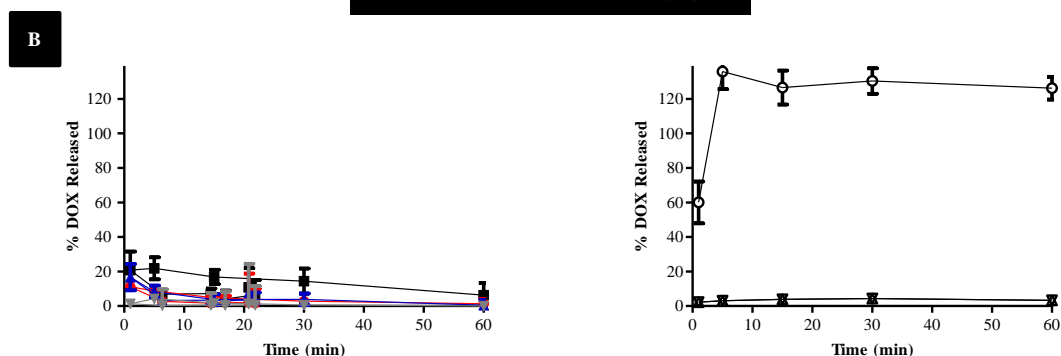


**Figure 4-13: Time dependent DOX release studies in HBS.**

The percentage of DOX release from Lp, Lp-Peptide hybrids, LTSL, TTSL & NTSL liposomes was quantified after incubation in HBS at A) 37 °C and B) 42 °C. Data represented as average  $\pm$  STD (n=3).

For comparison, CF release from Lp and Lp-Peptide 200:1 was also studied, both, at 37 °C and at 42 °C in serum and HBS as a model of low molecular weight compound (Figure 4-14). In contrast to DOX release study in HBS, triggered release of CF at 42 °C can be achieved even in HBS, which confirms that DOX crystallization is the reason behind its very low release in HBS (Figure 4-14 C). The enhancement effect of serum on content leakage from the liposome was not restricted to DOX, the percentage of CF released at both temperatures tested were higher in serum compared to HBS, which agrees with previous findings (Hashizaki *et al.* 2006; Hossann *et al.* 2007; Pradhan *et al.* 2010).

The drug release results indicated that bilayer anchoring of peptide up to a 200:1 lipid: peptide molar ratio did not preclude their responsiveness to temperature. Moreover, significant increase of drug retention of the Lp-Peptide vesicles under physiological conditions (50% serum and 37 °C) was achieved. These findings

highlighted the importance of peptide anchoring in the enhancement of drug retention at very low molar ratios and in a different way to that of cholesterol mediated bilayer rigidity. Therefore Lp-Peptide hybrid vesicles (200:1 ratio) were considered a candidate for further *in vivo* investigations.

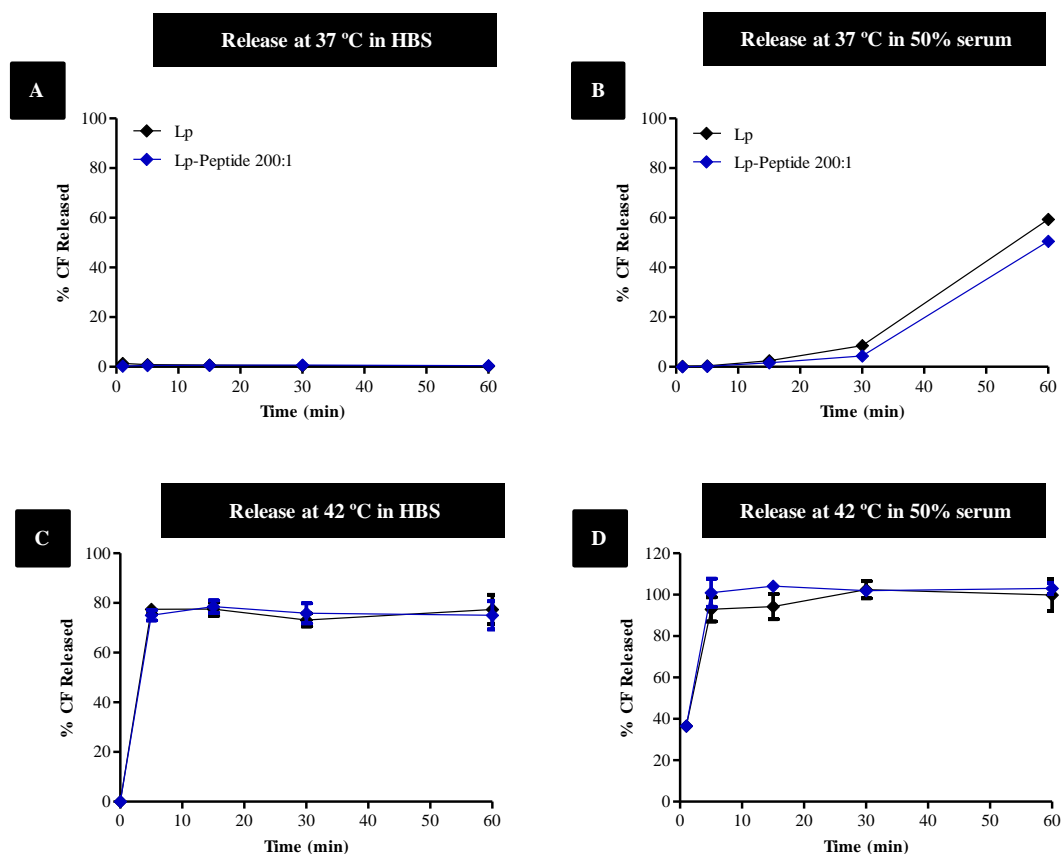


**Figure 4-14: CF release from DPPC:DSPC:DSPE-PEG<sub>2000</sub> liposomes with and without peptide.** The effect of Leucine zipper peptide incorporation on CF release profile was studied in HBS (A & C) and 50% serum (B & D) both at 37 °C and 42 °C. Data are expressed as mean  $\pm$  STD (n=3).

### 4.3 Discussion

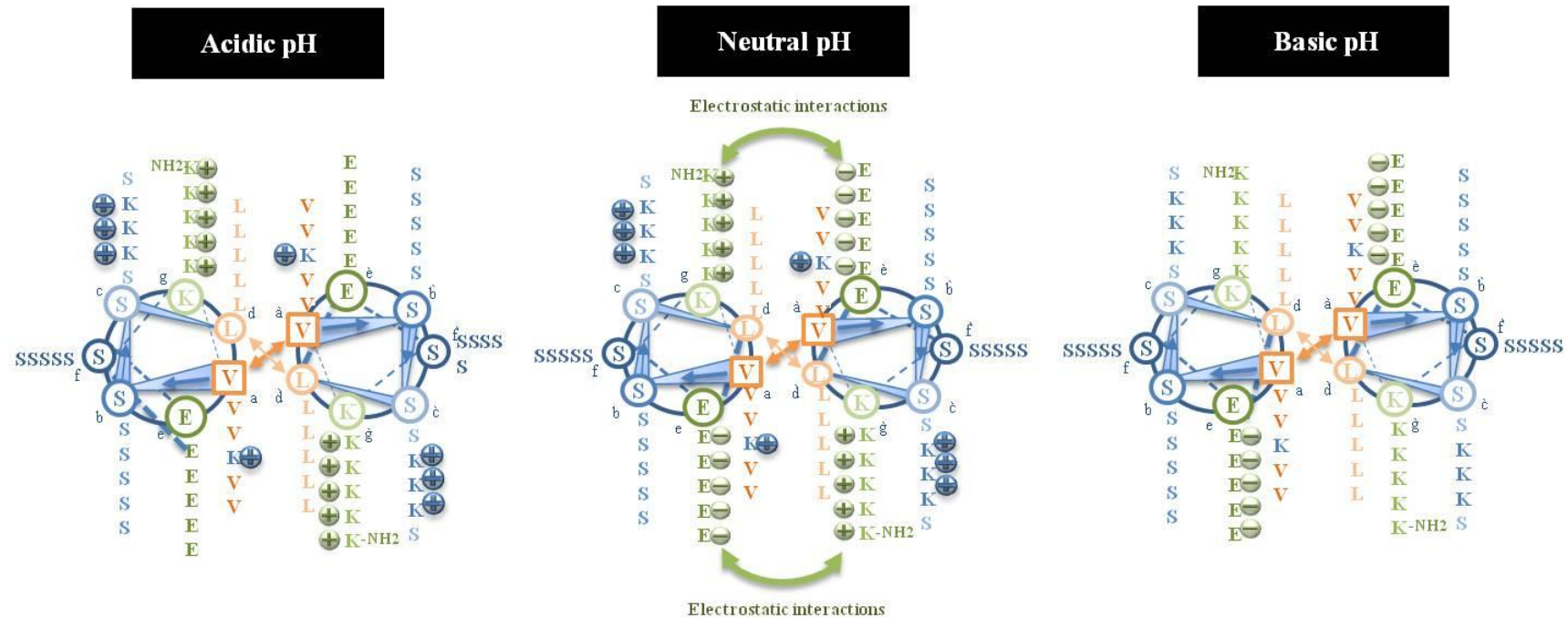
Interest in engineering peptide-modified delivery systems has increased with advances in biotechnology and genetically engineered biomaterials (Kopecek 2003). Polypeptides exhibit multiple characteristics that can provide biologically specific interactions, environmental responsiveness with opportunities to direct self-assembly and control over biodegradation. The majority of peptide-conjugated liposomes have been designed in an attempt to enhance therapeutic effectiveness and specificity using peptides as surface ligands to specifically target liposomes to tumours (Chang *et al.* 2009). Examples include RGD (Lestini *et al.* 2002; Negussie *et al.* 2010) and TAT modified liposomes (Torchilin 2002), engineered by covalent linking of the peptide to the liposome surface. Another reason for engineering peptide-modified liposomes is to induce liposomal content release in response to enzymes (Elegbede *et al.* 2008) or pH changes as a result of the ability of peptides to aggregate and form pores in the lipid bilayer (Parente *et al.* 1990; An *et al.* 2010a). The design of such hybrids involves either covalent linking to the liposome surface, peptide encapsulation inside the liposomes, or simple mixing (Parente *et al.* 1990; Brickner *et al.* 2002).

In this work, we engineered Lp-Peptide hybrids by anchoring temperature-sensitive amphiphilic peptides into the lipid bilayer by self-assembly. To our knowledge such peptide-modified liposomes have not been described previously. The Lp-Peptide hybrids at different peptide ratios maintained almost identical characteristics (mean vesicle diameter, surface charge, phase transition temperature and morphology). In addition, the anchored temperature-sensitive amphiphilic peptides rigidified the lipid bilayers and improved the liposome serum stability. More importantly, Lp-Peptide vesicles consisting of up to 200:1 lipid: peptide molar ratio exhibited high serum stability without significant changes in the overall vesicle temperature-sensitivity at 42 °C. Recently, DOX-loaded liposomes covalently modified with the thermosensitive peptide, ELP, have been described and shown to have enhanced cellular uptake by tumour cells after heating at the transition temperature of the peptide as a result of peptide dehydration at the liposomal surface (Na *et al.* 2012). Despite enhancing cellular uptake with ELP, its temperature

sensitivity was not enough to enhance drug release from the liposomes after heating at 42 °C as these liposomes were not temperature-responsive (Na *et al.* 2012).

Circular Dichroism (CD) has been shown to be capable of monitoring peptide secondary structure in a variety of environments, including vesicles (Lan *et al.* 2010b). Here, CD revealed that the leucine zipper peptide retained its secondary structure and temperature sensitivity after anchoring into liposomes. However, the CD spectra of the Lp-Peptide system as a function of temperature showed a less cooperative change upon melting compared with unbound peptide, which can be explained based on the stabilization effect imparted to the embedded peptide molecules by the adjacent lipid molecules. Interestingly, CD spectra after cooling indicated rapid and completely reversible conformational changes when anchored within the lipid bilayer compared with a slow and incomplete refolding of the unbound peptide.

The effect of pH on the peptide conformation was also studied with CD. Leucine zipper peptide showed increasing stability moving from acidic to basic pH. This effect is mainly related to the structure of the peptide and can be explained as the following (Figure 4-15), at basic pH values, only E residues were charged, which prevented the formation of electrostatic attraction between e and g residues. However, at the same time, no unwanted repulsive forces between c and g residues existed that might disturb the stabilization of the peptide by hydrophobic forces. This resulted in a stable coiled-coil structure, since hydrophobic forces are the main determinant for coiled-coil stability (Xu *et al.* 2005). Reducing the pH to a neutral value was associated with the ionization of both E and K residues. This leads to the formation of favourable electrostatic attraction between e & g residues. However, this is accompanied by unfavourable repulsive forces between c and g residues. This made the coiled-coil structure less stable compared to basic conditions. As the pH reduced to acidic, K were the only charged residues, which means that the electrostatic forces between e and g were absent. In addition, the unfavourable repulsion between c and g residues appeared. Moreover, the presence of charged K residues at position a was associated with disruption of hydrophobic forces at the helical core. The overall effect is that the coiled-coil structure was largely destabilized (Xu *et al.* 2005).



- Lys (+)
- No electrostatic attraction between e & g.
  - Electrostatic repulsion between c & g.
  - Disruption of the hydrophobic interactions.

Coiled-coil structure can not be established

- Lys (+) & Glu (-)
- Electrostatic attraction between e & g.
  - Electrostatic repulsion between c & g.
  - Disruption of the hydrophobic interactions.

Coiled-coil structure more stable compared to acidic pH

- Glu (-)
- No Electrostatic attraction between e & g.
  - No Electrostatic repulsion between c & g.
  - No Disruption of the hydrophobic interactions.

Stable coiled-coil structure  
(favourable condition for peptide incorporation)

Figure 4-15: Schematic presentation of the factors affecting the pH sensitivity of leucine zipper peptide.

The incorporation of leucine zipper peptides in liposomes was further studied by DSC and fluorescence anisotropy. No significant overall change in  $T_m$  was observed despite previous studies reporting that peptide incorporation in lipid bilayer can result in increased transition temperature (Reig *et al.* 2005; Zoonens *et al.* 2008). DPH anisotropy data showed that the incorporation of the peptide in the bilayer may be associated with a decrease in the fluidity of the hydrophobic core at temperatures below the vesicle  $T_m$  in agreement with Sospedra *et al.* (Sospedra *et al.* 1999). At the same time, ANS anisotropy measurements indicated increased membrane fluidity in the region of head group moieties (that ANS interacts with) (Engelke *et al.* 2001) when the peptide was incorporated. Therefore, the indications from both anisotropy probes suggested that the peptide interacted with both the hydrophobic and hydrophilic regions of the lipid membrane. However, determination of the exact orientation of the peptide will require further work. Solid-state NMR of chain perdeuterated lipids incorporated in the Lp-Peptide hybrid system revealed a dose dependent ordering effect of the peptide on the DPPC lipid acyl chains. Overall, our results were in agreement with others showing that peptide incorporation can have a rigidifying effect on the lipid bilayer without affecting their transition temperature (Sospedra *et al.* 1999).

It has been demonstrated before that incorporation of peptides within the lipid membrane could rigidify the lipid bilayer as has been reported previously by fluorescence anisotropy studies of other peptides such as viscotoxin A3 and laminin (Sospedra *et al.* 1999; Coulon *et al.* 2002; Zoonens *et al.* 2008) . However, limited information exists on the impact of such effects on drug release from the vesicles. DOX leakage at 37 °C indicated that the permeability of the liposome bilayer below  $T_m$  decreased in serum after peptide incorporation in a concentration-dependent manner, while at higher temperatures (where an ordering effect of the peptide was readily detected), DOX release was substantially reduced when incorporated at 1 mol%. These data are consistent with a tightening effect in phospholipid packing that can improve liposome stability and suggest that an optimal peptide-to-lipid ratio is required to ensure liposome stability does not compromise drug release under hyperthermic conditions.

In order to gain better understanding of the effect of peptide anchoring on lipid bilayer fluidity and the release rate of encapsulated drug molecules, bilayer incorporation of an equivalent molar ratio of cholesterol was studied. Cholesterol is commonly used to modulate the release rate from liposomes and increase their *in vitro* and *in vivo* stability by protecting against serum destabilization effects (Kirby *et al.* 1980; Gaber *et al.* 1995). It is well-documented that incorporation of small amounts of cholesterol into phosphatidylcholine liposome (less than 20 mol%) decreases  $T_m$  by approximately 0.24 °C/mole (Taylor *et al.* 1995). However, no change in  $T_m$  was detected when we included 0.5 mol% of cholesterol, and, at Lp-CHOL (200:1), higher DOX leakage was obtained compared with both unmodified liposomes and Lp-Peptide under physiological conditions. The inclusion of the temperature-sensitive peptide at low molar ratios was sufficient to stabilize the lipid bilayer providing a superior stabilizing effect when compared with cholesterol at the same molar ratio. The stabilizing effect imparted by the peptide was equivalent to that effect observed from TTSL liposomes that contain up to 16 mol% of cholesterol. In addition to the substantial stability of Lp-Peptide hybrids, they were also characterized by faster drug release with HT compared to slow gradual release from TTSL liposomes.

It was difficult to investigate the difference in the release profile from the different liposome types, when the same experiment was conducted in HBS instead of 50% serum. The discrepancy of the release observed in serum compared to HBS, can be due to several factors. The first thing to take into consideration is the physical state of DOX inside the liposome. It is well established that DOX loaded via ammonium sulphate gradient has the tendency to interact with sulphate anions inducing precipitation/crystallization/gelation of DOX inside the liposomes as a fibre-like structure (X *et al.* 1998; Fritze *et al.* 2006; Gregoriadis 2006; de Smet *et al.* 2010). In addition to the physical state of DOX, the factors that affect drug release at  $T_m$  are also important. There are several hypotheses which explain the release of drug from liposomes at the transition temperature including, a) the appearance of a boundary between gel phase and liquid crystalline phase during lateral phase separation, b) the change in the lateral compressibility between the neighbouring phospholipid molecules by increasing membrane fluidity during transition and c) the formation of statistical pores by rotation of phospholipid molecules with

isomerisation (Ueno *et al.* 1991). However, all these are applied only to the permeation of ions and small molecular weight compounds and it is difficult to explain the release of large compounds based on these hypotheses (Ueno *et al.* 1991). Based on that, it is understandable that crystallization of intra-liposomal DOX restricts its release properties. This was also confirmed by observing that CF release in HBS was higher compared to DOX, especially at 42 °C.

Along with the change in the DOX physical state, the high release values observed in serum compared to HBS imply that the presence of serum itself has its own effect on the drug release, since DOX physical state is similar in the two cases. Near  $T_m$  discontinuity of the gel phase and liquid crystalline phase appear and such phase separation allowed more protein interaction with the membrane and increased the leakage process (Hashizaki *et al.* 2006). The presence of serum can result in the loss of phospholipids from the liposomes to serum proteins such as high-density lipoproteins leading to release of encapsulated drugs (Kirby *et al.* 1980). In addition, the presence of serum itself can result in slight reduction in the  $T_m$  of the liposomes and increase the release of the drug (Gaber 1998; Hosokawa *et al.* 2003).

The correlation between the peptide temperature sensitivity, the change in its conformation in response to heating, and the leakage of drug from the hybrid vesicles is rather complex and not yet fully understood. Although clear enhancement in content release after peptide incorporation was observed with DOPE:EPC:DSPE-PEG<sub>2000</sub> liposomes, this increase in drug release was not obvious with DPPC:DSPC:DSPE-PEG<sub>2000</sub> liposomes since these liposomes are thermosensitive in nature. In spite of that, the presence of peptide in DPPC:DSPC:DSPE-PEG<sub>2000</sub> vesicles does not interfere with the thermoresponsive properties of the individual components. We speculate that the thermal responsiveness of Lp-Peptide hybrid vesicles can be further optimized by better understanding and reconfiguring the interaction of the peptide within the lipid bilayer.



#### 4.4 Conclusion

In conclusion, the results of this chapter showed for the first time that we successfully engineered lipid vesicles modified with temperature-sensitive peptide. The newly developed systems retained the temperature sensitivity of both the peptide and the liposomes and did not interfere with the liposome formation and the DOX loading process. Anchoring coiled-coil temperature-sensitive peptides into liposomes, up to a certain concentration (200:1 Lipid:Peptide mol/mol), significantly increases their *in vitro* long term serum stability at physiological temperature (~50% of drug retention over 24 h), without affecting their temperature sensitivity. Lp-Peptide hybrids present a promising new class of TSL, engineered by the anchoring of amphiphilic coiled-coil peptides within the lipid bilayer. This opens new opportunities for application in different clinical strategies that require the drug to circulate in the blood for a long time and passively accumulate in the tumour site by EPR effect before triggering drug release under the effect of mild hyperthermia.

## **CHAPTER 5**

---

### **BIOLOGICAL PERFORMANCE OF LP- PEPTIDE HYBRIDS**

In the previous chapter we represented the development of new type of TSL, Lp-Peptide hybrids, which showed promising rapid drug release after exposure to mild hyperthermia and good drug retention at physiological temperature. These interesting properties suggested that Lp-Peptide hybrids can be a good candidate for clinical and biomedical applications in combination with mild HT.

In this chapter, the biological activity of DOX-loaded Lp-Peptide hybrids was further investigated at the cellular level by studying their cellular uptake and cytotoxic activity with and without exposure to mild HT. In addition, the *in vivo* performance of the system was explored by studying its blood kinetics, tumour and other tissues accumulation. Therapeutic activity of Lp-Peptide hybrids was also studied compared to LTSL and TTSL by looking at the tumour growth retardation and survival. In addition, DOX retention at the tumour was also studied by *in vivo* life imaging of DOX fluorescent signal. Two different heating protocols were applied here to assess intravascular and interstitial drug release, by changing the timing between intravenous administration and heat application.

The studies in this chapter suggest that matching the drug release kinetics of TSL with the heating protocol applied is a critical factor in determining the safety and therapeutic efficacy.

## 5.1 Introduction

The previous chapter explained the development of novel lipid-Peptide hybrids (Lp-Peptide) that showed promising enhancement in drug release by mild HT together with reasonable drug retention at physiological conditions (~50 % of DOX retention 24 h in 50% serum). These hybrid vesicles are formulated by anchoring temperature-sensitive leucine zipper peptide within the liposomal lipid bilayer. The self-assembly of the peptide into super-helix coiled-coil structure at low temperatures and its dissociation by mild HT is thought to be responsible for triggering drug release. Triggered drug release (80-90 % in 15-30 min) and good serum stability data of Lp-Peptide hybrids suggested that the hybrid system can be suitable for both intravascular and interstitial triggered drug release in response to mild HT.

Previously published studies of TSL in combination with mild HT showed a clear enhancement in tumour uptake and tumour growth delay. However, only few studies correlated the choice of the HT protocol selected with the physicochemical properties of the TSL and their tumour accumulation (Kong *et al.* 2000a; Ponce *et al.* 2007; Manzoor *et al.* 2012). In most of these studies HT was applied directly after injection (Yatvin *et al.* 1981; Ishida *et al.* 2000; Kong *et al.* 2000a; Chen *et al.* 2004; Lindner *et al.* 2004; de Smet *et al.* 2011; Ranjan *et al.* 2012) or shortly after (1-3 h) while the TSL were still in circulation (Gaber *et al.* 1996; Ishida *et al.* 2000).

In this chapter, Lp-Peptide hybrids biological activity was investigated by studying the biocompatibility of the system, cellular uptake and cytotoxicity after DOX-loading. The effect of the peptide incorporation on blood profile, tissues and tumour accumulation was also studied. *In vivo* pharmacokinetics and biodistribution data suggested that Lp-Peptide hybrids can increase both immediate and long-term drug accumulation in the tumour. Therefore, we studied their therapeutic activity comparing two different heating protocols to mimic intravascular and interstitial drug release. To release drug inside the tumour vasculature, local HT was applied immediately after injection to trigger drug release as liposomes reach the heated tumour micro vessels. In addition, we examined the suitability of Lp-Peptide hybrids for interstitial trigger release after their tumour extravasation. For this purpose we applied a primary HT session to take advantage of HT in enhancing tumour vasodilatation as explained in details in chapter 1 (Kong *et al.* 2000b; Kong *et al.*

2001; Li *et al.* 2013a). At the end of 1st HT, TSL were administered and followed by a second HT treatment 24 h after injection to trigger their content release within the tumour. In order to link the efficacy of the HT protocols to the physicochemical properties of TSL, two different types of TSL were included for comparison. LTSL formulation was included since it has proved to be the most successful TSL (currently in phase III clinical trial) (Celsion.com 2013c) against which all newly developed TSL formulations must be compared. LTSL liposomes offer a rapid drug release profile with short DOX blood circulation times (0.92-1.3h) as shown by preclinical and clinical data (Banno *et al.* 2010; Wood *et al.* 2012). TTSL liposomes characterized by long blood circulation times (Al-Jamal *et al.* 2012) and intermediate drug release capability (60% DOX release in 30 min at 42 °C) (Gaber *et al.* 1995) were also included for comparison. We tested the ability of each system on the overall DOX tumour accumulation using live optical imaging and investigated the tumour growth rate, survival rate and safety of treatments using SW480, a human xenograft model.

## 5.2 Results

### 5.2.1 Lp-Peptide Hybrids Biocompatibility Studies

The biocompatibility of Lp-Peptide hybrids was assessed at the cellular level by studying their effect on cellular viability. Biocompatibility studies were performed by incubating Lp-Peptide hybrids (without DOX) with B16F10 cells and HUVEC cells to check the effect on tumour and endothelial cells, respectively. In addition, the possibility of immune response triggering by peptide incorporation into liposomes was also tested after *in vivo* administration.

#### 5.2.1.1 Biocompatibility with B16F10 and HUVEC Cells

To test the biocompatibility of Lp-Peptide hybrids with tumour cells, B16F10 cells were incubated with Lp and Lp-Peptide hybrids for 3 h and 24 h before assessing the effect on cell viability with MTT assay. Figure 5-1A & B shows that incubation of both Lp and Lp-Peptide hybrids up to 24 h did not significantly affect their viability of all the concentrations tested. This indicated that the incorporation of the peptide did not compromise biocompatibility of the liposomes.

In addition, we evaluated their effect on HUVEC cells by incubation at 0.145 mM final lipid concentration for 4 h and 24 h. Similar to B16F10 cells, both Lp and Lp-Peptide hybrids did not show any toxic effect on HUVEC cells after 4 h incubation (Figure 5-1 C), and moderate reduction in cell viability by 10% was observed after 24 h incubation. In both cases, no significant differences were seen between liposomes with and without peptide which confirmed the biocompatibility of the hybrids.

#### 5.2.1.2 ELISA Studies

In order to study the impact of systemic injection of Lp-Peptide hybrids on the development of immune response against leucine zipper peptide, serum was obtained from mice treated with empty Lp-Peptide hybrids 200:1 and Lp-Peptide hybrids 200:1-DOX 1 week after *in vivo* administration. ELISA was used to quantify the total antibodies level in the serum of treated mice in comparison to control mice.

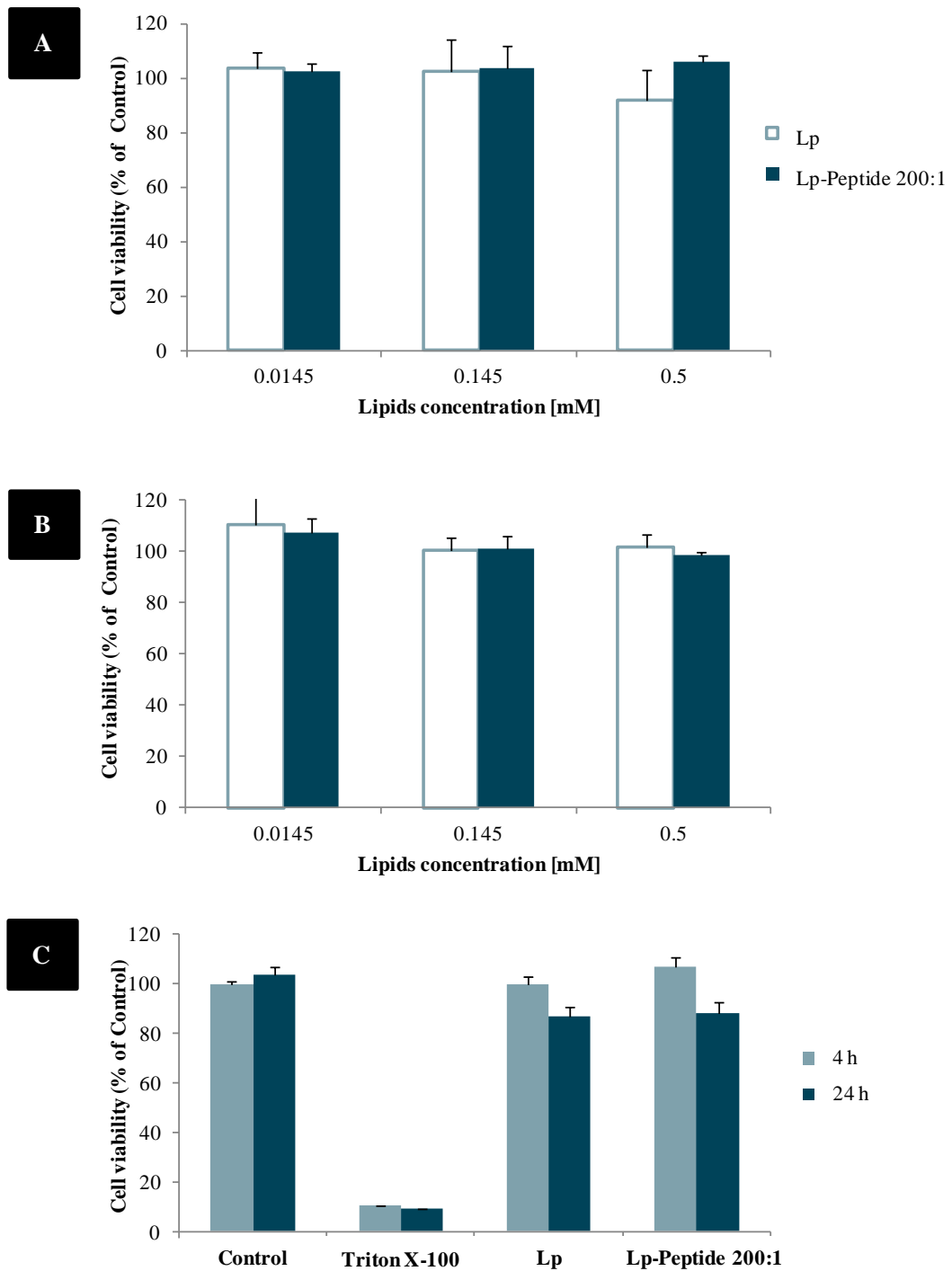


**Figure 5-1: Biocompatibility studies of Lp-Peptide hybrids with B16F10 and HUVEC cells.**

To assess the biocompatibility of Lp-Peptide 200:1 hybrids, B16F10 cellular monolayer were treated with Lp and Lp-Peptide hybrids at different lipid concentrations for A) 3 h and B) 24 h. C) Biocompatibility of Lp-Peptide 200:1 hybrids on HUVEC cells were checked at 0.145 mM lipid concentration for 4 h and 24 h. At the end of the incubation time, liposomes-containing media were removed and cellular viability was assessed with MTT assay. The results are expressed as percentage of cell viability compared to the control (untreated cells). Results are represented as average  $\pm$  STD.

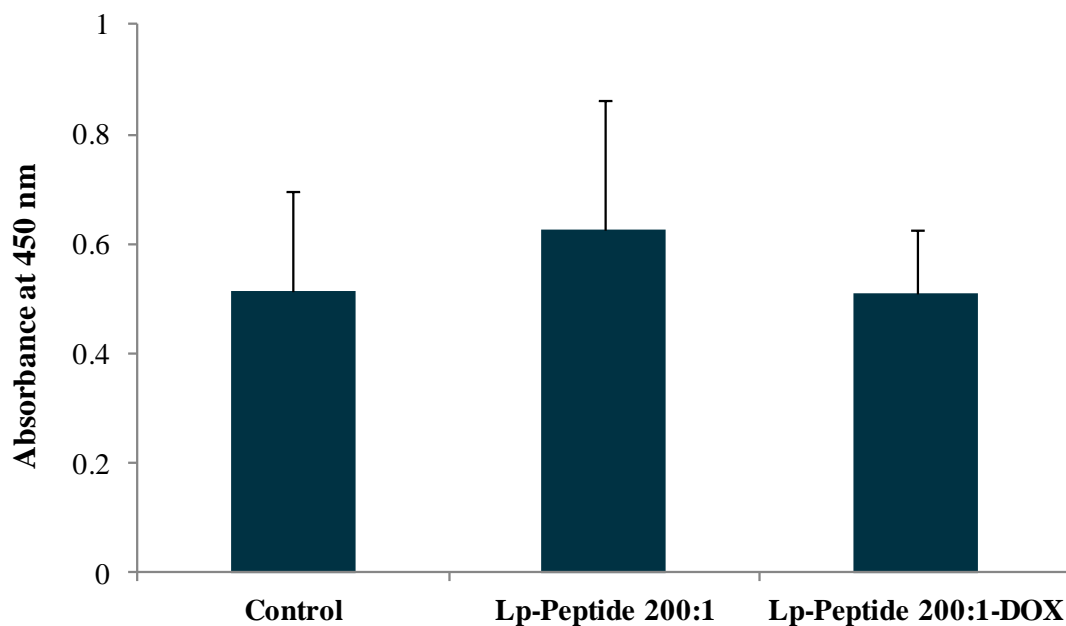


**Figure 5-2: ELISA studies to check for Lp-Peptide hybrids immunogenicity *in vivo*.**

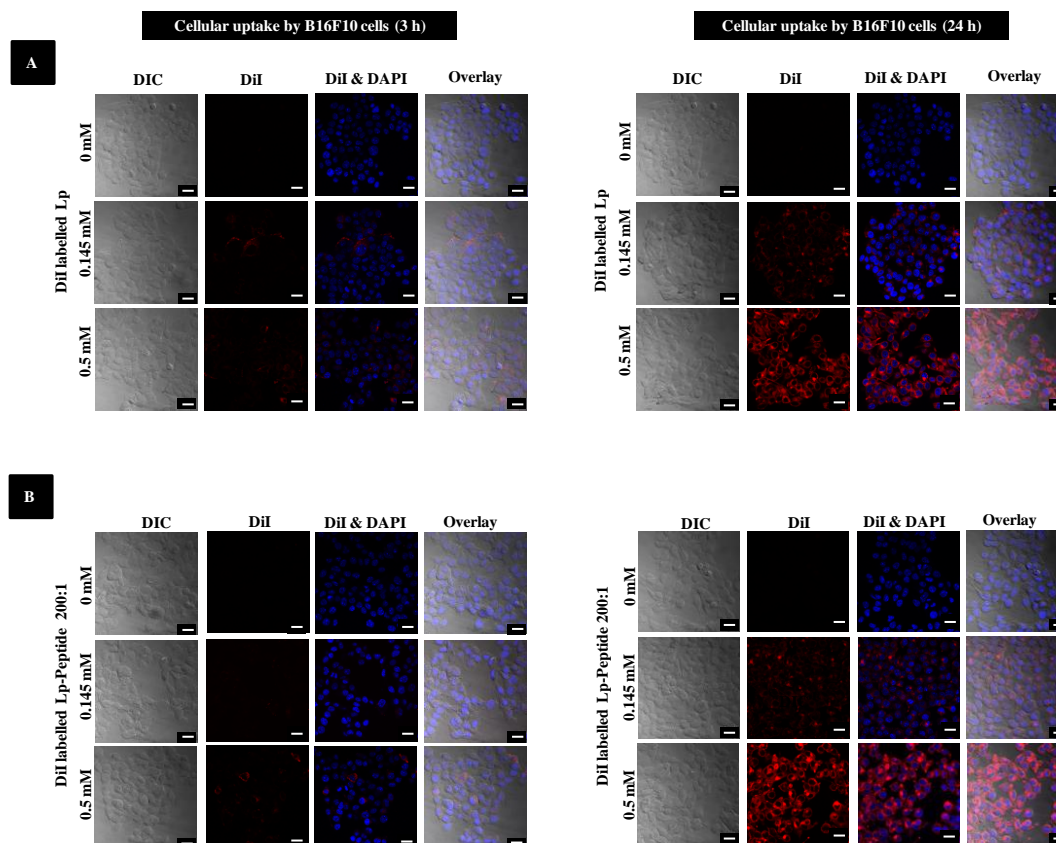
To study the possibility of development of immune response against Lp-Peptide hybrids after systemic administration, mice were injected with Lp-Peptide hybrids with or without DOX and total antibodies level were quantified in the serum 1 week after injection by ELISA. The absorbance values of each group are presented and compared to control. (data represent average  $\pm$  STD, n=4).

Figure 5-2 shows that there is no significant increase in the total immunoglobulins levels after injection with Lp-Peptide hybrids with and without DOX compared to control. These findings indicate the lack of immunogenicity of Lp-Peptide hybrids under the experimental conditions tested.

### 5.2.1.3 Cellular Uptake of Lp-Peptide Hybrids

DiI-labelled Lp-Peptide hybrids were then studied with confocal microscopy after 3 h and 24 h incubation with B16F10 cells. Figure 5-3, clearly shows that both Lp and Lp-Peptide hybrids were taken up by the cells to the same extent. Cellular uptake was both concentration and time dependent and the highest uptake was observed after 24 h incubation at 0.5 mM lipid concentration. Overall the Lp-Peptide hybrids did not show any cytotoxic side-effect on the cells.





**Figure 5-3: Cellular uptake studies of Lp and Lp-Peptide 200:1 into B16F10 cells.**

Confocal microscopy imaging of monolayer of B16F10 cells showed the uptake of DiI-labelled; A) Lp and B) Lp-Peptide hybrids 200:1 after 3 h and 24 h incubation at 37°C. Red signal represents the uptake of liposomes (signals from DiI-labelled liposomes). Co-localization with DAPI staining (blue) of the nucleus is shown in the overlay images. Scale bar is 20  $\mu\text{m}$ .

### 5.2.2 Cytotoxicity of DOX-Loaded TSL

The next step was to evaluate the cytotoxic activity of DOX-loaded hybrids compared to other TSL and their potential for triggered drug release. Cytotoxicity was assessed by measuring the cellular viability with MTT assay in B16F10 and SW480 cell lines. The choice of these cell lines was based on their sensitivity to DOX treatment and their cell division rate in order to have good correlation with the *in vivo* biodistribution and therapeutic data.

Liposomes were diluted in media to either 1  $\mu\text{M}$  & 10  $\mu\text{M}$  DOX concentrations (0.0145 and 0.145 mM lipid), then cells were treated with liposomes for 3 h with and without 1 h pre-heating at 42 °C. Liposomes were then removed and replaced with fresh media and incubation was continued for up to 24 h or 48 h before assessment of cytotoxicity (MTT assay). Figure 5-4 A shows that incubation with TSL at 10  $\mu\text{M}$

DOX concentration without preheating did not significantly affect cell viability of both B16F10 cells and SW480, with the exception of LTSL liposomes which resulted in significant cytotoxicity even without preheating due to their DOX leakage tendency in serum (de Smet *et al.* 2010). After a prolonged incubation time (48 h), reduction in cell viability observed from LTSL and a similar effect was observed from other TSL that was thought to be due to intracellular drug release (Figure 5-4 B). Alternatively, incubating the cells with preheated TSL of all types resulted in significant enhancement in cellular toxicity (almost identical to the effect observed for free DOX), that indicated complete drug release from liposomes (Figure 5-4). In comparison, no significant cytotoxicity was observed with NTSL, included as a negative control, both with and without preheating. The variations in cytotoxicity observed in both cell lines studied are due to the difference in the sensitivity among cell lines to DOX.

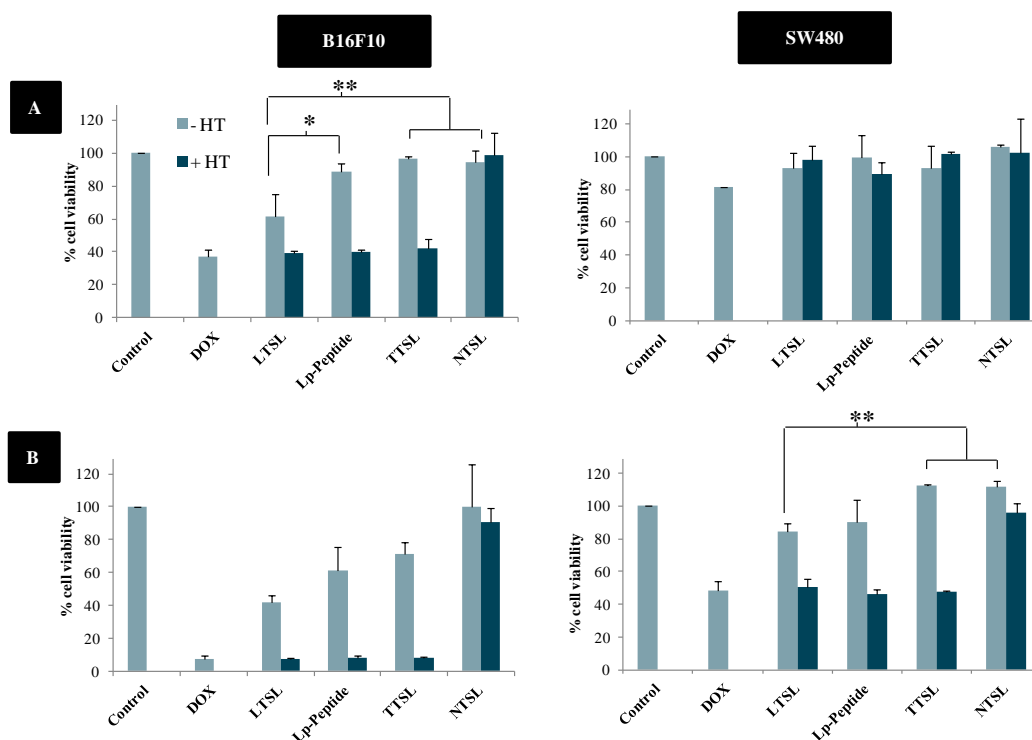


**Figure 5-4: MTT assay of different types of TSL in comparison to NTSL.**

The cytotoxicity of DOX loaded TSL was studied at 10 uM DOX concentration (0.145 mM lipid) on B16F10 and SW480 cells after A) 24 h and B) 48 h incubation. To study the effect of HT on drug release and cytotoxicity of TSL, liposomes were heated for 1 h at 42°C prior to cell treatment and compared to non-heated liposomes. Cellular monolayers were treated for 3 h then the liposome-containing media were removed and replaced with fresh media. MTT assay was performed at 24 h and 48 h after treatment and expressed as percentage of cell viability. Results represented as average  $\pm$  STD of at least 2 independent experiments (6 wells per treated group). \* indicates  $p < 0.05$  and \*\* indicates  $p < 0.01$

Similar data were observed with B16F10 cells treated at 1  $\mu$ M DOX concentration, however, no clear cytotoxic activity on SW480 cells was observed with both heated and non-heated TSL at this concentration (Figure 5-5).

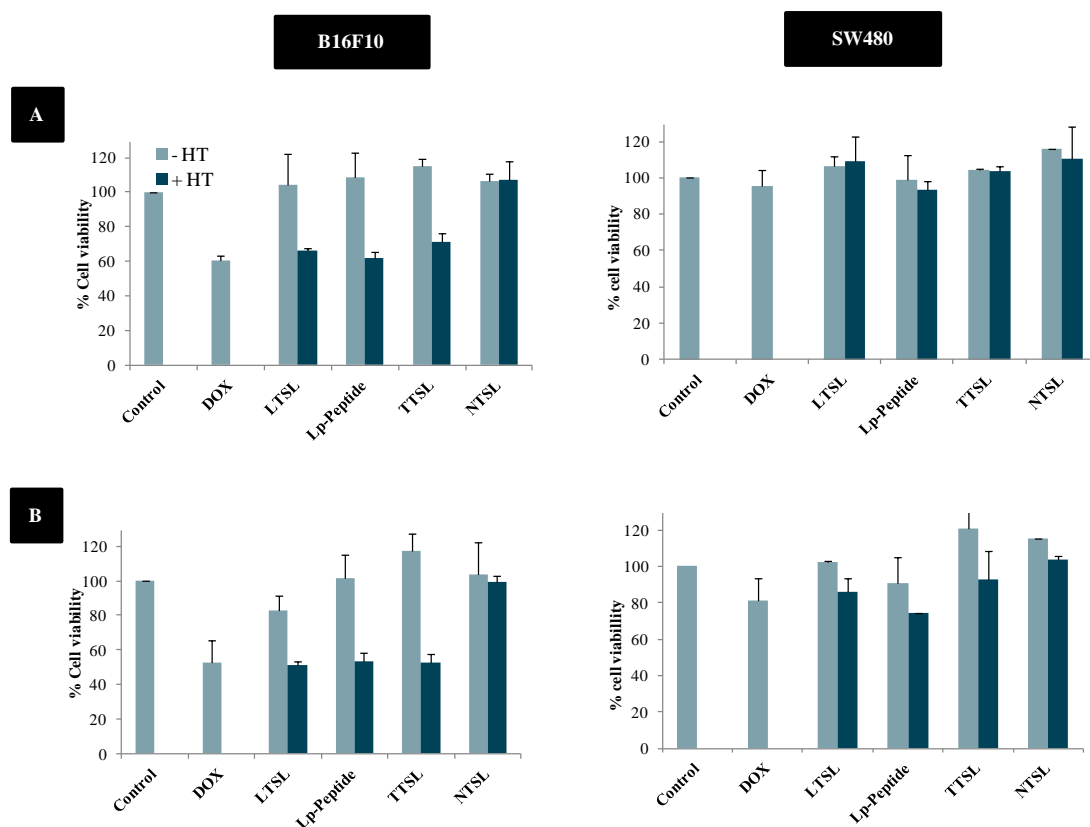


**Figure 5-5: MTT assay of different types of TSL in comparison to NTSL.**

The cytotoxicity of DOX loaded TSL was studied at 1  $\mu$ M DOX concentration, 0.0145 mM lipid on B16F10 and SW480 cells after A) 24 h and B) 48 h incubation. To study the effect of HT on drug release and cytotoxicity of TSL, liposomes were heated for 1 h at 42  $^{\circ}$ C prior to cell treatment and compared to non-heated liposomes. Cellular monolayers were treated for 3 h then the liposomes containing media were removed and replaced with fresh media. MTT assay was performed at 24 h and 48 h after treatment and expressed as percentage of cell viability. Results represented as average  $\pm$  STD of at least 2 independent experiments (6 wells per treated group).

### 5.2.3 Pharmacokinetics and Biodistribution Studies

Pharmacokinetics and biodistribution parameters of Lp-Peptide hybrid system were then studied after systemic administration. Lp-Peptide hybrids 200:1 were used for these studies since at this lipid:peptide molar ratio a balance between serum stability and temperature responsiveness was achieved.



Longer blood circulation of  $^{14}\text{C}$ -DOX was observed from Lp-Peptide hybrids compared to liposomes without peptide. Interestingly, drug retention can be further improved by replacing this peptide with another leucine zipper peptide (peptide II) with a different amino acid sequence (VSSLESK)<sub>6</sub>, Figure 5-6, resulting in a higher overall hydrophobic character and transition temperature (~83 °C).

### 5.2.3.2 Blood Profile of Lp-Peptide Hybrids in Comparison to LTSL and TTSL

Blood circulation time of Lp-Peptide hybrids was also compared to LTSL and TTSL (Figure 5-7). In comparison to LTSL, Lp-Peptide hybrids and TTSL showed 50% blood retention of DOX 1 h after injection compared to <20% from LTSL. Previous published data with LTSL reported 50% of DOX retained in blood 1 h after injection (Banno *et al.* 2010). However DOX loading in that study as well as the clinically tested LTSL formulation was performed using pH gradient method (citrate) compared to ammonium sulphate gradient method applied in this study.

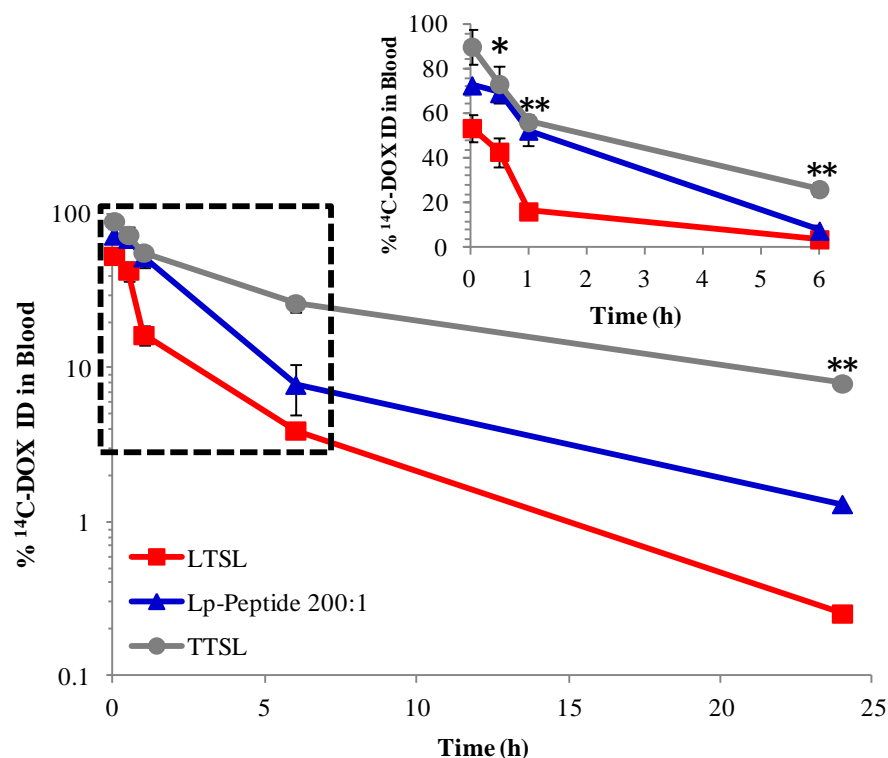


**Figure 5-7: Blood profile of  $^{14}\text{C}$ -Dox loaded LTSL, Lp-Peptide hybrids (200:1) and TTSL.**  $^{14}\text{C}$ -Dox loaded TSL were injected intravenously into B16F10 tumor-bearing C57BL6 mice and the  $^{14}\text{C}$  DOX blood clearance profile were compared over 24 h (inset:  $^{14}\text{C}$ -Dox blood level up to 6 h).  $^{14}\text{C}$ -labelled Dox was analyzed by liquid scintillation counting ( $n = 4 \pm \text{S.D.}$ ). \* indicates  $p < 0.05$  and \*\* indicates  $p < 0.01$ . Data are expressed as average  $\pm$  SEM ( $n=3-4$ ).

$^{14}\text{C}$ -DOX from Lp-Peptide hybrids decreased over time to around 10% 6 h after injection, while TTSL-DOX showed longer blood circulation with more than 20% ID and 10% ID of  $^{14}\text{C}$ -DOX detection in the blood 6 h and 24 h, respectively.

Our *in vivo* results were consistent with the *in vitro* release data. The rate of  $^{14}\text{C}$ -DOX clearance from the blood compartment observed with Lp-peptide 200:1 hybrids was much lower compared with LTSL, indicating higher serum stability. Although lysolipid desorption was not observed in buffer as reported by Mills *et al* (Mills *et al.* 2005), the loss of lysolipid component of LTSL at 37°C (70% 1 h after *in vivo* administration) in the presence of biological media might be responsible for drug leakage at body temperature and leads to short blood circulation (Banno *et al.* 2010).

### 5.2.3.3 Tumour Accumulation

The effect of localized mild HT on  $^{14}\text{C}$ -DOX accumulation in the tumour was also studied by heating the tumour site at 43 °C in a water bath for 1 h immediately after injection. Careful monitoring of mice body temperature was performed throughout HT application using a rectal thermocouple. Body temperature was maintained at less than 37 °C in all studies and, in particular, during HT (Figure 5-8) because the mice were maintained under anaesthesia.

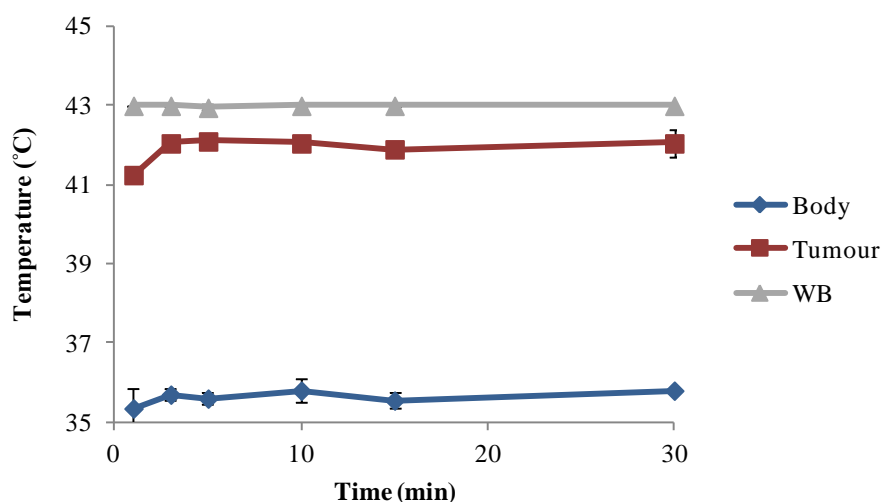


**Figure 5-8: Body and tumour temperatures monitoring during HT application.**

HT experiments were performed by immersing the tumour-bearing leg in water bath (WB) stabilized at 43 °C. Body temperature was monitored over time with rectal thermocouple. Tumour temperature was also checked with thermocouple, however, these mice were excluded from the analysis due to the invasiveness of the technique.

External cooling system was also used to regulate body temperature. To make sure that we are reaching the right temperature in the tumour, thermocouple was also used to record the temperature in the tumour over time. Figure 5-8 shows that tumour temperature increased rapidly to 41 °C within 1 minute after heating and stabilized at 42 °C throughout the study.

DOX accumulation in the tumour was studied by injecting B16F10 melanoma tumour-bearing mice intravenously with <sup>14</sup>C-DOX loaded LTSL, Lp-Peptide hybrids (200:1) and TTSL followed by localized HT immediately after injection. <sup>14</sup>C-DOX was quantified in the tumours 1 h and 24 h after injection and HT application. 1 h after injection, equivalent amount of DOX accumulated at the tumour site from LTSL and Lp-Peptide hybrids, 6.7% of ID and 5.8% of ID, respectively, 2 folds higher than TTSL tumour level (2.8% of ID) (Figure 5-9). The high DOX level in the tumour, immediately after HT, is presumably due to rapid intravascular release of DOX upon reaching the heated tumour, which agrees with rapid *in vitro* release profile. These observations agree with previous findings by Kong *et al* that showed 3.5 folds increase in total DOX (free and encapsulated) levels in FaDu tumour 1 h after treatment with LTSL compared to TTSL and HT at 42 °C (Kong *et al.* 2000a).

Interestingly, Lp-peptide hybrids (200:1) and TTSL showed significant ( $p < 0.05$ ) increase in DOX accumulation in the heated tumour compared to LTSL 24 h post-HT (Figure 5-9). Quantification of total <sup>14</sup>C-DOX (free and encapsulated) accumulation levels in the tumour 24h after injection and HT showed almost 13.5% of ID and 8.6% from TTSL and Lp-Peptide, respectively. This increase in long term tumour DOX accumulation from Lp-Peptide hybrids is because of their long blood circulation. In contrast DOX level from LTSL was reduced 24 h after injection and HT to 2.6% of ID. This could be an indication that DOX was mainly released in the tumour vasculature followed by only a fraction of drug taken up by tumour cells. These finding are consistent with previously publish data by Dromi *et al.* using HIFU (Dromi *et al.* 2007).

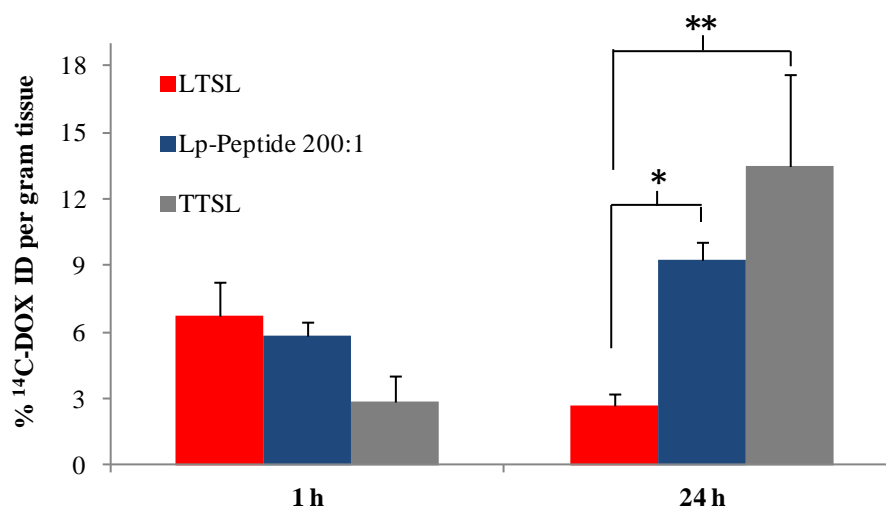


**Figure 5-9: Tumour accumulation of  $^{14}\text{C}$ -Dox after injection of different TSL with HT.**

$^{14}\text{C}$ -Dox accumulation in B16F10 melanoma tumours was quantified 1 h and 24 h post hyperthermia treatment (HT for 60 min) and injection of LTSL, Lp-Peptide 200:1 and TTSL.  $^{14}\text{C}$ -labelled DOX was analyzed by liquid scintillation counting ( $n = 4 \pm \text{S.D.}$ ). \* and \*\* indicates  $p < 0.05$  and  $P < 0.01$ , respectively, for the Lp-Peptide and TTSL liposomes when compared with the LTSL group. Data are expressed as average  $\pm$  SEM.

#### 5.2.3.4 Organs Accumulation

Organs biodistribution of DOX from different types of TSL was also studied. Very low level of  $^{14}\text{C}$ -DOX was detected in the heart and lung 1 h after administration in the presence and absence of HT and the level decreased further over 24 h. No significant difference in the organs uptake of  $^{14}\text{C}$ -DOX was detected 1 h after injection with and without hyperthermia, with exception of higher DOX level in the kidney and liver from LTSL which can be due to their drug leakage possibility (Figure 5-10 A & B).  $^{14}\text{C}$ -DOX accumulation in the kidney of Lp-Peptide group was also high, but less than that quantified from LTSL. However, kidney DOX-level from these two groups significantly reduced with HT which can be due to rapid clearance of drug after triggered release at the tumour site. DOX accumulation in the spleen was significantly high from TTSL at all time points studied which correlates with their long blood circulation and intermediate drug release rate. No significant difference in DOX level was observed 24 h after injection in the presence or absence of HT except in TTSL treated mice which showed higher drug level in the liver and kidney in the absence of HT (Figure 5-10 C & D).



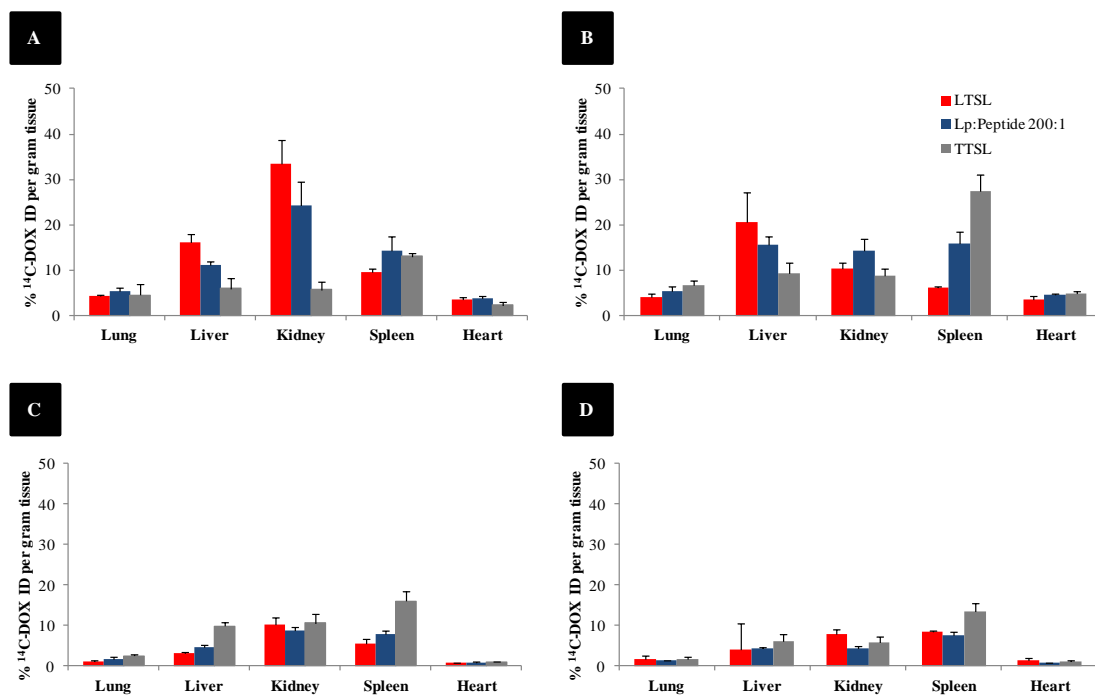
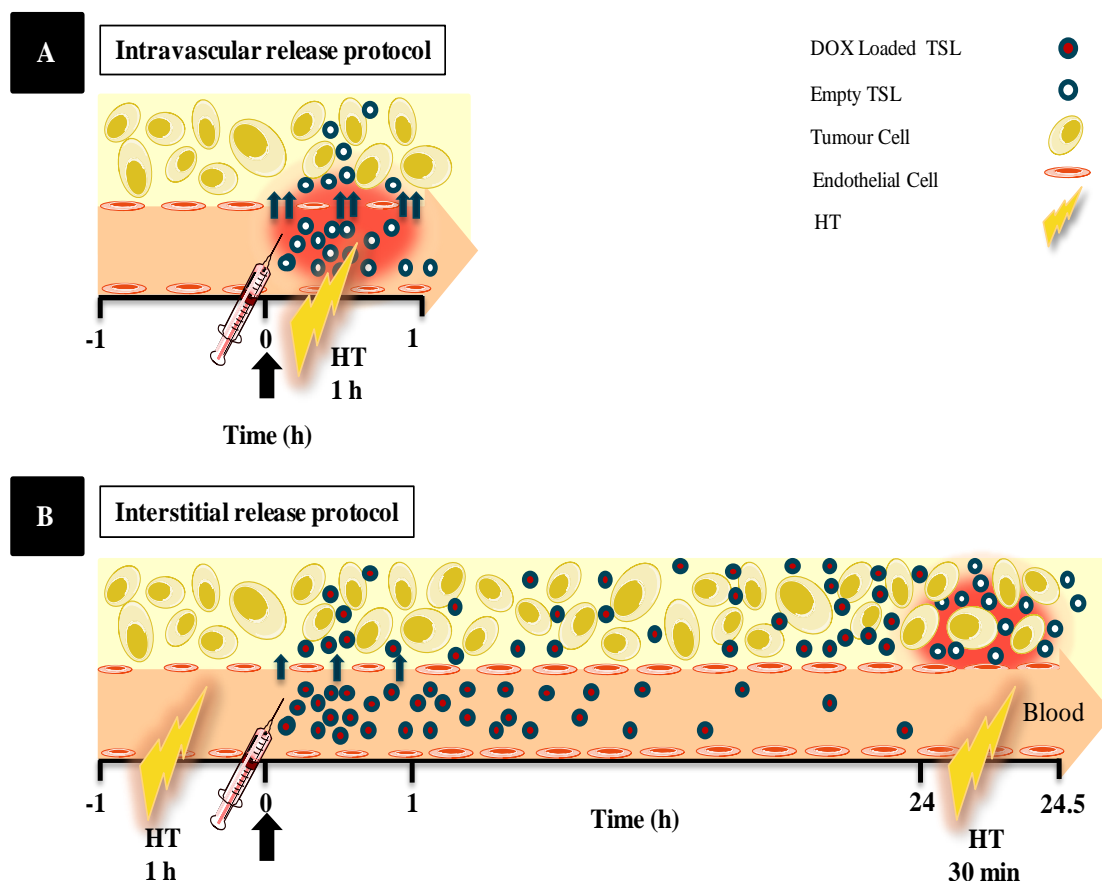


**Figure 5-10: Organ biodistribution of <sup>14</sup>C-DOX loaded LTSL, Lp-Peptide 200:1 and TTSL.** Accumulation of <sup>14</sup>C-DOX in the organs with different types of TSL was quantified after intravenous injection into B16F10 tumour-bearing C57BL6 mice 1 h post administration A) without and B) with HT. Biodistribution in the organs was also quantified 24 h after injection C) & D) in the absence and presence of HT, respectively. Data are expressed as average  $\pm$  SEM.

#### 5.2.4 Pharmacological Activity of Lp-Peptide Hybrids; Choosing the Right Heating Protocol to Maximize Therapeutic Activity

Biodistribution data into B16F10 tumour-bearing mice showed that Lp-Peptide hybrids delivered high level of DOX to the tumour following localized mild HT application which was comparable to LTSL. Besides, a further increase (3-fold) in tumour accumulation 24 h after heat application suggested the Lp-Peptide hybrids can be suitable for both intravascular and interstitial release approaches depending on the timing between the liposomes administration and hyperthermia application. To explore these possibilities, we studied DOX tumour retention, therapeutic activity and safety of Lp-Peptide hybrids applying the intravascular and interstitial release protocols presented in Scheme 5-1.

LTSL and TTSL liposomes were also included in these studies for comparison and in order to understand the effect of changing the physicochemical properties of TSL on the choice of the proper heating protocol.



**Scheme 5-1: Schematic presentation of intravascular and interstitial release protocols.**

The combination of hyperthermia and liposome systems can be utilized to enhance the drug release from TSL in two different protocols based on the timing between liposomes administration and heat application. A) In the intravascular release protocol, TSL are administered during the heating process, resulting in drug release inside blood vessels when reaching the heated area. (drug release is presented by red gradient seen in the blood vessels). This process is then followed by drug taken up by both tumour and endothelial cells. B) The increased vascular permeability of the blood vessels in response to the 1st HT treatment increases the level of liposomes accumulation in the tumour. The interstitial release approach takes advantage of the fact that stealth small size liposomes have the ability to extravasate the malformed tumour vasculature compared to normal blood vessels. After tumour accumulation a 2nd heating is applied to trigger drug release interstitially (drug release is represented by the red gradient close to tumour cells).

#### 5.2.4.1 Optical Imaging of DOX Retention into SW480 Tumour

*In vivo* optical imaging was performed to compare the accumulation of DOX into SW480 tumour-bearing mice treated with the three types of TSL applying both, intravascular and interstitial drug release protocols.

IVIS imaging of animals treated with the intravascular release protocol showed that the highest tumour DOX accumulation was achieved from LTSL and Lp-Peptide hybrids due to their fast drug release properties (Figure 5-11 A). Quantification of

DOX fluorescent signal at the tumour site showed that Lp-Peptide hybrids resulted in equivalent DOX accumulation to LTSL, and significantly higher than TTSL liposomes (Figure 5-11 B). 24 h after injection, reduction in DOX signal at the tumour site was observed from all TSL, that indicated a degree of wash-out of DOX molecules from the tumour (Dromi *et al.* 2007).

In the interstitial drug release protocol, TSL were intravenously injected immediately after the 1st HT session to increase liposome accumulation into the tumour, but not trigger drug release. Once liposomes accumulated in the tumour, a 2nd HT was applied (24 h after injection) to induce drug release interstitially. IVIS imaging was performed 24 h after injection before and after the 2nd HT.

Unlike the intravascular drug release LTSL liposomes resulted in significantly low DOX accumulation compared to Lp-Peptide hybrids and TTSL (Figure 5-12). This can be understood based on the differences in blood circulation profile and the ability to retain DOX after *in vivo* administration (Hauck *et al.* 2006; Banno *et al.* 2010; Wood *et al.* 2012). In addition, the application of 2nd HT did not significantly affect the overall DOX accumulation levels.

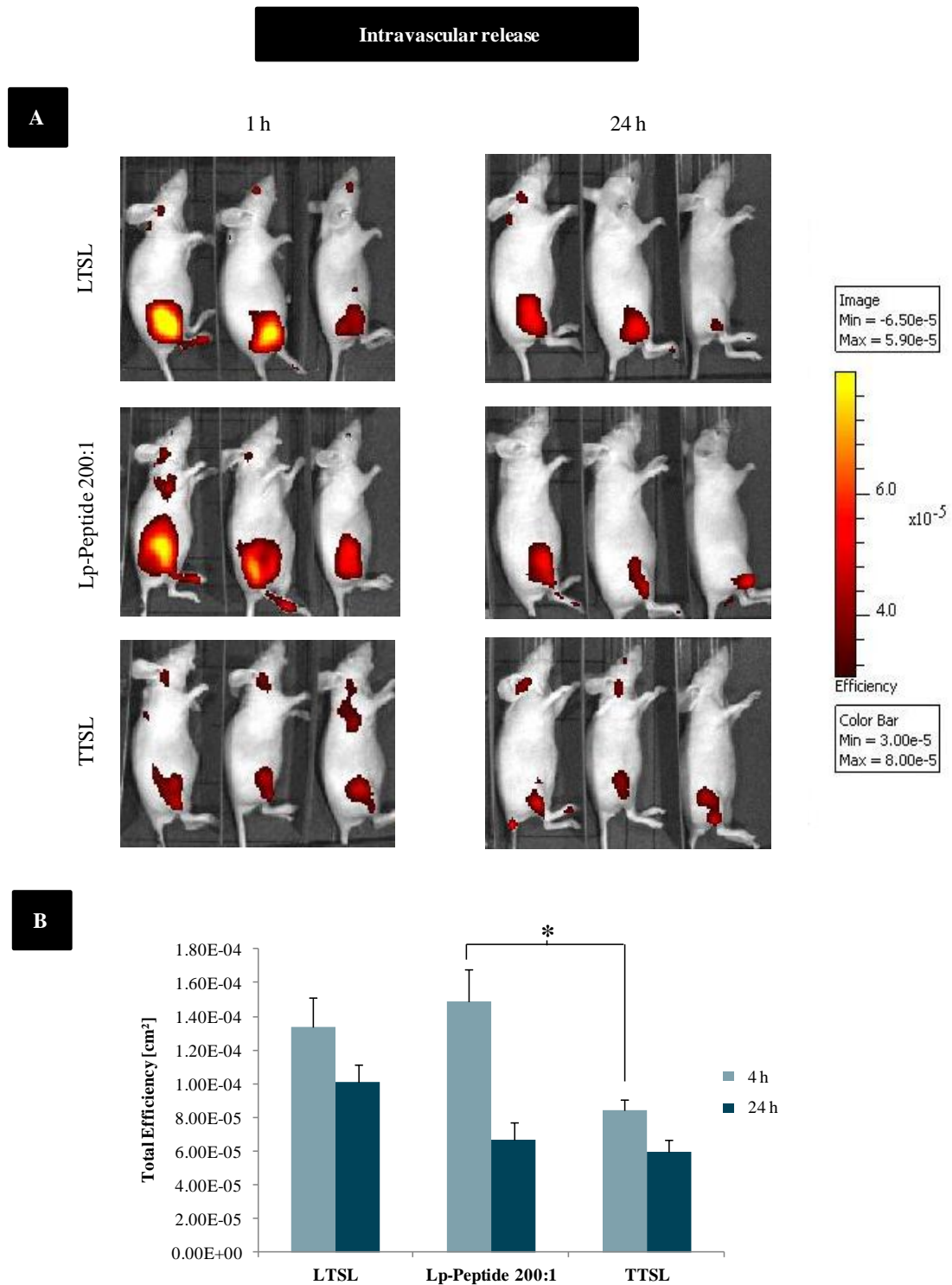


**Figure 5-11: *In vivo* optical imaging of DOX fluorescence in athymic mice treated with the intravascular release protocol.**

LTSL, Lp-Peptide 200:1 and TTSL were injected into SW480 tumour-bearing mice followed by immediate HT at 42 °C to trigger intravascular drug release. Mice were then imaged with IVIS Lumina II imaging system 1 h and 24 h after injection and heating. A) Represents the live fluorescence imaging of anaesthetised mice. B) DOX fluorescence intensity signals from the tumour (region of interest) were quantified and expressed as total efficiency. Results expressed as mean  $\pm$  SEM.

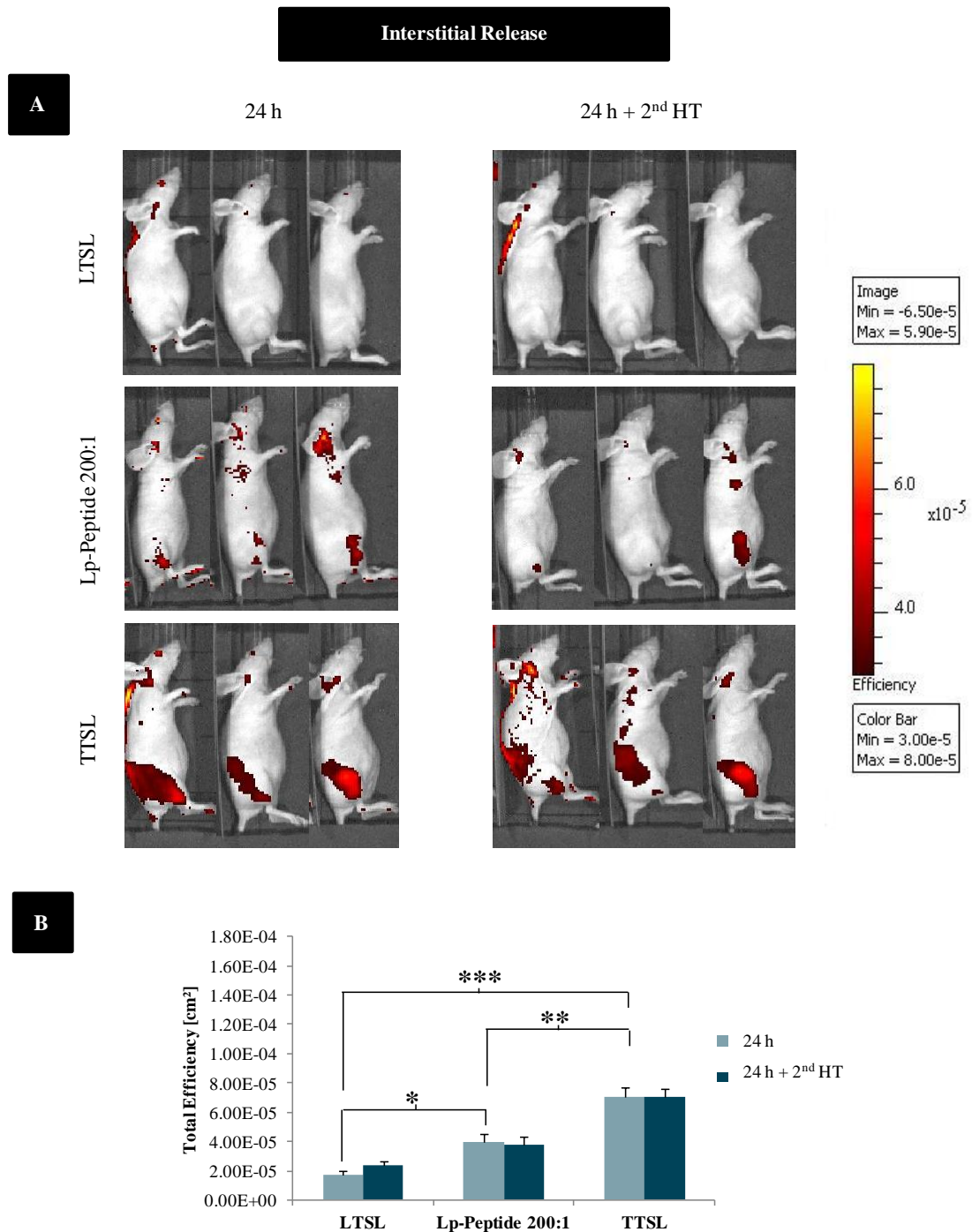


**Figure 5-12: *In vivo* optical imaging of DOX fluorescence in athymic mice treated with the interstitial release protocol.**

SW480 tumour-bearing mice were exposed to 1 h local HT (42 °C) prior to injection with LTSL, Lp-Peptide 200:1 and TTSL liposomes. 24 h after injection 2<sup>nd</sup> session of local HT was applied to trigger interstitial drug release after tumour accumulation. Mice were imaged with IVIS Lumina II imaging system 24 h after injection before and after 2<sup>nd</sup> heating. A) Represents the live fluorescence imaging of anaesthetised mice. B) DOX fluorescence intensity signals from the tumour (region of interest) were quantified and expressed as total efficiency. Results expressed as mean  $\pm$  SEM.

#### **5.2.4.2 Tumour Growth Retardation and Survival Studies (Intravascular Versus Interstitial Protocol)**

The therapeutic activity of LTSL, Lp-Peptide hybrids and TTSL was studied by looking at the change in tumour volume over time as well as by assessing the survival of treated mice compared to the control. Based on the change in tumour volume (Figure 5-13 A), we observed that all animals treated for intravascular release showed significant tumour growth retardation compared to control mice. Lp-Peptide hybrids and LTSL liposomes had equivalent therapeutic activity and were significantly more effective compared to TTSL because of their rapid release properties (In agreement with the IVIS tumour accumulation data). No signs of toxicity were observed from all treated groups using the intravascular release protocol and no significant change in the weight of the mice was observed (Figure 5-13 B).

When the HT protocol was changed to release DOX interstitially, we observed that LTSL did not show any improvement compared to control. This effect is mainly because of the poor serum stability for this protocol and short blood circulation that limits LTSL tumour accumulation (Hauck *et al.* 2006). TTSL treatment on the other hand showed tumour growth control up to 10 days after treatment because of their long blood circulation profile that resulted in the highest total DOX tumour accumulation as can be seen from IVIS. However, this was also accompanied with significant weight loss that suggested non-specific systemic toxicity. The best tumour growth retardation obtained from the interstitial protocol was from Lp-Peptide hybrids. Lp-Peptide was significantly more effective than LTSL because of their longer blood circulation that resulted in good tumour accumulation (Figure 5-12 B). In comparison to TTSL, no signs of toxicity or change in body weight were observed with LTSL and Lp-Peptide treated mice.

Similar findings were observed in survival rates that agreed with the tumour growth delay and DOX accumulation data (Figure 5-13 C). With the case of intravascular release, significant increase in life span ( $P < 0.001$ ) was achieved from LTSL and Lp-Peptide hybrid treatment (Table 5-1). However, with interstitial drug release, only Lp-Peptide hybrids treated mice showed increased life span (14.9%) compared to other TSL. In this case LTSL treated group survival was not

significantly different from the controlled group (treated with HT only). On the other hand, TTSL treated mice exhibited 50% reduction in survival compared to the control group and significant weight loss (>15% or more drop in body weight), that indicated systemic toxicity from TTSL treatment in this protocol.

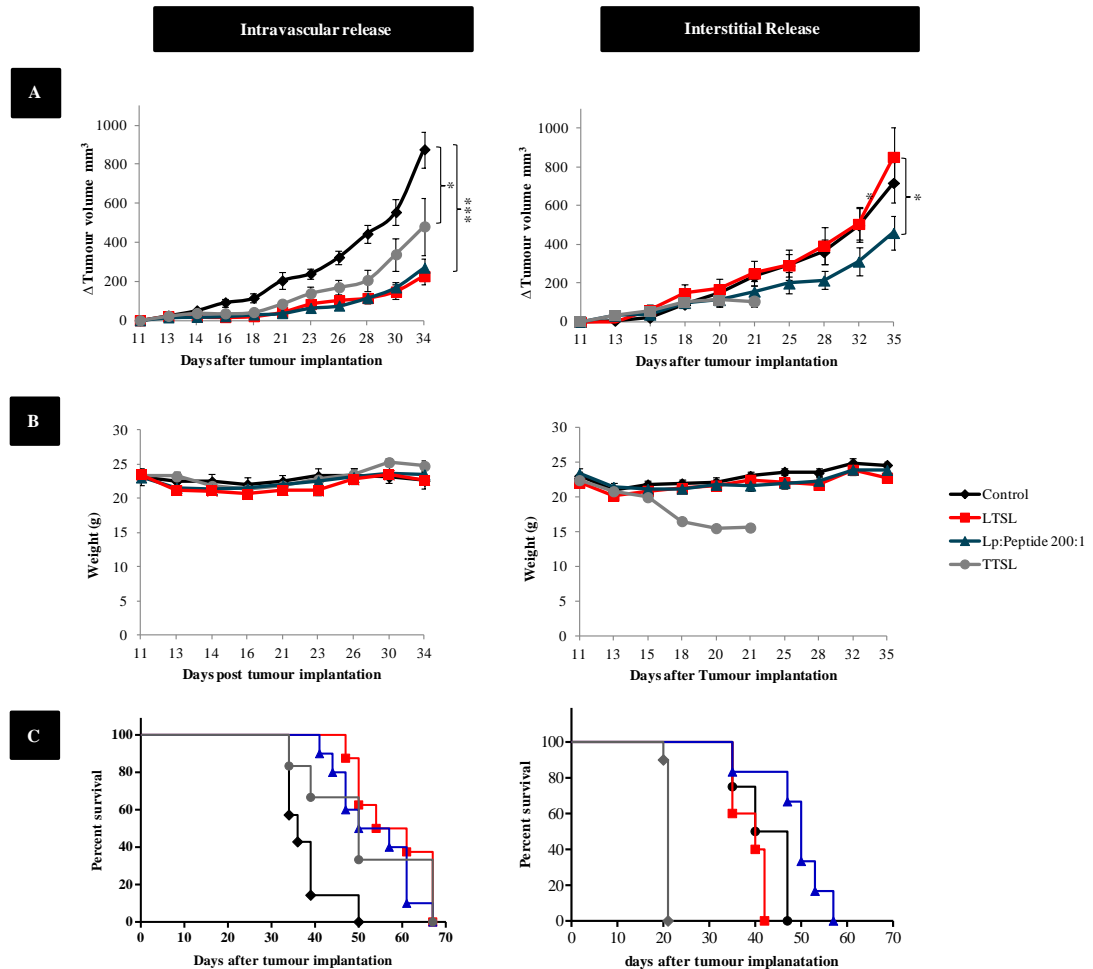


**Figure 5-13: *In vivo* tumour growth delay and survival studies.**

SW480 tumour-bearing mice were treated with LTSL, Lp-Peptide 200:1 and TTSL liposomes comparing intravascular and interstitial release protocols. A) Change in tumour volume; B) body weight; and C) survival analysis. SW480 ( $5 \times 10^6$ ) cells were injected subcutaneously in the right leg. Therapy started on day 11 after implantation with average tumour size of  $100 \text{ mm}^3$ . Animals were injected intravenously with LTSL, Lp-Peptide 200:1 and TTSL at  $5 \text{ mg DOX/kg}$ . Local HT was applied by immersing the tumour-bearing leg into  $43^\circ\text{C}$  water bath. Control animals are non-injected mice treated with HT only. Results expressed as average  $\pm$  SEM. \* indicates  $p < 0.05$  and \*\* indicates  $p < 0.01$ .

**Table 5-1: Therapeutic effect of TSL using the intravascular and interstitial release protocols**

Treatment	Dose (mg/kg)	Mean survival time (days)	Increase in life span (%) <sup>a</sup>	Significance (p) vs control
Intravascular release protocol (injection with HT)				
Control	-	36	0	
LTSL	1 × 5	57.5	+59.7	<0.001
Lp-Peptide 200:1	1 × 5	53.5	+48.6	<0.001
TTSL	1 × 5	50	+38.9	NS <sup>b</sup>
Interstitial release protocol (injection post HT + 24 h 2nd HT)				
Control	-	43.5	0	
LTSL	1 × 5	40	-8.0	NS <sup>b</sup>
Lp-Peptide 200:1	1 × 5	50	+14.9	NS <sup>b</sup>
TTSL	1 × 5	21	-51.7	<0.001

<sup>a</sup> % of increase in life span = mean survival time of treated / mean survival of control × 100 -100.

<sup>b</sup> NS, not significant.

### 5.2.4.3 Histopathological Analysis

Histological examination of tissues was performed 3-5 weeks after treatment. Figure 5-14 and Figure 5-15 showed representative images of mice treated with LTSL, Lp-Peptide hybrids and TTSL with both intravascular and interstitial heating protocols are expressed in comparison with control mice (treated with HT only). In general, histological analysis showed no sign of tissue damage in any of the groups tested with the exception of TTSL treated mice using the interstitial release protocol.

Cardiotoxicity is the most common problem associated with free DOX treatment, which is usually represented as vacuolization of cardiac myocytes or some degree of extensive loss of myocyte components (Rahman *et al.* 1982; Rahman *et al.* 1985). However, no histological changes in the heart were observed in any of the treated mice in both protocols in comparison with the control. This agrees with previous findings for NTSL (Doxil), that improved the safety of DOX after encapsulation in liposomes (Ewer *et al.* 2004).



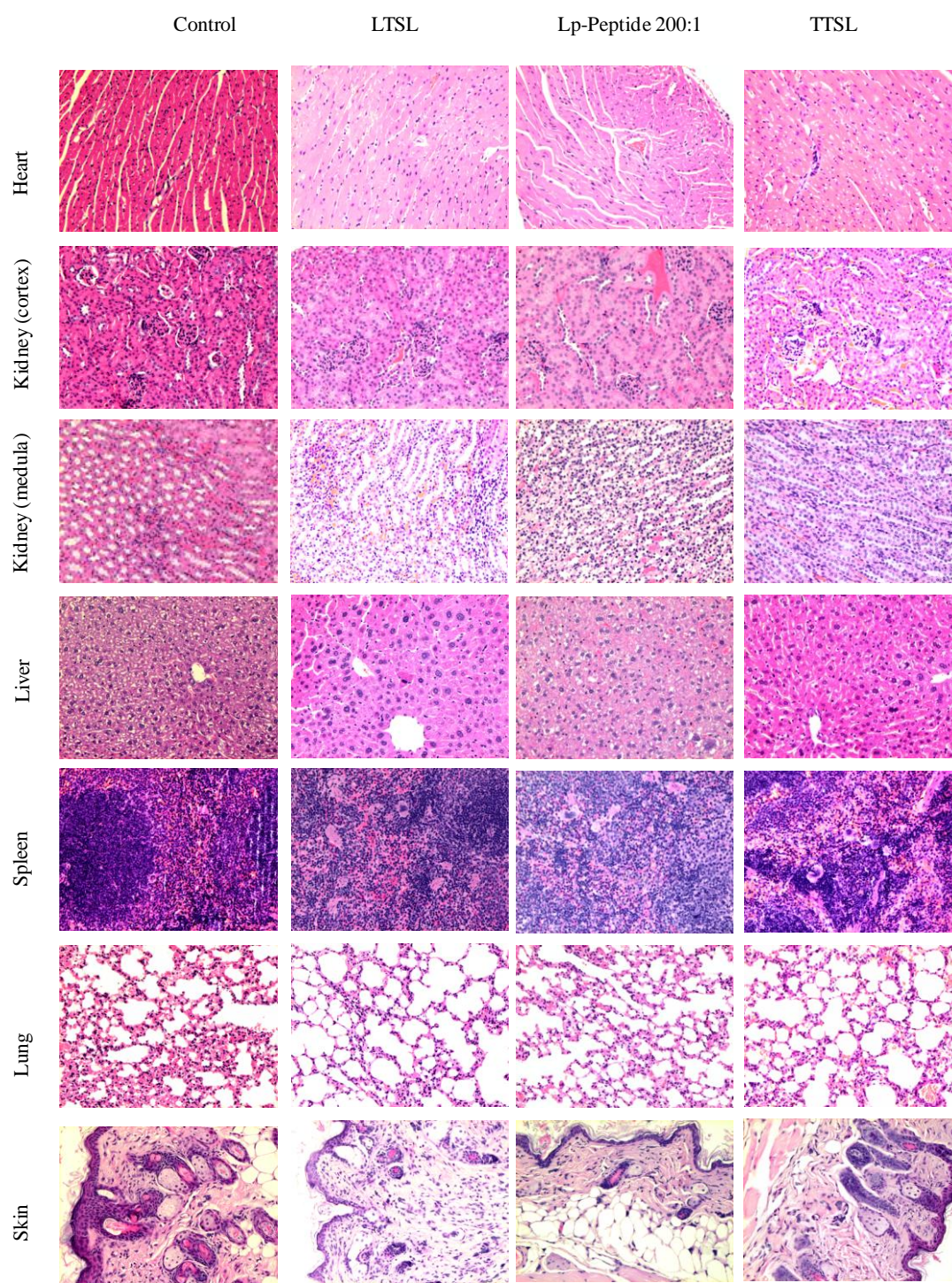


**Figure 5-14: Histological analysis of tissues following treatment using the avascular release protocol.**

Heart, kidney, liver, spleen, lung and skin tissues were stained with H&E staining. Images are shown at 10x magnification.

Nephrotoxicity is the other critical issue associated with free DOX treatment since the kidney is involved in the excretion of the drug (Burke *et al.* 1977; Lahoti *et al.*

2012). No pathological observations were noticed in kidney sections from LTSL, Lp-Peptide hybrids and TTSL mice treated with intravascular release protocol.

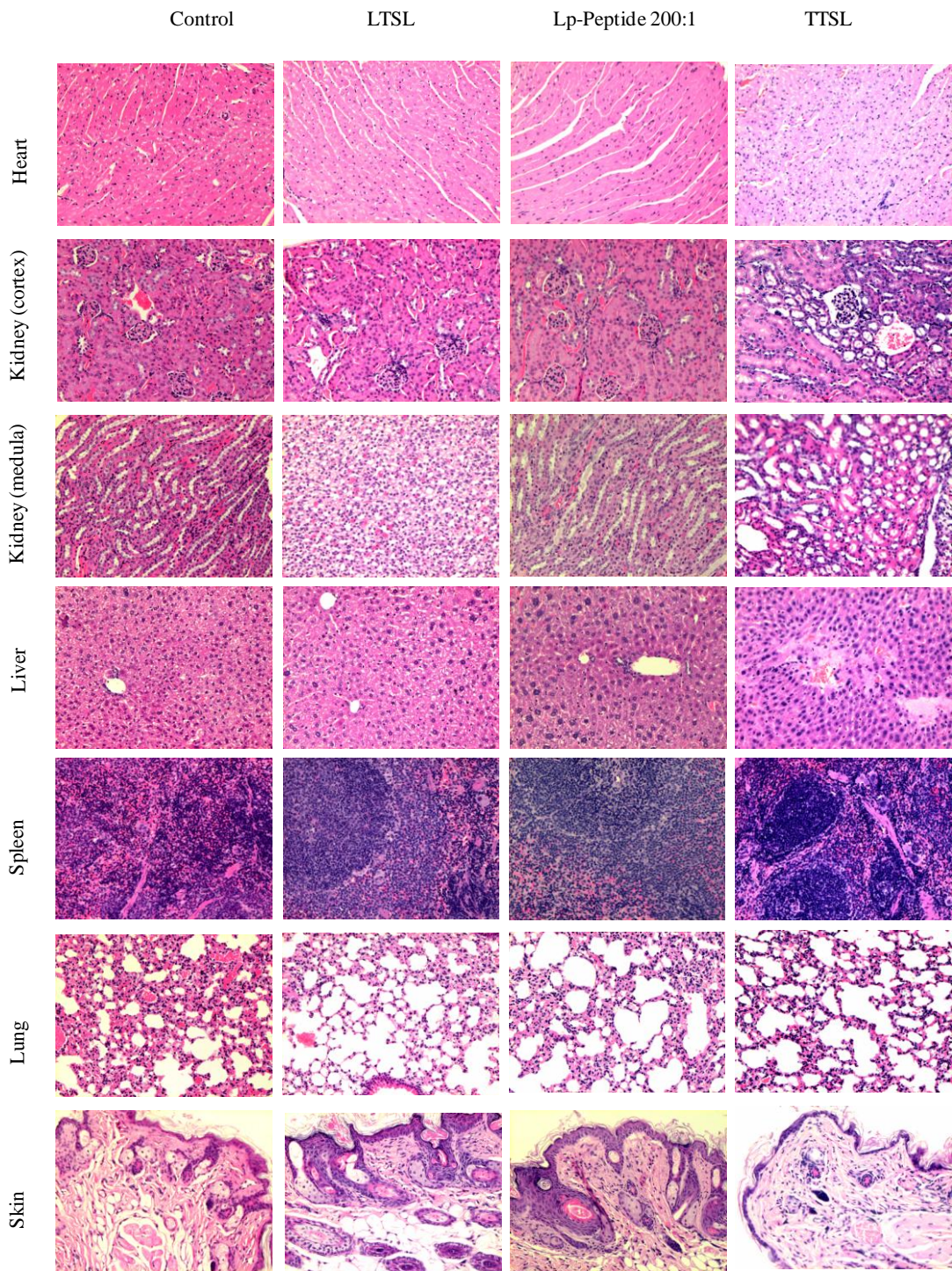


**Figure 5-15: Histological analysis of tissues following treatment using the interstitial release protocol.**

Heart, kidney, liver, spleen, lung and skin tissues were stained with H&E staining. Images are shown at 10x magnification.

In contrast, there were pathological abnormalities in the kidneys from the TTSL group treated with interstitial release protocol. Histological analysis of kidney sections from these animals revealed deposition of protein within tubular lumen and Bowman's space in the glomeruli. In addition, necrosis of the renal papilla was seen in one animal (1/3 TTSL treated mice) (Figure 5-16 C), consistent with previous reports of DOX toxicity (Wang *et al.* 2000). Milder pathological changes were observed in the kidneys of LTSL and Lp-Peptide treated mice with the interstitial release protocol, however these changes were not very severe to cause any clinical or biochemical changes.

Liver and spleen tissues were also examined for any pathological changes because of their high tendency to scavenge liposomes (Huang *et al.* 1992), however, no significant changes were observed.

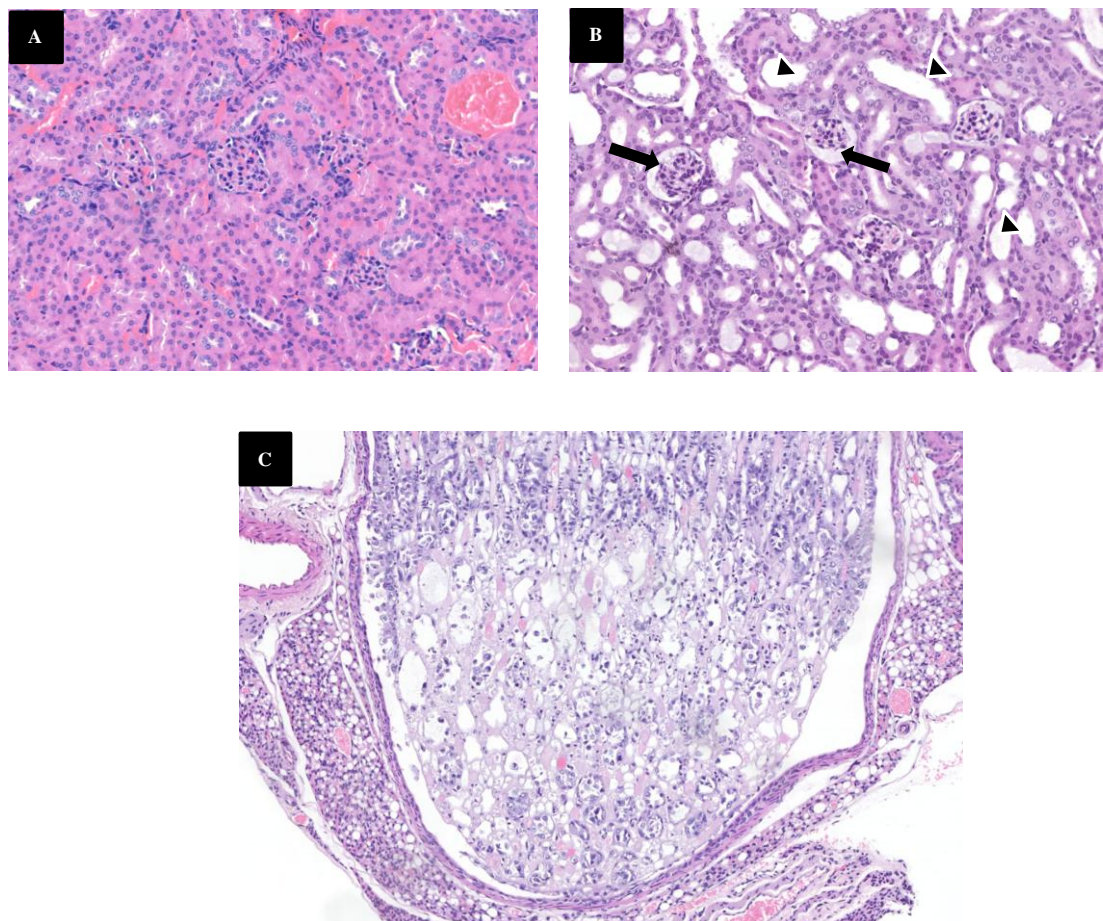


**Figure 5-16: Histopathological changes in the kidney 10 days after treatment with TTSL (interstitial protocol).**

H & E staining of kidney tissues from TTSL treated group represent the major pathological changes detected. A) normal Kidney. B) Pathological changes – arrows demonstrate protein in Bowmans space, arrow heads show dilated tubules with flattened epithelium. C) Papillary necrosis.

No pathological observations were noticed in the lungs of any treated mice compared to controls. All animals had abnormal skin structure consistent with the nude mouse strains. Although, minimally increased levels of dermal inflammation were noticed in some of TTSL treated mice (interstitial release protocol), the significance of this finding is unclear based on the small sample size.

### 5.3 Discussion

In the previous chapter, we explained the development of a new type of TSL, Lp-Peptide hybrids that showed somewhat promising rapid drug release under mild HT and substantial *in vitro* serum stability (50% drug retention in 24 h at 37°C). These interesting properties make this system eligible for *in vivo* application. In this chapter, we demonstrated in details the biocompatibility and cytotoxic activity *in vitro* before Lp-Peptide hybrids were tested for *in vivo* administration. Moreover, the immunogenicity of system was also studied and the results were encouraging to move forward with the *in vivo* evaluation. First blood profile, organs and tumour accumulation of the hybrid system were tested and compared to LTSL and TTSL. Then, the therapeutic activity of Lp-Peptide hybrids was also examined using two HT protocols in order to identify the best HT protocol for the hybrid system to maximize therapeutic effects.

The biocompatibility of liposomes at the therapeutic doses makes them attractive vehicles for drug delivery. This is because liposomes are mainly composed from natural lipids and well tolerated polymerized lipids (DSPE-PEG) (Drummond *et al.* 1999). To make sure the presence of leucine zipper peptide in Lp-Peptide hybrid system did not compromise their biocompatibility, we tested their effect on the *in vitro* viability of both cancer cells and endothelial cells using the MTT assay up to 24 h incubation time. The data did not show any significant cytotoxic effect on both cell types tested, which confirmed the biocompatibility of the hybrid system even after being effectively taken up by the cells as revealed by cellular uptake studies. In addition, ELISA studies confirm lack of antigenicity of the system after systemic administration.

The therapeutic activity of DOX-loaded Lp-Peptide hybrids in comparison to LTSL and TTSL was then studied at the cellular level with and without triggering drug release with mild HT. All TSL in combination with HT showed significant cytotoxic activity equivalent to that of free DOX which indicated complete drug release. No significant cytotoxic activity was observed from NTSL because no drug release is expected even under mild HT. Cytotoxicity data of TSL without exposure to HT were in good agreement with our *in vitro* release data and previous serum stability studies (de Smet *et al.* 2010). Non-heated Lp-Peptide vesicles, TTSL and

NTSL maintained good cellular viability, whereas, significant reduction in cell viability was observed from LTSL even without HT as a result of their leaky character (Banno *et al.* 2010).

In order to examine whether these interesting findings can be replicated *in vivo*, pharmacokinetic studies were performed and the data were consistent with *in vitro* results revealed prolonged blood circulation time of DOX with Lp-Peptide hybrids compared to LTSL. This increase in DOX blood level was clearly reflected on the amount of DOX ended up in the tumour 24 h after injection. *In vivo* administration of Lp-Peptide hybrids with HT resulted in substantial DOX tumour accumulation 1 h after injection which was equivalent to that observed from LTSL. Moreover, tumour DOX level significantly increased (3-fold) 24 h after injection of the hybrid system compared to LTSL. The increase in long term DOX level is due to the prolong blood circulation of Lp-Peptide hybrids leading to continuous extravasation into the tumour area even when HT ceased. Therefore, these findings suggest the suitability of the hybrid system for intravascular drug release while they are circulating in the blood stream because of their fast drug release properties. At the same time, this system enhances the long-term tumour drug-levels suggesting that the Lp-Peptide hybrids can also be useful if HT is applied after their accumulation in the tumour area to release drug interstitially.

Despite the great progress witnessed in the field of TSL over the last few decades, only few studies correlated the type of TSL with the HT protocol applied (Ponce *et al.* 2007) or offered direct comparison between the different types of TSL (Kong *et al.* 2000a; Manzoor *et al.* 2012). The impact of the sequence between LTSL injection and HT treatment on its therapeutic efficacy has been illustrated previously in preclinical studies by Ponce *et al.* (Ponce *et al.* 2007). In a rat fibrosarcoma model injection of LTSL into pre-warmed tumour (injection during HT) showed the optimum drug delivery as indicated by the amount of DOX delivered to the tumour and therapeutic effectiveness (Ponce *et al.* 2007). Almost doubled drug concentration was achieved with this protocol compared to injection before HT and was associated with greater antitumor effect as evidenced by longer time of tumour progression (34 days for LTSL injected during HT compared to 18.5 days for LTSL given before HT).

In FaDu tumour model Kong *et al* compared the therapeutic effects of TTSL and LTSL to NTSL with HT (1 h at 42 °C immediately after injection) (Kong *et al.* 2000a). DOX-loaded LTSL liposomes demonstrated improved therapeutic efficacy compared to TTSL and NTSL liposomes. LTSL-DOX treatment with HT showed complete tumour growth regression out to 60 days after treatment compared to only 30-35 days from TTSL and NTSL. This increase in therapeutic efficacy is attributed to the amount of DOX tumour accumulation which was found to be 25 ng DOX/mg tissue from LTSL compared to only 7-8 ng DOX/mg tissue from TTSL and NTSL (Kong *et al.* 2000a). In addition to increased total tumour DOX accumulation with LTSL, bioavailability of DOX was also improved. LTSL was also the only formulation that showed significant DNA-bound fraction of DOX (quantified by sliver nitrate extraction). Almost half of the DOX delivered to the tumour was bioavailable to tumour cells just 1 h after HT (Kong *et al.* 2000a).

In addition to increase drug accumulation and bioavailability into the tumour, intravascular drug release can also overcome the problems of heterogenous vascularity and limited penetration as it does not depend on liposomal extravasation (Landon *et al.* 2011). This was confirmed recently by Manzoor *et al.* that showed intravascular DOX release from LTSL injection into preheated tumour was associated with deeper tumour penetration as observed using intravital fluorescence imaging of DOX delivery into FaDu tumour model (Manzoor *et al.* 2012). Intravascular release of DOX from LTSL significantly increased free drug penetration distance into the interstitial space and the time to which tumour cells exposed to maximum drug concentration compared to free DOX and Doxil-like NTSL (Manzoor *et al.* 2012). LTSL injection into warm tumour delivered 3.5 times higher DOX level than free drug up to 78  $\mu\text{m}$  from both sides from blood vessels (double the penetration distance of Doxil<sup>®</sup> (Manzoor *et al.* 2012). Similar to Kong *et al* study, the focus of Manzoor *et al* study was mainly on the early time after injection (20 min).

Little is known about the use of HT in combination with liposomes after their accumulation into the tumour (Huang *et al.* 1994; Ning *et al.* 1994; Gaber *et al.* 1996). Although these studies showed prolonged survival, they were mainly performed with NTSL because of their well known passive accumulation in the

tumour by EPR effect even without HT application. The release of DOX from the extravasated liposomes (TTSL) was described previously by Gaber *et al.* by the application of HT 24 h after injection. However, the effect of this interstitial drug release from TTSL was not linked to therapeutic activity (Gaber *et al.* 1996). We designed our *in vivo* experiments using an interstitial drug release protocol to examine this in more detail and also to correlate it with drug release rate and pharmacokinetic parameters of different TSL.

Ultimately, our goal was to define the parameters that can affect the choice between intravascular and interstitial drug release in order to achieve the best efficacy of HT-assisted TSL treatment. *In vivo* therapeutic efficacy studies were performed using the SW480 tumour model rather than B16F10 because of the rapid growth and aggressive nature of B16F10 tumour model that makes comparison between the treatment groups challenging, especially since our experiments were designed on single and not multiple injection regimes. Previous reports have shown that tumour drug concentration correlated directly to therapeutic efficacy (Huang *et al.* 1994; Kong *et al.* 2000a; Yarmolenko *et al.* 2010) and *in vivo* optical imaging, therefore, IVIS imaging studies were performed to correlate tumour DOX accumulation with growth retardation and survival studies.

LTSL treated animals using intravascular release protocol showed pronounced tumour growth retardation and prolonged survival compared to the control because of their fast drug release that resulted in the highest tumour DOX level immediately after HT. On the other hand, LTSL treatment with interstitial release protocol did not show any improvement in tumour growth retardation and survival which was predicted from its limited tumour DOX accumulation. LTSL released most their encapsulated drug in circulation before accumulation in the tumour; therefore the fraction of bioavailable drug that reached the tumour was significantly less. The decrease in drug retention of LTSL was due to significant loss (~70%) of the lysolipid component shortly after contact with biological fluid as previously stipulated (Banno *et al.* 2010).

In the case of TTSL treatment using the intravascular protocol, tumour growth retardation and survival were significantly improved compared to control. However, the therapeutic effect was less pronounced compared to LTSL treatment because of



their intermediate drug release rate in response to HT. Although TTSL treatment with the interstitial release protocol showed the highest DOX accumulation among the three types of TSL tested, as expected from their long blood circulation time and drug retention, this was also accompanied by severe weight loss and resulted in 50% reduced survival. The rapid toxicity profile observed with the TTSL treatment using the interstitial protocol suggested toxicities, other than cardiotoxicity, are involved, since the cardiotoxicity of DOX is mainly a cumulative effect (Allen *et al.* 2005). This agrees with the findings of Allen *et al.*, where they observed similar toxicity profile (gastrointestinal as an example) from mice treated with DOX-loaded DPPC/POPC:CHOL:DSPE-PEG (2:1:0.1) liposomes which has intermediate release properties (Allen *et al.* 2005). Histopathological analysis of organs pooled from TTSL treated mice with interstitial release protocol showed significant pathological changes in the kidneys which were consistent with findings previously reported with free drug (Wang *et al.* 2000). We observed similar toxicity profile with DOX loaded TTSL treatment without HT application. Whereas, no toxicity was observed from drug-free TTSL liposomes, which indicate that this toxicity was not due to the lipid composition. Conversely, TTSL formulation tested using the intravascular protocol did not show any toxicity.

The possible explanation of the above is the intermediate drug retention of TTSL and their longer blood circulation time when the interstitial protocol was used. This could cause drug leakage at a rate that corresponded to the turn-over properties of the tissues showing significant toxicity (Allen *et al.* 2005). This discrepancy in blood profile of TTSL between the two protocols is believed to be due to the release of DOX from TTSL at the tumour site when the HT is applied simultaneously after injection (de Smet *et al.* 2011). Although mild HT is expected to affect liposome accumulation only in the tumour, the change in blood profile of TSL as a result of changing the HT protocol can be reflected in the amount of drug that accumulates in the other tissues. Our *in vivo* organs biodistribution studies revealed a significant increase in DOX levels in the liver and kidney from TTSL liposomes when administered without HT compared to HT application. The rate of drug release is another determinant factor for liposomes toxicity. It has been reported before by Mayer *et al.* and Allen *et al.* that relatively long circulation time of liposomes with intermediate release rate had higher toxicity compared to those with fast and slow

release (Mayer *et al.* 1989; Charrois *et al.* 2004). Interestingly, this toxicity was reduced by conjugation to anti CD-19 antibodies to increase the specificity of liposomes (Allen *et al.* 2005).

In agreement with our hypothesis, Lp-Peptide hybrids showed good therapeutic efficacy in both heating protocols tested compared to LTSL and TTSL. Lp-Peptide hybrids treatment with intravascular protocol showed equally effective tumour growth retardation and survival to that of LTSL treatment. Lp-Peptide hybrids were the only TSL that showed modest therapeutic response using the interstitial release protocol. Almost 15% increase in life span was observed from Lp-Peptide hybrids, with no signs of toxicity.

Obviously, higher DOX accumulation was achieved from intravascular release compared to interstitial release protocols. This can be understood based on the advantageous effect of HT on the tumour accumulation of liposomes as well as the triggering of DOX release. Despite the well known effect of HT on increasing liposomal extravasation into the same tumour that can last up to 6-8 h after stopping HT, this effect decays over time (Kong *et al.* 2001; Li *et al.* 2013a). Maximum increase in nanoparticles extravasation can be achieved when administered with HT due to the contribution from increased in blood flow and triggered local release of DOX from TSL (Matteucci *et al.* 2000; Kong *et al.* 2001).

As noted above, the choice of the heating protocol is a critical parameter in determining the safety and the therapeutic efficacy of TSL. This also highlights the impact of better understanding of the pharmacokinetic parameters on the outcome in the clinical setting.

## 5.4 Conclusion

*In vitro* and *in vivo* biocompatibility studies showed that Lp-Peptide hybrids did not have any negative effect on cell viability and did not show any signs of immunogenicity. *In vivo* pharmacokinetics and biodistribution studies were in good agreement with *in vitro* release and cytotoxicity data. Lp-Peptide hybrids characterized by prolong blood circulation profile resulted in higher tumour drug accumulation following hyperthermia in tumour-bearing animals. Therapy data demonstrated that the drug release properties of TSL are not the only factors that determine their therapeutic activity. The design and the timing of heating and injection based on the proper understanding of their physicochemical properties and pharmacokinetics parameters also play a pivotal role in the therapeutic effectiveness as well as in the toxicity of TSL. In agreement with our hypothesis, Lp-Peptide hybrids showed good therapeutic efficacy in both heating protocols tested compared to LTSL and TTSL. The clinical benefits of this study lies in the understanding of the critical parameters to take in consideration in the design of clinical HT protocol based on the type of TSL formulation.

## **CHAPTER 6**

---

### **THE ENGINEERING OF ANTI-MUC-1 TARGETED TSL**

In this chapter, we explore the opportunities to further enhance the therapeutic potential of TSL, by designing MUC-1 targeted TSL (TTSL-Ab). For this purpose we focused our interest on traditional TSL (TTSL) because of their long circulation kinetics and high tumour accumulation. TTSL-Ab should, ideally, have the potential to bind and be internalised into tumour cells with great specificity. Once inside the cells, HT can be applied to trigger drug release inside the tumour cells. We characterized these liposomes by studying their size, surface properties, serum stability and thermal sensitivity before and after conjugation to MUC-1 antibody. Receptor mediated cellular uptake and cytotoxic efficacy of MUC-1 TTSL-Ab were investigated using 2D and 3D cell culture techniques. Significant enhancement in cellular uptake and cytotoxic activity after 1 h heating at 42 °C was observed from TTSL-Ab compared to non-targeted liposomes in MUC-1 over-expressing breast cancer cells (MDA-MB-435). *In vivo* performance of TTSL-Ab was tested comparing three different heating protocols. Blood circulation kinetics, biodistribution and tumour accumulation were thoroughly studied using <sup>14</sup>C-DOX radiolabelled liposomes and live imaging technology (IVIS). *In vivo* tumour uptake of TTSL-Ab improved compared to TTSL when injected post or with HT. Anticancer activity in MDA-MB-435 breast cancer xenografts was also studied applying simultaneous heating and injection protocol. *In vivo* therapeutic experiments were designed with and without 2nd heating 24 h after injection to trigger liposomal drug release after tumour accumulation. Slight improvement in therapeutic activity and survival was observed from TTSL-Ab plus 2nd HT compared to TTSL (49% and 45% increase in life span, respectively), which might be further optimized by increasing dosing frequency and by changing the timing of 2nd HT. Ultimately, our results suggested that TTSL-Ab in combination with mild HT can reveal new avenues in anticancer therapy.

## 6.1 Introduction

In order to enhance the therapeutic potential of liposomal anticancer drugs, interest in developing new generation of liposomes that aim to combine the advantages of both active targeting and triggered release properties has increased. Targeted TSL might be useful in slowing the transient time in the blood, by targeting antigens expressed on the angiogenic tumour vasculature (Negussie *et al.* 2010), and it can be directed towards tumour-specific or tumour-associated antigens (Puri *et al.* 2008; Pradhan *et al.* 2010). Once bound to the specific antigen on their target tumour cells, targeted TSL can then release their contents by the application of HT either at the surface of the cells (Sullivan *et al.* 1986) or inside the tumour cells after conjugation to an internalising ligands (Puri *et al.* 2008; Smith *et al.* 2011). Several examples of targeted TSL have been reported recently and showed promising biological activity *in vitro*. Examples on that are the folate targeted DPPC:CHOL:DSPE-PEG<sub>2000</sub>:DSPE-PEG<sub>2000</sub>-Folate (80:20:4.5:0.5) liposomes co-encapsulating iron oxide magnetic nanoparticles and DOX (Pradhan *et al.* 2010) (MagFolDox). Physical targeting and cellular uptake of MagFolDox into folate expressing cells using permanent magnetic field increased cellular uptake by 50 folds compared to Doxil-like liposomes. Synergistic increase in cytotoxicity (<10% cell viability at 30µM DOX) was observed from MagFolDox in combination with magnetic HT that was thought to be mediated by intracellular triggered drug release (Pradhan *et al.* 2010). In recent study by Smith *et al* thermosensitive DPPC:Mal-DSPE-PEG<sub>2000</sub>:DSPE-PEG<sub>2000</sub> (88:5.5:5.5) liposomes were conjugated with anti-HER2 affibody (HER2<sup>+</sup> affisomes) (Smith *et al.* 2011). Conjugation to anti-HER2 affibody increased binding specificity by 10 folds to HER2<sup>+</sup> SK-BR-3, human breast adenocarcinoma cells without HT. This also resulted in 2-3 folds increase in cellular cytotoxicity from DOX-loaded HER2<sup>+</sup> affisomes (at 45 °C) compared to non-targeted liposomes (Smith *et al.* 2011).

However, *in vivo* evaluation of targeted TSL in combination with mild HT and the effects of HT on targeted TSL accumulation and drug release at the tumour site have not been previously performed.

In this chapter we attempt to unravel the potential of combining monoclonal antibody targeted TSL with local HT *in vivo*. We designed MUC-1 targeted TSL, by

conjugation of clinically tested hCTMO1 mAb directed against MUC-1 antigen to the termini of traditional TSL (TTSL).

MUC-1 (mucin antigen), a transmembrane glycoprotein, is an attractive target for cancer immunotherapy. Although, MUC-1 is expressed on the surface of many normal epithelial cells, its expression is up-regulated in the majority of epithelial cancers. In the tumour MUC-1 loses its apical distribution and it becomes hypoglycosylated (Limacher *et al.* 2007). MUC-1 is over-expressed in 90% of adenocarcinomas, including cancers of the ovary, breast, and pancreas (Mukherjee *et al.* 2003). It is involved in the signal transduction pathways that regulate the mobility, invasion and metastasis of cancer. These tumour associated changes and cellular internalisation properties by receptor recycling (Moase *et al.* 2001) make it an attractive candidate for cancer therapy.

CTMO1 is a murine monoclonal antibody that recognises MUC-1 epitope and has a potential in the therapy of breast and ovarian cancers (Baker *et al.* 1994). In order to decrease the immunogenicity and permit repeated administration, CMT01 was genetically engineered with high level of re-expression by grafting the complementarity determining regions (CDR) into human immunoglobulin resulting in the formation of recombinant humanized antibody (hCTMO1) with superior binding affinity to MUC-1 antigen compared to CMT01 (Baker *et al.* 1994; Gillespie *et al.* 2000). Biodistribution and therapeutics potential of hCTMO1 has been clinically assessed (Davies *et al.* 1997; Prinssen *et al.* 1998). In addition, the internalising capability of hCTMO1 antibody offers a great potential to improve local drug delivery of anticancer drugs and reduce systemic toxicity through antibody drug conjugates. An example of that is the conjugation of hCTMO1 antibody to calicheamicin, a highly cytotoxic drug via amide linker and the resulting immunoconjugate (called CMB-401) which reserved the properties of both the antibody and the drug (Hinman *et al.* 1993). This conjugate showed very promising results *in vitro* and *in vivo* against ovarian carcinoma and progressed into clinical testing (Gillespie *et al.* 2000). However, the results of phase II clinical trial did not meet the end point criteria. The type of the amide linker used for the design of this conjugate and the pre-injection of hCTMO1 may be responsible for the reduction in pharmacological activity which warranted more work (Chan *et al.* 2003). Although

the results of this clinical study was disappointing it opens the doors for further investigations in order to establish a more effective treatment strategy for cancer.

TTSL is a long circulating temperature sensitive liposome with an intermediate capacity to temperature triggered drug release (Gaber *et al.* 1996). TTSL exhibit a long blood circulation profile and high accumulation at the tumour site that can be further substantiated by HT (Gaber *et al.* 1996; de Smet *et al.* 2011). Due to these attractive properties, we hypothesized that the biological activity of TTSL liposomes could be further improved by conjugation of anti-MUC-1 IgG antibody to achieve specific interaction with cancer cells and subsequent internalisation. Once inside target cancer cells, content release could be triggered by the application of HT.

To achieve these goals, we studied the biodistribution and tumour accumulation of MUC-1 targeted TTSL (TTSL-Ab) in comparison to non targeted TTSL, applying different protocols varying the timing between HT and injection to allow HT to vasodilate tumour vessels and increase TTSL tumour accumulation. *In vivo* therapeutic experiments were designed, with and without a second heating at 24 h after administration, to trigger liposomal drug release after tumour accumulation. Moderate improvement in the biological activity and survival was observed from TTSL-Ab plus second HT compared to non-targeted TTSL. Our results suggest that targeted TTSL in combination with mild HT can offer new opportunities in the development of advanced cancer therapeutics.



## 6.2 Results

### 6.2.1 Preparation and Characterization MUC-1 TTSL-Ab Liposomes

Anti-MUC-1 Ab conjugation to TTSL liposomes was performed by the post-insertion method (Moreira *et al.* 2002). The conjugation of Ab by post-insertion method depends on the translocation of mal-DSPE-PEG<sub>2000</sub> Ab micelles into the liposomes. By this, the Ab ligand will be exposed at the outer surface of liposomes and, thus, maintain its binding capacity (Sofou *et al.* 2008). Briefly, mal-DSPE-PEG<sub>2000</sub> Ab micelles were prepared by conjugation of thiolated Ab (Ab-SH) with mal-DSPE-PEG<sub>2000</sub> micelles (Figure 6-1).

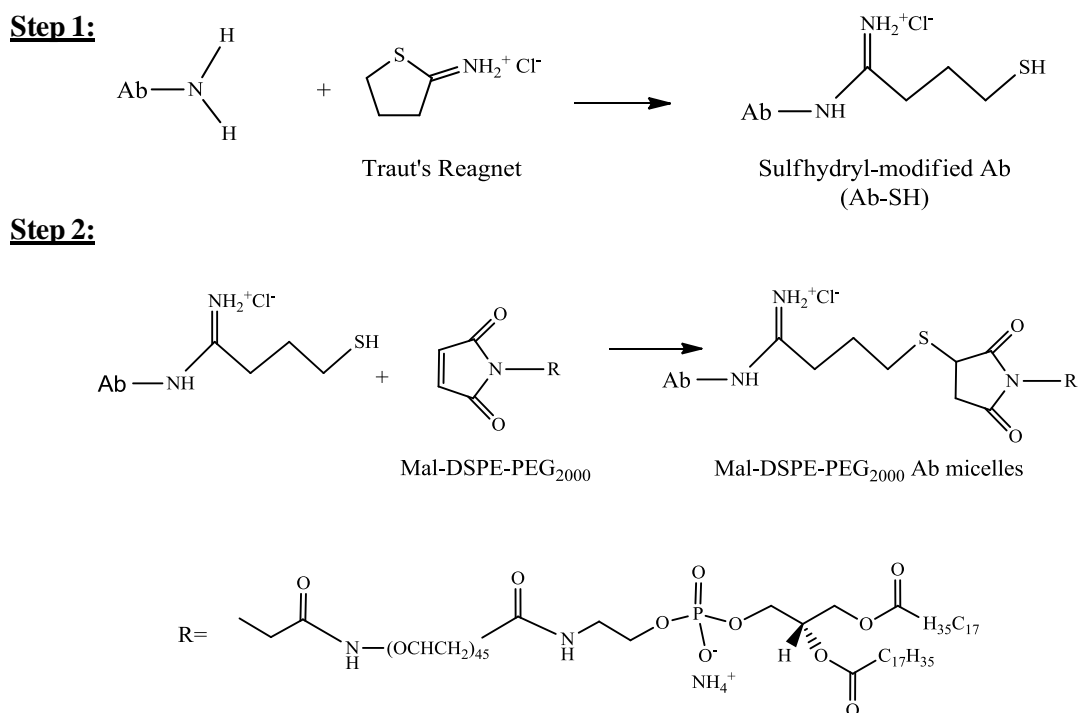
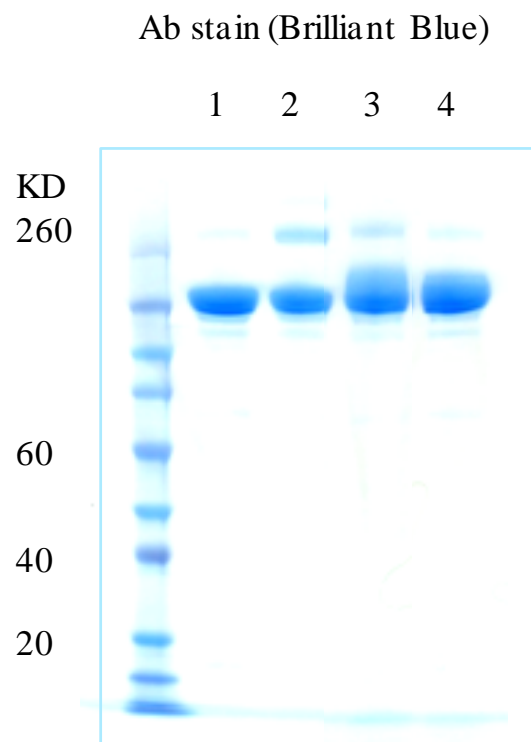


**Figure 6-1: Conjugation of anti-MUC-1 Ab to mal-DSPE-PEG<sub>2000</sub> micelles.**

Thiolation of anti-MUC-1 Ab by mixing with Traut's reagent at room temperature for 1h, followed by mixing with mal-DSPE-PEG<sub>2000</sub> micelles overnight. Both reactions were preformed under oxygen-free environment

The conjugation process was confirmed by an upper shift in anti-MUC-1 Ab band on SDS-PAGE (band 3) indicating an increase in its molecular weight after conjugation (Figure 6-2).



- 1 Ab.
- 2 Ab-SH.
- 3 Ab-SH conjugated to mal-DSPE-PEG<sub>2000</sub> micelles.
- 4 Ab mixed with mal-DSPE-PEG<sub>2000</sub> micelles.

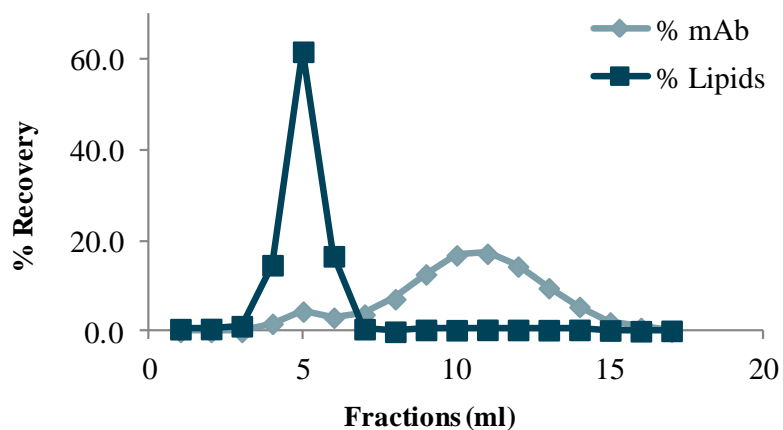
**Figure 6-2: SDS-PAGE electrophoresis of anti-MUC-1 antibody.**

SDS-PAGE gel of anti-MUC-1 Ab before and after conjugation to mal-DSPE-PEG<sub>2000</sub> micelles. SDS-PAGE gel was stained with Instant Blue stain to visualize the Ab. An upper shift in of Ab band in lane 3 was observed indicated an increase in anti-MUC-1 Ab molecular weight after conjugation.

In order to determine the best post-insertion temperature, post-insertion was done at three different conditions; 60 °C (1 h), 45 °C (1 h) and 39 °C (5 h) (Figure 6-3 A). The amount of antibody post-inserted into TTSL liposomes was then determined in each elution fraction by quantification of both Ab using BCA assay and lipids using the Steward assay (Figure 6-3 B). The best post-insertion efficiency was obtained after 1 h incubation at 60 °C. A clear co-localization of mal-DSPE-PEG<sub>2000</sub> Ab micelles with the liposome fractions was observed (Figure 6-3 B). The amount of Ab conjugation obtained was 13 µg Ab/µmole lipid at Ab:lipid 1:1000 molar ratio and 26.5 µg Ab/µmole lipid at Ab:lipid 1:500 molar ratio.

**A**

Incubation temp (°C)	Duration	$\mu\text{g Ab}/\mu\text{mole lipid}$
60	1h	26.46
45	1h	8.82
39	5h	2.94

**B**

**Figure 6-3: Quantification of anti-MUC-1 after post insertion into TTSL liposomes.**

A) The effect of post-insertion temperature on the amount of anti-MUC-1 Ab post-inserted into TTSL liposomes. The best antibody conjugation was achieved after 1 h incubation at 60 °C. B) Size exclusion chromatographic fractions of mal-DSPE-PEG<sub>2000</sub> Ab micelles after post-insertion into TTSL liposomes. Ab and lipids in each fraction were quantified by BCA assay and the Stewart assay, respectively.

SPR was used to check the integrity of the anti-MUC-1 antibody after the different conjugation steps to TTSL liposomes. SPR sensorgrams of mal-DSPE-PEG<sub>2000</sub> Ab micelles & TTSL-Ab showed that the antibody reserved its binding capability evidenced by the increase in response unit (RU) in a concentration dependent manner (Figure 6-4).

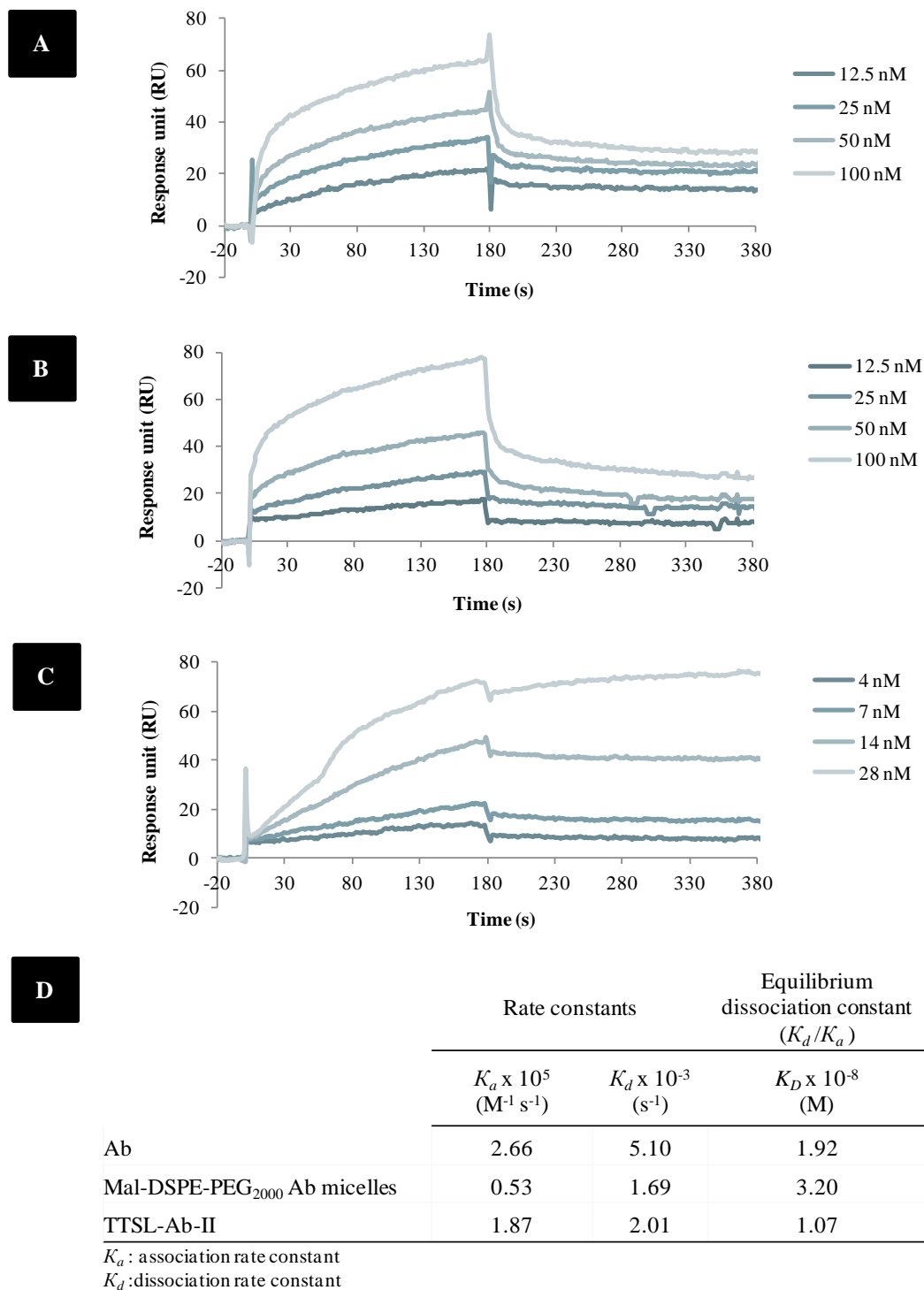


**Figure 6-4: SPR sensograms of anti-MUC-1 antibody binding to MUC-1 epitope.**

Different concentrations of; A) Anti-MUC-1 antibody, B) Mal-DSPE-PEG<sub>2000</sub> Ab micelles and C) TTSL-Ab were injected over immobilized MUC-1 epitope. D) Rate constants and dissociation constants for the interaction of anti-MUC-1 antibody with immobilized MUC-1 epitope.

Interestingly, we observed that the equilibrium dissociation constant of Ab after conjugation to liposomes was lower than the Ab itself indicating higher binding affinity (Figure 6-4 D).

No significant change in the size of liposomes was observed after Ab conjugation. Both TTSL and TTSL-Ab liposomes were slightly larger than 100 nm in size with low PDI. Moreover, DOX was successfully encapsulated (> 90%) without affecting the particle size of the liposomes (Figure 6-5 B). Interestingly, a decrease in zeta potential was observed after Ab conjugation and the reduction was proportional to the amount of the Ab conjugated which agrees with other previous studies (Chen 2011; Yang *et al.* 2012a).

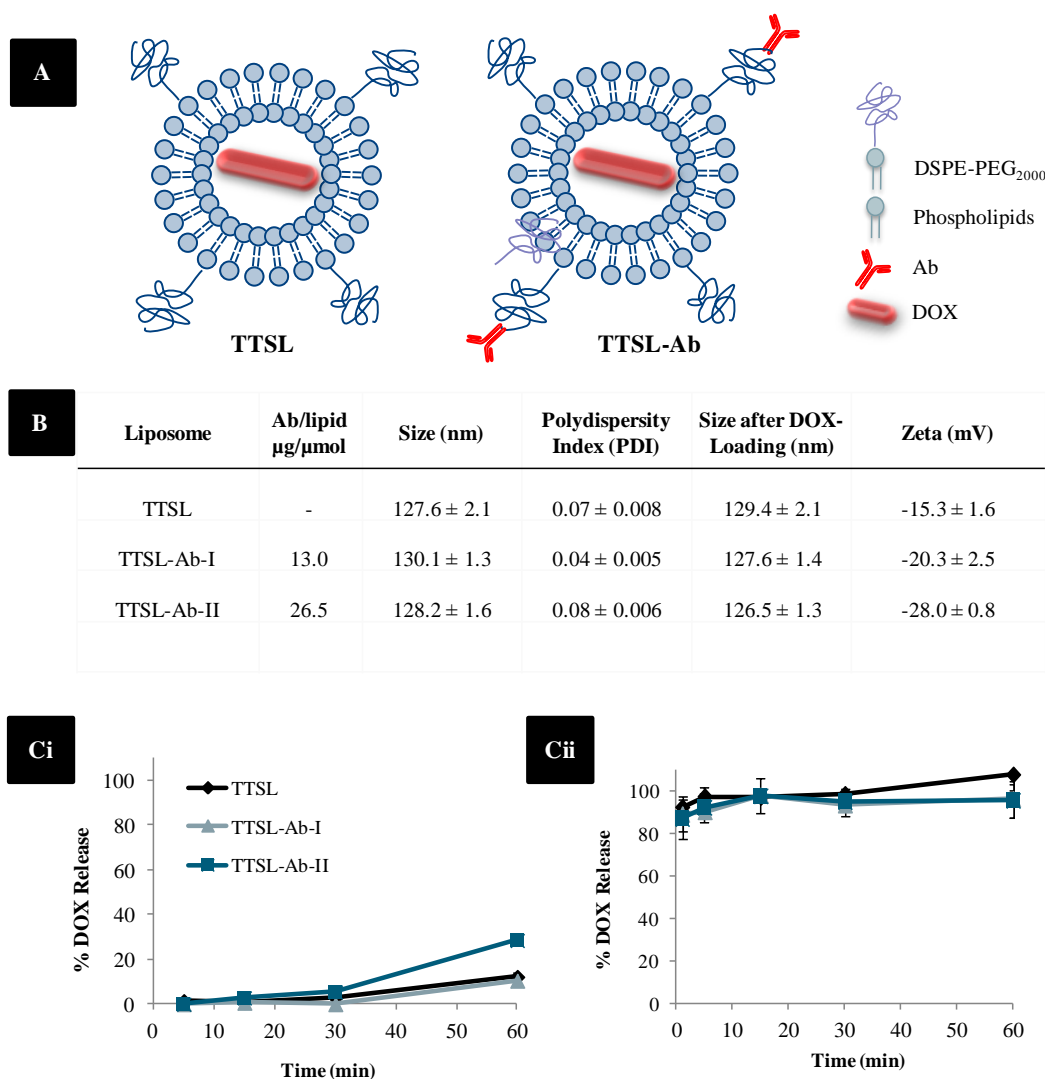


**Figure 6-5: Design and characterization of TTSL and TTSL-Ab.**

A) Schematic presentation of non-targeted TTSL and targeted TTSL-Ab. B) Size, PDI and surface properties of TTSL before and after post-insertion of MUC-1 antibody at two different ratios. Ci) DOX release from TTSL and TTSL-Ab liposomes after incubation at 37 °C. Cii) DOX release after heating at 42 °C. DOX release experiments were performed in 50% CD-1 mouse serum to simulate physiological conditions. Data represented as mean  $\pm$  STD (n=3).

### 6.2.2 DOX Release Studies

Serum stability and thermal responsiveness of TTSL and TTSL-Ab liposomes were studied by quantifying the amount of encapsulated DOX release at 37°C and 42°C, respectively. No significant leakage of DOX from both TTSL and TTSL-Ab was observed after incubation for 60 min in 50% serum at 37 °C (Figure 6-5 Ci). DOX release at 42°C showed rapid release, more than 80% of drug release after 1 min incubation from TTSL liposomes with and without Ab (Figure 6-5 Cii). DOX release data showed that TTSL-Ab liposomes maintained their serum stability and temperature sensitivity after Ab conjugation.

### 6.2.3 Cellular Binding of Anti-MUC-1 Antibody

We tested the expression of MUC-1 antigen in various human cancer cell lines (MDA-MB-435, MCF-7 and C33a) (Figure 6-6 A).

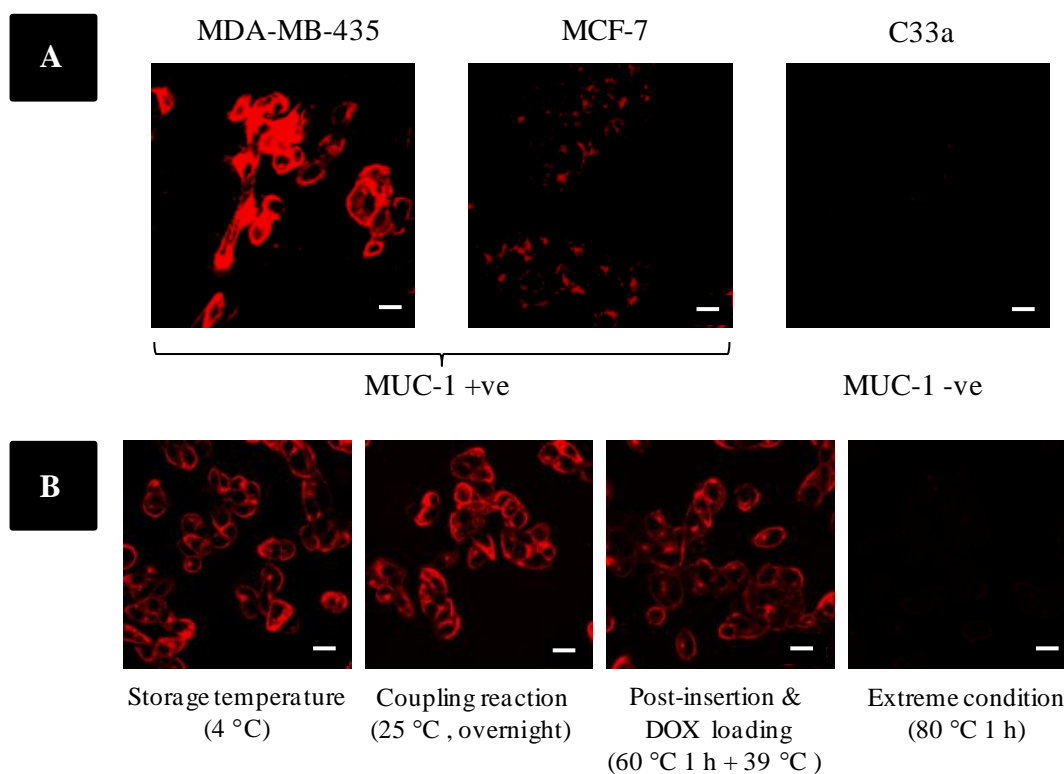


**Figure 6-6: Cellular binding of anti-MUC-1 antibody.**

A) CLSM images of MDA-MB-435, MCF-7 and C33a after 3 h incubation with Anti MUC-1 Ab (1 $\mu$ g/ml) at 37 °C. B) Anti MUC-1 Ab binding to MDA-MB-435 cells at each step of conjugation process to TTSL liposomes by 1 h incubation with anti-MUC-1 antibody (1 $\mu$ g/ml) at 37 °C. After incubation with anti-MUC-1 antibody cells were washed and stained with Cy3-labelled secondary antibody and imaged with CLSM. Scale bar is 20  $\mu$ m.

The binding capacity of anti-MUC-1 antibody after each step of conjugation to TTSL liposomes was studied by looking at their binding to MDA-MB-435 cells using immunostaining with Cy3-labelled secondary antibody and visualization with confocal microscopy (Figure 6-6 B). Binding data confirmed that the antibody maintained its binding efficiency after incorporation into TTSL-Ab liposomes, in contrast to complete loss of binding after 1h incubation at 80°C.

#### 6.2.4 Cellular Uptake of TTSL and TTSL-Ab

We then examined the cellular uptake of TTSL-Ab liposomes by confocal microscopy (Figure 6-7).

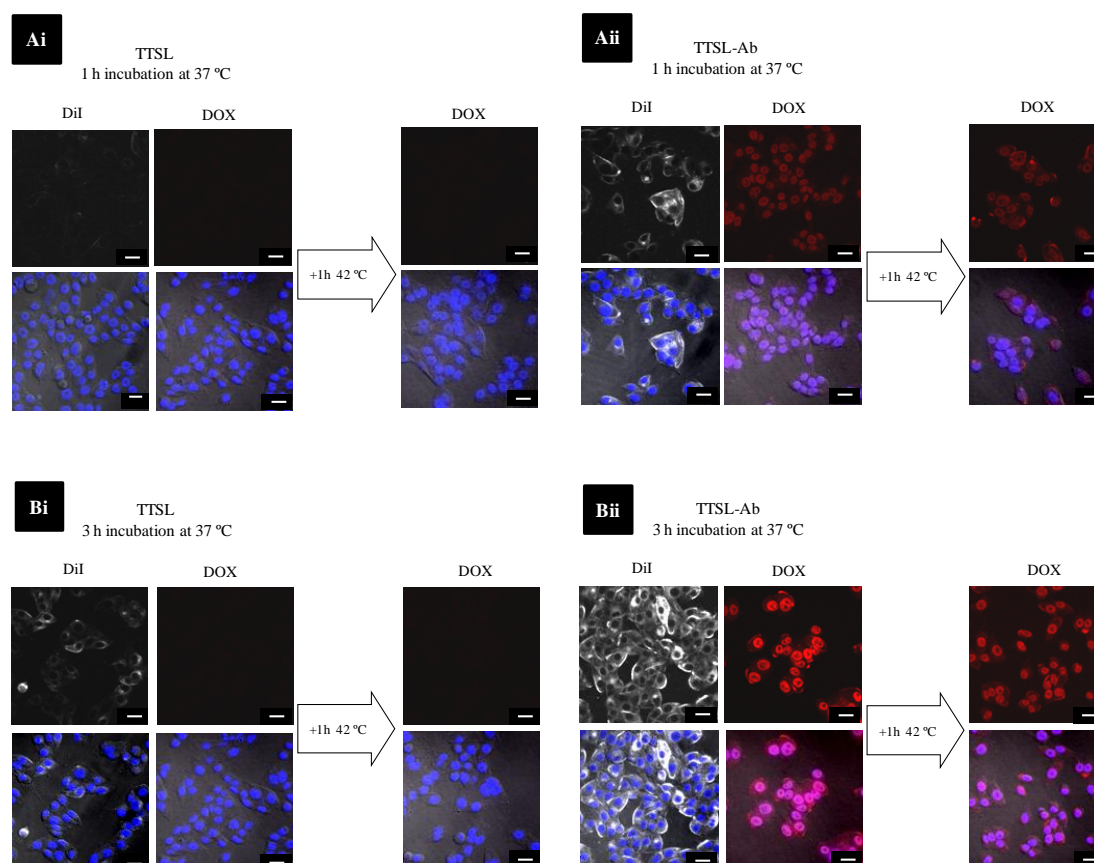


**Figure 6-7: Cellular uptake studies of TTSL and TTSL-Ab into MDA-MB-435 cells.**

Confocal microscopy imaging of monolayer of MDA-MB-435 cells (MUC-1+ve) showed the uptake of DiI-labelled and DOX encapsulated TTSL and TTSL-Ab (26  $\mu\text{g Ab}/\mu\text{mol lipid}$ ) after: Ai) & Aii) 1 h and Bi) & Bii) 3 h incubation. White channel represents the uptake of DiI-labelled liposomes. Red channel represents DOX before and after 1 h heating at 42°C. Co-localization with DAPI stain (blue channel) of the nucleus is shown in the overlay images. Top images are fluorescence images from excitation of DiI (left) and DOX (centre and right). Bottom images represent the overlay with DAPI and bright field images. Scale bar is 20  $\mu\text{m}$ . DiI was imaged at 514 nm laser excitation source and 585 nm output filter. DOX fluorescence signal was detected at 488 nm laser excitation source and 535–674 nm output filters.

Antibody targeted TTSL were internalised by MUC-1+ve cells with higher levels of intracellular accumulation compared to non-targeted TTSL liposomes. Figure 6-7 also depicts that the uptake of both lipids (DiI signal; white) and the encapsulated drug (DOX signal, red) were increased by conjugation with anti-MUC-1 antibody after 1 h and 3 h incubation. In comparison, only moderate cellular uptake was observed from non-targeted TTSL (DiI signal) after 3 h incubation, presumably through non-specific endocytosis. No internalisation of non-targeted TTSL was observed based on DOX fluorescence, further indicating the poor levels of cellular uptake compared to targeted TTSL (amount of DOX internalised close to the background level (Figure 6-7 Bi middle and right panels)).

The kinetics of cellular uptake were also studied by imaging DOX-loaded TTSL and TTSL-Ab (Figure 6-8). Rapid binding and internalisation of TTSL-Ab liposomes into MDA-Mb-435 cells was observed as early as 1 h after incubation and increased over 24 h. Cellular uptake can be further enhanced by increasing the density of anti-MUC-1 antibody per liposome from 13  $\mu\text{g Ab}/\mu\text{mole lipid}$  to 26.5  $\mu\text{g Ab}/\mu\text{mole lipid}$  in TTSL-Ab-I and TTSL-Ab-II, respectively (Figure 6-8). The enhancement in cellular uptake was specific to MUC-1+ve cells, since no significant difference was observed in internalisation within C33a cells (MUC-1-ve).

We also investigated the potential of MUC-1 targeted TTSL liposomes for triggered DOX delivery by exposing the cells to mild HT (1 h incubation at 42 °C). Confocal microscopy did not show a significant difference in the signal intensity and location of DOX.

### **6.2.5 Cytotoxic Activity of DOX-Loaded TTSL and TTSL-Ab**

To evaluate the cytotoxic activity of targeted TTSL compared to TTSL, cellular viability was measured using the MTT assay in both MUC-1+ve and MUC-1-ve cell lines with and without exposure to HT. To evaluate temperature sensitivity of targeted TTSL, mild HT was applied to trigger release from liposomes after cellular uptake. Moderate cytotoxic activity (~90% cell viability) was observed from cells treated with TTSL-Ab without exposure to HT. In comparison, intracellularly triggered DOX release from targeted TTSL-Ab liposomes in MDA-MB-435 (MUC-1+ve) cells resulted in a significant ( $p < 0.01$ ) enhancement in cytotoxicity compared



to that without heating (only 60% cell viability) (Figure 6-9 A). The observed cytotoxic effect was also dependent on the density of anti-MUC-1 antibody conjugation to liposomes. This data followed in agreement with the cellular uptake findings above and indicated that although some spontaneous release of DOX could occur after TTSL-Ab internalisation, the amount of bioavailable drug can be significantly enhanced by triggering release with HT.

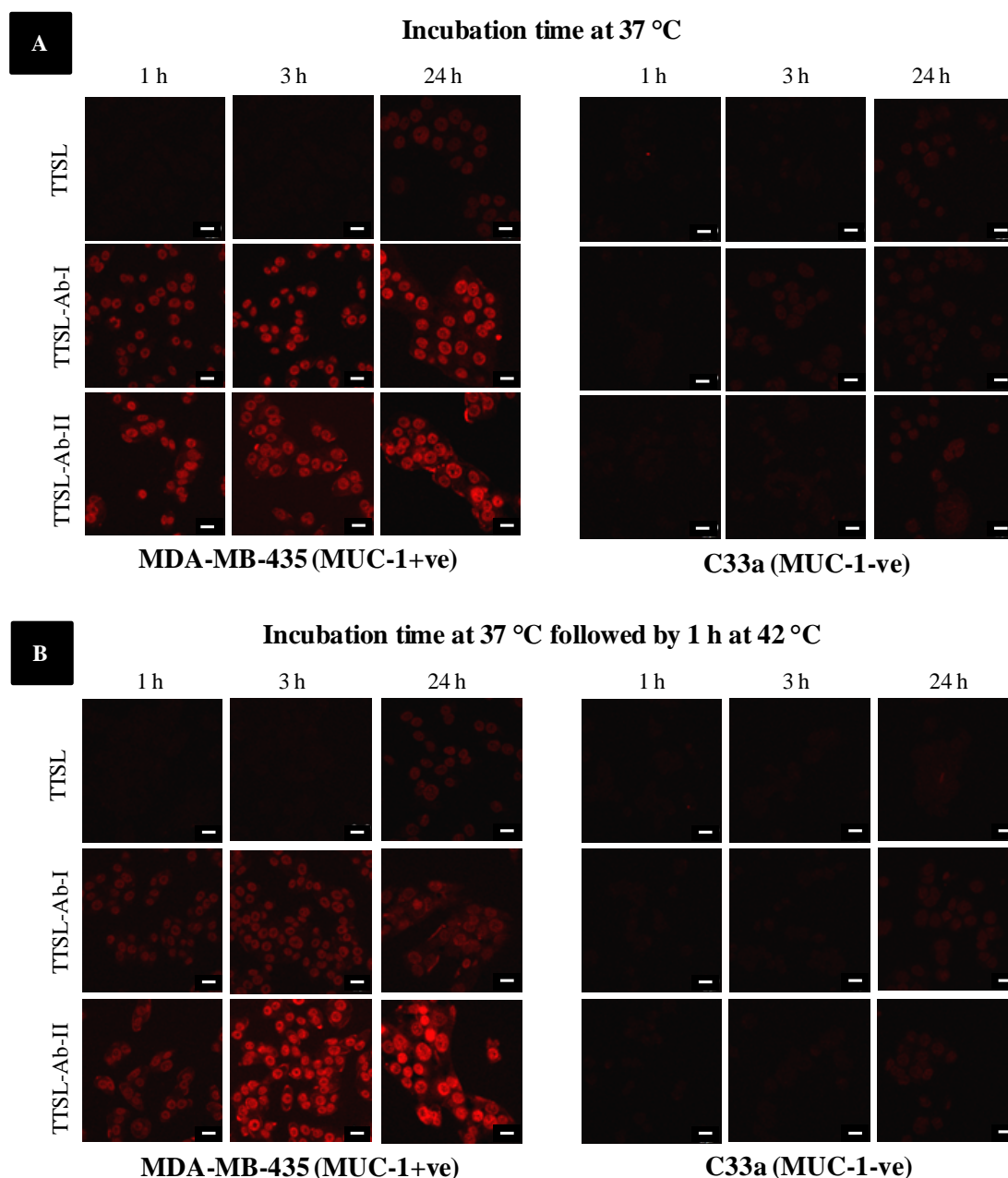


**Figure 6-8: Cellular uptake of DOX-loaded TTSL, TTSL-Ab-I & TTSL-Ab-II.**

Cellular uptake of TTSL liposomes with and without conjugation to two different ratios of anti-MUC-1 antibody was studied with CLSM after 1 h, 3 h & 24 h incubation at: A) 37 °C with MDA-MB-435

cells (MUC-1+ve) and C33a (MUC-1-ve) and B) after 1 h additional incubation at 42 °C at the end of incubation time at 37 °C. Scale bar is 20 µm.

No cytotoxic activity was observed from non-targeted TTSL with and without HT. Also, both targeted and non-targeted TTSL did not have any cytotoxic activity in C33a (MUC-1-ve) cells, which further confirmed the selective activity of MUC-1 targeted TTSL (Figure 6-9 B).

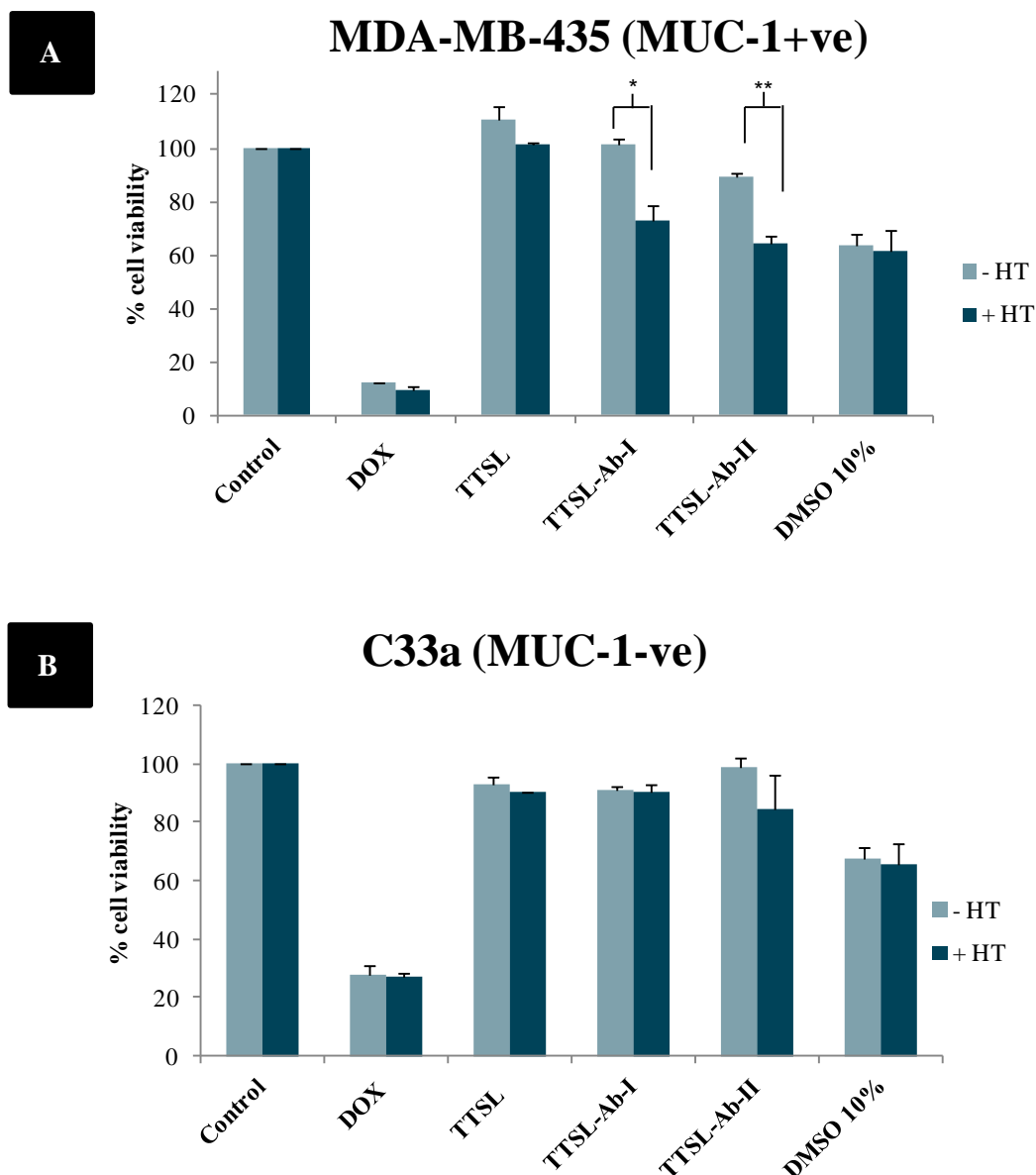


**Figure 6-9: MTT assay of TTSL and TTSL-Ab in: A) MDA-MB-435 and B) C33a cells.** Cellular monolayers were treated with TTSL and TTSL-Ab at 10µM DOX concentration for 3 h at 37 °C. After 3 h incubation, the liposomes containing media were removed and replaced with fresh media. To test the effect of heat trigger release, cells were incubated at 42 °C (1 h, in CO<sub>2</sub> incubator) and compared to no heating condition. MTT assay was performed 48 h after treatment and expressed as percentage of cell viability. Results represent average ± STD of at least 2 independent experiments (6 wells per treated group). \* indicates  $p < 0.05$  and \*\* indicates  $p < 0.01$ .

### 6.2.6 Localisation and Cytotoxic Activity of TTSL and TTSL-Ab in Multicellular Spheroids (MCS)

The therapeutic efficacy of targeted TTSL-Ab liposomes will depend not only on their cell receptor binding and internalisation, but also on their capability to penetrate into the tumour. MCS were used to better mimic the avascular region of tumour tissue. MCF-7 (MUC-1+ve) MCS were used in these experiments instead of MDA-MB-435 due to the inability of the later to form MCS Figure 6-10.

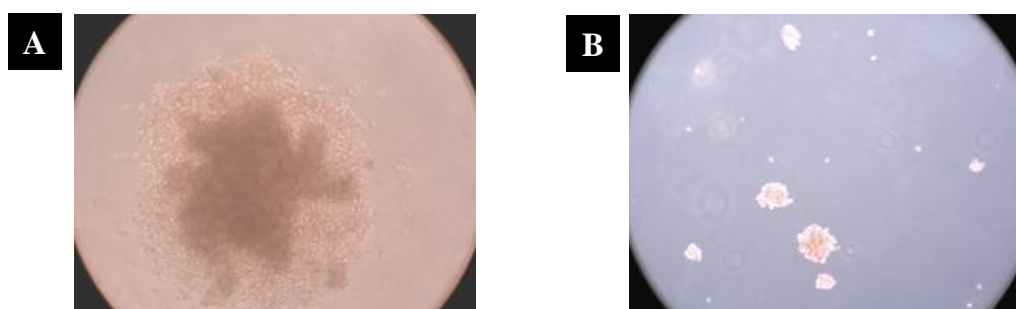


**Figure 6-10: Optical microscopy images of MDA-MB-435 MCS.**

Inverted phase microscope images of MDA-MB-435 MCS; A) before and B) after harvesting showed clearly the disintegration of spheroids during harvesting process.

TTSL-Ab-II liposome showed better cellular uptake and cytotoxicity results compared to TTSL-Ab-I, therefore we have chosen this formulation to be tested further in MCS and *in vivo*. MCF-7 (MUC-1+ve) MCS were treated with DOX-loaded TTSL and TTSL-Ab and compared to free DOX. After 24 h incubation at 37 °C, liposomes were removed and MCS were washed with PBS while DOX localisation was assessed by confocal microscopy (Figure 6-11 A). No significant enhancement in the fluorescence intensity of DOX was observed from TTSL-Ab compared to TTSL as expected which can be due to the restricted penetration of liposomes into MCS compared to monolayer. A moderate increase in DOX penetration was observed from TTSL-Ab after 15 min heating at 42 °C.

The cytotoxic activity of targeted TTSL was compared to TTSL by evaluation of spheroids growth retardation. Figure 6-11 B represents the photographic images of MCF-7 MCS and the change in the size over time. Both TTSL and TTSL-Ab retarded significantly spheroids growth compared to control (at day 22  $p < 0.05$  and  $p < 0.001$ , respectively). Spheroids growth retardation observed by TTSL-Ab was

comparable to free DOX. In both cases normalised spheroids volumes were less than double up to 22 days after treatment (Figure 6-11 C).

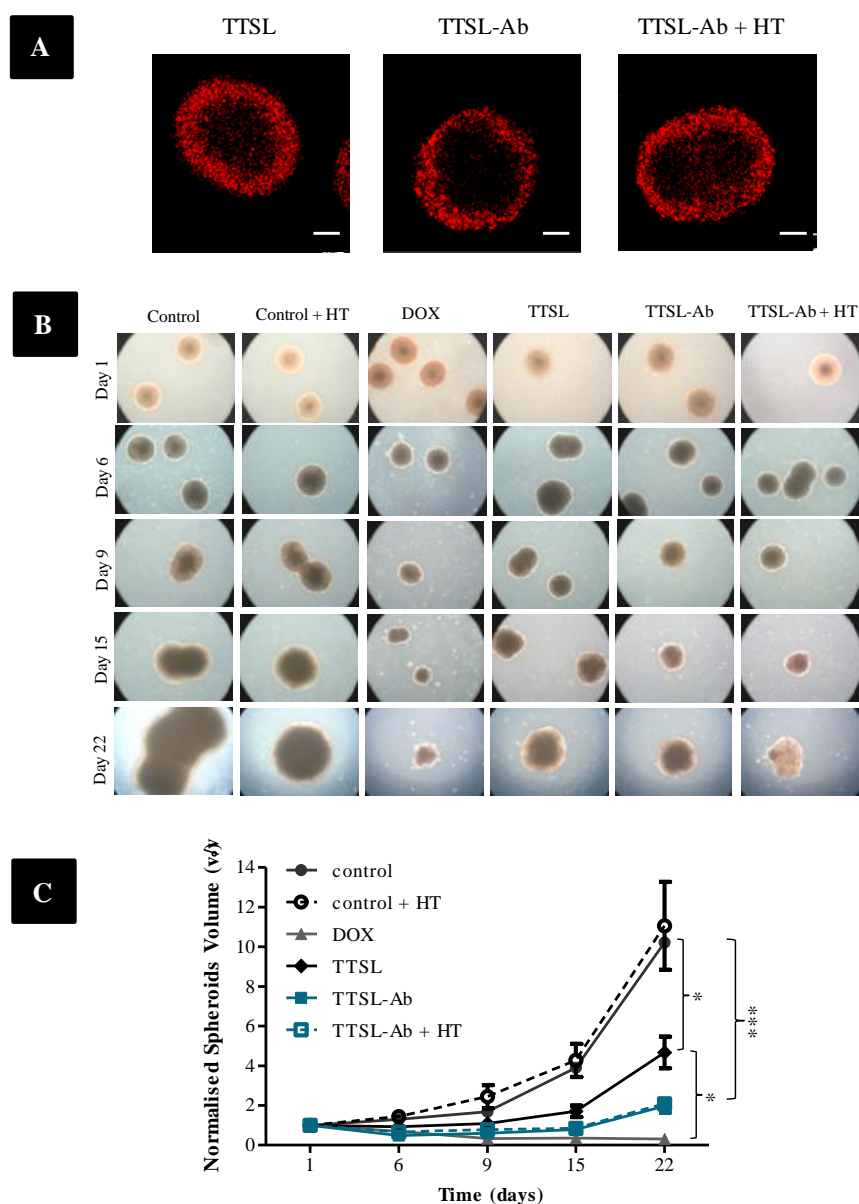


**Figure 6-11: Evaluation of TTSL and TTSL-Ab liposomes localisation and cytotoxicity on MCS.** The penetration and cytotoxicity of DOX-loaded TTSL and TTSL-Ab on MCF-7 MCS (MUC-1+ve) were evaluated following single 24 h incubation at 37 °C. Spheroids treated with TTSL-Ab were further heated for 15 min at 42 °C to demonstrate the effect of HT on DOX penetration and MCF-MCS proliferation. Untreated MCS with and without HT were used as controls. A) CLSM images of MCF-7 spheroids treated with DOX loaded TTSL, TTSL-Ab and TTSL-Ab plus 15 min HT at 42 °C. At the end of 24 h incubation MCS were washed with PBS and DOX penetration was imaged at 488 nm laser excitation source and 535–674 nm output filter, scale bar 100  $\mu$ m. B) Inverted phase-contrast microscope images of MCF-7 spheroids showed clearly smaller size with free DOX and TTSL-Ab + HT compared to other groups. C) Mean normalized spheroids volume (v/v) as a function of time after treatment showed more significant reduction in spheroids volume treated with TTSL-Ab compared to TTSL ( $P < 0.001$  compared to  $P < 0.5$ , respectively). The MCF growth retardation effect observed from TTSL-Ab was statistically equivalent to the effect of free drug.

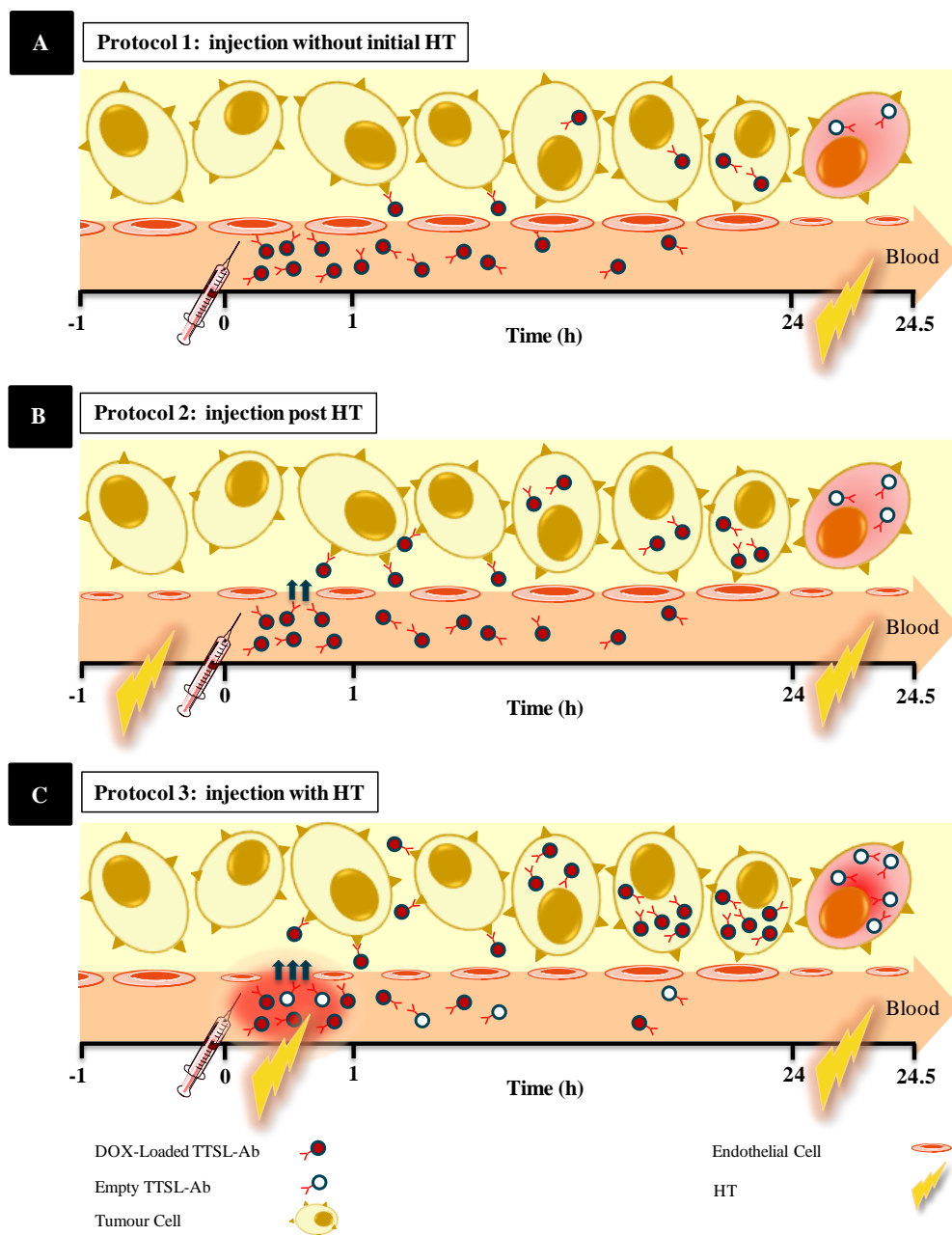
Targeted TTSL-Ab with and without HT showed greater control on MCS growth compared to non-targeted TTSL. Although DOX penetration into MCS from TTSL and TTSL-Ab was not significantly different, this enhancement in cytotoxicity might be explained by the increase in DOX concentration at the periphery, which is the proliferating layer of MCS (Figure 6-11 C). Although, free DOX showed the highest MCS growth retardation, this effect is not representative of *in vivo* conditions because free DOX is eliminated rapidly from the blood and thus minimises its interaction with tumour cells.

### **6.2.7 Biodistribution and Optical Imaging Studies of TTSL and TTSL-Ab Liposomes**

Then we evaluated the behaviour of our targeted TTSL-Ab *in vivo*. To the best of our knowledge, targeted TTSL *in vivo* combined with mild local HT have not been previously reported. Our experiments were designed to evaluate the effect of localized HT on the accumulation of TTSL-Ab and if triggering drug release from targeted TTSL-Ab after their tumour accumulation can offer better drug bioavailability. To answer the first question we designed our biodistribution experiments comparing three different heating protocols (Scheme 6-1). In each protocol two heating sessions were applied. The purpose of the 1st HT was to increase drug accumulation by HT mediated tumour vasodilatation (Kong *et al.* 2001). The 2nd HT aimed to release drug interstitially following accumulation inside the tumour tissue. We classified the protocols we studied based on whether the 1st HT session was applied and its timing in relation to the liposome injection. To answer the second question, the *in vivo* therapeutic efficacy of the targeted TTSL-Ab was compared to non-targeted TTSL.

First, we studied the blood circulation profile of TTSL and TTSL-Ab due to the importance of prolonged blood circulation on the level of tumour accumulation (Gabizon *et al.* 1994). Figure 6-12 showed that both TTSL and TTSL-Ab exhibited prolonged DOX circulation half-life, irrespective to the HT protocol applied. This indicated that conjugation of anti-MUC-1 Ab on the TTSL surface did not compromise their blood circulation time. TTSL-Ab had 26.5  $\mu\text{g Ab}/\mu\text{mole lipid}$  that is equivalent to 15 Ab molecules per liposome. According to previous studies

conjugation of MUC-1 antibody at this density should not interfere with blood circulation (Moase *et al.* 2001).



**Scheme 6-1: Schematic presentation of the three different heating protocols applied to study the biodistribution of TTSL-Ab compared to TTSL liposomes.**

The three heating protocols are classified based on the timing of liposome injection in relation to the initial HT. A) Liposomes were injected without application of initial HT, B) local HT was applied at the tumour area for 1 h followed by liposome injection; and C) local heating of the tumour was performed immediately after injection. Initial HT was applied with the aim to increase tumour accumulation of liposomes and/or to initially trigger drug release at the tumour vasculature. A 2nd localised heating session of 30 min was applied 24 h after injection to trigger drug release from liposomes after accumulation within the tumour for all three protocols.

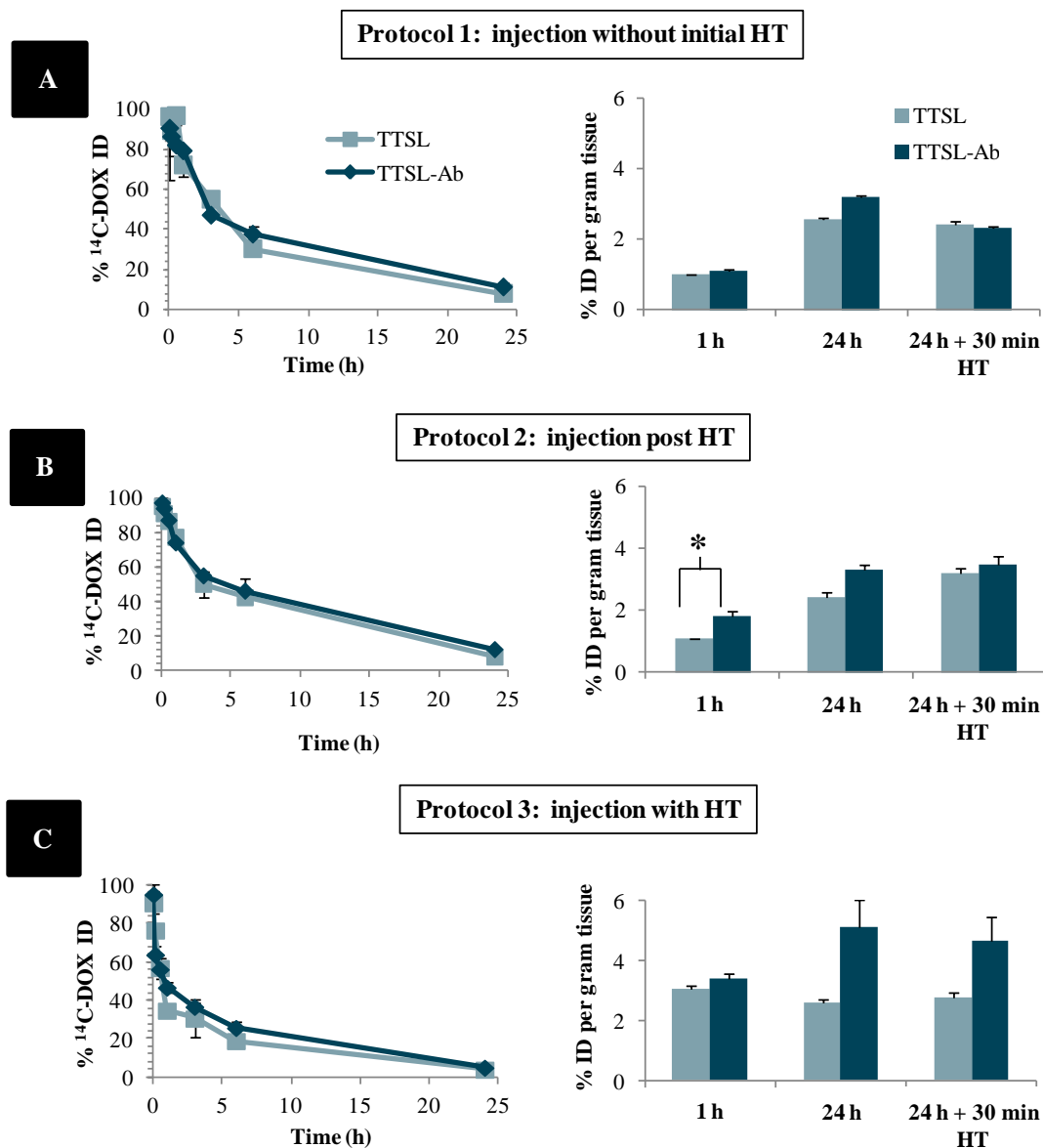


**Figure 6-12: Blood profile and tumour accumulation of TTSL and TTSL-Ab.**

TTSL and TTSL-Ab were injected intravenously into MDA-MB-435 (MUC-1+ve) tumour-bearing mice applying the three heating protocols described in Scheme 6-1. Blood profile data (right) and tumour accumulation (left) of  $^{14}\text{C}$ -DOX; A) injection without initial HT, B) injection post HT (tumour was heated for 1 h at 42 °C prior to injection); and C) injection followed by immediate heating for 1 h at 42 °C. Data represented as mean  $\pm$  SEM (n=3-4). \* indicates  $p < 0.05$ .

The shortest blood circulation was obtained with heating protocol 3 compared to protocols 1 and 2. In protocol 1 and 2 both TTSL and TTSL-Ab DOX blood circulation  $t_{1/2}$  were  $\sim 4$  h compared to only  $\sim 1$  h observed in heating protocol 3. This difference was thought to be due to the possibility of drug release at the tumour site when the 1st HT session was applied simultaneously with liposome injection. On the

other hand, in the other two protocols the liposome injection was either done in the absence of 1st HT (protocol 1) or immediately after (protocol 2).

To evaluate the effect of active targeting on tumour accumulation,  $^{14}\text{C}$ -DOX in the tumour from mice treated with TTSL-Ab was quantified and compared to TTSL. 1 h after injection, the highest tumour accumulation was achieved from simultaneous injection and heating (protocol 3), which resulted in almost 2-3 fold increase in  $^{14}\text{C}$ -DOX compared to the other two protocols (Figure 6-12). This advantageous effect of HT in enhanced tumour accumulation of liposomes and monoclonal antibodies has been well-demonstrated before (Hauck *et al.* 1997a; Kong *et al.* 2000b). The accumulation  $^{14}\text{C}$ -DOX from both TTSL and TTSL-Ab increased over time by 2-3 fold (24 h post injection) with the exception of TTSL liposomes under protocol 3. No significant difference in DOX tumour levels were noticed after a (30 min) 2nd HT 24 h after injection (Figure 6-12).

Comparing the  $^{14}\text{C}$ -DOX tumour levels from both TTSL and TTSL-Ab, almost identical values were obtained without HT (protocol 1) at all time points studied (Figure 6-12 A). Interestingly, TTSL-Ab injected post-HT (protocol 2) resulted in higher tumour accumulation compared to TTSL liposomes 1 h after injection ( $p < 0.05$ ). Similar increase in  $^{14}\text{C}$ -DOX within the tumour by TTSL-Ab was also observed in the case of injections with HT (protocol 3) (Figure 6-12 C). The equivalent  $^{14}\text{C}$ -DOX tumour levels from TTSL and TTSL-Ab 1 h after injection (protocol 3) is a result of tumour accumulation of DOX in its free and encapsulated form, since both TTSL and TTSL-Ab showed similar thermal responsiveness *in vitro*. This could explain the similar amounts of drug observed in the tumour immediately after HT.

In addition, the effects of antibody conjugation on the tissue biodistribution of TTSL and TTSL-Ab along with the effects of the different heating protocols were also evaluated (Figure 6-13). Due to triggered drug release during protocol 3, higher levels of  $^{14}\text{C}$ -DOX were detected in the tissues as early as 1 h after injection. This effect was observed in liver, kidney and heart, we believe due to free drug circulation in the blood. Quantification  $^{14}\text{C}$ -DOX level in different organs at 24 h before and after application of the 2nd HT session showed the opposite effect. The accumulation



of  $^{14}\text{C}$ -DOX was generally higher after treatment with protocols 1 and 2 due to their longer circulation without release of DOX.

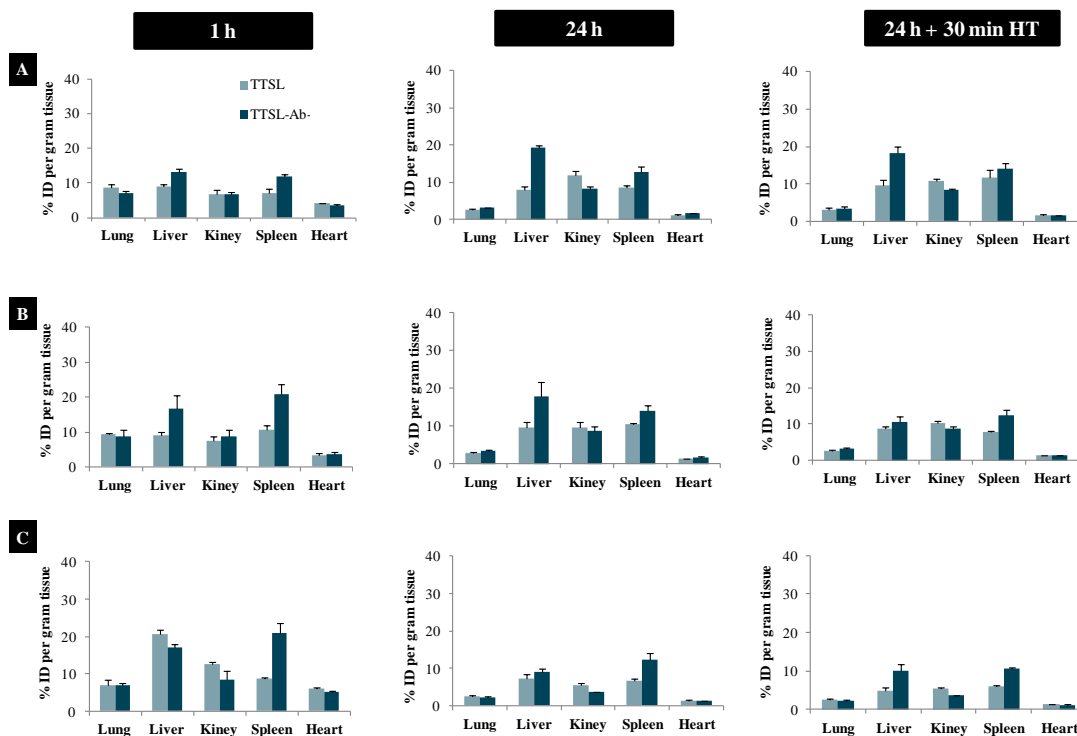


**Figure 6-13: Biodistribution study of  $^{14}\text{C}$ -DOX loaded TTSL and TTSL-Ab in the organs.** Quantification of the accumulation of  $^{14}\text{C}$ -DOX loaded TTSL and TTSL-Ab-II in the organs 1 h, 24 h and 24 h after 30 min 2nd HT using; A) protocol 1, B) protocol 2 and C) protocol 3.

Tissue distribution of DOX from TTSL and TTSL-Ab was almost identical with some increase in the spleen and liver accumulation with TTSL-Ab. This finding agreed with previous studies (Pastorino *et al.* 2006; Fondell *et al.* 2011) illustrating entrapment of the liposomes in the filtering apparatuses of these organs.

After treatment with TTSL and TTSL-Ab under the three HT protocols described earlier, whole-body optical imaging 1 h and 24 h after injection before and after 2nd HT was performed utilizing IVIS camera (Figure 6-14). In agreement with  $^{14}\text{C}$ -DOX tissue distribution, IVIS imaging showed that protocol 1 and 2 were associated with higher whole-body background in DOX signal due to the higher tissues accumulation level compared to protocol 3. This was more obvious with TTSL-Ab compared to TTSL (Figure 6-14 Ai & Bi). Also in agreement with  $^{14}\text{C}$ -DOX quantification levels within the tumour, total DOX fluorescence intensity at the tumour site, showed that

the TTSL-Ab resulted in significantly higher tumour accumulation using protocols 2 and 3 only (Figure 6-14 Bii & Cii).

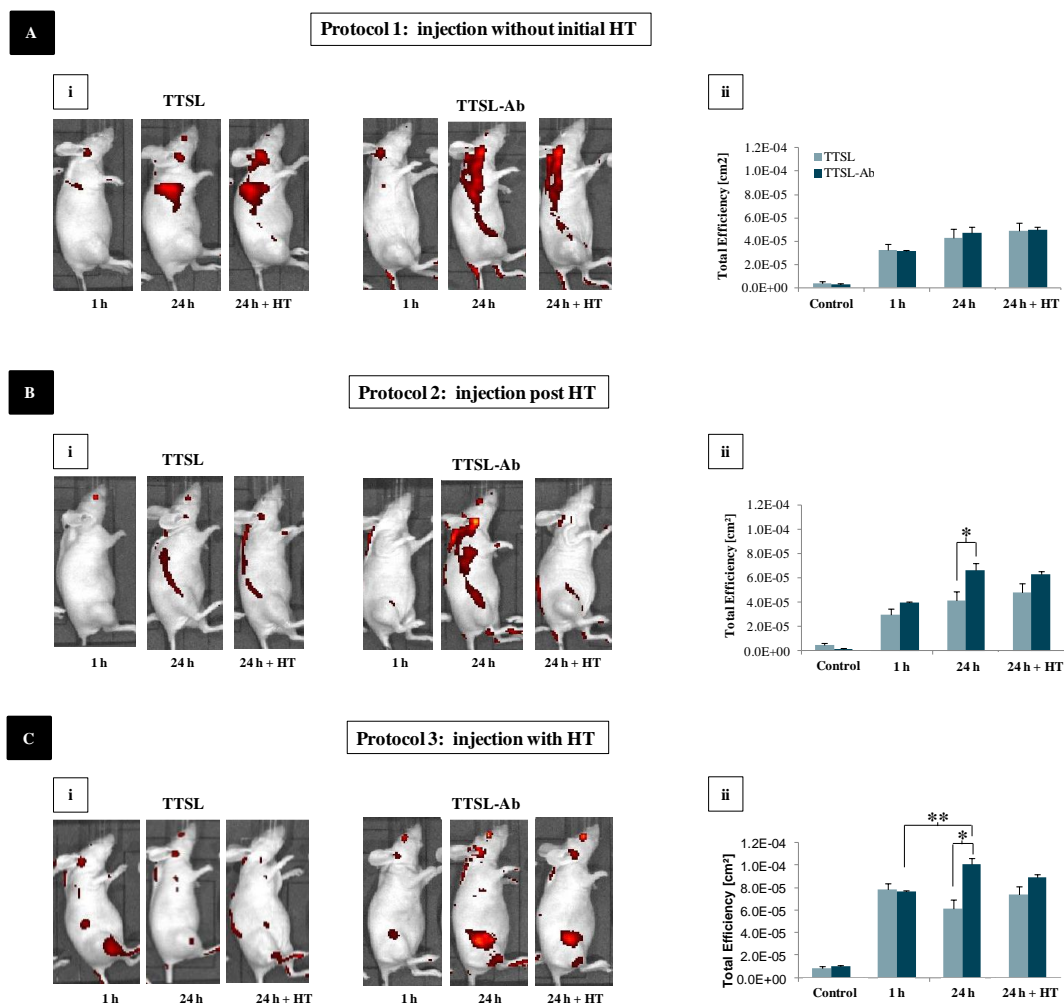


**Figure 6-14: *In vivo* imaging of athymic nude mice after injection with TTSL and TTSL-Ab.** Live fluorescence imaging of DOX-loaded TTSL and TTSL-Ab injected mice by application of the three heating protocols using the IVIS Lumina II imaging system. (Ai), (Bi) & (Ci) represent the live fluorescence imaging. (Aii), (Bii) & (Cii) show DOX fluorescence intensity signal quantification at 500 nm/DsRed excitation and emission filters from the tumour (ROI). In the first two HT protocols the high background signal from DOX accumulation into vital organs limited the signal of DOX in the tumour under this imaging scale used.

## 6.2.8 Tumour Growth Retardation and Survival Studies

Our biodistribution and whole body imaging data showed 2-fold increase in tumour uptake of MUC-1 TTSL-Ab compared to TTSL. The highest DOX accumulation was achieved by application of protocol 3 (injection with HT). Therefore, we took this heating protocol forward for evaluation of the therapeutic activity of TTSL-Ab. MDA-MB-435 bearing nude mice were treated with both

TTSL and TTSL-Ab applying protocol 3, with and without application of 2nd HT (24 h post injection). The purpose of the 2nd heating was to examine the potential of triggering DOX release from TTSL-Ab after tumour accumulation and perhaps tumour cell internalisation. Tumour growth retardation (Figure 6-15 A) indicated that injection with both TTSL and TTSL-Ab loaded with DOX showed significant growth retardation compared to untreated animals. On day 30 and 34, tumour growth delay from treatment with TTSL liposome without 2nd HT was not statistically significant compared to control mice. However, TTSL +2nd HT, TTSL-Ab and TTSL-Ab+2nd HT treatments resulted in significant growth retardation compared to the control group. However, no statistical significance was observed between those treatment groups.

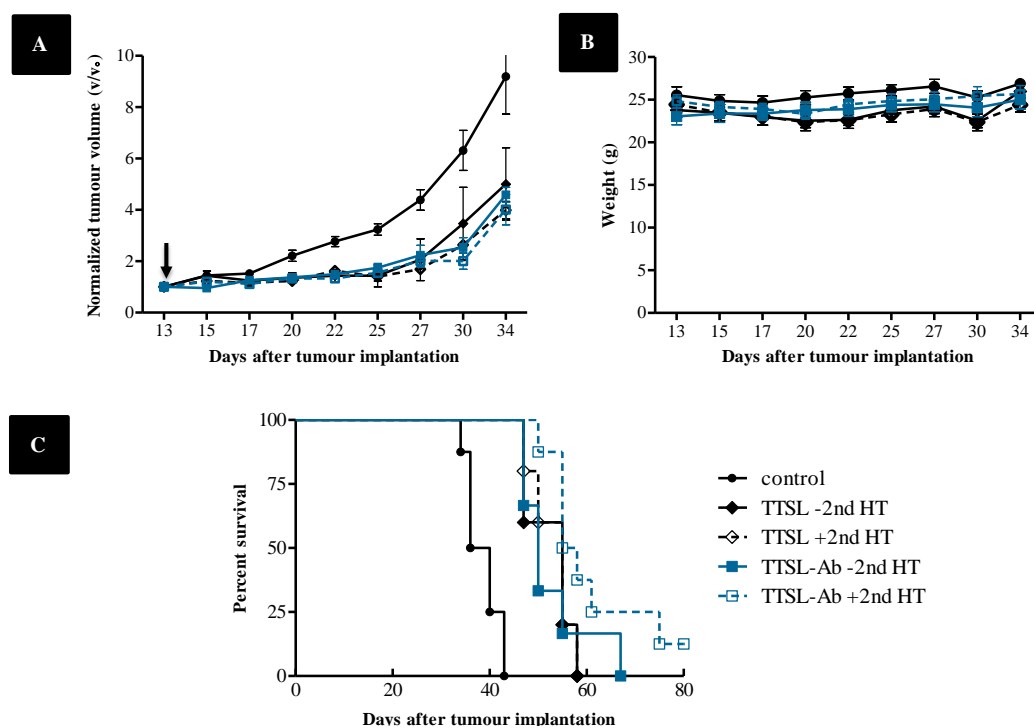


**Figure 6-15: *In vivo* tumour growth delay and survival studies.**

MDA-MB-435 tumour-bearing mice treated with TTSL and TTSL-Ab liposomes applying (protocol 3) with and without 30 min 2nd HT 24h after injection. A) Normalized tumour volume. One way ANOVA followed by Tukey's multiple comparison tests indicated significant tumour growth retardation of treated mice compared to control. At day 30, the p values of control vs TTSL + 2nd HT, control vs TTSL-Ab – 2nd HT and control vs TTSL-Ab + 2nd HT were <0.05, < 0.01 and < 0.001 respectively. At day 34 the p values of control vs TTSL + 2nd HT, control vs TTSL-Ab – 2nd HT and control vs TTSL-Ab + 2nd HT were <0.05, < 0.05 and < 0.01 respectively.; B) Body weight and C) Survival curves following single administration. Therapy started on day 13 after implantation with average tumour size of 100 mm<sup>3</sup>. Animals were injected intravenously with TTSL and TTSL-Ab at 5mg/kg DOX followed by immediate 1 h HT. Control animals were not injected, and treated with a single session of HT. Each group (n=5-7, average ± SEM).

All treated animals did not show any signs of toxicity, abnormal behaviour and no significant fluctuation in their weight until they died (Figure 6-15 B). In terms of survival, all treatment groups displayed significantly prolonged survival ( $p < 0.001$ ) compared to the untreated group (Table 6-1). The highest Increase in life span was from TTSL-Ab treatment accompanied with 2nd HT compared to the other treatment groups (Figure 6-15 C), but not statistically significant.

**Table 6-1: Survival analysis of MDA-MB-435 tumour-bearing mice treated with DOX-loaded TTSL and TTSL-Ab.**

Treatment	Dose (mg/kg)	Mean survival time (days)	Increase in life span (%) <sup>a</sup>	Significance (p) vs control
Intravascular release protocol (injection with HT)				
Control	-	36	0	-
TTSL -2nd HT	1 × 5	55.0	+45.0	0.0010
TTSL +2nd HT	1 × 5	55.0	+45.0	0.0010
TTSL-Ab-II -2nd HT	1 × 5	50	+32.0	0.0027
TTSL-Ab-II +2nd HT	1 × 5	56.5	+49.0	<0.0001

<sup>a</sup> Percentage of increase in life span = mean survival time of treated / mean survival of control × 100 - 100.

### 6.3 Discussion

The effect of chemotherapeutics is usually limited by their widespread toxicity to normal tissues and organs. Liposomes can enhance the localization of cytotoxic agents in some solid tumours and decrease drug uptake by sensitive organs, (Ewer *et al.* 2004). However, these advantages are usually hampered by difference in the permeability of the tumour vasculature that resulted in heterogeneous passive tumour targeting process that may vary in the same tumour and between different tumour types (Yuan *et al.* 1994a; Li *et al.* 2013a). EPR effect could be minimum or even absent among other tumour models (Gaber *et al.* 1996; Kong *et al.* 2001; Manzoor *et al.* 2012). Moreover, clinical benefits of EPR effect in passive tumour accumulation is not yet conclusive (Prabhakar *et al.* 2013).

A further optimized liposomal formulation would also have active targeting and triggered drug release capabilities (Pradhan *et al.* 2010). Several targeted liposomes have been developed with increased cellular uptake *in vitro*; however, none of them have been successfully translated to the clinic (Lammers 2012). Interest in designing specifically targeted liposomes with temperature sensitivity has increased, with some previous studies reported promising cell-specific cytotoxic activity after heating *in vitro* (Pradhan *et al.* 2010; Smith *et al.* 2011). Whether such concept can be replicated *in vivo* by triggering intracellular drug release after tumour accumulation, a question remained unanswered.

In an attempt to offer an answer, we designed anti-MUC-1 targeted TSL (TTSL-Ab) which have the potential to internalise specifically into tumour cells and offer on-demand drug release in response to HT. TTSL liposomes were chosen intentionally for this purpose for their long blood circulation and substantial accumulation in the tumour specially when combined with moderate HT (<42 °C). In the previous chapter, we have shown that TTSL administration into B16-F10 tumour-bearing mice in combination with mild HT could result in up to 13.5 % of ID DOX tumour accumulation 24 h after administration and heat application. This finding was a result of three factors: a) prolonged blood circulation ( $t_{1/2} \sim 4$  h); b) the stability of TTSL ( $\sim 50\%$  DOX retention after 24 h incubation in serum at 37 °C), and c) the enhanced tumour extravasation following HT ( $\sim 5$  folds increase in DOX accumulation 24 h after injection and heating). We hypothesized here that the

therapeutic activity of TTSL can be further improved by conjugation of anti MUC-1 antibodies to increase their binding specificity and cellular internalisation, followed by content release inside tumour cells triggered by application of mild HT (30 min at 42 °C).

Anti-MUC-1 TTSL-Ab were successfully prepared by post-insertion of anti-MUC-1 mal-DSPE-PEG<sub>2000</sub> micelles into preformed TTSL, resulting in antibody conjugation to the external termini of the pegylated lipid bilayer and therefore reserve the antibody binding capacity (Allen *et al.* 2002) as confirmed by SPR and cellular uptake studies. TTSL-Ab liposomes retained their characteristics, drug-loading capacity and thermal-responsiveness that agreed with previously described targeted TSL (Puri *et al.* 2008; Negussie *et al.* 2010).

Similar to other examples of targeted TSL designed for intracellular drug delivery (Puri *et al.* 2008; Smith *et al.* 2011), TTSL-Ab showed specific increase in cellular uptake and internalisation. Consequently TTSL-Ab liposomes were able to mediate significant improvement in cytotoxicity on MDA-MB-435 (MCU-1+ve) cells after exposure to HT and this effect was proportional to anti-MUC-1 antibody density. On the contrary, we did not observe any significant effect on C33a (MCU-1-ve) cells viability, that confirmed the biological specificity of the liposomes. No cytotoxic activity was observed from non-targeted TTSL in both MUC-1+ve and MUC-1-ve cells, with and without HT application.

The potential of targeted TTSL-Ab was then evaluated *in vivo*. First pharmacokinetic parameters and organ distribution of TTSL-Ab were studied and compared to TTSL by radiolabelling the drug content using <sup>14</sup>C-DOX. Antibody conjugation did not compromise liposome blood circulation half-life. This indicated that antibody conjugation to the DSPE-PEG<sub>2000</sub> terminus at this density (26.5 Ab µg/µmol lipid) did not trigger enhanced recognition by phagocytes which agreed with previous studies (Allen 2002).

The biodistribution of DOX-loaded TTSL-Ab and TTSL was evaluated in vital organs, especially the heart, an important indicator for risk of DOX mediated cardiac toxicity (Fulbright *et al.* 2010). At all time points tested, the accumulation of DOX in the heart from both targeted and non-targeted TTSL was low, confirming that both

liposome types were able to minimize non-specific cardiac uptake similar to Doxil<sup>®</sup> (Safra *et al.* 2000). <sup>14</sup>C-DOX quantification in spleen and liver showed higher levels for TTSL-Ab compared to non-targeted TTSL. Similar findings have been reported before (Pastorino *et al.* 2006; Fondell *et al.* 2011) and can be due to the recognition of the Fc region of mAb by macrophages (Allen 2002; Torchilin 2008). However, the prolonged circulation time of TTSL-Ab suggested that this might not be the case.

Besides studying the organ distribution, we also quantified <sup>14</sup>C-DOX accumulation in MDA-MB-435 (MUC-1+ve) tumour from both TTSL-Ab and TTSL. Previous studies from mAb-targeted liposomes have shown that there was no improvement in overall accumulation in solid tumours (Kirpotin *et al.* 2006). Despite significant improvements observed in cellular uptake in vitro by many groups using mAb-targeted liposomes, enhancements were not obtained in vivo. Kirpotin *et al.* showed previously similar tumour accumulation of both anti-HER2 targeted and non-targeted liposomes. However, the intratumoral microdistribution and cellular localisation of targeted and non targeted anti-HER2 liposomes were different due to their cellular internalisation capacity (Mamot *et al.* 2005; Kirpotin *et al.* 2006).

The ability of antibody-targeted liposomes to be internalise can result in improvements in drug bioavailability, especially for drugs acting against intracellular targets (Sapra *et al.* 2002) even though this is not always associated with improvements in the overall accumulation within solid tumours. The reason for that is because the accumulation process of both targeted and non-targeted pegylated liposomes is dependent on the EPR effect. After escape from the tumour vasculature, targeted liposomes face a number of barriers to transport through the tumour interstitium before reaching their cellular targets (Lammers 2012). These factors are in most cases tumour-type specific. Among these, is the leakiness of the tumour vasculature that in turn depends on the density of the pericytes and smooth muscle cells that cover the blood microvessels. Other factors include the density of the tumour cells and the building of high interstitial fluid pressure. The only cases in which mAb-targeted liposomes have shown better tumour accumulation is in very rapidly growing tumours in which tumour cells are located immediately adjacent to their vasculature (Lammers 2012) and the other case is in non-solid tumours (Fondell *et al.* 2011).

Different approaches have been investigated in an attempt to increase the penetration of both liposomes and immunoliposomes into solid tumours. One approach involved the use of the extracellular matrix (ECM) degrading enzyme, Hyaluronidase, prior to liposome administration (Eikenes 2005) or X-ray irradiation that also acted against ECM integrity (Davies *et al.* 2004). Liposomal accumulation into OHS, human osteosarcoma tumour increased four times when administered intravenously 1 h after hyaluronidase (1500 IU) (Eikenes 2005). This was thought to be due to induction of transcapillary pressure gradient as a result of almost 40% reduction in IFP (Eikenes 2005). A similar 2 folds increase in liposomal DOX accumulation into the same tumour model was observed when combined with ionizing radiation 1 day after liposomes administration or in three fractionating doses (Davies *et al.* 2004).

In addition, HT has also been a well-established method to augment liposomal accumulation into solid tumours (Gaber *et al.* 1996; Kong *et al.* 1999). Dewhirst and colleagues observed significant enhancement in the extravasation of nanoparticles including liposomes, monoclonal antibodies and antibody fragments into solid tumours by the application of mild HT (Cope *et al.* 1990; Schuster *et al.* 1995; Hauck *et al.* 1997b; Kong *et al.* 2000b). Application of local HT at 42 °C for 4 h increased tumour specific Mel-14 monoclonal antibody fragments accumulation into D-54 MG, human glioma xenografts by 3-4 folds (Cope *et al.* 1990). In another experiment the effect of heating temperature on the tumour uptake of Mel-14 mAb was studied and compared to nonspecific mAb (Schuster *et al.* 1995). After 4 h heating at 42 °C and 44 °C maximum tumour accumulation was observed with tumour specific antibody compared to control. Measuring tumour mAb 12 h after heating showed that at 42 °C specific mAb level was maintained at ~ 6% of ID compared to washout of control. This indicated that Mel-14 mAb accumulation is mainly due to specific binding rather than vascular occlusion (Schuster *et al.* 1995).

This enhancement of nanoparticles accumulation into tumour by HT is due to the increase in local blood flow (Karino *et al.* 1988), 40-60% increase at 41 °C, and increase microvascular permeability (Fujiwara *et al.* 1990; Kong *et al.* 2000b; Kong *et al.* 2001). Increased microvascular permeability of ferritin particles (Molecular weight 450,000 dalton, size 10-11 nm) was observed 1-3 days after HT (Fujiwara *et*



*al.* 1990). Kong *et al* studied the effect of HT on pore size of the tumour vasculature by quantifying the extravasation of liposomes of different size, 100-400 nm compared to albumin (7 nm) into SKOV-3 tumour (Kong *et al.* 2000b). In the absence of HT albumin easily extravasated from the tumour vasculature in addition to only small fraction of 100 nm liposomes. HT (1 h at 42 °C) increased the extravasation of liposomes of all sizes and the increase was inversely proportional to their sizes. On the other hand no significant difference in the extravasation of albumin was observed with and without HT. This indicated that HT increase pore size of this tumour model from ~100 nm at normothermic conditions to ~400 nm (Kong *et al.* 2000b).

To find out whether HT will have any effect on the accumulation of targeted TTSL-Ab, we quantified <sup>14</sup>C-DOX accumulation in the tumour by injecting the liposomes with and without HT and varying the time between HT and injection. <sup>14</sup>C-DOX was quantified 1 h and 24 h after injection. In addition, <sup>14</sup>C-DOX in the tumour was also measured after 30 min of 2nd HT that was applied 24 h after injection with the aim to release DOX after tumour accumulation and internalisation. As expected our results showed that TTSL and TTSL-Ab accumulated to the same extent when injected without applying HT first, similar to what was observed in other studies because of their similar penetration into the tumour (Kirpotin *et al.* 2006). On the contrary, significant increase in <sup>14</sup>C-DOX accumulation from TTSL-Ab was achieved when injected after or during HT application that was thought to be due to improvement in tumour penetration by local HT. The observed increase in <sup>14</sup>C-DOX from TTSL-Ab can be a result of increased retention of the liposomes within the tumour. Active binding and internalisation via the receptors on MDA-MS-435 tumour cells allowed them to be retained in the tumour for a longer time and prevented them to be washed out back to the circulation (Lammers 2012). Application of 30 min mild HT to trigger drug release from accumulated liposomes 24 h after injection did not significantly change drug levels in the tumour or efficacy.

Similar findings were observed from *in vivo* imaging confirmed the above organ distribution and tumour accumulation data. Significant increase in DOX tumour accumulation was achieved from TTSL-Ab when HT was combined with injection (Protocols 2 & 3) compared to TTSL ( $p < 0.05$ ).

Despite the two-fold increase in tumour uptake of TTSL-Ab liposomes compared to TTSL, no significant improvement in tumour growth retardation and survival was achieved compared to TTSL with and without application of a 2nd HT. Moderate improvements in therapeutic efficacy has been observed previously by triggering intracellular release after tumour accumulation using pH-sensitive anti-HER2 targeted liposomes administered in three doses (Bandekar *et al.* 2012). We may therefore, suggested that the therapeutic activity of TTSL-Ab developed here can be optimised after repeated administration.

Targeted temperature sensitive DOX-loaded liposomes (TTSL-Ab) have been successfully developed as cancer thermo-chemotheraputices. TTSL-Ab liposomes maintain their physicochemical and structural integrity with retention of their thermal properties after conjugation to anti-MUC-1 antibodies (IgG). TTSL-Ab in combination with mild HT increased tumour DOX level, however this was not associated with significant improvement in therpautic efficacy.

## 6.4 Conclusion

In conclusion, we have shown a potential role of mild HT as an effective modality to increase the therapeutic specificity *in vitro* and augment drug accumulation in the tumour from targeted temperature-sensitive liposomes *in vivo*. These observations showed that HT might be used as an alternative physical penetration enhancer to other pharmacological methods to improve tumour accumulation of targeted liposomes. These results may have implications for other actively targeted drug delivery systems, and suggest that such approach can be utilized for efficient penetration and internalisation. Despite anti-MUC-1 TTSL liposomes capability to accumulate and internalise into MUC-1+ve tumour cells, no significant improvement in therapeutic efficacy was observed under the experimental conditions tested.

## **CHAPTER 7**

---

### **FINAL REMARKS AND FUTURE PERSPECTIVE**

The use of HT to trigger local drug release is a promising and a rapidly evolving area. Local triggered release from TSL by mild HT has proven to be a precise and effective method for cancer treatment in many preclinical studies and as such it holds a great potential to be translated into an effective treatment modality for cancer therapy in the near future, especially for advanced local tumours that cannot be cured by conventional anticancer drugs. The evolution of advanced technology for applying and monitoring HT allows remote non-invasive local heating to be delivered with a great degree of control. Besides, remarkable advances in the design and development of TSL have been accomplished over the last few years and the progress is still ongoing. Different types of TSL have been developed, however most of the work was directed towards developing TSL with ultrafast release properties such as the lysolipids-containing TSL that was designed to release their loaded drug within seconds on reaching the heated tumour. A promising example on that is ThermoDox<sup>®</sup>, the LTSL formulation that progressed into phase II/III clinical trials. However, there are still some limitations recognized with this formulation which opens the scope for further improvements. The desorption of temperature-sensitive component (lysolipid) from this formulation and its consequences on drug retention at body temperature, blood circulation time, systemic toxicity and the fraction of the drug to be released, indicates that further work needs to be done to overcome those issues. The unsuccessful outcome of phase III clinical trial of ThermoDox<sup>®</sup> imposes a lot of hurdles for the clinical translation of other TSL technologies. The delicate design of ThermoDox<sup>®</sup> put lots of limitations for its application into clinical practice. Ideally for TSL to be therapeutically effective, compared to conventional chemotherapeutics or non-temperature-sensitive liposomes, they should have a reasonable drug retention capability in order to deliver effective therapeutic dose at the tumour site and reduce the associate systemic toxicity. In addition, it is critical to heat the tumour area to the right temperature and at proper time relative to TSL administration.

The development of new TSL technologies holds a great promise and opens the space for further improvements. Polymer-modified TSL can overcome some of the limitations involving the design of relatively stable TSL since their temperature sensitivity is mainly dependent on the polymer component itself. Nevertheless, more work is warranted in that area to develop temperature-sensitive polymers that

respond to narrow temperature changes, maintain good stability under physiological conditions and ensure effective drug release under mild HT. In addition, TSL decorated with metallic nanoparticles have the advantages of providing localized non-invasive self-heating to the liposomal bilayer at the nanoscale level after exposure to external energy such as MF or NIR light. Further *in vivo* evaluation of the performance of those systems is required to optimize their therapeutic potential. This is in addition to the need for the development of proper clinical techniques for the application of MF and NIR light and controls their penetration depth into the tissues. A final promising, yet challenging, area in the field TSL is the design of image-guided drug delivery from TSL by co-entrapment of imaging agents. The live information that can be provided from these systems about liposomes accumulation into tumour area could help to optimise the timing of HT application to trigger drug release and to monitor tumour temperature. However, the complicated design of these systems and the heating technologies applied might require further optimisation to be clinically applicable. Based on the lessons learned from ThermoDox<sup>®</sup> clinical trial, the translation of the newly developed TSL technologies will depend greatly on the development of relatively stable TSL systems that could be adapted into practical clinical applications.

In this thesis we attempted to address the aforementioned limitations by looking at different aspects, starting from the rationale in the design of novel TSL formulations all the way through understanding the pharmacological critical parameters that affect their clinical translation and exploring new opportunities to increase their therapeutic benefits. Below are the main outcomes of this thesis:

**Lipid-Peptide hybrid vesicles modified with a temperature-responsive peptide can be successfully engineered.**

We have successfully engineered Lp-Peptide hybrid vesicles for triggered drug release by mild HT. Lp-Peptide hybrids retained the temperature sensitivity of both the peptide and the liposomes and did not interfere with neither the liposome formation nor the effective DOX loading. Anchoring of the self-associated  $\alpha$ -helical, temperature-sensitive peptides into lipid bilayers significantly enhanced the hybrid vesicle serum stability *in vitro* and *in vivo* without affecting their thermoresponsive character.

**Lipid-Peptide hybrids system is a good candidate for intravascular and interstitial triggered drug release by mild HT.**

Administration of Lp-Peptide hybrids into tumour-bearing mice followed by immediate HT resulted in substantial DOX tumour accumulation within 1 h after injection which was comparable to LTSL. The prolonged blood circulation profile of Lp-Peptide hybrids resulted in continuous DOX accumulation into the tumour even when the heating was stopped. A three-fold increase in DOX level in the tumour, 24 h after injection and heat application, was achieved from Lp-Peptide hybrids as compared to LTSL. These interesting observations suggested that Lp-peptide hybrids can be suitable for both intravascular and interstitial drug release depending on the timing between the liposomes administration and hyperthermia application.

**The choice of the heating protocol is a critical parameter in determining the safety and the therapeutic efficacy of TSL.**

The therapeutic activity of Lp-Peptide hybrids system was studied by comparing two different heating protocols to mimic intravascular and interstitial drug release relative to other TSL. Therapy data demonstrated that the drug release profile of TSL is not the only factor that determines their therapeutic activity. The design and the timing of heating and injection based on proper understanding of the TSL physicochemical properties and pharmacokinetics parameters played a pivotal role in the therapeutic effectiveness as well as in the toxicity of TSL. In agreement with our hypothesis, Lp-Peptide hybrids showed better therapeutic efficacy in both heating protocols tested compared to LTSL and TTSL. However, the therapeutic activity of Lp-Peptide hybrids system was much higher with the intravascular release protocol. The reason for this variation is because DOX accumulation into the tumour with the intravascular release approach is a combination of the free drug and the long term accumulation of liposomal DOX. Despite the well known effect of HT on increasing liposomal extravasation into the tumour that can last up to 6-8 h after stopping HT, maximum extravasation occurred when the liposomes were injected during HT. This emphasizes the potential of simultaneous heating and injection not only to trigger intravascular drug release, but also to achieve the maximum liposomal extravasation.

TTSL had prolonged drug profile and good drug retention. As a result, the maximal DOX accumulation in the tumour was seen during the interstitial release phase of the protocol. However, this was associated with unexpected systemic toxicity that resulted in 50% reduction in the life span compared to the control. This was precipitated by the long circulation time and the intermediate drug release while the TTSL was still in the blood stream leading to continuous DOX leakage and, hence, the increased exposure time of the healthy tissues to the chemotherapeutic agent. Conversely, TTSL formulation treated with the intravascular protocol did not show any toxicity. This suggests the importance of local initial triggered drug release, even for intermediate release formulation, since this will reduce the overall amount of drug circulating in the blood stream. This highlights the impact of better understanding of the pharmacokinetic parameters on the outcome in the clinical setting.

**The use of HT in combination with targeted TTSL is an effective modality to increase the therapeutic specificity and augment drug accumulation in the tumour.**

We successfully developed and characterized targeted temperature-sensitive doxorubicin loaded liposome (TTSL-Ab) for cancer thermo-chemotherapy. TTSL-Ab liposome maintained its physicochemical and thermal properties after conjugation to anti-MUC-1 Ab. TTSL-Ab increased the binding specificity and cellular uptake into MUC-1+ve cells compared to non-targeted TTSL liposome. Triggering intracellular DOX release by the application of mild hyperthermia significantly enhanced the cytotoxicity of TTSL-Ab compared to non-targeted TTSL.

The accumulation of targeted TTSL-Ab into MUC-1+ve tumour after *in vivo* administration was greatly enhanced when combined with HT prior to or immediately after the injection, compared to non-heated tumours. These observations highlighted the potential role of HT as a physical penetration enhancer to improve targeted liposomes penetration into solid tumours. HT can be used as a useful alternative to other pharmacological methods to improve the efficacy of targeted liposomes. Further work is warranted to understand this effect in details including the penetration distance of the liposomes and the drug and their distribution in the tumour interstitium. Single injection of TTSL-Ab with HT followed by 24 h 2nd



heating resulted in moderate improvement in the therapeutic activity and survival compared to non-targeted TTSL. We suggested that this therapeutic activity of TTSL-Ab might be further optimised by increasing the dosing frequency or by modifying the timing of 2nd heating.

The studies presented in this thesis revealed the importance of rational design of TSL system and the factors that should be considered in the design of the proper HT protocol for their pharmacological evaluation. Therefore, besides the attempts to develop TSL with ultrafast release properties, more efforts should be made to get a balance between thermosensitivity, stability and safety profiles of TSL. The development of such systems would offer greater chance for clinical translation and would give much flexibility to adapt to the complications of clinical procedures.

## APPENDENCES

### ▪ Publications

Zahraa S. Al-Ahmady, Al-Jamal WT, Bossche JV, Bui TT, Drake AF, Mason AJ, Kostarelos K, Lipid-Peptide vesicle nanoscale hybrids for triggered drug release by mild hyperthermia *in vitro* and *in vivo*. *ACS Nano* (2012).

Al-Jamal WT, Zahraa S. Al-Ahmady, Kostarelos K, Pharmacokinetics & tissue distribution of temperature-sensitive liposomal doxorubicin in tumor-bearing mice triggered with mild hyperthermia. *Biomaterials* (2012).

### ▪ Abstracts and Proceedings

Zahraa S. Al-Ahmady & Kostas Kostarelos. Engineering Lipid-Peptide Hybrid Vesicles for Triggered Drug Release by Mild Hyperthermia. KCL, UK, 2012. Seminar.

Zahraa S. Al-Ahmady & Kostas Kostarelos. Lipid-Peptide Hybrid Vesicles for Triggered Drug Release by Mild Hyperthermia *in vitro* and *in vivo*. COST Action TD1004 Annual Meeting, UK, 2012. Oral Presentation.

Zahraa S. Al-Ahmady, Wafa' T. Al-Jamal, Tam T. Bui, Alex F. Drake, James Mason, Jeroen V. Bossche, Kostas Kostarelos. Self-assembled leucine zipper peptide-lipid hybrid vesicles for the engineering of temperature-responsive doxorubicin-loaded liposomes. ACS meeting, San Diego, 2012. Oral Presentation.

Zahraa S. Al-Ahmady, Wafa' T. Al-Jamal, Tam T. Bui, Alex F. Drake, James Mason, Jeroen V. Bossche, Kostas Kostarelos. Coiled-coil leucine zipper peptides anchored onto lipid bilayers for the design of temperature sensitive liposomes. ACS meeting, San Diego, 2012. Oral Presentation.

Al-Jamal WT, Zahraa S. Al-Ahmady, Kostarelos K. Thermosensitive Liposomal Doxorubicin and Tumor Hyperthermia: Matching the Heating protocol with the Liposome System. ACS meeting, San Diego, 2012. Oral Presentation.

### ▪ Awards

*Postgraduate Research Day Prize* for the best poster presentation (UCL School of Pharmacy, University of London), Sep. 2011

## BIBLIOGRAPHY

- Abulateefeh, S. R., Spain, S. G., Aylott, J. W., Chan, W. C., Garnett, M. C. and Alexander, C. (2011). "Thermoresponsive polymer colloids for drug delivery and cancer therapy." Macromolecular Bioscience 11(12): 1722-1734.
- Ahmed, M., Brace, C. L., Lee, F. T., Jr. and Goldberg, S. N. (2011). "Principles of and advances in percutaneous ablation." Radiology 258(2): 351-369.
- Ahmed, M., Moussa, M. and Goldberg, S. N. (2012). "Synergy in cancer treatment between liposomal chemotherapeutics and thermal ablation." Chemistry and Physics of Lipids 165(4): 424-437.
- Al-Jamal, W. T., Al-Ahmady, Z. S. and Kostarelos, K. (2012). "Pharmacokinetics & tissue distribution of temperature-sensitive liposomal doxorubicin in tumor-bearing mice triggered with mild hyperthermia." Biomaterials 33(18): 4608-4617.
- Al-Jamal, W. T., Al-Jamal, K. T., Cakebread, A., Halket, J. M. and Kostarelos, K. (2009a). "Blood circulation and tissue biodistribution of Lipid-Quantum Dot (L-QD) hybrid vesicles intravenously administered in mice." Bioconjugate Chemistry 20(9): 1696-1702.
- Al-Jamal, W. T., Al-Jamal, K. T., Tian, B., Cakebread, A., Halket, J. M. and Kostarelos, K. (2009b). "Tumor targeting of functionalized Quantum Dot-Liposome hybrids by intravenous administration." Molecular Pharmaceutics 6(2): 520-530.
- Al-Jamal, W. T., Al-Jamal, K. T., Tian, B., Lacerda, L., Bornans, P. H., Frederik, P. M. and Kostarelos, K. (2008). "Lipid-quantum dot bilayer vesicles enhance tumor cell uptake and retention in vitro and in vivo." ACS Nano 2(3): 408-418.
- Al-Jamal, W. T. and Kostarelos, K. (2011). "Liposomes: From a clinically established drug delivery system to a nanoparticle platform for theranostic nanomedicine." Accounts of Chemical Research 44(10): 1094-1104.
- Alkilany, A. M., Thompson, L. B., Boulos, S. P., Sisco, P. N. and Murphy, C. J. (2012). "Gold nanorods: Their potential for photothermal therapeutics and drug delivery, tempered by the complexity of their biological interactions." Advanced Drug Delivery Reviews 64(2): 190-199.
- Allen, T. (2013). "Liposomal drug delivery systems: From concept to clinical applications." Advanced Drug Delivery Reviews 65(1): 36-48.
- Allen, T. M. (2002). "Ligand-targeted therapeutics in anticancer therapy." Nature Reviews Cancer 2(10): 750-763.
- Allen, T. M. and Chonn, A. (1987). "Large unilamellar liposomes with low uptake into the reticuloendothelial system." FEBS Letters 223(1): 42-46.
- Allen, T. M. and Cleland, L. G. (1980). "Serum-induced leakage of liposome contents." Biochimica et Biophysica Acta (BBA) - Biomembranes 597(2): 418-426.
- Allen, T. M. and Hansen, C. (1991a). "Pharmacokinetics of stealth versus conventional liposomes - effect of dose." Biochimica et Biophysica Acta 1068(2): 133-141.
- Allen, T. M., Hansen, C., Martin, F., Redemann, C. and Yau-Young, A. (1991b). "Liposomes containing synthetic lipid derivatives of poly(ethylene glycol) show prolonged circulation half-lives in vivo." Biochimica et Biophysica Acta 1066(1): 29-36.

- Allen, T. M., Hansen, C. and Rutledge, J. (1989). "Liposomes with prolonged circulation times: factors affecting uptake by reticuloendothelial and other tissues." Biochimica et Biophysica Acta (BBA) - Biomembranes 981(1): 27-35.
- Allen, T. M., Mumbengegwi, D. R. and Charrois, G. J. R. (2005). "Anti-CD19-targeted liposomal doxorubicin improves the therapeutic efficacy in murine B-cell lymphoma and ameliorates the toxicity of liposomes with varying drug release Rates." Clinical Cancer Research 11(9): 3567-3573.
- Allen, T. M., Sapra, P. and Moase, E. (2002). "Use of the post-insertion method for the formation of ligand-coupled liposomes." Cellular & Molecular Biology Letters 7(3): 889-894.
- Aluri, S., Janib, S. M. and Mackay, J. A. (2009). "Environmentally responsive peptides as anticancer drug carriers." Advanced Drug Delivery Reviews 61(11): 940-952.
- An, M., Wijesinghe, D., Andreev, O. A., Reshetnyak, Y. K. and Engelman, D. M. (2010a). "pH-(low)-insertion-peptide (pHLIP) translocation of membrane impermeable phalloidin toxin inhibits cancer cell proliferation." Proceedings of the National Academy of Sciences 107(47): 20246-20250.
- An, X., Zhan, F. and Zhu, Y. (2013). "Smart photothermal-triggered bilayer phase transition in AuNPs-liposomes to release drug." Langmuir 29(4): 1061-1068.
- An, X., Zhang, F., Zhu, Y. and Shen, W. (2010b). "Photoinduced drug release from thermosensitive AuNPs-liposome using a AuNPs-switch." Chemical Communications 46(38): 7202-7204.
- Anyambhatla, G. R. and Needham, D. (1999). "Enhancement of the phase transition permeability of dppc liposomes by incorporation of mppc: a new temperature-sensitive liposome for use with mild hyperthermia." Journal of Liposome Research 9(4): 491-506.
- Bacic, G., Niesman, M. R., Bennett, H. F., Magin, R. L. and Swartz, H. M. (1988). "Modulation of water proton relaxation rates by liposomes containing paramagnetic materials." Magnetic Resonance in Medicine 6(4): 445-458.
- Baker, T. S., Bose, C. C., Caskey-Finney, H. M., King, D. J., Lawson, A. D., Lyons, A., Mountain, A., Owens, R. J., Rolfe, M. R., Sehdev, M. and et al. (1994). "Humanization of an anti-mucin antibody for breast and ovarian cancer therapy." Advances in Experimental Medicine and Biology 353: 61-82.
- Bandekar, A., Karve, S., Chang, M. Y., Mu, Q., Rotolo, J. and Sofou, S. (2012). "Antitumor efficacy following the intracellular and interstitial release of liposomal doxorubicin." Biomaterials 33(17): 4345-4352.
- Bangham, A. D. and Horne, R. W. (1964). "Negative staining of phospholipids and their structural modification by surface-active agents as observed in the electron microscope." Journal of Molecular Biology 8: 660-668.
- Bangham, A. D., Standish, M. M. and Watkins, J. C. (1965). "Diffusion of univalent ions across the lamellae of swollen phospholipids." Journal of Molecular Biology 13(1): 238-IN227.
- Banno, B., Ickenstein, L. M., Chiu, G. N. C., Bally, M. B., Thewalt, J., Brief, E. and Wasan, E. K. (2010). "The functional roles of poly(ethylene glycol)-lipid and lysolipid in the drug retention and release from lysolipid-containing thermosensitive liposomes in vitro and in vivo." Journal of Pharmaceutical Sciences 99(5): 2295-2308.
- Barenholz, Y. (2003). "Relevancy of drug loading to liposomal formulation therapeutic efficacy." Journal of Liposome Research 13(1): 1-8.

- Barenholz, Y. Amphipathic weak base loading into preformed liposomes having a transmembrane ammonium ion gradient: from the bench to approved doxil. In Liposome Technology: (2006), 1-25.
- Barenholz, Y. (2012). "Doxil<sup>®</sup> The first FDA-approved nano-drug: Lessons learned." Journal of Controlled Release 160(2): 117-134.
- Bassett, J. B., Anderson, R. U. and Tacker, J. R. (1986). "Use of temperature-sensitive liposomes in the selective delivery of methotrexate and cis-platinum analogues to murine bladder tumor." Journal of Urology 135(3): 612-615.
- Bealle, G., Di Corato, R., Kolosnjaj-Tabi, J., Dupuis, V., Clement, O., Gazeau, F., Wilhelm, C. and Menager, C. (2012). "Ultra magnetic liposomes for MR imaging, targeting, and hyperthermia." Langmuir 28(32): 11834-11842.
- Ben-Yosef, R. and Kapp, D. S. (1992). "Persistent and/or late complications of combined radiation therapy and hyperthermia." International Journal of Hyperthermia 8(6): 733-745.
- Bettaieb, A., Wrzal, P. K. and Averill-Bates, D. A. Hyperthermia: Cancer treatment and beyond. In Cancer treatment - conventional and innovative approaches: (2013), 257-283.
- Bibi, S., Lattmann, E., Mohammed, A. R. and Perrie, Y. (2012). "Trigger release liposome systems: local and remote controlled delivery?" Journal of Microencapsulation 29(3): 262-276.
- Bikram, M. and West, J. L. (2008). "Thermo-responsive systems for controlled drug delivery." Expert opinion on drug delivery 5(10): 1077-1091.
- Blum, R. H. and Carter, S. K. (1974). "Adriamycin. A new anticancer drug with significant clinical activity." Annals of Internal Medicine 80(2): 249-259.
- Bothun, G. D. (2008). "Hydrophobic silver nanoparticles trapped in lipid bilayers: Size distribution, bilayer phase behavior, and optical properties." Journal of Nanobiotechnology 6: 13.
- Bothun, G. D. and Preiss, M. R. (2011). "Bilayer heating in magnetite nanoparticle-liposome dispersions via fluorescence anisotropy." Journal of Colloid and Interface Science 357(1): 70-74.
- Brickner, M. L., Yusuf, C., Vogel, K. M. and Chmielewski, J. A. Design and use of amphiphilic peptides in liposomes as pH-triggered releasing agents. In Peptides Frontiers of Peptide Science, Tam, J. and Kaumaya, P. P., Eds.; Springer Netherlands: (2002); 5, 461-462.
- Buiting, A. M., Zhou, F., Bakker, J. A., van Rooijen, N. and Huang, L. (1996). "Biodistribution of clodronate and liposomes used in the liposome mediated macrophage 'suicide' approach." Journal of Immunological Methods 192(1-2): 55-62.
- Burke, J. F., Jr., Laucius, J. F., Brodovsky, H. S. and Soriano, R. Z. (1977). "Doxorubicin hydrochloride-associated renal failure." Archives of Internal Medicine 137(3): 385-388.
- Celsion.com. (2013a). "Celsion announces results of phase III HEAT study of ThermoDox<sup>®</sup> in primary liver cancer." Retrieved 31-01-2013, from <http://investor.celsion.com/releasedetail.cfm?ReleaseID=737033>.
- Celsion.com. (2013b). "Celsion announces ThermoDox<sup>®</sup> HEAT study findings to be reviewed at the 9th annual world conference on interventional oncology (WCIO) in New York city on May 16, 2013." Retrieved 06-05-2013.
- Celsion.com. (2013c). "Inovation in oncology celsion corporation." Retrieved 01-01-2013, from [www.celsion.com](http://www.celsion.com).

- Chan, S. Y., Gordon, A. N., Coleman, R. E., Hall, J. B., Berger, M. S., Sherman, M. L., Eten, C. B. and Finkler, N. J. (2003). "A phase 2 study of the cytotoxic immunoconjugate CMB-401 (hCTM01-calicheamicin) in patients with platinum-sensitive recurrent epithelial ovarian carcinoma." Cancer Immunology, Immunotherapy 52(4): 243-248.
- Chang, D.-K., Lin, C.-T., Wu, C.-H. and Wu, H.-C. (2009). "A novel peptide enhances therapeutic efficacy of liposomal anti-cancer drugs in mice models of human lung cancer." Plos One 4(1): e4171.
- Charrois, G. J. R. and Allen, T. M. (2004). "Drug release rate influences the pharmacokinetics, biodistribution, therapeutic activity, and toxicity of pegylated liposomal doxorubicin formulations in murine breast cancer." Biochimica et Biophysica Acta (BBA) - Biomembranes 1663(1-2): 167-177.
- Chen, C.-W. (2011). "Novel RGD-lipid conjugate-modified liposomes for enhancing siRNA delivery in human retinal pigment epithelial cells." International Journal of Nanomedicine 6: 2567-2580.
- Chen, Q., Krol, A., Wright, A., Needham, D., Dewhirst, M. W. and Yuan, F. (2008). "Tumor microvascular permeability is a key determinant for antivascular effects of doxorubicin encapsulated in a temperature sensitive liposome." International Journal of Hyperthermia 24(6): 475-482.
- Chen, Q., Tong, S., Dewhirst, M. W. and Yuan, F. (2004). "Targeting tumor microvessels using doxorubicin encapsulated in a novel thermosensitive liposome." Molecular Cancer Therapeutics 3(10): 1311-1317.
- Chen, Y., Bose, A. and Bothun, G. D. (2010). "Controlled release from bilayer-decorated magnetoliposomes via electromagnetic heating." ACS Nano 4(6): 3215-3221.
- Cheng, W. W. K. and Allen, T. M. (2008). "Targeted delivery of anti-CD19 liposomal doxorubicin in B-cell lymphoma: A comparison of whole monoclonal antibody, Fab' fragments and single chain Fv." Journal of Controlled Release 126(1): 50-58.
- Chithrani, D. B., Dunne, M., Stewart, J., Allen, C. and Jaffray, D. A. (2010). "Cellular uptake and transport of gold nanoparticles incorporated in a liposomal carrier." Nanomedicine: Nanotechnology, Biology and Medicine 6(1): 161-169.
- Chiu (2005). "Encapsulation of doxorubicin into thermosensitive liposomes via complexation with the transition metal manganese." Journal of Controlled Release 104(2): 271-288.
- Chrastina, A., Massey, K. A. and Schnitzer, J. E. (2011). "Overcoming in vivo barriers to targeted nanodelivery." Wiley interdisciplinary reviews. Nanomedicine and nanobiotechnology 3(4): 421-437.
- ClinicalTrials.gov. (2012a). "MRI guided high intensity focused ultrasound (HIFU) and ThermoDox for palliation of painful bone metastases." Retrieved 03-05-2013, from <http://clinicaltrials.gov/ct2/show/NCT01640847>.
- ClinicalTrials.gov. (2012b). "Phase 3 study of ThermoDox with radiofrequency ablation (RFA) in treatment of hepatocellular carcinoma (HCC)." Retrieved 06-03-2013, from <http://clinicaltrials.gov/show/NCT00617981>.
- ClinicalTrials.gov. (2013a). "Phase 1/2 study of ThermoDox with approved hyperthermia in treatment of breast cancer recurrence at the chest wall (DIGNITY)." Retrieved 19/04/2013, from <http://clinicaltrials.gov/show/NCT00826085>.

- ClinicalTrials.gov. (2013b). "Phase 2 study of ThermoDox as adjuvant therapy with thermal ablation (RFA) in treatment of metastatic colorectal cancer(mCRC) (ABLATE)." Retrieved 03/05/2013, from <http://clinicaltrials.gov/ct2/show/NCT01464593>.
- Cope, D. A., Dewhirst, M. W., Friedman, H. S., Bigner, D. D. and Zalutsky, M. R. (1990). "Enhanced delivery of a monoclonal antibody F(ab')<sub>2</sub> fragment to subcutaneous human glioma xenografts using local hyperthermia." Cancer Research 50(6): 1803-1809.
- Coulon, A., Berkane, E., Sautereau, A. M., Urech, K., Rouge, P. and Lopez, A. (2002). "Modes of membrane interaction of a natural cysteine-rich peptide: viscotoxin A3." Biochimica et Biophysica Acta-Biomembranes 1559(2): 145-159.
- Davies, L., Lundstrom, L. M., Frengen, J., Eikenes, L., Bruland, S. O., Kaalhus, O., Hjelstuen, M. H. and Brekken, C. (2004). "Radiation improves the distribution and uptake of liposomal doxorubicin (caelyx) in human osteosarcoma xenografts." Cancer Research 64(2): 547-553.
- Davies, Q., Perkins, A. C., Frier, M., Watson, S., Lalani, E. and Symonds, E. M. (1997). "The effect of circulating antigen on the biodistribution of the engineered human antibody hCTM01 in a nude mice model." European Journal of Nuclear Medicine 24(2): 206-209.
- Davis, J. H. (1983). "The description of membrane lipid conformation, order and dynamics by H-2-NMR." Biochimica et Biophysica Acta 737(1): 117-171.
- Davis, M. E., Chen, Z. G. and Shin, D. M. (2008). "Nanoparticle therapeutics: an emerging treatment modality for cancer." Nature Reviews Drug Discovery 7(9): 771-782.
- de Senneville, B. D., Mougnot, C., Quesson, B., Dragonu, I., Grenier, N. and Moonen, C. T. (2007). "MR thermometry for monitoring tumor ablation." European Radiology 17(9): 2401-2410.
- de Smet, M., Heijman, E., Langereis, S., Hijnen, N. M. and Grull, H. (2011). "Magnetic resonance imaging of high intensity focused ultrasound mediated drug delivery from temperature-sensitive liposomes: an in vivo proof-of-concept study." Journal of Controlled Release 150(1): 102-110.
- de Smet, M., Hijnen, N. M., Langereis, S., Elevelt, A., Heijman, E., Dubois, L., Lambin, P. and Grull, H. (2013). "Magnetic resonance guided high-intensity focused ultrasound mediated hyperthermia improves the intratumoral distribution of temperature-sensitive liposomal doxorubicin." Investigative Radiology 48(6): 395-405.
- de Smet, M., Langereis, S., van den Bosch, S. and Grull, H. (2010). "Temperature-sensitive liposomes for doxorubicin delivery under MRI guidance." Journal of Controlled Release 143(1): 120-127.
- Dewhirst, M. W., Vujaskovic, Z., Jones, E. and Thrall, D. (2005). "Re-setting the biologic rationale for thermal therapy." International Journal of Hyperthermia 21(8): 779-790.
- Dicheva, B. M., Hagen, T. L., Li, L., Schipper, D., Seynhaeve, A. L., Rhoon, G. C., Eggermont, A. M., Lindner, L. H. and Koning, G. A. (2012). "Cationic thermosensitive liposomes: a novel dual targeted heat-triggered drug delivery approach for endothelial and tumour cells." Nano Letters 13: 13.
- Dromi, S., Frenkel, V., Luk, A., Traugher, B., Angstadt, M., Bur, M., Poff, J., Xie, J., Libutti, S. K., Li, K. C. and Wood, B. J. (2007). "Pulsed-high intensity focused ultrasound and low temperature-sensitive liposomes for enhanced

- targeted drug delivery and antitumor effect." Clinical Cancer Research 13(9): 2722-2727.
- Drummond, D. C., Meyer, O., Hong, K., Kirpotin, D. B. and Papahadjopoulos, D. (1999). "Optimizing liposomes for delivery of chemotherapeutic agents to solid tumors." Pharmacological Reviews 51(4): 691-744.
- Dupuy, D. E., DiPetrillo, T., Gandhi, S., Ready, N., Ng, T., Donat, W. and Mayo-Smith, W. W. (2006). "Radiofrequency ablation followed by conventional radiotherapy for medically inoperable stage I non-small cell lung cancer." Chest 129(3): 738-745.
- Dvorak, H. F., Nagy, J. A., Dvorak, J. T. and Dvorak, A. M. (1988). "Identification and characterization of the blood vessels of solid tumors that are leaky to circulating macromolecules." American Journal of Pathology 133(1): 95-109.
- Eikenes, L. (2005). "Hyaluronidase induces a transcapillary pressure gradient and improves the distribution and uptake of liposomal doxorubicin (Caelyx) in human osteosarcoma xenografts." British Journal of Cancer 93(1): 81-88.
- Elegbede, A. I., Banerjee, J., Hanson, A. J., Tobwala, S., Ganguli, B., Wang, R., Lu, X., Srivastava, D. K. and Mallik, S. (2008). "Mechanistic studies of the triggered release of liposomal contents by matrix metalloproteinase-9." Journal of the American Chemical Society 130(32): 10633-10642.
- Engelke, M., Bojarski, P., Bloss, R. and Diehl, H. (2001). "Tamoxifen perturbs lipid bilayer order and permeability: comparison of DSC, fluorescence anisotropy, Laurdan generalized polarization and carboxyfluorescein leakage studies." Biophysical Chemistry 90(2): 157-173.
- Evans, E. and Needham, D. (1987). "Physical properties of surfactant bilayer membranes: thermal transitions, elasticity, rigidity, cohesion and colloidal interactions." The Journal of Physical Chemistry 91(16): 4219-4228.
- Ewer, M. S., Martin, F. J., Henderson, C., Shapiro, C. L., Benjamin, R. S. and Gabizon, A. A. (2004). "Cardiac safety of liposomal anthracyclines." Seminars in Oncology 31(6 Suppl 13): 161-181.
- Fenske, D. B. and Cullis, P. R. Encapsulation of drugs within liposomes by pH-gradient techniques. In Liposome Technology: (2006), 27-50.
- Fondell, A., Edwards, K., Unga, J., Kullberg, E., Park, J. W. and Gedda, L. (2011). "In vitro evaluation and biodistribution of HER2-targeted liposomes loaded with an 125I-labelled DNA-intercalator." Journal of Drug Targeting 19(9): 846-855.
- Francis, R. J., Sharma, S. K., Springer, C., Green, A. J., Hope-Stone, L. D., Sena, L., Martin, J., Adamson, K. L., Robbins, A., Gumbrell, L., O'Malley, D., Tsiompanou, E., Shahbakhti, H., Webley, S., Hochhauser, D., Hilson, A. J., Blakey, D. and Begent, R. H. (2002). "A phase I trial of antibody directed enzyme prodrug therapy (ADEPT) in patients with advanced colorectal carcinoma or other CEA producing tumours." British Journal of Cancer 87(6): 600-607.
- Frich, L., Bjornerud, A., Fossheim, S., Tillung, T. and Gladhaug, I. (2004). "Experimental application of thermosensitive paramagnetic liposomes for monitoring magnetic resonance imaging guided thermal ablation." Magnetic Resonance in Medicine 52(6): 1302-1309.
- Fritze, A., Hens, F., Kimpfler, A., Schubert, R. and Peschka-Süss, R. (2006). "Remote loading of doxorubicin into liposomes driven by a transmembrane phosphate gradient." Biochimica et Biophysica Acta (BBA) - Biomembranes 1758(10): 1633-1640.



- Fujiwara, K. and Watanabe, T. (1990). "Effects of hyperthermia, radiotherapy and thermoradiotherapy on tumor microvascular permeability." Acta Pathologica Japonica 40(2): 79-84.
- Fulbright, J. M., Huh, W., Anderson, P. and Chandra, J. (2010). "Can anthracycline therapy for pediatric malignancies be less cardiotoxic?" Current Oncology Reports 12(6): 411-419.
- Gaber, M. H. (1998). "Effect of bovine serum on the phase transition temperature of cholesterol-containing liposomes." Journal of Microencapsulation 15(2): 207-214.
- Gaber, M. H., Hong, K. L., Huang, S. K. and Papahadjopoulos, D. (1995). "Thermosensitive sterically stabilized liposomes - formulation and in-vitro studies on mechanism of doxorubicin release by bovine serum and human plasma." Pharmaceutical Research 12(10): 1407-1416.
- Gaber, M. H., Wu, N. Z., Hong, K., Huang, S. K., Dewhirst, M. W. and Papahadjopoulos, D. (1996). "Thermosensitive liposomes: extravasation and release of contents in tumor microvascular networks." International Journal of Radiation Oncology, Biology, Physics 36(5): 1177-1187.
- Gabizon, A., Catane, R., Uziely, B., Kaufman, B., Safra, T., Cohen, R., Martin, F., Huang, A. and Barenholz, Y. (1994). "Prolonged circulation time and enhanced accumulation in malignant exudates of doxorubicin encapsulated in polyethylene-glycol coated liposomes." Cancer Research 54(4): 987-992.
- Gabizon, A. and Martin, F. (1997). "Polyethylene glycol-coated (pegylated) liposomal doxorubicin. Rationale for use in solid tumours." Drugs 4: 15-21.
- Gabizon, A., Tzemach, D., Gorin, J., Mak, L., Amitay, Y., Shmeeda, H. and Zalipsky, S. (2010). "Improved therapeutic activity of folate-targeted liposomal doxorubicin in folate receptor-expressing tumor models." Cancer Chemotherapy and Pharmacology 66(1): 43-52.
- Gabizon, A. A., Shmeeda, H. and Zalipsky, S. (2006). "Pros and cons of the liposome platform in cancer drug targeting\*." Journal of Liposome Research 16(3): 175-183.
- Gasselhuber, A., Dreher, M. R., Partanen, A., Yarmolenko, P. S., Woods, D., Wood, B. J. and Haemmerich, D. (2012). "Targeted drug delivery by high intensity focused ultrasound mediated hyperthermia combined with temperature-sensitive liposomes: computational modelling and preliminary in vivo validation." International Journal of Hyperthermia 28(4): 337-348.
- Gervais, D. A., McGovern, F. J., Arellano, R. S., McDougal, W. S. and Mueller, P. R. (2003). "Renal cell carcinoma: clinical experience and technical success with radio-frequency ablation of 42 tumors." Radiology 226(2): 417-424.
- Gillespie, A. M., Broadhead, T. J., Chan, S. Y., Owen, J., Farnsworth, A. P., Sopwith, M. and Coleman, R. E. (2000). "Phase I open study of the effects of ascending doses of the cytotoxic immunoconjugate CMB-401 (hCTMO1-calicheamicin) in patients with epithelial ovarian cancer." Annals of Oncology 11(6): 735-741.
- Goldberg, S. N., Gazelle, G. S., Compton, C. C., Mueller, P. R. and Tanabe, K. K. (2000a). "Treatment of intrahepatic malignancy with radiofrequency ablation: radiologic-pathologic correlation." Cancer 88(11): 2452-2463.
- Goldberg, S. N., Gazelle, G. S. and Mueller, P. R. (2000b). "Thermal ablation therapy for focal malignancy: a unified approach to underlying principles, techniques, and diagnostic imaging guidance." American Journal of Roentgenology 174(2): 323-331.

- Gregoriadis, G. (1973). "Drug entrapment in liposomes." FEBS Letters 36(3): 292-296.
- Gregoriadis, G. (2006). Liposome technology: volume II entrapment of drugs and other materials into liposomes, Informa Healthcare.
- Gregoriadis, G. and Neerunjun, D. E. (1974a). "Control of the rate of hepatic uptake and catabolism of liposome-entrapped proteins injected into rats. Possible therapeutic applications." European Journal of Biochemistry 47(1): 179-185.
- Gregoriadis, G. and Senior, J. (1980). "The phospholipid component of small unilamellar liposomes controls the rate of clearance of entrapped solutes from the circulation." FEBS Letters 119(1): 43-46.
- Gregoriadis, G., Swain, C. P., Wills, E. J. and Tavill, A. S. (1974b). "Drug-carrier potential of liposomes in cancer chemotherapy." The Lancet 303(7870): 1313-1316.
- Grull, H. and Langereis, S. (2012). "Hyperthermia-triggered drug delivery from temperature-sensitive liposomes using MRI-guided high intensity focused ultrasound." Journal of Controlled Release 161(2): 317-327.
- Han, H., BC, S. and HS, C. (2006a). "Doxorubicin-encapsulated thermosensitive liposomes modified with poly(N-isopropylacrylamide-co-acrylamide): drug release behavior and stability in the presence of serum." European Journal of Pharmaceutics and Biopharmaceutics 62(1): 110.
- Han, H. D., Choi, M. S., Hwang, T., Song, C. K., Seong, H., Kim, T. W., Choi, H. S. and Shin, B. C. (2006b). "Hyperthermia-induced antitumor activity of thermosensitive polymer modified temperature-sensitive liposomes." Journal of Pharmaceutical Sciences 95(9): 1909-1917.
- Haran, G., Cohen, R., Bar, L. K. and Barenholz, Y. (1993). "Transmembrane ammonium sulfate gradients in liposomes produce efficient and stable entrapment of amphipathic weak bases." Biochimica et Biophysica Acta (BBA) - Biomembranes 1151(2): 201-215.
- Harbury, P. B. (1993). "A switch between two-, three-, and four-stranded coiled coils in GCN4 leucine zipper mutants." Science 262(5138): 1401-1407.
- Harbury, P. B., Kim, P. S. and Alber, T. (1994). "Crystal structure of an isoleucine-zipper trimer." Nature 371(6492): 80-83.
- Hashizaki, K., Taguchi, H., Sakai, H., Abe, V., Saito, Y. and Ogawa, N. (2006). "Carboxyfluorescein leakage from poly(ethylene glycol)-grafted liposomes induced by the interaction with serum." Chemical & Pharmaceutical Bulletin 54(1): 80-84.
- Hauck, M. L., Coffin, D. O., Dodge, R. K., Dewhirst, M. W., Mitchell, J. B. and Zalutsky, M. R. (1997a). "A local hyperthermia treatment which enhances antibody uptake in a glioma xenograft model does not affect tumour interstitial fluid pressure." International Journal of Hyperthermia 13(3): 307-316.
- Hauck, M. L., Dewhirst, M. W., Bigner, D. D. and Zalutsky, M. R. (1997b). "Local hyperthermia improves uptake of a chimeric monoclonal antibody in a subcutaneous xenograft model." Clinical Cancer Research 3(1): 63-70.
- Hauck, M. L., LaRue, S. M., Petros, W. P., Poulson, J. M., Yu, D., Spasojevic, I., Pruitt, A. F., Klein, A., Case, B., Thrall, D. E., Needham, D. and Dewhirst, M. W. (2006). "Phase I trial of doxorubicin-containing low temperature sensitive liposomes in spontaneous canine tumors." Clinical Cancer Research 12(13): 4004-4010.

- Hayashi, H., Kono, K. and Takagishi, T. (1996). "Temperature-controlled release property of phospholipid vesicles bearing a thermo-sensitive polymer." Biochimica et Biophysica Acta-Biomembranes 1280(1): 127-134.
- Hayashi, H., Kono, K. and Takagishi, T. (1998). "Temperature-dependent associating property of liposomes modified with a thermosensitive polymer." Bioconjugate Chemistry 9(3): 382-389.
- Hayashi, H., Kono, K. and Takagishi, T. (1999). "Temperature sensitization of liposomes using copolymers of N-isopropylacrylamide." Bioconjugate Chemistry 10(3): 412-418.
- Hildebrandt, B., Wust, P., Ahlers, O., Dieing, A., Sreenivasa, G., Kerner, T., Felix, R. and Riess, H. (2002). "The cellular and molecular basis of hyperthermia." Critical Reviews in Oncology/Hematology 43(1): 33-56.
- Hilger, I. and Kaiser, W. A. (2012). "Iron oxide-based nanostructures for MRI and magnetic hyperthermia." Nanomedicine 7(9): 1443-1459.
- Hinman, L. M., Hamann, P. R., Wallace, R., Menendez, A. T., Durr, F. E. and Upešlaciš, J. (1993). "Preparation and characterization of monoclonal antibody conjugates of the calicheamicins: a novel and potent family of antitumor antibiotics." Cancer Research 53(14): 3336-3342.
- Hosokawa, T., Sami, M., Kato, Y. and Hayakawa, E. (2003). "Alteration in the temperature-dependent content release property of thermosensitive liposomes in plasma." Chemical & pharmaceutical bulletin 51(11): 1227-1232.
- Hossann, M., Syunyaeva, Z., Schmidt, R., Zengerle, A., Eibl, H., Issels, R. D. and Lindner, L. H. (2012). "Proteins and cholesterol lipid vesicles are mediators of drug release from thermosensitive liposomes." Journal of Controlled Release 162(2): 400-406.
- Hossann, M., Wang, T. T., Wiggenghorn, M., Schmidt, R., Zengerle, A., Winter, G., Eibl, H., Peller, M., Reiser, M., Issels, R. D. and Lindner, L. H. (2010). "Size of thermosensitive liposomes influences content release." Journal of Controlled Release 147(3): 436-443.
- Hossann, M., Wiggenghorn, M., Schwerdt, A., Wachholz, K., Teichert, N., Eibl, H., Issels, R. D. and Lindner, L. H. (2007). "In vitro stability and content release properties of phosphatidylglyceroglycerol containing thermosensitive liposomes." Biochimica Et Biophysica Acta-Biomembranes 1768: 2491-2499.
- Huang, S. K., Mayhew, E., Gilani, S., Lasic, D. D., Martin, F. J. and Papahadjopoulos, D. (1992). "Pharmacokinetics and therapeutics of sterically stabilized liposomes in mice bearing c-26 colon carcinoma." Cancer Research 52(24): 6774-6781.
- Huang, S. K., Stauffer, P. R., Hong, K., Guo, J. W. H., Phillips, T. L., Huang, A. and Papahadjopoulos, D. (1994). "Liposomes and hyperthermia in mice: increased tumor uptake and therapeutic efficacy of doxorubicin in sterically stabilized liposomes." Cancer Research 54(8): 2186-2191.
- Huang, X., El-Sayed, I. H. and El-Sayed, M. A. (2010). "Applications of gold nanorods for cancer imaging and photothermal therapy." Methods in Molecular Biology 624: 343-357.
- Huang, X., Jain, P. K., El-Sayed, I. H. and El-Sayed, M. A. (2007). "Gold nanoparticles: interesting optical properties and recent applications in cancer diagnostics and therapy." Nanomedicine 2(5): 681-693.
- Hynynen, K. (2011). "MRIGHIFU: A tool for image-guided therapeutics." Journal of Magnetic Resonance Imaging 34(3): 482-493.

- Iacobucci, V., Di Giuseppe, F., Bui, T. T., Vermeer, L. S., Patel, J., Scherman, D., Kichler, A., Drake, A. F. and Mason, A. J. (2012). "Control of pH responsive peptide self-association during endocytosis is required for effective gene transfer." Biochimica et biophysica acta. Biomembranes(0).
- Iden, D. L. and Allen, T. M. (2001). "In vitro and in vivo comparison of immunoliposomes made by conventional coupling techniques with those made by a new post-insertion approach." Biochimica et Biophysica Acta-Biomembranes 1513(2): 207-216.
- Iga, K., Hamaguchi, N., Igari, Y., Ogawa, Y., Gotoh, K., Ootsu, K., Toguchi, H. and Shimamoto, T. (1991). "Enhanced antitumor-activity in mice after administration of thermosensitive liposome encapsulating cisplatin with hyperthermia." Journal of Pharmacology and Experimental Therapeutics 257(3): 1203-1207.
- Ishida, O., Maruyama, K., Yanagie, H., Eriguchi, H. and Iwatsuru, M. (2000). "Targeting chemotherapy to solid tumors with long-circulating thermosensitive liposomes and local hyperthermia." Japanese Journal of Cancer Research 91(1): 118-126.
- Issels, R. (1999). "Hyperthermia combined with chemotherapy a biological rationale, clinical application, and treatment results." Onkologie 22(5): 374-381.
- Issels, R. D., Lindner, L. H., Verweij, J., Wust, P., Reichardt, P., Schem, B.-C., Abdel-Rahman, S., Daugaard, S., Salat, C., Wendtner, C.-M., Vujaskovic, Z., Wessalowski, R., Jauch, K.-W., Dürr, H. R., Ploner, F., Baur-Melnyk, A., Mansmann, U., Hiddemann, W., Blay, J.-Y. and Hohenberger, P. (2010). "Neo-adjuvant chemotherapy alone or with regional hyperthermia for localised high-risk soft-tissue sarcoma: a randomised phase 3 multicentre study." The Lancet Oncology 11(6): 561-570.
- Iyer, A. K., Khaled, G., Fang, J. and Maeda, H. (2006). "Exploiting the enhanced permeability and retention effect for tumor targeting." Drug Discovery Today 11(17-18): 812-818.
- Jaattela, M. (1999). "Heat shock proteins as cellular lifeguards." Annals of Medicine 31(4): 261-271.
- Jain, R. K. (1987a). "Transport of molecules across tumor vasculature." Cancer and Metastasis Reviews 6(4): 559-593.
- Jain, R. K. (1987b). "Transport of molecules in the tumor interstitium: a review." Cancer Research 47(12): 3039-3051.
- Jain, R. K. and Stylianopoulos, T. (2010). "Delivering nanomedicine to solid tumors." Nature reviews. Clinical oncology. 7(11): 653-664.
- Johannsen, M., Thiesen, B., Wust, P. and Jordan, A. (2010). "Magnetic nanoparticle hyperthermia for prostate cancer." International Journal of Hyperthermia 26(8): 790-795.
- Juliano, R. L. and Stamp, D. (1975). "The effect of particle size and charge on the clearance rates of liposomes and liposome encapsulated drugs." Biochemical and Biophysical Research Communications 63(3): 651-658.
- Kaasgaard, T. and Andresen, T. L. (2010). "Liposomal cancer therapy: exploiting tumor characteristics." Expert Opinion on Drug Delivery 7(2): 225-243.
- Karino, T., Koga, S. and Maeta, M. (1988). "Experimental studies of the effects of local hyperthermia on blood flow, oxygen pressure and pH in tumors." Japanese Journal of Surgery 18(3): 276-283.
- Katagiri, K., Imai, Y., Koumoto, K., Kaiden, T., Kono, K. and Aoshima, S. (2011). "Magneto-responsive on-demand release of hybrid liposomes formed from

- fe(3)o(4) nanoparticles and thermosensitive block copolymers." Small 7(12): 1683-1689.
- Kim, J. C., Bae, S. K. and Kim, J. D. (1997). "Temperature-sensitivity of liposomal lipid bilayers mixed with poly(N-isopropylacrylamide-co-acrylic acid)." The Journal of Biochemistry 121(1): 15-19.
- Kirby, C., Clarke, J. and Gregoriadis, G. (1980). "Effect of the cholesterol content of small unilamellar liposomes on their stability in vivo and in vitro." Biochemical Journal 186(2): 591-598.
- Kirchmeier, M. J., Ishida, T., Chevrette, J. and Allen, T. M. (2001). "Correlations between the rate of intracellular release of endocytosed liposomal doxorubicin and cytotoxicity as determined by a new assay." Journal of Liposome Research 11(1): 15-29.
- Kirpotin, D. B., Drummond, D. C., Shao, Y., Shalaby, M. R., Hong, K., Nielsen, U. B., Marks, J. D., Benz, C. C. and Park, J. W. (2006). "Antibody targeting of long-circulating lipidic nanoparticles does not increase tumor localization but does increase internalization in animal models." Cancer Research 66(13): 6732-6740.
- Kobayashi, D., Kawai, N., Sato, S., Naiki, T., Yamada, K., Yasui, T., Tozawa, K., Kobayashi, T., Takahashi, S. and Kohri, K. (2013). "Thermotherapy using magnetic cationic liposomes powerfully suppresses prostate cancer bone metastasis in a novel rat model." Prostate 73(9): 913-922.
- Kobayashi, T. (2011). "Cancer hyperthermia using magnetic nanoparticles." Biotechnology Journal 6(11): 1342-1347.
- Kong, G., Anyambhatla, G., Petros, W. P., Braun, R. D., Colvin, O. M., Needham, D. and Dewhirst, M. W. (2000a). "Efficacy of liposomes and hyperthermia in a human tumor xenograft model: importance of triggered drug release." Cancer Research 60(24): 6950-6957.
- Kong, G., Braun, R. D. and Dewhirst, M. W. (2000b). "Hyperthermia enables tumor-specific nanoparticle delivery: Effect of particle size." Cancer Research 60(16): 4440-4445.
- Kong, G., Braun, R. D. and Dewhirst, M. W. (2001). "Characterization of the effect of hyperthermia on nanoparticle extravasation from tumor vasculature." Cancer Research 61(7): 3027-3032.
- Kong, G. and Dewhirst, M. W. (1999). "Hyperthermia and liposomes." International Journal of Hyperthermia 15(5): 345-370.
- Koning, G. A., Eggermont, A. M. M., Lindner, L. H. and ten Hagen, T. L. M. (2010). "Hyperthermia and thermosensitive liposomes for improved delivery of chemotherapeutic drugs to solid tumors." Pharmaceutical Research 27(8): 1750-1754.
- Kono, K. (2001). "Thermosensitive polymer-modified liposomes." Advanced Drug Delivery Reviews 53(3): 307-319.
- Kono, K., Hayashi, H. and Takagishi, T. (1994). "Temperature-sensitive liposomes: liposomes bearing poly (N-isopropylacrylamide)." Journal of Controlled Release 30(1): 69-75.
- Kono, K., Henmi, A., Yamashita, H., Hayashi, H. and Takagishi, T. (1999a). "Improvement of temperature-sensitivity of poly(N-isopropylacrylamide)-modified liposomes." Journal of Controlled Release 59(1): 63-75.
- Kono, K., Murakami, T., Yoshida, T., Haba, Y., Kanaoka, S., Takagishi, T. and Aoshima, S. (2005). "Temperature sensitization of liposomes by use of thermosensitive block copolymers synthesized by living cationic

- polymerization: Effect of copolymer chain length." Bioconjugate Chemistry 16(6): 1367-1374.
- Kono, K., Nakai, R., Morimoto, K. and Takagishi, T. (1999b). "Temperature-dependent interaction of thermo-sensitive polymer-modified liposomes with CV1 cells." FEBS Letters 456(2): 306-310.
- Kono, K., Nakai, R., Morimoto, K. and Takagishi, T. (1999c). "Thermosensitive polymer-modified liposomes that release contents around physiological temperature." Biochimica et Biophysica Acta 12: 1-2.
- Kono, K., Nakashima, S., Kokuryo, D., Aoki, I., Shimomoto, H., Aoshima, S., Maruyama, K., Yuba, E., Kojima, C., Harada, A. and Ishizaka, Y. (2011). "Multi-functional liposomes having temperature-triggered release and magnetic resonance imaging for tumor-specific chemotherapy." Biomaterials 32(5): 1387-1395.
- Kono, K., Ozawa, T., Yoshida, T., Ozaki, F., Ishizaka, Y., Maruyama, K., Kojima, C., Harada, A. and Aoshima, S. (2010). "Highly temperature-sensitive liposomes based on a thermosensitive block copolymer for tumor-specific chemotherapy." Biomaterials 31(27): 7096-7105.
- Kono, K., Yoshino, K. and Takagishi, T. (2002). "Effect of poly(ethylene glycol) grafts on temperature-sensitivity of thermosensitive polymer-modified liposomes." Journal of Controlled Release 80(1-3): 321-332.
- Kopecek, J. (2003). "Smart and genetically engineered biomaterials and drug delivery systems." European Journal of Pharmaceutical Sciences 20(1): 1-16.
- Koudelka, Š. and Turánek, J. (2012). "Liposomal paclitaxel formulations." Journal of Controlled Release 163(3): 322-334.
- Kowal, C. D. (1979). "Possible benefits of hyperthermia to chemotherapy." Cancer Research 39(6): 2285.
- Kullberg, M., Mann, K. and Owens, J. L. (2009). "A two-component drug delivery system using Her-2-targeting thermosensitive liposomes." Journal of Drug Targeting 17(2): 98-107.
- Kullberg, M., Owens, J. L. and Mann, K. (2010). "Listeriolysin O enhances cytoplasmic delivery by Her-2 targeting liposomes." Journal of Drug Targeting 18(4): 313-320.
- Laginha, K. M., Verwoert, S., Charrois, G. J. R. and Allen, T. M. (2005). "Determination of doxorubicin levels in whole tumor and tumor nuclei in murine breast cancer tumors." Clinical Cancer Research 11(19): 6944-6949.
- Lahoti, T. S., Patel, D., Thekkemadom, V., Beckett, R. and Ray, S. D. (2012). "Doxorubicin-induced in vivo nephrotoxicity involves oxidative stress-mediated multiple pro- and anti-apoptotic signaling pathways." Current Neurovascular Research 9(4): 282-295.
- Lammers, T. (2012). "Drug targeting to tumors: Principles, pitfalls and (pre-) clinical progress." Journal of Controlled Release 161(2): 175-187.
- Lan, Y., Langlet-Bertin, B., Abbate, V., Vermeer, L. S., Kong, X., Sullivan, K. E., Leborgne, C., Scherman, D., Hider, R. C., Drake, A. F., Bansal, S. S., Kichler, A. and Mason, A. J. (2010a). "Incorporation of 2,3-diaminopropionic acid into linear cationic amphipathic peptides produces pH-sensitive vectors." Chembiochem : a European journal of chemical biology 11(9): 1266-1272.
- Lan, Y., Ye, Y., Kozłowska, J., Lam, J. K. W., Drake, A. F. and Mason, A. J. (2010b). "Structural contributions to the intracellular targeting strategies of antimicrobial peptides." Biochimica et Biophysica Acta (BBA) - Biomembranes 1798(10): 1934-1943.

- Landon, C. D., Park, J.-Y., Needham, D. and Dewhirst, M. W. (2011). "Nanoscale drug delivery and hyperthermia: the materials design and preclinical and clinical testing of low temperature-sensitive liposomes used in combination with mild hyperthermia in the treatment of local cancer." The Open Nanomedicine Journal 3: 38-64.
- Lasic, D. D. and Needham, D. (1995). "The "stealth" liposome: A prototypical biomaterial." Chemical Reviews 95(8): 2601-2628.
- Laurent, S., Forge, D., Port, M., Roch, A., Robic, C., Vander Elst, L. and Muller, R. N. (2008). "Magnetic iron oxide nanoparticles: synthesis, stabilization, vectorization, physicochemical characterizations, and biological applications." Chemical Reviews 108(6): 2064-2110.
- Lestini, B. J., Sagnella, S. M., Xu, Z., Shive, M. S., Richter, N. J., Jayaseharan, J., Case, A. J., Kottke-Marchant, K., Anderson, J. M. and Marchant, R. E. (2002). "Surface modification of liposomes for selective cell targeting in cardiovascular drug delivery." Journal of Controlled Release 78(1-3): 235-247.
- Leunig, M. (1992). "Interstitial fluid pressure in solid tumors following hyperthermia: possible correlation with therapeutic response." Cancer Research 52(2): 487-490.
- Li, L., Ten Hagen, T. L., Bolkestein, M., Gasselhuber, A., Yatvin, J., van Rhooon, G. C., Eggermont, A. M., Haemmerich, D. and Koning, G. A. (2013a). "Improved intratumoral nanoparticle extravasation and penetration by mild hyperthermia." Journal of Controlled Release 167(2): 130-137.
- Li, L., Ten Hagen, T. L., Hossann, M., Suss, R., van Rhooon, G. C., Eggermont, A. M., Haemmerich, D. and Koning, G. A. (2013b). "Mild hyperthermia triggered doxorubicin release from optimized stealth thermosensitive liposomes improves intratumoral drug delivery and efficacy." Journal of Controlled Release 168(2): 142-150.
- Li, L., ten Hagen, T. L. M., Schipper, D., Wijnberg, T. M., Van Rhooon, G., Eggermont, A. M. M., Lindner, L. H. and Koning, G. A. (2010). "Triggered content release from optimized stealth thermosensitive liposomes using mild hyperthermia." Journal of Controlled Release 143(2): 274-279.
- Li, P. Z., Zhu, S. H., He, W., Zhu, L. Y., Liu, S. P., Liu, Y., Wang, G. H. and Ye, F. (2012). "High-intensity focused ultrasound treatment for patients with unresectable pancreatic cancer." Hepatobiliary & Pancreatic Diseases International 11(6): 655-660.
- Liaubet, A., Egretcharlier, M. and Kuhry, J. G. (1994). "Influence of the clathrin coat on the membrane lipidic organization of endocytic vesicles – A fluorescence study." Biochimica et Biophysica Acta-Biomembranes 1195(1): 164-168.
- Limacher, J. M. and Acres, B. (2007). "MUC1, a therapeutic target in oncology." Bull Cancer 94(3): 253-257.
- Lindner, L. H., Eichhorn, M. E., Eibl, H., Teichert, N., Schmitt-Sody, M., Issels, R. D. and Dellian, M. (2004). "Novel temperature-sensitive liposomes with prolonged circulation time." Clinical Cancer Research 10(6): 2168-2178.
- Lindner, L. H., Hossann, M., Vogeser, M., Teichert, N., Wachholz, K., Eibl, H., Hiddemann, W. and Issels, R. D. (2008). "Dual role of hexadecylphosphocholine (miltefosine) in thermosensitive liposomes: Active ingredient and mediator of drug release." Journal of Controlled Release 125(2): 112-120.

- Lindner, L. H., Reinl, H. M., Schlemmer, M., Stahl, R. and Peller, M. (2005). "Paramagnetic thermosensitive liposomes for MR-thermometry." International Journal of Hyperthermia 21(6): 575-588.
- Livraghi, T., Goldberg, S. N., Lazzaroni, S., Meloni, F., Ierace, T., Solbiati, L. and Gazelle, G. S. (2000). "Hepatocellular carcinoma: Radio-frequency ablation of medium and large lesions." Radiology 214(3): 761-768.
- Livraghi, T., Meloni, F., Di Stasi, M., Rolle, E., Solbiati, L., Tinelli, C. and Rossi, S. (2008). "Sustained complete response and complications rates after radiofrequency ablation of very early hepatocellular carcinoma in cirrhosis: Is resection still the treatment of choice?" Hepatology 47(1): 82-89.
- Livraghi, T., Solbiati, L., Meloni, M. F., Gazelle, G. S., Halpern, E. F. and Goldberg, S. N. (2003). "Treatment of focal liver tumors with percutaneous radio-frequency ablation: complications encountered in a multicenter study." Radiology 226(2): 441-451.
- Loomis, K., Smith, B., Feng, Y., Garg, H., Yavlovich, A., Campbell-Massa, R., Dimitrov, D. S., Blumenthal, R., Xiao, X. and Puri, A. (2010). "Specific targeting to B cells by lipid-based nanoparticles conjugated with a novel CD22-ScFv." Experimental and Molecular Pathology 88(2): 238-249.
- Lorenzato, C., Cernicanu, A., Meyre, M. E., Germain, M., Pottier, A., Levy, L., de Senneville, B. D., Bos, C., Moonen, C. and Smirnov, P. (2013). "MRI contrast variation of thermosensitive magnetoliposomes triggered by focused ultrasound: a tool for image-guided local drug delivery." Contrast Media & Molecular Imaging 8(2): 185-192.
- Mackay, J. A. and Chilkoti, A. (2008). "Temperature sensitive peptides: Engineering hyperthermia-directed therapeutics." International Journal of Hyperthermia 24(6): 483-495.
- Maeda, H. (2001). "The enhanced permeability and retention (EPR) effect in tumor vasculature: the key role of tumor-selective macromolecular drug targeting." Advances in Enzyme Regulation 41: 189-207.
- Maier-Hauff, K., Rothe, R., Scholz, R., Gneveckow, U., Wust, P., Thiesen, B., Feussner, A., von Deimling, A., Waldoefner, N., Felix, R. and Jordan, A. (2007). "Intracranial thermotherapy using magnetic nanoparticles combined with external beam radiotherapy: results of a feasibility study on patients with glioblastoma multiforme." Journal of Neuro-Oncology 81(1): 53-60.
- Maier-Hauff, K., Ulrich, F., Nestler, D., Niehoff, H., Wust, P., Thiesen, B., Orawa, H., Budach, V. and Jordan, A. (2011). "Efficacy and safety of intratumoral thermotherapy using magnetic iron-oxide nanoparticles combined with external beam radiotherapy on patients with recurrent glioblastoma multiforme." Journal of Neuro-Oncology 103(2): 317-324.
- Mamot, C., Drummond, D. C., Noble, C. O., Kallab, V., Guo, Z., Hong, K., Kirpotin, D. B. and Park, J. W. (2005). "Epidermal growth factor receptor-targeted immunoliposomes significantly enhance the efficacy of multiple anticancer drugs in vivo." Cancer Research 65(24): 11631-11638.
- Manzoor, A. A., Lindner, L. H., Landon, C. D., Park, J. Y., Simnick, A. J., Dreher, M. R., Das, S., Hanna, G., Park, W., Chilkoti, A., Koning, G. A., ten Hagen, T. L., Needham, D. and Dewhirst, M. W. (2012). "Overcoming limitations in nanoparticle drug delivery: triggered, intravascular release to improve drug penetration into tumors." Cancer Research 72(21): 5566-5575.
- Maruyama, K., Unezaki, S., Takahashi, N. and Iwatsuru, M. (1993). "Enhanced delivery of doxorubicin to tumor by long-circulating thermosensitive



- liposomes and local hyperthermia." Biochimica et Biophysica Acta (BBA) - Biomembranes 1149(2): 209-216.
- Matsumura, Y. and Maeda, H. (1986). "A new concept for macromolecular therapeutics in cancer chemotherapy: mechanism of tumortropic accumulation of proteins and the antitumor agent smancs." Cancer Research 46(12 Pt 1): 6387-6392.
- Matteucci, M. L., Anyarambhatla, G., Rosner, G., Azuma, C., Fisher, P. E., Dewhirst, M. W., Needham, D. and Thrall, D. E. (2000). "Hyperthermia increases accumulation of technetium-99m-labeled liposomes in feline sarcomas." Clinical Cancer Research 6(9): 3748-3755.
- May, J. P. and Li, S. D. (2013). "Hyperthermia-induced drug targeting." Expert Opinion on Drug Delivery 10(4): 511-527.
- Mayer, L. D., Bally, M. B. and Cullis, P. R. (1986). "Uptake of adriamycin into large unilamellar vesicles in response to a pH gradient." Biochimica et Biophysica Acta 857(1): 123-126.
- Mayer, L. D., Tai, L. C. L., Ko, D. S. C., Masin, D., Ginsberg, R. S., Cullis, P. R. and Bally, M. B. (1989). "Influence of vesicle size, lipid composition, and drug-to-lipid ratio on the biological activity of liposomal doxorubicin in mice." Cancer Research 49(21): 5922-5930.
- McFarlane, A. A., Orriss, G. L. and Stetefeld, J. (2009). "The use of coiled-coil proteins in drug delivery systems." European Journal of Pharmacology 625(1-3): 101-107.
- McIntyre, J. C. and Sleight, R. G. (1991). "Fluorescence assay for phospholipid membrane asymmetry." Biochemistry 30(51): 11819-11827.
- Mills, J. K. and Needham, D. (2005). "lysolipid incorporation in dipalmitoylphosphatidylcholine bilayer membranes enhances the ion permeability and drug release rates at the membrane phase transition." Biochimica et Biophysica Acta-Biomembranes 1716(2): 77-96.
- Moase, E. H., Qi, W., Ishida, T., Gabos, Z., Longenecker, B. M., Zimmermann, G. L., Ding, L., Krantz, M. and Allen, T. M. (2001). "Anti-MUC-1 immunoliposomal doxorubicin in the treatment of murine models of metastatic breast cancer." Biochimica et Biophysica Acta (BBA) - Biomembranes 1510(1-2): 43-55.
- Moghimi, S. M. and Patel, H. M. (1989). "Differential properties of organ-specific serum opsonins for liver and spleen macrophages." Biochimica et Biophysica Acta 984(3): 379-383.
- Moreira, J. N., Ishida, T., Gaspar, R. and Allen, T. M. (2002). "Use of the post-insertion technique to insert peptide ligands into pre-formed stealth liposomes with retention of binding activity and cytotoxicity." Pharmaceutical Research 19(3): 265-269.
- Morimoto, R. I. (1993). "Cells in stress: transcriptional activation of heat shock genes." Science 259(5100): 1409-1410.
- Mukherjee, P., Madsen, C. S., Ginardi, A. R., Tinder, T. L., Jacobs, F., Parker, J., Agrawal, B., Longenecker, B. M. and Gendler, S. J. (2003). "Mucin 1-specific immunotherapy in a mouse model of spontaneous breast cancer." Journal of Immunotherapy 26(1): 47-62.
- Na, K., Lee, S. A., Jung, S. H., Hyun, J. and Shin, B. C. (2012). "Elastin-like polypeptide modified liposomes for enhancing cellular uptake into tumor cells." Colloids and surfaces. B, Biointerfaces 91: 130-136.

- Nagy, I. B., Alsina, M. A., Haro, I., Reig, F. and Hudecz, F. (2000). "Phospholipid-model membrane interactions with branched polypeptide conjugates of a Hepatitis A virus peptide epitope." Bioconjugate Chemistry 11(1): 30-38.
- Needham, D., Anyarambhatla, G., Kong, G. and Dewhirst, M. W. (2000). "A new temperature-sensitive liposome for use with mild hyperthermia: characterization and testing in a human tumor xenograft model." Cancer Research 60(5): 1197-1201.
- Needham, D. and Dewhirst, M. Materials science and engineering of the low temperature sensitive liposome (LTSL): Composition-structure-property relationships that underlie its design and performance. In Smart materials for drug delivery, Eds.; The Royal Society of Chemistry: (2012); 1.
- Needham, D. and Dewhirst, M. W. (2001). "The development and testing of a new temperature-sensitive drug delivery system for the treatment of solid tumors." Advanced Drug Delivery Reviews 53(3): 285-305.
- Needham, D., McIntosh, T. J. and Evans, E. (1988). "Thermomechanical and transition properties of dimyristoylphosphatidylcholine/cholesterol bilayers." Biochemistry 27(13): 4668-4673.
- Needham, D., McIntosh, T. J. and Zhelev, D. V. Surface chemistry of the sterically stabilized PEG-liposome: General principles. In Liposomes: Rational Design, Janoff, A. and Dekker, M.: (1998), 13-62.
- Needham, D. and Nunn, R. S. (1990). "Elastic deformation and failure of lipid bilayer membranes containing cholesterol." Biophysical Journal 58(4): 997-1009.
- Needham, D., Park, J.-Y., Wright, A. M. and Tong, J. (2013). "Materials characterization of the low temperature sensitive liposome (LTSL): effects of the lipid composition (lysolipid and dspe-peg2000) on the thermal transition and release of doxorubicin." Faraday Discussions 161(0): 515-534.
- Negussie, A. H., Miller, J. L., Reddy, G., Drake, S. K., Wood, B. J. and Dreher, M. R. (2010). "Synthesis and in vitro evaluation of cyclic NGR peptide targeted thermally sensitive liposome." Journal of Controlled Release 143(2): 265-273.
- Negussie, A. H., Yarmolenko, P. S., Partanen, A., Ranjan, A., Jacobs, G., Woods, D., Bryant, H., Thomasson, D., Dewhirst, M. W., Wood, B. J. and Dreher, M. R. (2011). "Formulation and characterisation of magnetic resonance imageable thermally sensitive liposomes for use with magnetic resonance-guided high intensity focused ultrasound." International Journal of Hyperthermia 27(2): 140-155.
- Ning, S., Macleod, K., Abra, R. M., Huang, A. H. and Hahn, G. M. (1994). "Hyperthermia induces doxorubicin release from long-circulating liposomes and enhances their anti-tumor efficacy." International Journal of Radiation Oncology, Biology, Physics 29(4): 827-834.
- Otte, J. (1988). "Hyperthermia in cancer therapy." European Journal of Pediatrics 147(6): 560-569.
- Paasonen, L., Laaksonen, T., Johans, C., Yliperttula, M., Kontturi, K. and Urtti, A. (2007a). "Gold nanoparticles enable selective light-induced contents release from liposomes." Journal of Controlled Release 122(1): 86-93.
- Paasonen, L., Romberg, B., Storm, G., Yliperttula, M., Urtti, A. and Hennink, W. E. (2007b). "Temperature-sensitive poly(N-(2-hydroxypropyl)methacrylamide mono/dilactate)-coated liposomes for triggered contents release." Bioconjugate Chemistry 18: 2131-2136.

- Paasonen, L., Sipila, T., Subrizi, A., Laurinmaki, P., Butcher, S. J., Rappolt, M., Yaghmur, A., Urtti, A. and Yliperttula, M. (2010). "Gold-embedded photosensitive liposomes for drug delivery: triggering mechanism and intracellular release." Journal of Controlled Release 147(1): 136-143.
- Pankhurst, Q. A. (2003). "Applications of magnetic nanoparticles in biomedicine." Journal of Physics D: Applied Physics 36(13): R167-R181.
- Papahadjopoulos, D., Allen, T. M., Gabizon, A., Mayhew, E., Matthay, K., Huang, S. K., Lee, K. D., Woodle, M. C., Lasic, D. D., Redemann, C. and Martin, F. J. (1991). "Sterically stabilized liposomes - improvements in pharmacokinetics and antitumor therapeutic efficacy." Proceedings of the National Academy of Sciences of the United States of America 88(24): 11460-11464.
- Papahadjopoulos, D., Jacobson, K., Nir, S. and Isac, I. (1973). "Phase transitions in phospholipid vesicles fluorescence polarization and permeability measurements concerning the effect of temperature and cholesterol." Biochimica et Biophysica Acta (BBA) - Biomembranes 311(3): 330-348.
- Parente, R. A., Nir, S. and Szoka, F. C. (1990). "Mechanism of leakage of phospholipid vesicle contents induced by the peptide GALA." Biochemistry 29(37): 8720-8728.
- Park, J. H., von Maltzahn, G., Xu, M. J., Fogal, V., Kotamraju, V. R., Ruoslahti, E., Bhatia, S. N. and Sailor, M. J. (2010). "Cooperative nanomaterial system to sensitize, target, and treat tumors." Proceedings of the National Academy of Sciences of the United States of America 107(3): 981-986.
- Park, J. W., Kirpotin, D. B., Hong, K., Shalaby, R., Shao, Y., Nielsen, U. B., Marks, J. D., Papahadjopoulos, D. and Benz, C. C. (2001). "Tumor targeting using anti-HER2 immunoliposomes." Journal of Controlled Release 74(1-3): 95-113.
- Park, S. H., Oh, S. G., Mun, J. Y. and Han, S. S. (2005). "Effects of silver nanoparticles on the fluidity of bilayer in phospholipid liposome." Colloids and Surfaces B-Biointerfaces 44(2-3): 117-122.
- Park, S. H., Oh, S. G., Mun, J. Y. and Han, S. S. (2006). "Loading of gold nanoparticles inside the DPPC bilayers of liposome and their effects on membrane fluidities." Colloids and Surfaces B-Biointerfaces 48(2): 112-118.
- Pastorino, F. (2003). "Vascular damage and anti-angiogenic effects of tumor vessel-targeted liposomal chemotherapy." Cancer Research 63(21): 7400-7409.
- Pastorino, F., Brignole, C., Di Paolo, D., Nico, B., Pezzolo, A., Marimpietri, D., Pagnan, G., Piccardi, F., Cilli, M., Longhi, R., Ribatti, D., Corti, A., Allen, T. M. and Ponzoni, M. (2006). "Targeting liposomal chemotherapy via both tumor cell-specific and tumor vasculature-specific ligands potentiates therapeutic efficacy." Cancer Research 66(20): 10073-10082.
- Peer, D., Karp, J. M., Hong, S., Farokhzad, O. C., Margalit, R. and Langer, R. (2007). "Nanocarriers as an emerging platform for cancer therapy." nature nanotechnology 2(12): 751-760.
- Petka, W. A., Harden, J. L., McGrath, K. P., Wirtz, D. and Tirrell, D. A. (1998). "Reversible hydrogels from self-assembling artificial proteins." Science 281(5375): 389-392.
- Ponce, A. M., Viglianti, B. L., Yu, D., Yarmolenko, P. S., Michelich, C. R., Woo, J., Bally, M. B. and Dewhirst, M. W. (2007). "Magnetic resonance imaging of temperature-sensitive liposome release: drug dose painting and antitumor effects." Journal of the National Cancer Institute 99(1): 53-63.

- Ponce, A. M., Vujaskovic, Z., Yuan, F., Needham, D. and Dewhirst, M. W. (2006a). "Hyperthermia mediated liposomal drug delivery." International Journal of Hyperthermia 22(3): 205-213.
- Ponce, A. M., Wright, A., Dewhirst, M. W. and Needham, D. (2006b). "Targeted bioavailability of drugs by triggered release from liposomes." Future Lipidology 1(1): 25-34.
- Poon, R. T. and Borys, N. (2009). "Lyso-thermosensitive liposomal doxorubicin: a novel approach to enhance efficacy of thermal ablation of liver cancer." Expert Opinion on Pharmacotherapy 10(2): 333-343.
- Prabhakar, U., Blakey, D. C., Maeda, H., Jain, R. K., Sevick-Muraca, E. M., Zamboni, W., Farokhzad, O. C., Barry, S. T., Gabizon, A. and Grodzinski, P. (2013). "Challenges and key considerations of the enhanced permeability and retention effect (EPR) for nanomedicine drug delivery in oncology." Cancer Research.
- Pradhan, P., Giri, J., Rieken, F., Koch, C., Mykhaylyk, O., Doblinger, M., Banerjee, R., Bahadur, D. and Plank, C. (2010). "Targeted temperature sensitive magnetic liposomes for thermo-chemotherapy." Journal of Controlled Release 142(1): 108-121.
- Preiss, M. R. and Bothun, G. D. (2011). "Stimuli-responsive liposome-nanoparticle assemblies." Expert Opinion on Drug Delivery 8(8): 1025-1040.
- Prinssen, H. M., Molthoff, C. F., Verheijen, R. H., Broadhead, T. J., Kenemans, P., Roos, J. C., Davies, Q., van Hof, A. C., Frier, M., den Hollander, W., Wilhelm, A. J., Baker, T. S., Sopwith, M., Symonds, E. M. and Perkins, A. C. (1998). "Biodistribution of <sup>111</sup>In-labelled engineered human antibody CTM01 (hCTM01) in ovarian cancer patients: influence of prior administration of unlabelled hCTM01." Cancer Immunology, Immunotherapy 47(1): 39-46.
- Puri, A., Kramer-Marek, G., Campbell-Massa, R., Yavlovich, A., Tele, S. C., Lee, S. B., Clogston, J. D., Patri, A. K., Blumenthal, R. and Capala, J. (2008). "HER2-specific affibody-conjugated thermosensitive liposomes (affisomes) for improved delivery of anticancer agents." Journal of Liposome Research 18(4): 293-307.
- Rahman, A., More, N. and Schein, P. S. (1982). "Doxorubicin-induced chronic cardiotoxicity and its protection by liposomal administration." Cancer Research 42(5): 1817-1825.
- Rahman, A., White, G., More, N. and Schein, P. S. (1985). "Pharmacological, toxicological, and therapeutic evaluation in mice of doxorubicin entrapped in cardiolipin liposomes." Cancer Research 45(2): 796-803.
- Ranjan, A., Jacobs, G. C., Woods, D. L., Negussie, A. H., Partanen, A., Yarmolenko, P. S., Gacchina, C. E., Sharma, K. V., Frenkel, V., Wood, B. J. and Dreher, M. R. (2012). "Image-guided drug delivery with magnetic resonance guided high intensity focused ultrasound and Temperature Sensitive Liposomes in a rabbit Vx2 tumor model." Journal of Controlled Release 158(3): 487-494.
- Reig, F., Juve, A., Ortiz, A., Sospedra, P. and Alsina, M. A. (2005). "Effect of a laminin amphiphatic sequence on DPPC ordered bilayers." Luminescence 20(4-5): 326-330.
- Safra, T., Muggia, F., Jeffers, S., Tsao-Wei, D. D., Groshen, S., Lyass, O., Henderson, R., Berry, G. and Gabizon, A. (2000). "Pegylated liposomal doxorubicin (doxil): Reduced clinical cardiotoxicity in patients reaching or

- exceeding cumulative doses of 500 mg/m<sup>2</sup>." Annals of Oncology 11(8): 1029-1033.
- Salomir, R., Vimeux, F. C., de Zwart, J. A., Grenier, N. and Moonen, C. T. (2000). "Hyperthermia by MR-guided focused ultrasound: accurate temperature control based on fast MRI and a physical model of local energy deposition and heat conduction." Magnetic Resonance in Medicine 43(3): 342-347.
- Sapra, P. and Allen, T. M. (2002). "Internalizing antibodies are necessary for improved therapeutic efficacy of antibody-targeted liposomal drugs." Cancer Research 62(24): 7190-7194.
- Sawant, R. R. and Torchilin, V. P. (2012). "Challenges in development of targeted liposomal therapeutics." The AAPS Journal 14(2): 303-315.
- Schafer, H., Madler, B. and Volke, F. (1995). "De-Pake-ing of NMR powder spectra by nonnegative least-squares analysis with Tikhonov regularization." Journal of Magnetic Resonance, Series A 116(2): 145-149.
- Schlemmer, M., Lindner, L. H., Abdel-Rahman, S. and Issels, R. D. (2004). "Principles, technology and indication of hyperthermia and part body hyperthermia." Radiologe 44(4): 301-309.
- Schuster, J. M., Zalutsky, M. R., Noska, M. A., Dodge, R., Friedman, H. S., Bigner, D. D. and Dewhirst, M. W. (1995). "Hyperthermic modulation of radiolabeled antibody uptake in a human glioma xenograft and normal-tissues." International Journal of Hyperthermia 11(1): 59-72.
- Seetharamu, N., Kim, E., Hochster, H., Martin, F. and Muggia, F. (2010). "Phase II study of liposomal cisplatin (SPI-77) in platinum-sensitive recurrences of ovarian cancer." Anticancer Research 30(2): 541-545.
- Senior, J. and Gregoriadis, G. (1982). "Is half-life of circulating liposomes determined by changes in their permeability?" FEBS Letters 145(1): 109-114.
- Seynhaeve, A. L., Hoving, S., Schipper, D., Vermeulen, C. E., de Wiel-Ambagtsheer, G., van Tiel, S. T., Eggermont, A. M. and Ten Hagen, T. L. (2007). "Tumor necrosis factor alpha mediates homogeneous distribution of liposomes in murine melanoma that contributes to a better tumor response." Cancer Research 67(19): 9455-9462.
- Shen, W., Lammertink, R. G. H., Sakata, J. K., Kornfield, J. A. and Tirrell, D. A. (2005). "Assembly of an artificial protein hydrogel through leucine zipper aggregation and disulfide bond formation." Macromolecules 38(9): 3909-3916.
- Shibayama, M., Mizutani, S.-y. and Nomura, S. (1996). "Thermal properties of copolymer gels containing N-isopropylacrylamide." Macromolecules 29(6): 2019-2024.
- Silva, A. C., Lee, J. H., Aoki, I. and Koretsky, A. P. (2004). "Manganese-enhanced magnetic resonance imaging (MEMRI): methodological and practical considerations." NMR in Biomedicine 17(8): 532-543.
- Smith, B., Lyakhov, I., Loomis, K., Needle, D., Baxa, U., Yavlovich, A., Capala, J., Blumenthal, R. and Puri, A. (2011). "Hyperthermia-triggered intracellular delivery of anticancer agent to HER2(+) cells by HER2-specific affibody (ZHER2-GS-Cys)-conjugated thermosensitive liposomes (HER2(+) affisomes)." Journal of controlled Release 153(2): 187-194.
- Sofou, S. and Sgouros, G. (2008). "Antibody-targeted liposomes in cancer therapy and imaging." Expert Opinion on Drug Delivery 5(2): 189-204.

- Solomon, R. and Gabizon, A. A. (2008). "Clinical pharmacology of liposomal anthracyclines: focus on pegylated liposomal doxorubicin." Clinical Lymphoma and Myeloma 8(1): 21-32.
- Song, C. W., Lokshina, A., Rhee, J. G., Patten, M. and Levitt, S. H. (1984). "Implication of blood flow in hyperthermic treatment of tumors." IEEE Transactions on Biomedical Engineering 31(1): 9-16.
- Sospedra, P., Nagy, I. B., Haro, I., Mestres, C., Hudecz, F. and Reig, F. (1999). "Physicochemical behavior of polylysine-[HAV-VPS peptide] constructs at the air-water interface." Langmuir 15(15): 5111-5117.
- Staruch, R., Chopra, R. and Hynynen, K. (2011). "Localised drug release using MRI-controlled focused ultrasound hyperthermia." International Journal of Hyperthermia 27(2): 156-171.
- Staruch, R. M., Ganguly, M., Tannock, I. F., Hynynen, K. and Chopra, R. (2012). "Enhanced drug delivery in rabbit VX2 tumours using thermosensitive liposomes and MRI-controlled focused ultrasound hyperthermia." International Journal of Hyperthermia 28(8): 776-787.
- Sternin, E., Bloom, M. and Mackay, A. L. (1983). "De-Pake-ing of NMR-spectra." Journal of Magnetic Resonance 55(2): 274-282.
- Storm, G., Roerdink, F. H., Steerenberg, P. A., de Jong, W. H. and Crommelin, D. J. (1987). "Influence of lipid composition on the antitumor activity exerted by doxorubicin-containing liposomes in a rat solid tumor model." Cancer Research 47(13): 3366-3372.
- Sullivan, S. M. and Huang, L. (1985). "Preparation and characterization of heat-sensitive immunoliposomes." Biochimica et Biophysica Acta 812(1): 116-126.
- Sullivan, S. M. and Huang, L. (1986). "Enhanced delivery to target cells by heat-sensitive immunoliposomes." Proceedings of the National Academy of Sciences 83(16): 6117-6121.
- Ta, T., Convertine, A. J., Reyes, C. R., Stayton, P. S. and Porter, T. M. (2010). "Thermosensitive liposomes modified with poly(N-isopropylacrylamide-co-propylacrylic acid) copolymers for triggered release of doxorubicin." Biomacromolecules 11(8): 1915-1920.
- Ta, T. and Porter, T. M. (2013). "Thermosensitive liposomes for localized delivery and triggered release of chemotherapy." Journal of Controlled Release 169(1-2): 112-125.
- Tagami, T., Ernsting, M. J. and Li, S.-D. (2011a). "Efficient tumor regression by a single and low dose treatment with a novel and enhanced formulation of thermosensitive liposomal doxorubicin." Journal of Controlled Release 152(2): 303-309.
- Tagami, T., Ernsting, M. J. and Li, S.-D. (2011b). "Optimization of a novel and improved thermosensitive liposome formulated with DPPC and a Brij surfactant using a robust in vitro system." Journal of Controlled Release 154(3): 290-297.
- Tagami, T., Foltz, W. D., Ernsting, M. J., Lee, C. M., Tannock, I. F., May, J. P. and Li, S.-D. (2011c). "MRI monitoring of intratumoral drug delivery and prediction of the therapeutic effect with a multifunctional thermosensitive liposome." Biomaterials 32(27): 6570-6578.
- Tagami, T., May, J. P., Ernsting, M. J. and Li, S.-D. (2012). "A thermosensitive liposome prepared with a Cu<sup>2+</sup> gradient demonstrates improved

- pharmacokinetics, drug delivery and antitumor efficacy." Journal of Controlled Release 161(1): 142-149.
- Tai, L.-A., Tsai, P.-J., Wang, Y.-C., Wang, Y.-J., Lo, L.-W. and Yang, C.-S. (2009). "Thermosensitive liposomes entrapping iron oxide nanoparticles for controllable drug release." Nanotechnology 20(13): 135101.
- Tai, L.-A., Wang, Y.-C. and Yang, C.-S. (2010). "Heat-activated sustaining nitric oxide release from zwitterionic diazeniumdiolate loaded in thermo-sensitive liposomes." Nitric Oxide 23(1): 60-64.
- Taylor, K. M. G. and Morris, R. M. (1995). "Thermal analysis of phase transition behaviour in liposomes." Thermochimica Acta 248: 289-301.
- Terentyuk, G. S., Maslyakova, G. N., Suleymanova, L. V., Khlebtsov, N. G., Khlebtsov, B. N., Akchurin, G. G., Maksimova, I. L. and Tuchin, V. V. (2009). "Laser-induced tissue hyperthermia mediated by gold nanoparticles: toward cancer phototherapy." Journal of Biomedical Optics 14(2): 3122371.
- Thacker, P. G., Callstrom, M. R., Curry, T. B., Mandrekar, J. N., Atwell, T. D., Goetz, M. P. and Rubin, J. (2011). "Palliation of painful metastatic disease involving bone with imaging-guided treatment: comparison of patients' immediate response to radiofrequency ablation and cryoablation." AJR. American Journal of Roentgenology 197(2): 510-515.
- Thompson, K. S., Vinson, C. R. and Freire, E. (1993). "Thermodynamic characterization of the structural stability of the coiled-coil region of the bZIP transcription factor GCN4." Biochemistry 32(21): 5491-5496.
- Thrall, D. E., Prescott, D. M., Samulski, T. V., Dewhirst, M. W., Cline, J. M., Lee, J., Page, R. L. and Oleson, J. R. (1992). "Serious toxicity associated with annular microwave array induction of whole-body hyperthermia in normal dogs." International Journal of Hyperthermia 8(1): 23-32.
- Tian, B., Al-Jamal, W. T., Al-Jamal, K. T. and Kostarelos, K. (2011). "Doxorubicin-loaded lipid-quantum dot hybrids: surface topography and release properties." International Journal of Pharmaceutics 416(2): 443-447.
- Tong, L., Zhao, Y., Huff, T. B., Hansen, M. N., Wei, A. and Cheng, J. X. (2007). "Gold nanorods mediate tumor cell death by compromising membrane integrity." Advanced Materials 19: 3136-3141.
- Torchilin (2003). Liposomes : A practical approach
- Torchilin, V. (2008). "Antibody-modified liposomes for cancer chemotherapy." Expert Opinion on Drug Delivery 5(9): 1003-1025.
- Torchilin, V. P. (2002). "TAT peptide-modified liposomes for intracellular delivery of drugs and DNA." Cellular & Molecular Biology Letters 7(2): 265-267.
- Turner, D. C., Moshkelani, D., Shemesh, C. S., Luc, D. and Zhang, H. (2012). "Near-infrared image-guided delivery and controlled release using optimized thermosensitive liposomes." Pharmaceutical Research 29(8): 2092-2103.
- Ueno, M., Yoshida, S. and Horikoshi, I. (1991). "Characteristics of the membrane-permeability of temperature-sensitive liposome." Bulletin of the Chemical Society of Japan 64(5): 1588-1593.
- Unezaki, S., Maruyama, K., Takahashi, N., Koyama, M., Yuda, T., Suginaka, A. and Iwatsuru, M. (1994). "Enhanced delivery and antitumor-activity of doxorubicin using long-circulating thermosensitive liposomes containing amphipathic polyethylene-glycol in combination with local hyperthermia." Pharmaceutical Research 11(8): 1180-1185.
- Van Der Zee, J. (2002). "Heating the patient: a promising approach?" Annals of Oncology 13(8): 1173-1184.

- Van Der Zee, J., De Bruijne, M., Mens, J. W., Ameziane, A., Broekmeyer-Reurink, M. P., Drizdal, T., Linthorst, M. and Van Rhoon, G. C. (2010). "Reirradiation combined with hyperthermia in breast cancer recurrences: overview of experience in Erasmus MC." International Journal of Hyperthermia 26(7): 638-648.
- Viglianti, B. L., Abraham, S. A., Michelich, C. R., Yarmolenko, P. S., MacFall, J. R., Bally, M. B. and Dewhirst, M. W. (2004). "In vivo monitoring of tissue pharmacokinetics of liposome/drug using MRI: Illustration of targeted delivery." Magnetic Resonance in Medicine 51(6): 1153-1162.
- Viglianti, B. L., Ponce, A. M., Michelich, C. R., Yu, D., Abraham, S. A., Sanders, L., Yarmolenko, P. S., Schroeder, T., MacFall, J. R., Barboriak, D. P., Colvin, O. M., Bally, M. B. and Dewhirst, M. W. (2006). "Chemodosimetry of in vivo tumor liposomal drug concentration using MRI." Magnetic Resonance in Medicine 56(5): 1011-1018.
- Viroonchatapan, E., Sato, H., Ueno, M., Adachi, I., Tazawa, K. and Horikoshi, I. (1997). "Release of 5-fluorouracil from thermosensitive magnetoliposomes induced by an electromagnetic field." Journal of Controlled Release 46(3): 263-271.
- Volodkin, D. V., Skirtach, A. G. and Mohwald, H. (2009). "Near-IR remote release from assemblies of liposomes and nanoparticles." Angewandte Chemie. International Ed. In English 48(10): 1807-1809.
- Wang, L., Wang, Z., Liu, J., Zhang, J. and Zhang, D. (2011a). "Preparation of a new nanosized As<sub>2</sub>O<sub>3</sub>/Mn<sub>0.5</sub>Zn<sub>0.5</sub>Fe<sub>2</sub>O<sub>4</sub> thermosensitive magnetoliposome and its antitumor effect on MDA\_MB\_231 cells." Journal of Nanoscience and Nanotechnology 11(12): 10755-10759.
- Wang, L., Zhang, J., An, Y., Wang, Z., Liu, J., Li, Y. and Zhang, D. (2011b). "A study on the thermochemotherapy effect of nanosized As<sub>2</sub>O<sub>3</sub>/MZP thermosensitive magnetoliposomes on experimental hepatoma in vitro and in vivo." Nanotechnology 22(31): 0957-4484.
- Wang, Q. and Liu, J. Nanoparticles enhanced hyperthermia. In Intracellular delivery: Fundamentals and applications, Prokop, A.: (2011c); 5, 567-598.
- Wang, Y., Wang, Y. P., Tay, Y. C. and Harris, D. C. (2000). "Progressive adriamycin nephropathy in mice: sequence of histologic and immunohistochemical events." Kidney International 58(4): 1797-1804.
- Waterhouse, D. N., Tardi, P. G., Mayer, L. D. and Bally, M. B. (2001). "A comparison of liposomal formulations of doxorubicin with drug administered in free form: changing toxicity profiles." Drug Safety 24(12): 903-920.
- Webb, M. S., Harasym, T. O., Masin, D., Bally, M. B. and Mayer, L. D. (1995). "Sphingomyelin-cholesterol liposomes significantly enhance the pharmacokinetic and therapeutic properties of vincristine in murine and human tumour models." British Journal of Cancer 72(4): 896-904.
- Weiss, R. B. (1992). "The anthracyclines: Will we ever find a better doxorubicin?" Seminars in Oncology 19(6): 670-686.
- Weissleder, R. (2001). "A clearer vision for in vivo imaging." Nature Biotechnology 19(4): 316.
- Wilkie, S., Picco, G., Foster, J., Davies, D. M., Julien, S., Cooper, L., Arif, S., Mather, S. J., Taylor-Papadimitriou, J., Burchell, J. M. and Maher, J. (2008). "Retargeting of human T cells to tumor-associated MUC1: the evolution of a chimeric antigen receptor." Journal of Immunology 180(7): 4901-4909.



- Wood, B. J., Poon, R. T., Locklin, J. K., Dreher, M. R., Ng, K. K., Eugeni, M., Seidel, G., Dromi, S., Neeman, Z., Kolf, M., Black, C. D., Prabhakar, R. and Libutti, S. K. (2012). "Phase I study of heat-deployed liposomal doxorubicin during radiofrequency ablation for hepatic malignancies." Journal of Vascular and Interventional Radiology 23(2): 248-255.
- Wu, G. (2008). "Remotely triggered liposome release by near-infrared light absorption via hollow gold nanoshells." Journal of the American Chemical Society 130(26): 8175-8177.
- X, L., DJ, H., D, C.-L., A, Z., SM, G., AS, J. and WR, P. (1998). "Doxorubicin physical state in solution and inside liposomes loaded via a pH gradient." Biochimica et biophysica acta. Biomembranes 1415(1): 23-40.
- Xu, C. Y., Breedveld, V. and Kopecek, J. (2005). "Reversible hydrogels from self-assembling genetically engineered protein block copolymers." Biomacromolecules 6(3): 1739-1749.
- Yang, F. Y., Wang, H. E., Liu, R. S., Teng, M. C., Li, J. J., Lu, M., Wei, M. C. and Wong, T. T. (2012a). "Pharmacokinetic analysis of 111 in-labeled liposomal doxorubicin in murine glioblastoma after blood-brain barrier disruption by focused ultrasound." Plos One 7(9): e45468.
- Yang, T., Choi, M.-K., Cui, F.-D., Kim, J. S., Chung, S.-J., Shim, C.-K. and Kim, D.-D. (2007). "Preparation and evaluation of paclitaxel-loaded PEGylated immunoliposome." Journal of Controlled Release 120(3): 169-177.
- Yang, W., Ahmed, M., Tasawwar, B., Levchenko, T., Sawant, R. R., Torchilin, V. and Goldberg, S. N. (2012b). "Combination radiofrequency (RF) ablation and IV liposomal heat shock protein suppression: reduced tumor growth and increased animal endpoint survival in a small animal tumor model." Journal of Controlled Release 160(2): 239-244.
- Yarmolenko, P. S., Zhao, Y., Landon, C., Spasojevic, I., Yuan, F., Needham, D., Viglianti, B. L. and Dewhirst, M. W. (2010). "Comparative effects of thermosensitive doxorubicin-containing liposomes and hyperthermia in human and murine tumours." International Journal of Hyperthermia 26(5): 485-498.
- Yatvin, M. B., Muhlensiepen, H., Porschen, W., Weinstein, J. N. and Feinendegen, L. E. (1981). "Selective delivery of liposome-associated cis-dichlorodiammineplatinum(II) by heat and its influence on tumor drug uptake and growth." Cancer Research 41(5): 1602-1607.
- Yatvin, M. B., Weinstein, J. N., Dennis, W. H. and Blumenthal, R. (1978). "Design of liposomes for enhanced local release of drugs by hyperthermia." Science 202(4374): 1290-1293.
- Yoshida, M., Sato, M., Yamamoto, Y., Maehara, T., Naohara, T., Aono, H., Sugishita, H., Sato, K. and Watanabe, Y. (2012). "Tumor local chemohyperthermia using docetaxel-embedded magnetoliposomes: Interaction of chemotherapy and hyperthermia." Journal of Gastroenterology and Hepatology 27(2): 406-411.
- Yoshino, K., Kadowaki, A., Takagishi, T. and Kono, K. (2004). "Temperature sensitization of liposomes by use of N-isopropylacrylamide copolymers with varying transition endotherms." Bioconjugate Chemistry 15(5): 1102-1109.
- Yuan, F., Leunig, M., Huang, S. K., Berk, D. A., Papahadjopoulos, D. and Jain, R. K. (1994a). "Microvascular permeability and interstitial penetration of sterically stabilized (stealth) liposomes in a human tumor xenograft." Cancer Research 54(13): 3352-3356.

- Yuan, F., Salehi, H. A., Boucher, Y., Vasthare, U. S., Tuma, R. F. and Jain, R. K. (1994b). "Vascular permeability and microcirculation of gliomas and mammary carcinomas transplanted in rat and mouse cranial windows." Cancer Research 54(17): 4564-4568.
- Yuhas, J. M., Li, A. P., Martinez, A. O. and Ladman, A. J. (1977). "A simplified method for production and growth of multicellular tumor spheroids." Cancer Research 37(10): 3639-3643.
- Zagar, T. M., Oleson, J. R., Vujaskovic, Z., Dewhurst, M. W., Craciunescu, O. I., Blackwell, K. L., Prosnitz, L. R. and Jones, E. L. (2010). "Hyperthermia combined with radiation therapy for superficial breast cancer and chest wall recurrence: a review of the randomised data." International Journal of Hyperthermia 26(7): 612-617.
- Zhou, Y. F. (2011). "High intensity focused ultrasound in clinical tumor ablation." World Journal of Clinical Oncology 2(1): 8-27.
- Zhu, L., Huo, Z. L., Wang, L. L., Tong, X., Xiao, Y. and Ni, K. Y. (2009). "Targeted delivery of methotrexate to skeletal muscular tissue by thermosensitive magnetoliposomes." International Journal of Pharmaceutics 370(1-2): 136-143.
- Zhu, L. and Torchilin, V. P. (2013). "Stimulus-responsive nanopreparations for tumor targeting." Integrative Biology 5(1): 96-107.
- Zitzewitz, J. A., Bilsel, O., Luo, J., Jones, B. E. and Matthews, C. R. (1995). "Probing the folding mechanism of a leucine zipper peptide by stopped-flow circular dichroism spectroscopy." Biochemistry 34(39): 12812-12819.
- Zoonens, M., Reshetnyak, Y. K. and Engelman, D. M. (2008). "Bilayer interactions of pHLIP, a peptide that can deliver drugs and target tumors." Biophysical Journal 95(1): 225-235.